VAPB regulation of ER stress and its potential involvement in ALSVIII

Christos G. Gkogkas

A thesis submitted for the degree of Doctor of Philosophy

The University of Edinburgh

2008

Declaration

I declare that this thesis was composed entirely by myself and the work on which it is based is my own, unless clearly stated in the text.

Christos Gkogkas

Abstract

A mis-sense point mutation in the human VAPB gene is associated with a familial form of motor neuron disease that has been classified as Amyotrophic Lateral Sclerosis type VIII. Affected individuals suffer from a spinal muscular atrophy (SMA), amyotrophic lateral sclerosis (ALS) or an atypical slowly progressing form of ALS.

Mammals have two homologous VAP genes, vapA and vapB. VAPA and VAPB share 76% similar or identical amino acid residues; both are COOH-terminally anchored membrane proteins enriched on the endoplasmic reticulum. Several functions have been ascribed to VAP proteins including membrane trafficking, cytoskeleton association and membrane docking interactions for cytoplasmic factors. It is shown here that VAPA and VAPB are expressed in tissues throughout the body but at different levels, and that they are present in overlapping but distinct regions of the endoplasmic reticulum. The disease-associated mutation in VAPB, VAPB (P56S) is within a highly conserved N-terminal region of the protein that shares extensive structural homology with the major sperm protein (MSP) from nematodes. The MSP domain of VAPA and VAPB is found to interact with the ER-localized transcription factor ATF6. Over expression of VAPB or VAPB (P56S) attenuates the activity of ATF6-regulated transcription and the mutant protein VAPB (P56S) appears to be a more potent inhibitor of ATF6 activity. Moreover VAP proteins affect the activity of XBP1 and BiP promoter elements, two major components of the Unfolded Protein Response (UPR) of the Endoplasmic Reticulum and the different domains of VAPB have a differential effect on UPR regulation. Finally, over expression of the MSP domain of VAPB leads to cell death via apoptosis, while overexpression of other VAPB domains renders cells more susceptible to apoptotic death after ER stress.

The data presented in this thesis indicate that VAP proteins interact directly with components of ER homeostatic and stress signalling systems and may therefore be parts of a previously unidentified regulatory pathway. The mis-function of such regulatory systems may contribute to the pathological mechanisms of degenerative motor neuron disease.

Acknowledgments

First and foremost I would like to thank my supervisor Dr. Paul A. Skehel for his help, support, ideas, guidance and patience throughout my PhD and for hosting me in his laboratory providing the means to learn and do research. He has been my family away from home and has helped me in numerous occasions, thus my gratitude to him is eternal.

I would like to thank my parents Γιώργος and Μαρία for their ongoing support and faith in me and especially my brother Μπάμπης.

During my PhD I had the privilege to interact with marvellous people in the Edinburgh Neuroscience community and I would like to thank Dr. Caroline Wardrope for her help and advice and for cloning various VAPB constructs, Dr. Susan Middleton for her help and guidance, Ms Helen Ibbotson, Dr. Giles Hardingham and Dr. Franscesc Soriano for invaluable help with luciferase transcriptional assays and advice and Dr. Tom Gillingwater for the muscle experiment.

I would like extend my gratitude to my PhD thesis committee chairman Dr. Richard R. Ribchester and my second supervisor Dr. Karen Horsburgh for their guidance throughout my studies.

I would like to thank Dr. Kazutoshi Mori for providing the ATF6, XBP1 and BiP reporters and Professor Steve Michnick for providing the PCA plasmids.

I would like to thank Professor Peter Brophy and the CNR for supporting my trip to Cold Spring Harbor in 2005. I would also like to thank the University of Edinburgh for financing my PhD.

I would like extend my gratitude to Ms Dorothy Watson and Mr Paul McGuire at the MVM Postgraduate office for their help.

Finally, I would like to thank my friend Dr. Alexandros Pantazis for his support and my friend Dr. Emanouil Rampakakis for his support and scientific advice.

Table of Contents

Chapter 1
Introduction

1.1 VAMP/synaptobrevin -Associated Proteins (VAPs)

1.1.1 Initial Characterisation

The first VAP protein (*VAP33*) was identified in the sea mollusc *Aplysia californica* as a 33 KDa protein in a yeast-two hybrid screen for proteins interacting with the synaptic vesicle protein VAMP (vesicle associated protein or synaptobrevin); this interaction was further validated by pull-down of a glutathione-S-transferase fused VAP33 and an *in vitro* translated VAMP (Skehel et al., 1995). VAMPs are synaptic vesicle SNARE (soluble N-ethylmaleimide-sensitive factor attachment protein receptor) proteins that participate in synaptic-vesicle fusion (Chen and Scheller, 2001, Scales et al., 2000). When the presynaptic sensory neuron of *A. californica* was injected with VAP33 specific antibodies, inhibition of EPSPs (Excitatory Post-Synaptic Potentials) recorded in the postsynaptic motor neuron was observed, while the overall structure of the synapses was not perturbed (Skehel et al., 1995). Expression of VAP33 was restricted in neuronal cells of *A. Californica.*

Soon after, the human homologue of VAP33 termed hVAP33 was identified (Weir et al., 1998) and its binding to human VAMP was shown; hVAP33 expression was not restricted to neuronal tissue like its *A.californica* homologue. Furthermore, in rat and human three homologues of VAP33 were characterised and termed VAPA (corresponding to the previously identified hVAP33), VAPB and VAPC (Nishimura et al., 1999). VAPA and VAPB share an overall 60% sequence similarity, while VAPC is a splice variant of the vapB gene. Mammalian VAPA and VAPB share the same basic architecture (Figure 1.1), consisting of three major structural protein domains:

- A N-terminal Major Sperm Protein Homology domain termed *MSP* domain
- A *Coiled-Coil* domain
- A C-terminal *transmembrane* domain.

VAPC lacks the coiled coil and transmembrane domains but contains the MSP domain and 24 amino acids, which are not found in VAPA or VAPB; however the evidence so far presented for the expression of this transcript is not substantial

Figure 1.1

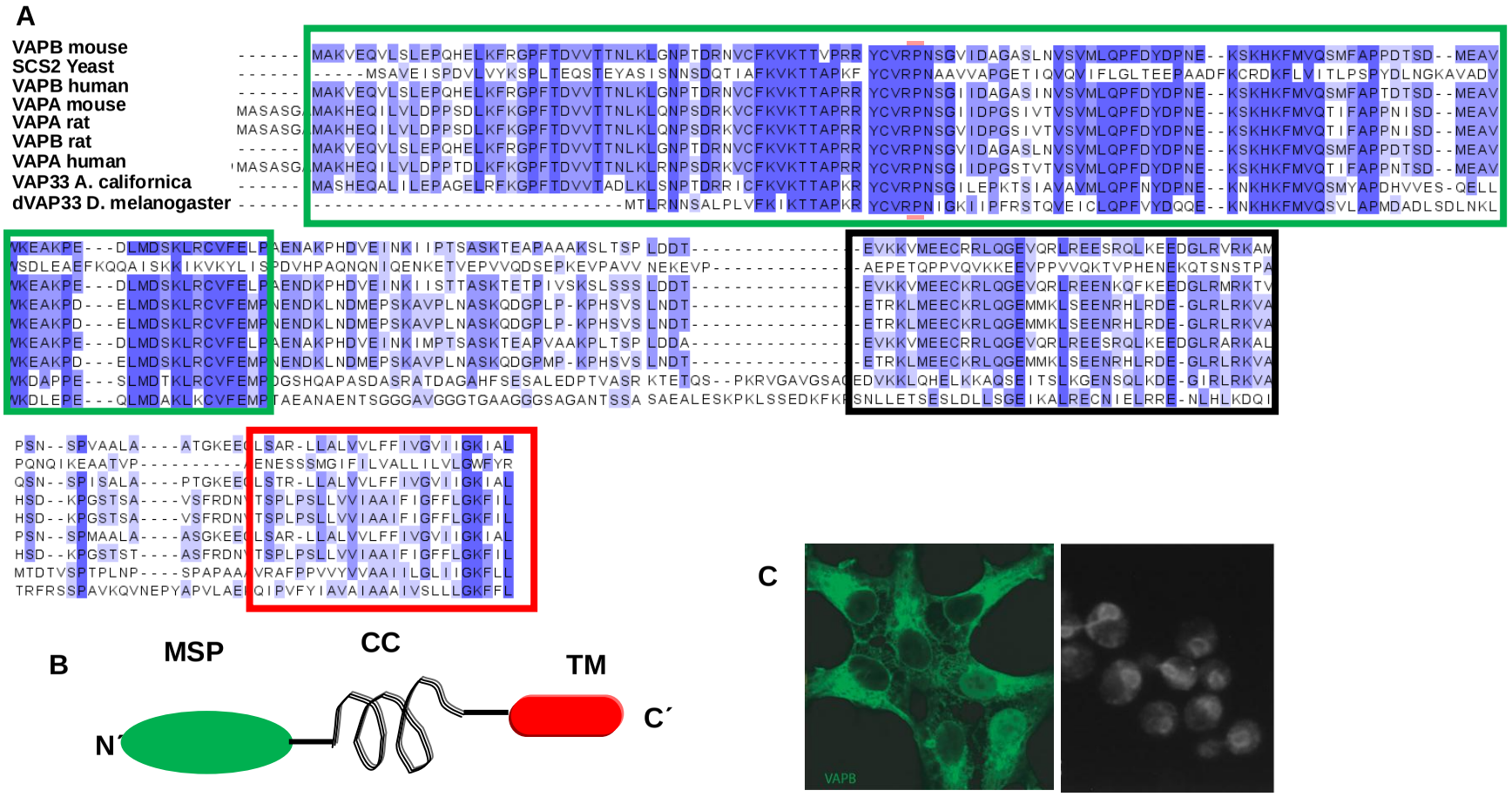
A
VAPB mouse
SCS2 Yeast
VAPB human
VAPA mouse
VAPA rat
VAPB rat
VAPA human
VAP33 A. californica
dVAP33 D. melanogaster
B
MSP
CC
TM
N
C´
C
VAPB

Figure 1.1 ***VAP proteins sequence, domains and subcellular localization***

A. Alignment of VAP proteins from human to *A. californica*. The conservation is high throughout the primary protein sequence, however the most conserved domain is the N-terminal MSP domain (conserved proline at position 56 highlighted in red). Colours correspond to the relative domains on the highlighted areas of the alignment. Alignment was done using Jalview (Clamp et al., 2004).

B. Schematic representation of the structural domains of mammalian VAPs.

C. VAP proteins in HEK293 cells and yeast YPH500 cells (Images respectively from (Gkogkas et al., 2008, Kagiwada et al., 1998, Pennetta et al., 2002)).

(Nishimura et al., 1999). Homologues of VAPA or VAPB have also been characterised in yeast (Kagiwada et al., 1998), Drosophila (Pennetta et al., 2002) and mouse (Skehel et al., 2000) and identified in other mammals; a VAP33 homologue (VAP27) was identified in plants (Laurent et al., 2000).

1.1.2 Subcellular localization

The yeast homologue of VAP33, *SCS2*, was shown to be C-terminally anchored to the Endoplasmic Reticulum membrane and the majority of the protein resided in the cytoplasm (Kagiwada et al., 1998). Human VAPA was shown to interact and colocalize with occludin, which is a transmembrane protein localized at tight junctions between endothelial and epithelial cells, or plasma membrane domains (Lapierre et al., 1999). Mouse VAP33 is associated with microtubules and Endoplasmic Reticulum membranes (Skehel et al., 2000), while in Drosophila it is localized at the neuromuscular junction (Pennetta et al., 2002).

1.1.3 VAP protein domains

The MSP domain (MSP)

The N-terminal domain of VAP proteins is the most conserved domain of the protein from Aplysia to human. This domain was termed MSP domain for its similarity to the nematode Major Sperm Protein (MSP). Nematode sperm displays an amoeboid like locomotion that is not mediated by the actin cytoskeleton, but by a dynamic structural web whose single component is MSP (Tarr and Scott, 2005b, Tarr and Scott, 2005a). Major Sperm Protein has no sequence similarity to actin and is the most abundant protein in nematode sperm. The MSP domain is an s-type Immunoglobulin-like fold (Ig-fold), which is also found in several other proteins, including human growth hormone receptor, fibronectin and CD4 (Bork et al., 1994). It comprises of a seven stranded b sandwich composed of a three-stranded sheet opposed by a four stranded sheet. These sheets of the Ig-fold interact with sheets of other Ig-like domains and therefore can mediate protein-protein interactions. The MSP domain of rat VAPA (amino acids 1-125) was crystallized (Kaiser et al., 2005)

and the structure 1z9L (Protein Data Bank) , as expected from the sequence identity was similar to Major Sperm Protein. It is noteworthy that VAPA MSP is monomeric in solution, while the nematode MSP and VAPB MSP domain dimerize (Kaiser et al., 2005).

Recently it was shown that the MSP of Drosophila VAPA is released after cleavage of the full length protein and the MSP domain is secreted and interacts with the Ephrin-B receptor (Tsuda et al., 2008). This is in agreement with the function of MSP in nematodes, as apart from a cytoskeletal element, the MSP monomer is exported from the sperm cytoplasm into the proximal gonad by a membrane-budding mechanism (Kosinski et al., 2005) and binds to the VAB-1 Eph receptor protein-tyrosine kinase (RPTK) (Miller et al., 2003). Moreover, in nematodes, binding of MSP to the VAB-1 Eph receptor stimulates NMR-1 (N-methyl D-aspartate type glutamate receptor) which in turn prevents signalling by the UNC-43 Ca2+/calmodulin-dependent protein kinase II (CaMKII) (Corrigan et al., 2005). Therefore, despite the fact that Ig-like domains are thought to be mainly involved in binding functions, a signalling role for the MSP domain architecture is emerging.

The Coiled-Coil domain (CC)

Amino acids 158-211 of VAP proteins are predicted to form a coiled- coil when the COILS prediction software is used (Lupas et al., 1991). The VAP protein CC domain resembles that of many SNARE proteins (syntaxin, synaptobrevin, SNAP25 (Brunger, 2005)) and therefore one would speculate that it is that domain that mediates the synaptobrevin-VAP interaction. The CC domain promotes VAP dimerization (Kaiser et al., 2005) and Coiled-Coil protein domains are known to participate in promiscuous protein-protein interactions (Weir et al., 1998); little is known so far about the structure-function association of the VAP CC domain.

The Transmembrane domain (CT)

VAP proteins have a C terminal transmembrane domain (amino acids 220-243) which anchors the protein to membranes (ER membranes, vesicle membranes etc.). VAPs are classified as type II membrane proteins (amino terminus on the cytoplasmic side and lack of an ER-targeting signal peptide), albeit VAP dimerisation

may classify them as type IV (multiple homologous domains)(Aturaliya et al., 2006, Matlack et al., 1998). In most metazoan VAPs, a GxxxG inner-membrane protein interactions motif (Russ and Engelman, 2000) is present in their C-terminal transmembrane domain. This suggests that VAP proteins can homo/hetero-dimerize via their transmembrane domains; yeast SCS2 does not contain the aforementioned motif and therefore is not observed as a dimer (Kagiwada et al., 1998, Kagiwada and Zen, 2003).

1.1.4 Cellular functions of VAPs

Proteins interacting with VAPs

VAPs interact with a plethora of other proteins and their known interactors so far are summarized in the Table 1.1 (taken from (Lev et al., 2008). This broad array of interactions has helped assign several functions to VAP proteins.

SNARE associated function

Human VAP proteins were shown to interact with synaptobrevin along with other v and tSNAREs, such as syntaxin 1a, bet1, sec22, αSNAP and NSF (Weir et al., 2001). Interestingly, they do not bind to syntaxin 17, a tSNARE involved in smooth ER traffic or to the plasma membrane tSNARE SNAP-25. The high degree of conservation of the SNARE core (coiled-coil) and VAP CC domain suggest that there might be an evolutionary conserved function as a result of the VAP-SNARE interaction. However, the physiological role of the VAP-SNARE interaction in mammals has not been yet revealed, although in *A. Californica* it was clearly demonstrated that antibodies to VAP33 block EPSPs and thus neurotransmitter release. The main hypothesis regarding SNARE function is that VAP proteins do not regulate SNAREs, but act as a chaperone that does not participate in SNARE fusion events; this hypothesis is strengthened by the fact that mouse VAPA does not co-localise with VAMP at synaptic structures, but at the cell body of neurons, in lower quantities (Skehel et al., 2000). VAPs could rather regulate ER to Golgi transport, similarly to sec22, which is required for retrograde transport to the ER (Brunger, 2005, Burri et al., 2003).

Table 1.1 ***VAP interacting proteins***

Interacting Protein	VAP protein	Interacting Domain	Reference
SNAREs			
VAMP	aVAP33	-	(Skehel et al., 1995)
VAMP-1	VAPA	MSP, CT	(Weir et al., 1998, Weir et al., 2001)
VAMP-2	VAPA	-	(Weir et al., 1998, Weir et al., 2001)
Syntaxin 1A	VAPA	-	(Weir et al., 2001)
bet1	VAPA	-	(Weir et al., 2001)
sec22	VAPA	-	(Weir et al., 2001)
αSNAP	VAPA	-	(Weir et al., 2001)
NSF	VAPA	-	(Weir et al., 2001)
Viral Proteins			
P48 Norwalk virus non-structural protein	VAPA	-	(Ettayebi and Hardy, 2003)
NS5A HCV non-structural (NS) protein	VAPB	CC	(Hamamoto et al., 2005)
NS5A	VAPA	CC, CT	(Tu et al., 1999)
NS5B	VAPA	MSP	(Hamamoto et al., 2005, Tu et al., 1999)
60K cowpea mosaic virus	VAP27	CC	(Carette et al., 2002)
FFAT-proteins			
Opi1p	SCS2p	MSP FFAT motif	(Loewen and Levine, 2005, Loewen et al., 2003)
Osh1, Osh2, Osh3	SCS2p	-	(Loewen et al., 2003)
OSBP	VAPA	-	(Wyles et al., 2002)
ORP1-4, 6, 7, 9	VAPA, VAPB	-	(Wyles and Ridgway, 2004)
CERT	VAPA, VAPB	-	(Kawano et al., 2006)
Nir1, Nir2, Nir3	VAPA, VAPB	-	(Amarilio et al., 2005)
Other Proteins			
VAPA, VAPB	VAPA, VAPB	CT required	(Nishimura et al., 1999)
Occludin	VAPA	-	(Lapierre et al., 1999)
Insig1, Insig2	VAPA, VAPB	-	(Gong et al., 2006)
Tubulin	dVAP33	-	(Pennetta et al., 2002)
PRA2	VAPA	-	(Gougeon and Ngsee, 2005)
PP2Cε	VAPA	CT required	(Saito et al., 2008)
Stt4p, Fks1p, Num1p, Rpn10p, YGR086Cp	SCS2p	-	(Gavin et al., 2002)

Lipid Metabolism

Yeast studies of the VAP homologue Scs2p highlight its extensive participation in lipid metabolism (Kagiwada and Hashimoto, 2007, Kagiwada et al., 1998, Kagiwada and Zen, 2003). The SCS2 gene was first identified as a suppressor of inositol auxotrophy of the yeast ire15 mutant and choline-sensitive dominant mutation, CSE1 (Hosaka et al., 1992, Nikawa et al., 1995), while the two auxotroph genes are on different alleles. The inositol metabolic pathway is well characterized in yeast and INO1 (inositol-1-phosphate synthase) is the key enzyme that catalyzes synthesis of Inosito-1-P from Glucose 6-P (Figure 1.2A). Notably, disruption of genes involved in the choline pathway reversed the INO1 auxotrophy caused by the SCS2-deficient yeast strains. Inositol and choline promote INO1 expression. Regulation of INO1 expression is mediated by an inositol-sensitive promoter (UAS_{INO}) and two transcription factors Ino2p and Ino4p that act on the UAS promoter. This transcriptional control is tightly repressed by binding of Opi1p to Ino2p. Dissociation of Opi1p promotes INO1 transcription and expression; the dynamics of this repression are modulated by phosphatidic acid (PA). PA, Opi1p and Scs2p all localize on the ER membrane and in addition, OPi1p binds to the MSP domain of Scs2p. This interaction suggests a potential role in regulating INO1 transcriptional activation via the Scs2p MSP domain.

FFAT and lipid sensing- Membrane Trafficking

The FFATT motif (two phenylalanines in an acidic tract) is a targeting signal that targets cytosolic proteins to the surface of the ER and the nuclear membrane and corresponds to the consensus sequence EFFDAxE. VAP proteins were found to interact with FFAT containing proteins (Wyles et al., 2002, Wyles and Ridgway, 2004); apart from the aforementioned Ssc2p-Opi1p interaction which his associated with inositol metabolism, VAPs interact with a multitude of lipid-binding, lipid-sensing or lipid-transport proteins (Table 1.1). Thus, FFAT motifs are targeted to ER membranes by interactions with VAP proteins. The FFAT motif binding site on VAP

Figure 1.2

A

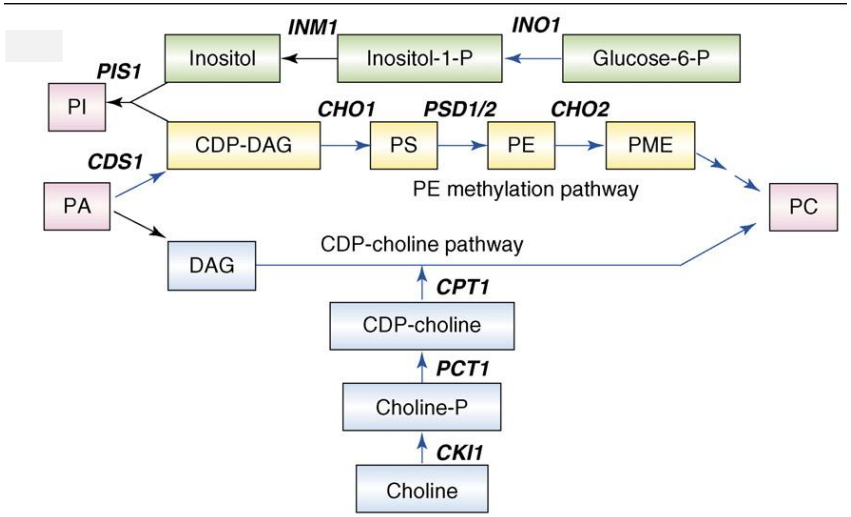
INM1
INO1
Inositol
Inositol-1-P
Glucose-6-P
PIS1
PI
CHO1
PSD1/2
CHO2
CDP-DAG
PS
PE
PME
CDS1
PE methylation pathway
PA
PC
DAG
CDP-choline pathway
CPT1
CDP-choline
PCT1
Choline-P
CKI1
Choline

B

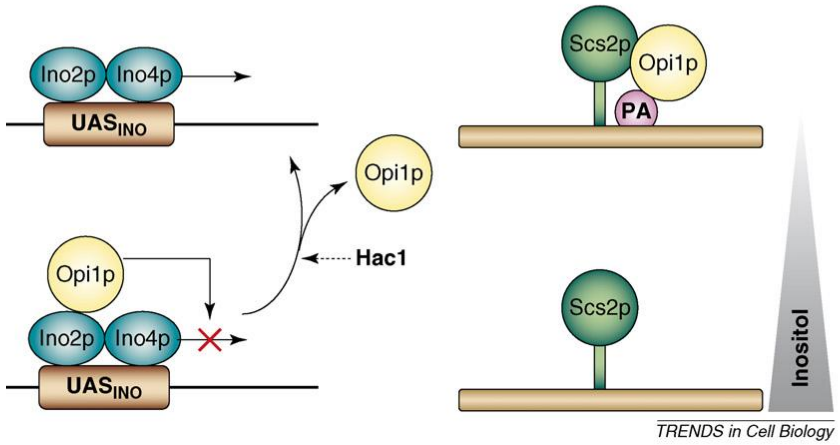
Ino2p
Ino4p
UAS$_{INO}$
Opi1p
Scs2p
PA
Hac1
Inositol
TRENDS in Cell Biology

Figure 1.2 ***Regulation of phospholipid biosynthesis in S.cerevisiae*** **(image from (Lev et al., 2008)).**

A. Inositol and Choline metabolism in *S. Cerevisiae.*

B. Op1p and Scs2 interplay in INO1 transcription.

Lipids**: DAG**, diacylglycerol; **PA**, phosphatidic acid; **PtdCho**, phosphatidylcholine; **PtdEtn**, phosphatidylethanolamine; **PtdIns**, phosphatidylinositol; **PME**, phosphatidylmonomethylethanolamine; **PS**, phosphatidylserine. Enzymes: **CDS1**, **CDP-DAG** synthase; **CHO1**, **PS** synthase; **CHO2**, PtdEtn methyltransferase; **CKI1**, choline kinase; **CPT1**, **CDP-choline**: 1,2-DAG choline phosphotransferase; **INO1**, inositol 1-phosphate synthase; **PCT1**, CTP: choline-phosphate cytidyltransferase; **PIS**, PtdIns synthase; **PSD1/2**, **PS** decarboxylase.

proteins was mapped to a highly conserved region of the MSP domain (Kaiser et al., 2005, Loewen and Levine, 2005, Loewen et al., 2003). Co-crystallization of rat VAPA MSP and FFAT reveals a MSP-FFAT complex that buries two FFATS between two VAPA MSP domains. FFAT binding on VAP MSP domain is considered to be a pivotal physiological function of mammalian VAPs.

Ceramide transport-Glucose transport

Sphingolipid synthesis, transport, sorting and turnover in cells are essential processes that preserve membrane structure of organelles and other membranous formations. Ceramide is converted to sphingomyelin(SM) in the Golgi by phosphatidylcholine ceramide cholinephosphotransferase (SM synthase); Ceramide is synthesized at the ER and then transported to the Golgi. The key factor participating in ceramide transport is CERT (Goodpasture antigen-binding protein). VAPA and VAPB were found to interact with CERT (Hanada et al., 2007, Kawano et al., 2006), a cytosolic protein that consists of three distinct domains:

- An N-terminal phosphoinositide-binding pleckstrin homology domain (PH). This domain recognises PI4P (phosphatidylinositol 4-monophosphate) and targets CERT to the Golgi apparatus.
- A middle domain with no similarity to any protein structures; however this domain contains an FFAT motif which mediates the interaction of CERT with VAPs
- A C-terminal START domain (lipid-transfer domain). This domain is responsible for ceramide transfer between membranes.

The VAP-CERT interaction modulates targeting of CERT to the Golgi apparatus via the FFAT interaction and this is dependent on the available amount of CERT protein(Kawano et al., 2006).

Insulin in muscle and fat cells, in order to increase glucose entry to the cell causes intracellular vesicles containing the GLUT4 glucose transporter to rapidly recruit to the plasma membrane (Foster et al., 2000). In these cells, GLUT4 transport requires participation of the SNARE machinery (VAMP-2, syntaxin-4 and synaptosome-associated protein of 23kDa (SNAP-23) in 3T3-l1 adipocytes). Moreover, VAPA co-localises with VAMP-2 in L6 myoblasts and 3T3-L1 adipocytes and partially co-localises with GLUT4 in L6 myoblasts. Overexpression of VAPA

Figure 1.3

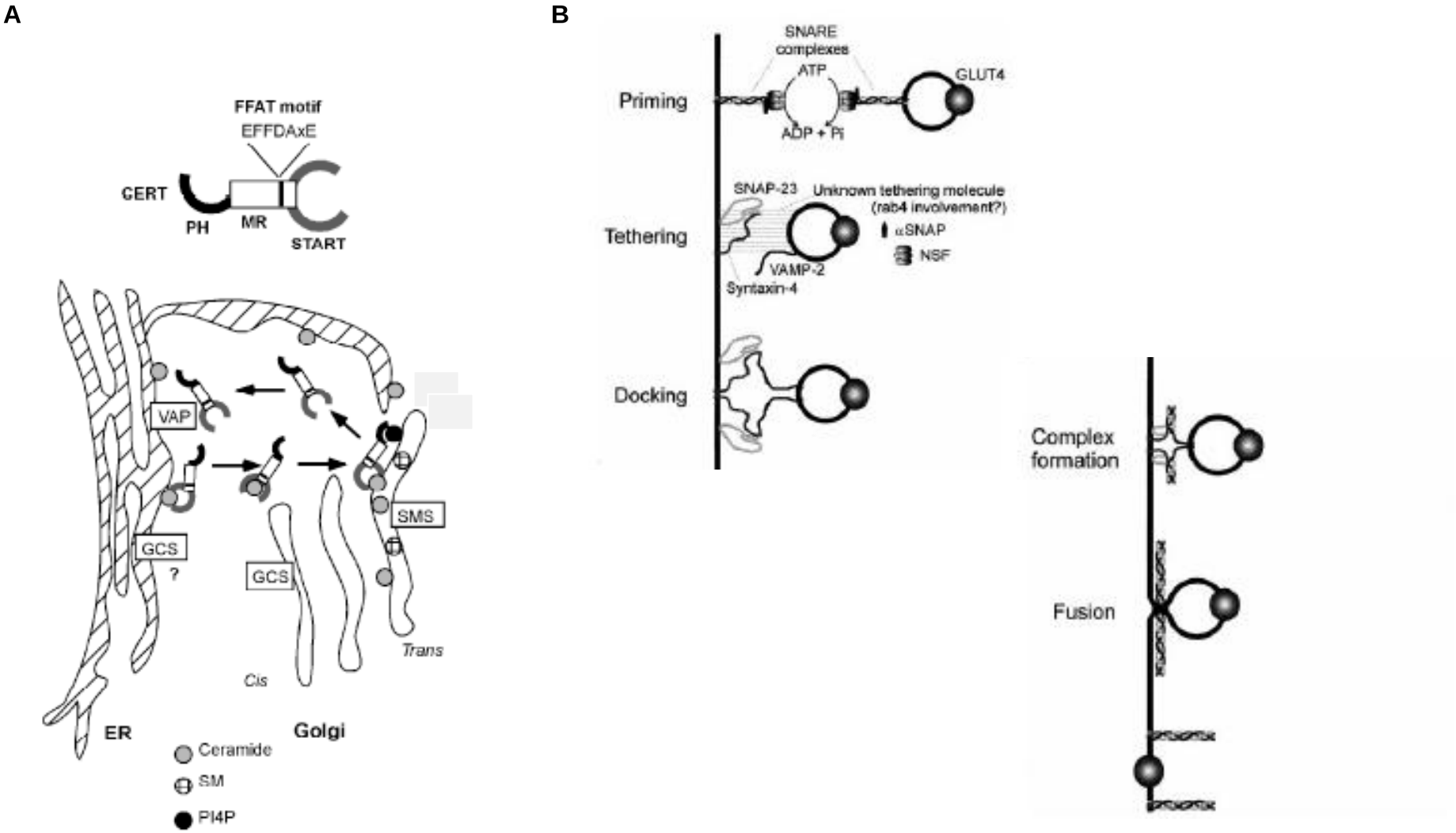
A
FFAT motif
EFFDAxE
CERT
PH
MR
START
VAP
GCS
?
GCS
SMS
Trans
Cis
ER
Golgi
Ceramide
SM
PI4P
B
SNARE complexes
ATP
ADP + Pi
GLUT4
Priming
SNAP-23
Unknown tethering molecule (rab4 involvement?)
αSNAP
NSF
Tethering
VAMP-2
Syntaxin-4
Docking
Complex formation
Fusion

Figure 1.3 ***Ceramide transport, glucose transport and VAP proteins***

A. (from (Kawano et al., 2006)) Ceramide transport by CERT via FFAT motif interactions with VAP proteins (see text). *SMS*: SM (sphingomyelin) synthase; *GCS*: GlcCer (glucosylceramide) synthase

B. (from (Foster et al., 2000)) Steps in vesicle docking and fusion applied to the glucose transporter 4 (GLUT-4) system. SNARE complexes on the plasma membrane and vesicle membranes must first be dissociated by the action of the ATPase *N*-ethylmaleimide-sensitive factor (NSF) and soluble NSF attachment protein (αSNAP) (vesicle priming). The vesicle then becomes associated with the plasma membrane (vesicle tethering). Once tethered, the SNAREs can *trans*-associate, causing the vesicle to become more tightly associated with the plasma membrane (docking). The classic SNARE complex is formed after docking.

reduced GLUT4 delivery to the surface, following application of insulin. In addition, antibodies to VAPA reduce levels of surface GLUT4 post insulin treatment, but do not affect basal levels of membrane GLUT4. Remarkably, when VAPA and VAMP-2 are co-expressed GLUT4 returned to its previous levels. Therefore, VAPA may limit the amount of endogenous VAMP-2 required to promote transport of GLUT4 to the membrane.

HCV replication

The Hepatitis C virus (HCV) is a single stranded RNA virus shown to be the major causative agent of non-A, non-B hepatitis (Moriishi and Matsuura, 2007). Its replication is based on the host cell protein machinery and therefore interactions of viral proteins with cellular components are important. VAPA and VAPB were found to interact with non-structural phopshoproteins NS5A and NS5B of the HCV (Tu et al., 1999). Overexpression of VAP proteins increases HCV replication, while blocking of VAPs with antibodies blocks viral replication. VAPA and VAPB homo/hetero-dimers modulate this interaction and there is no effect when VAPs don't have their CT domain that tethers them to the ER membranes (Hamamoto et al., 2005).

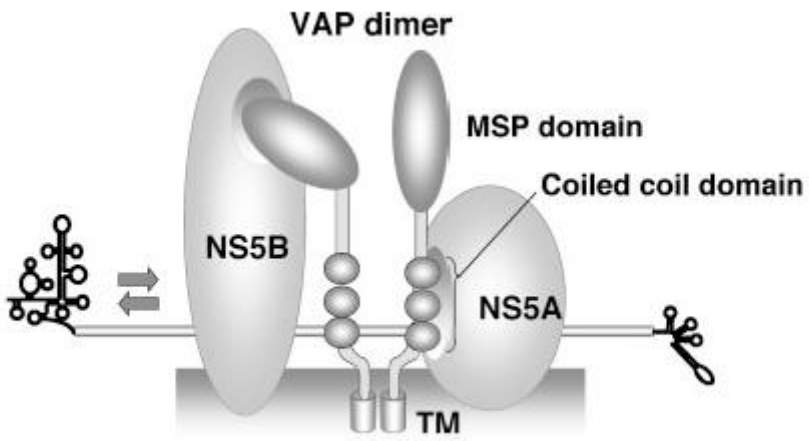

Figure 1.4 ***VAP proteins and the Hepatitis C virus (taken from (Moriishi and Matsuura, 2007).***

VAPA and VAPB bind to NS5B and NS5A non-structural HCV proteins and regulate HCV replication.

Unfolded Protein Response

VAP proteins have been implicated in the regulation of a cell's Unfolded Protein Response (UPR) of the ER (see 1.3.3); when misfolded or unfolded proteins are accumulated in the ER lumen, a network of genes and transcription factors is activated via a signalling cascade that signals to the nucleus and results in attenuation of translation and eventually leads to apoptotic death if the cell's capacity to handle the misfolded proteins is exceeded. The first report linking VAP proteins with this pathway comes from yeast (Kagiwada et al., 1998, Kagiwada and Zen, 2003). Scs2p was shown to be involved in yeast UPR via Hac1 (see Figure 1.2B). Hac1 is a transcription factor that initiates the UPR in yeast by binding to promoter elements of UPR associated genes; Hac1 regulates dissociation of Opi1 from the promoter element that controls transcription of the INO1 inositol associated gene. Therefore the Scs2-Opi1 interaction and the fact that UPR can be induced by inositol starvation in yeast, suggest that Scs2 might participate directly or indirectly in UPR regulation in yeast.

Apart from yeast, in HCV virus it was shown that VAP proteins may participate in the UPR of the host cell. NS5A and NS5B were shown to interact with VAPA and VAPB. NS5A can affect translocation and topology of another non-structural protein NS4B (Lundin et al., 2006). NS4B can induce an unfolded protein response in the host cell which seems to be an evolutionary adaptation of the virus that facilitates its replication by allowing synthesis of viral proteins in huge amounts in the host cell's ER (Zheng et al., 2005).

Finally, it was shown by Kanekura et al., 2006 that in a mammalian cell line, overexpression of VAPB can induce an unfolded protein response. Conversely, when endogenous VAPB is blocked with siRNA, the UPR response is attenuated. This study shows a global effect of VAP protein levels in regulating the UPR and suggests that this might be done through splicing of a UPR transcription factor, XBP1 (discussed in 1.3.3).

Hsp90

Hsp90 (Heat-Shock Protein of 90 KDa) is a molecular chaperone implicated in protein folding, cell signalling, and tumour repression (Pratt and Toft, 2003).

Hsp90 is known to control the folding of numerous cell-regulatory proteins such as steroid receptors and kinases. Recently it was shown that Hsp90 forms a complex with the co-chaperone tetratricopeptide repeat domain 1 (TPR1) that associates with VAPA on the ER membrane (Lotz et al., 2008). This novel interaction reveals a new regulatory pathway for VAP proteins.

Ephrin receptors

Ephrin receptors are transmembrane receptor tyrosine kinases that are implicated in cell signalling (angiogenesis, segmentation, axon guidance), development (cell guidance) and cancer (elevated levels in tumours); ephrins are the ligands of these receptors (O'Leary and Wilkinson, 1999, Boyd and Lackmann, 2001). Recently, Tsuda et al., 2008 showed that drosophila VAPB gets cleaved and is secreted from cells. Additionally, they showed that human MSP expressed protein binds expressed EphA4 extracellular domain in a pull-down assay; moreover MSP expression disrupts the interaction between mouse EphA4 and EphB2. The model proposed reveals a novel pathway for VAP proteins MSP domain to compete with ephrins for binding to ephrin receptors.

ER to Golgi transport

Transport of proteins between membranous organelles or on the plasma membrane is performed with 3 types of coated vesicles*: clathrin vesicles*, from the plasma membrane and trans-Golgi to endosomes; *COP I vesicles*, within Golgi cisternae and retrograde from cis-Golgi back to the rough ER; and *COP II* vesicles, from the rough ER to the cis-Golgi (Duden, 2003). Coated vesicles fuse with the acceptor membrane, release their cargo and then recycle the coat proteins for reuse. Uncoating of transport vesicles exposes specific v-SNARE proteins on the surface of each type of vesicle. V-SNAREs bind to t-SNARE proteins that are in complex with SNAP25 on the acceptor membrane. NSF and α-, β-, and γ-SNAP proteins then bind to the T-SNARE/V-SNARE/SNAP25 complex, and form the prefusion complex. After vesicle fusion the t-SNARE/ t-SNARE/SNAP25 may be dissociated via NSF and SAP proteins.

VAPA has been shown to participate in intra-Golgi and Golgi to ER transport

via COP I vesicles (Soussan et al., 1999). Blocking of VAP-B with antibodies blocks transport between Golgi cisternae and leads to accumulation of COP I coated vesicles(Soussan et al., 1999). More recently, Prosser et al., 2008 showed that VAPA but not VAPB overexpression blocks ER-Golgi transport as well as lateral diffusion, using the VSVG model (to follow movement of COP II vesicles from the ER to the Golgi in living cultured mammalian cells a construct encoding a chimeric protein consisting of green fluorescent protein fused to the cytosolic-facing C-terminus of the Vesicular Stomatitis Virus G glycoprotein, was used). Expression of the FFAT motif rescued this blocking of transport.

1.2 VAP proteins and ALS8

1.2.1 ALS8 and the P56S mutation

ALS/MND (Veldink et al., 2004)

The term Motor Neuron Disease (MND) is used to describe a number of illnesses concerning motor neuron malfunction. Known subtypes of MND are Amyotrophic Lateral Sclerosis (ALS), Progressive Muscular Atrophy (PMA), Progressive Bulbar Palsy (PBP) and Primary Lateral Sclerosis (PLS). The general term MND is widely used in Europe, whilst ALS is used more generically in the USA. Also this type of disease is often referred to as “maladie de Charcot” - first described by French physiologist Charcot in 1874 - aka “Lou Gehrig’s Disease” after the famous American baseball player who died of the disease.

ALS is one of the most common neurodegenerative disorders with an incidence of 2 per 100,000 of total population. Though it can affect anyone, ALS/MND is more often found in the 40-70 year group; juvenile cases have also been observed. The life expectancy for patients after diagnosis is about 3 years, although great deviations have been observed. The most typical feature of ALS is degeneration of cortical, bulbar and spinal motor neurons (spinal cord - brainstem - motor cortex), except for bladder controlling neurons (Onuf’s nuclei) and the ocular-motor neurons. The results of this degeneration are generalized muscle weakness, fasciculation, muscle atrophy, speech and swallowing disabilities, progressive

paralysis and ultimately death due to respiratory failure. However, there may be heterogeneity in the body regions affected, as well as the progression of the disease. Undoubtedly, the unique nature of the disease affects social life, family and career. The disease is progressing rapidly and this requires increased attention and adaptation to different levels of support and care for patients and their families.

Approximately 10% of ALS cases are dominantly inherited (Familial ALS-FALS) while 90% of them are sporadic. The main difference between FALS and sporadic ALS is the age onset, which is often lower for FALS.

ALS8-P56S (Nishimura et al., 2005, Nishimura et al., 2004)

After studying the genealogy tree of a large white Brazilian family, with 28 members affected across 4 generations a new locus for ALS/MND was mapped at 20q13.3 (chromosome 20, long arm, region q13.3), ALS8 (Figure 1.5). ALS8 is an autosomal dominant disorder with a slow progression of the disease (fasciculation, cramps, postural tremor). More elaborate studying of the genomic area in which the recombination events took place has revealed the existence of a missense mutation in VAPB in all affected members of this family. Moreover, the same mutation was found in six additional families with a different diagnosis. Although no immediate link could be found between those test cases, historical data points to a common Portuguese ancestor that expands the genealogy of affected patients throughout the various generations.

Mutation screening of the possible candidate genes identified that the missense mutation was a C→T substitution in exon 2 of the VAPB gene. The effect of the mutation is that a HaeIII restriction site is removed and at codon 56 a Proline (that is conserved) is substituted by a Serine (Pro56Ser or P56S). The proline is within the MSP domain and thus conserved in *H. sapiens, M. musculus, R. norvegicus, A. californica, D. melanogaster and S. Cerevisiae* (Figure 1.1A). Interestingly, this mutation was present in all affected members of the family, but not in unaffected relatives, or unrelated normal controls.

Figure 1.5

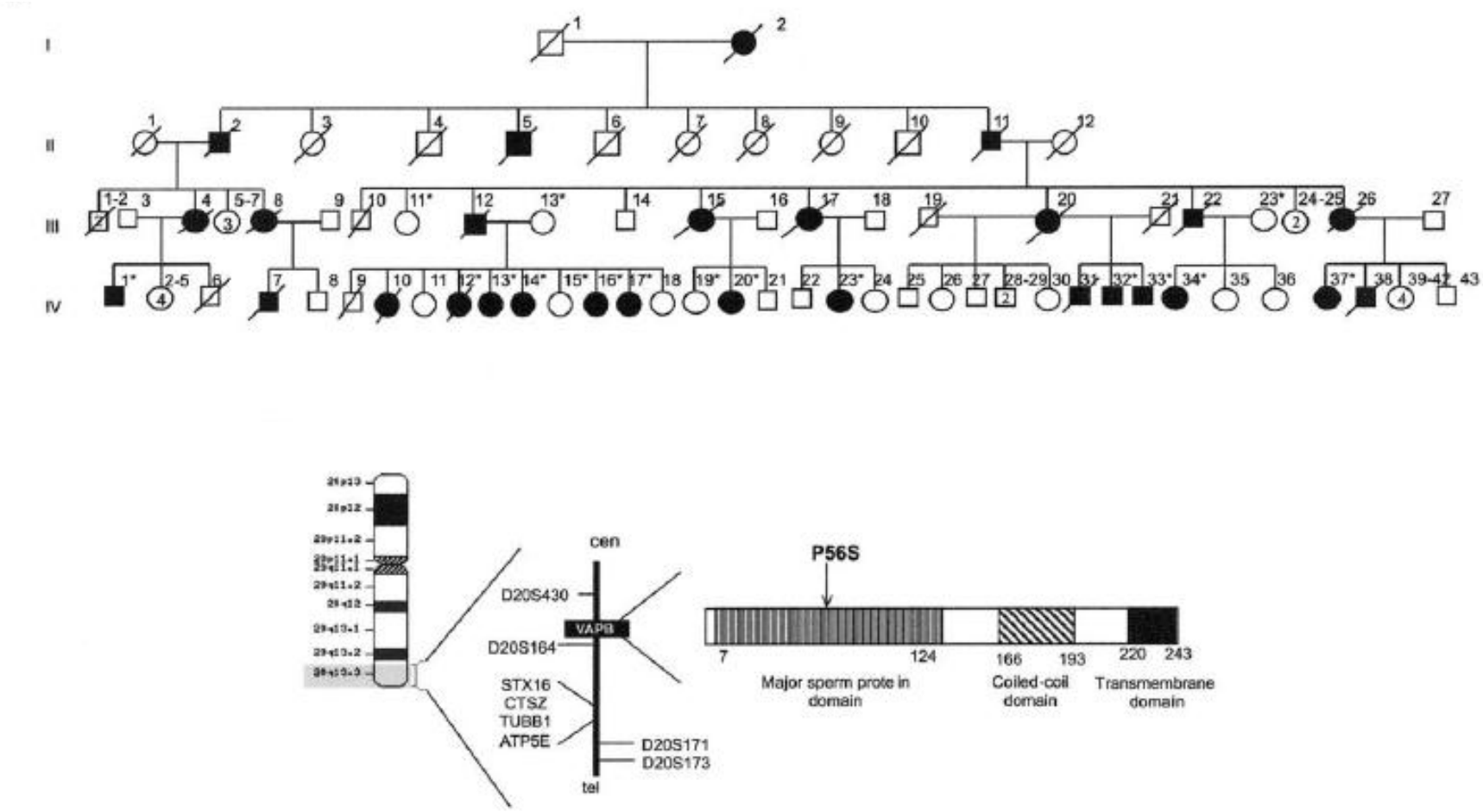
cen
D20S430
VAPB
D20S164
STX16
CTSZ
TUBB1
ATP5E
D20S171
D20S173
tel
P56S
7
124
166
193
220
243
Major sperm prote in domain
Coiled-coil domain
Transmembrane domain

Figure 1.5 ***Mapping of the VAPB locus and mutation analyses (taken from (Nishimura et al., 2004).***

Pedigree from the first family reported with a diagnosis of ALS/MND (an asterisk [*] indicates DNA was available). VAPB locus at 20q13.3 is shown. The mutation with homologous recombination reduces the region to 1.5 Mb, between marker D20S430 and the TUBB1 gene.

1.2.3 Cell biology of ALS associated P56S

Since 2004 when the P56S ALS8 associated mutation was identified in the large Brazilian pedigree, several groups have offered models on how the mutant behaves aberrantly and might lead to motor neuron degeneration. The theoretical prediction for changing a Proline to a Serine at P56S was that the 2 β-sheets of the Ig-like fold of the MSP domain would no longer be held together in their original conformation and either the structure would collapse leading to a non-functional MSP domain for the protein or the fold would change and therefore the domain might participate in a different subset of interactions-functions than the wild-type. Therefore, the mutant $VAPB^{P56S}$ would either be loss or gain of function mutation.

Protein Aggregates

The first observation in Nishimura et al., 2004 was that when the P56S mutant was expressed in mammalian cells and primary hippocampal rat neurons (as a GFP or myc fusion protein), it would form cytoplasmic aggregates (Figure 1.6). Protein aggregates are a common theme in many neurodegenerative diseases like Parkinson's, Alzheimer's, Huntington's and prion diseases; misfolded proteins aggregate and can lead to cell death (Gorman, 2008). This process does not necessarily happen immediately and aggregates can remain within cells for many years before starting to induce cell death. More groups have validated this result and additionally shown that these aggregates are tubular and immobile (Teuling et al., 2007), increase the insolubility of the protein (Kanekura et al., 2006) and are not localised in the ER. Moreover, Teuling et al, 2007 have shown that $VAPB^{P56S}$ cannot interact with the FFAT motif via its MSP domain which suggests that the mutation potentially leads to loss of the FFAT binding capacity of VAPB. However, a recent study by Prosser et al., 2008 has shown that overexression of FFAT can dissolve the P56S aggregates.

Trafficking

As previously mentioned in 1.1.4 overexpression of VAPA blocks ER to Golgi transport of membrane proteins; VAPB does not. $VAPB^{P56S}$ overexpression

Figure 1.6

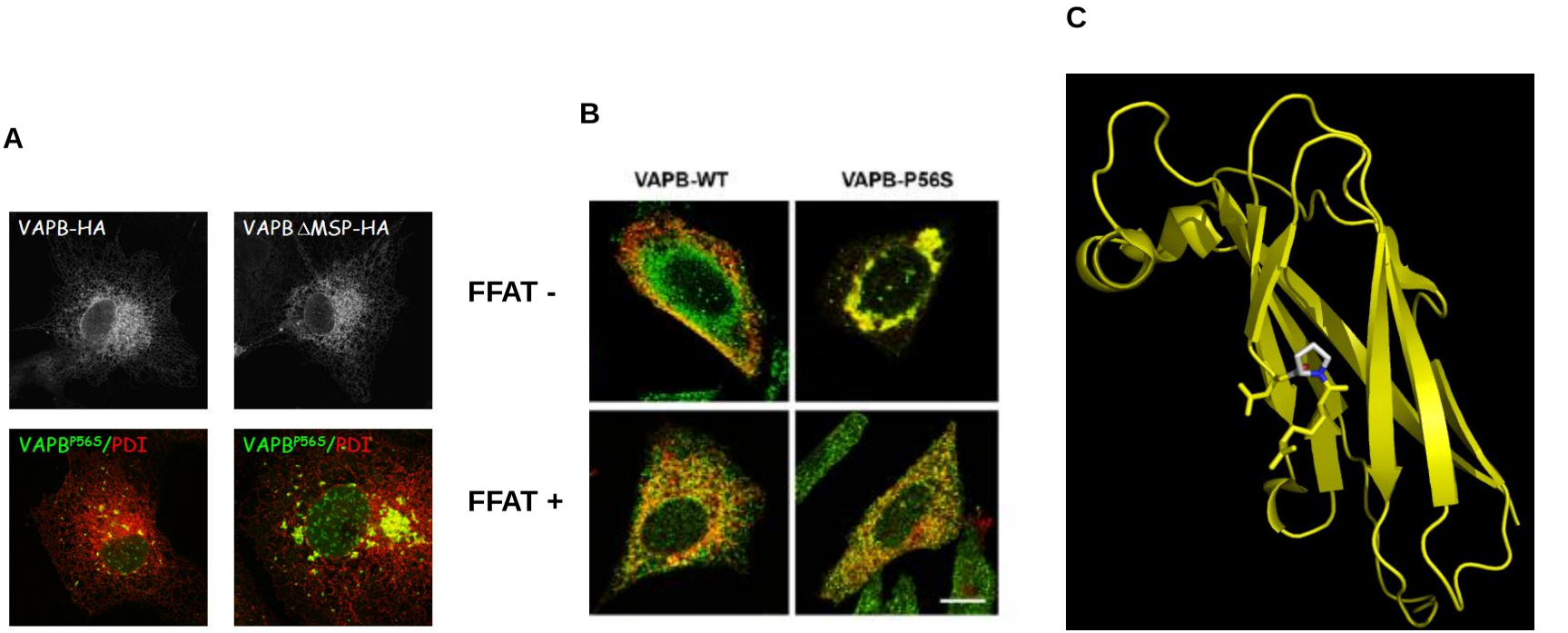
A
VAPB-HA
VAPB ΔMSP-HA
VAPB^P56S/PDI
VAPB^P56S/PDI
B
VAPB-WT
VAPB-P56S
FFAT -
FFAT +
C

Figure 1.6 ***The ALS8 associated mutant P56S of VAPB forms aggregates.***

A. (Skehel unpublished and (Nishimura et al., 2004)) $VAPB^{P56S}$ forms aggregates – PDI is an ER protein.

B. (From Prosser et al., 2008) FFAT rescues formation of P56S aggregates.

C. The P56S substitution in the VAPB MSP domain (here depicted rat 1z9L VAPA MSP domain) takes place in a pivotal position for the Ig-like fold of the MSP domain (image was made using the open-source visualization tool PyMol).

blocks trafficking by trapping the VSVG marker in the aggregates. FFAT application rescues this inhibition, restoring trafficking of proteins from the ER to Golgi (Prosser et al., 2008). However in this case they do not observe rescue of a "lost" function, as overexpression of VAPB had no effect on trafficking; it seems like the P56S mutant gains a novel negative function (inhibition) which is then relieved by application of FFAT.

UPR

Yeast, HCV and in mammalian cells studies have highlighted the role of VAP proteins in the Unfolded Protein Response (see 1.1.4).Although, most studies focus on the wild-type protein, only two of them propose a model for the P56S mutation. Kanekura et al., 2006 have shown that the P56S mutant cannot activate the Unfolded Protein Response through splicing of the UPR associated transcription factor XBP1. Therefore this study suggests that the P56S mutation is a loss of function mutation. Tsuda et al., 2008 have shown that overexpression of the mutant P56S of the drosophila homologue of VAP activates the UPR via the chaperone Hsc3 more than the wild-type protein. Thus, the effect of the P56S mutation on the UPR of a cell has not been extensively studied.

1.2.3 New VAPB mutations and ALS

In 2008, two new mutations of VAPB were described in ALS patients (Landers et al., 2008).:

- *D130E* (aspartic acid to glutamic acid at position 130). A missense T→G substitution was observed within exon 4 in 2 individuals. However, previously a study in southern Italy found the same ratio of the D130E substitution between ALS patients and healthy individuals suggesting that it might not be a causative gene of ALS (Conforti et al., 2006).

and

- *del160* (deletion of amino acid at position 160, which is a serine). A three base pair deletion of CTT at nucleotide 478 within exon 5 of the vapB gene (Figure 1.7). One individual of a family was identified as having the mutation.

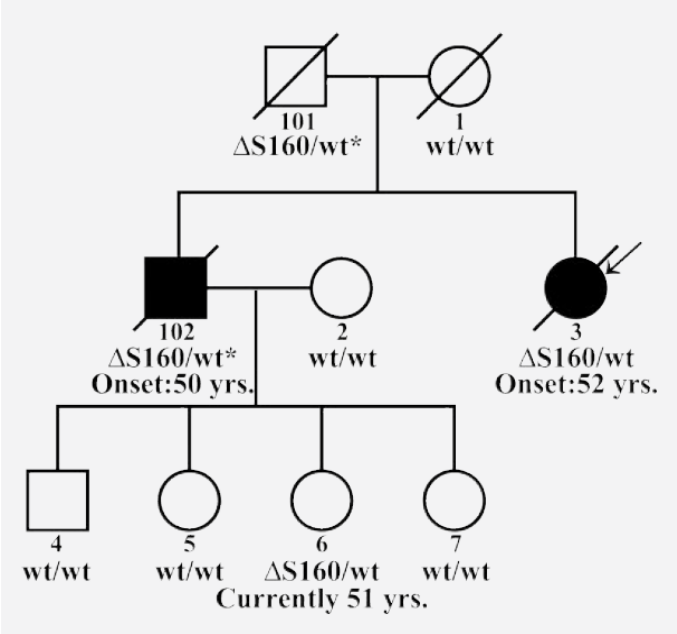

Figure 1.7 ***The del160 mutation in family F089 (from (Landers et al., 2008)).***

The asterisk denotes individuals whose DNA was not available for sequencing. The arrow indicates the individual that the mutation was first discovered. Disease onset is at about 50 years of age, while a 51 year old individual (6) is still asymptomatic.

Amino acids at positions 130 and 160 of VAPB are not conserved amongst different organisms. Both D130E and del160 mutants do not form cytoplasmic aggregates like the P56S mutant, which suggests that if they are causative genes for ALS8, they might act via a different mechanism or pathway than P56S.

1.3 The Endoplasmic Reticulum

1.3.1 A dynamic organelle (Borgese et al., 2006, Voeltz et al., 2002)

The Endoplasmic reticulum is a membranous organelle with diverse functions including the *translocation* of proteins (such as secretory proteins) across the ER membrane; the *integration* of proteins into the membrane; the *folding* and *modification* of proteins in the ER lumen; the *synthesis of phospholipids and steroids* on the cytosolic side of the ER; and the *storage of calcium ions* in the lumen and

their regulated release into the cytosol. The large amounts of membrane belonging to the ER are organized by folding into tubular and lamellar structures. The ER membranes vary not only between different cells but even within the same cell and form subdomains which serve the diverse functions of this organelle; therefore, although the ER is a continuous membrane formation, it is divided into various structural and functional subdomains (Voeltz et al., 2002).

The ER can be divided into two major parts: the nuclear ER (nuclear envelope-NE) and the peripheral ER (PE). The NE connects with the nucleus at the nuclear pores and a network of lamins underlies the entire ER-nuclear membrane complex. Continuous with the NE, the PE takes up 10% of the whole cell volume. The next division of the ER membranes is between the Rough ER (RER- enriched in ribosomes) and the Smooth ER (SER-smooth area) (see Figure 1.8).In different cell types, according to their function, there is a different relative distribution of RER and SER (Voeltz et al., 2002).

ER membranes are in contact with various other membranous organelles (plasma membrane, Golgi, vacuoles, mitochondria, peroxisomes, late endosomes and lysosomes) and at these junctions specialized ER microdomains are formed. Moreover, ER membranes are connected to the actin cytoskeleton and microtubules; elongation and retraction of ER tubules contribute to ER membrane rearrangement and maintenance of its shape and form. During cell division the ER maintains its structure and divides between cells with cytokinisis. In skeletal muscle, the ER is termed Sarcoplasmic reticulum (SR)(Rossi and Dirksen, 2006) and participates in calcium homeostasis which is essential for muscle cell function. Several calcium associated proteins (sarco(endo)plasmic reticulum Ca2+ -ATPase (SERCA) for Ca^{2+} exchange, calsequestrin for calcium binding), including ryanodine receptors (RyRs), which are ER calcium release channels are associated with SR subdomains.

1.3.2 ER in neurons

In neurons the ER is not limited in the soma, but also exists in the distal dendrites, where it has the capacity for local protein synthesis (Ju et al., 2004). The main type of ER in neurons is the SER. In axons, the ER is mostly tubular. From

Figure 1.8

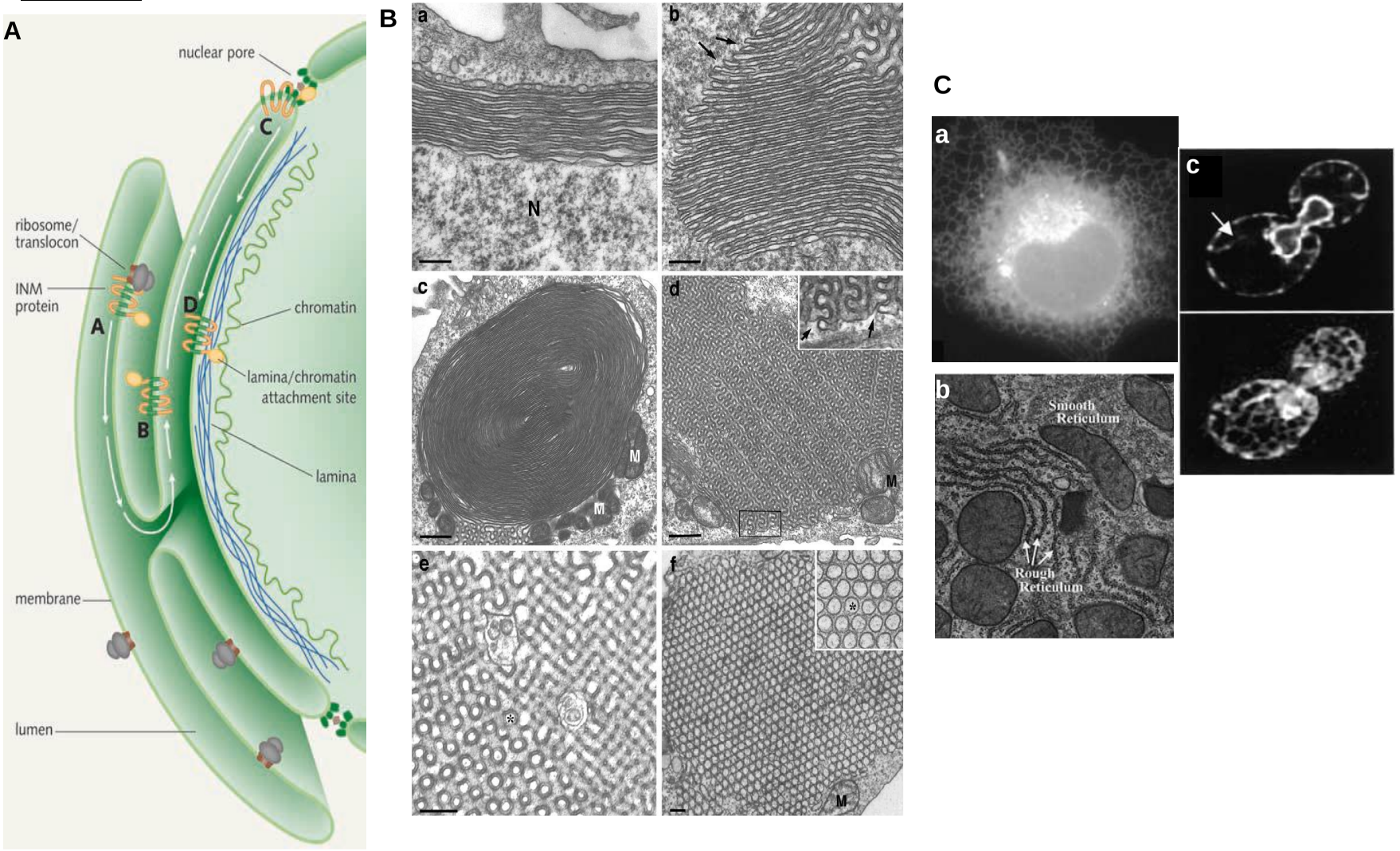
A
nuclear pore
C
ribosome/
translocon
INM
protein
A
D
chromatin
lamina/chromatin
attachment site
B
lamina
membrane
lumen
B
a
N
b
c
M
M
d
M
e
*
f
*
M
C
a
b
Smooth
Reticulum
Rough
Reticulum
c

Figure 1.8 ***The Endoplasmic reticulum architecture.***

A. (from (Voeltz et al., 2002))The Nuclear Envelope (NE). Targeting and retention of an inner nuclear membrane protein (ER membranes→ peripheral ER→ nuclear pore membrane→ inner nuclear membrane→ binding to nuclear lamina and chromatin).

B. (from (Borgese et al., 2006)) The different membrane organisations of the Endoplasmic Reticulum **(a)** a karmella, **(b)** a lamella, **(c)** a whorl, **(d,e)** sinusoidal arrays with cubic symmetry, and **(f)** a bundle of packed tubules with hexagonal symmetry. (N: nucleus, M: mitochondria)

C. (from (Voeltz et al., 2002)) Ultrastructure of the RER, SER and NE. (**a)** a GFP ER fusion protein is COS cells displaying a characteristic ER reticular pattern, **(b)** Electron micrograph of RER and SER in a liver cell, **(c)** connection between NE and peripheral ER in yeast dividing cells.

there it extends to the presynaptic terminal where it might enwrap mitochondria. In dendrites the ER terminates in the spines and effectively connects them with the ER lumen.

Regulation of Ca^{2+} in neurons by the ER is associated with synaptic plasticity and rapid response to signalling events coupled with protein synthesis or modifications or long term changes to synapses (Figure 1.9). Calcium is released from the ER and participates in activation of Ca^{2+} dependent pathways via calcium binding proteins or calcium membrane channels. Luminal calcium creates the driving force for the calcium wave that favours exit from the ER to the cytosol. Regulation of calcium release also receives a positive auto-feedback from cytosolic calcium accumulation.

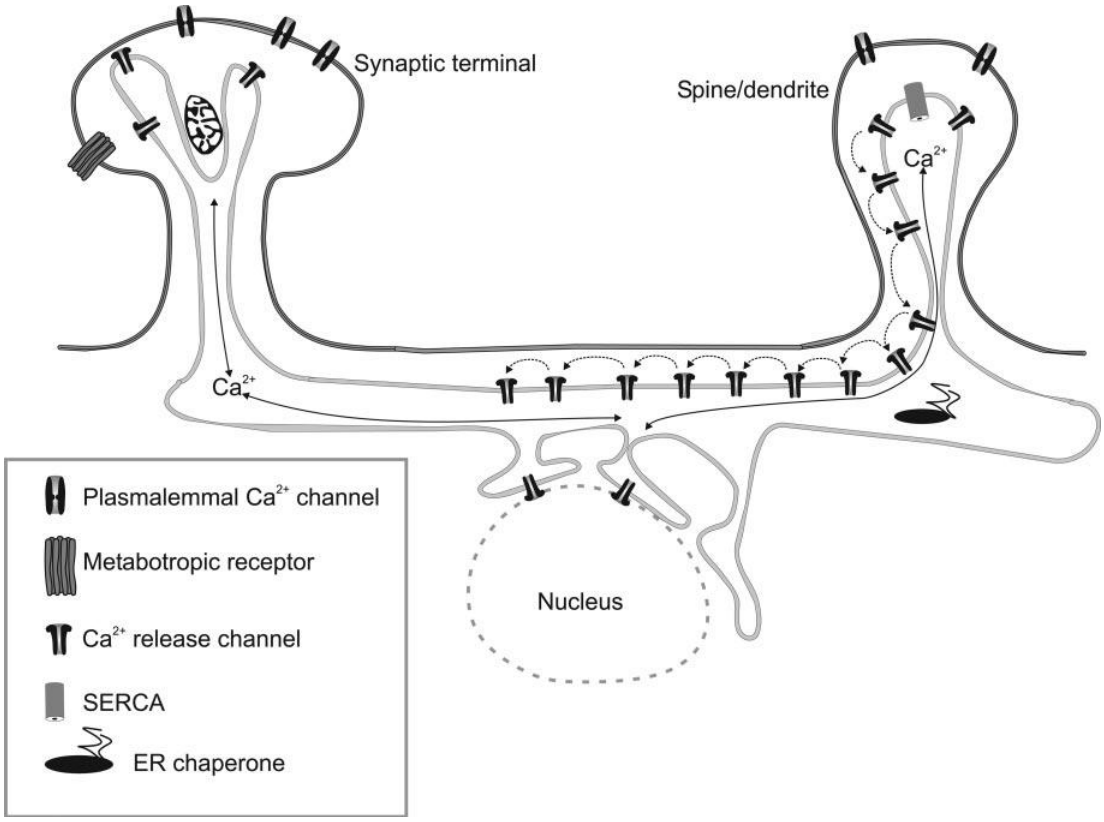

Figure 1.9 ***ER calcium signalling and neuronal integration (from (Verkhratsky, 2005).***

Regulation of calcium diffusion from the ER can modulate the propagating Ca^{2+} wave that can participate in rapid or long lasting (via the nucleus) responses.

1.3.3 The unfolded protein response (Back et al., 2005, Schroder and Kaufman, 2005).

When the influx of unfolded proteins in the ER lumen exceeds the folding capacity of the ER machinery (folding chaperones, or trafficking molecules) then the cell steps into a state of stress termed Unfolded Protein Response (UPR). This coordinated response starting from the ER involves activation of a complex gene cascade transferring the stress signal via second messengers to the nucleus. The purpose of this activation of the ER stress associated genes is to return the cell to its normal physiological state; this is done by halting protein translation and facilitating protein folding by producing more folding chaperones, or by sequestering unfolded products to the cytosol via a mechanism termed ERAD (Endoplasmic Reticulum Associated Degradation- unfolded proteins are selectively recognised and transported to the cytosol where they are degraded by the proteasome). If the insult caused by unfolded proteins persists and the cell cannot recover, programmed cell death may be initiated.

In yeast the only protein-sensor for induction of the UPR is Ire1p, a transmembrane ER protein that has a luminal dimerization domain and a cytosolic domain with serine/threonine kinase and RNAse activities. Ire1p is activated via dimerization and subsequent autophosphorylation. The activated Ire1p recognises an intron in HAC1 mRNA and cleaves it, producing a spliced form of HAC1 which yields an active transcription factor that binds to UPR responsive elements (UPRE) of UPPR associated genes in the nucleus.

In mammalian cells, the three major transducers of the UPR are inositol-requiring 1(*IRE1*), PKR-like endoplasmic reticulum kinase (*PERK*), and activating transcription factor 6 (*ATF6*), which sense the presence of unfolded proteins in the ER lumen; all three aforementioned proteins are transmembrane proteins with a cytosolic and a luminal part (Figure 1.10). All three UPR transducers luminal domains associate with *BiP* in their inactive state. BiP/GRP78 (immunoglobulin heavy chain-binding protein/glucose-regulated protein of molecular weight 78 kDa) is a member of the Hsp70 heat-shock protein family and a highly expressed ER resident chaperone. BiP binds via its C-terminal domain to premature proteins with a

Figure 1.10

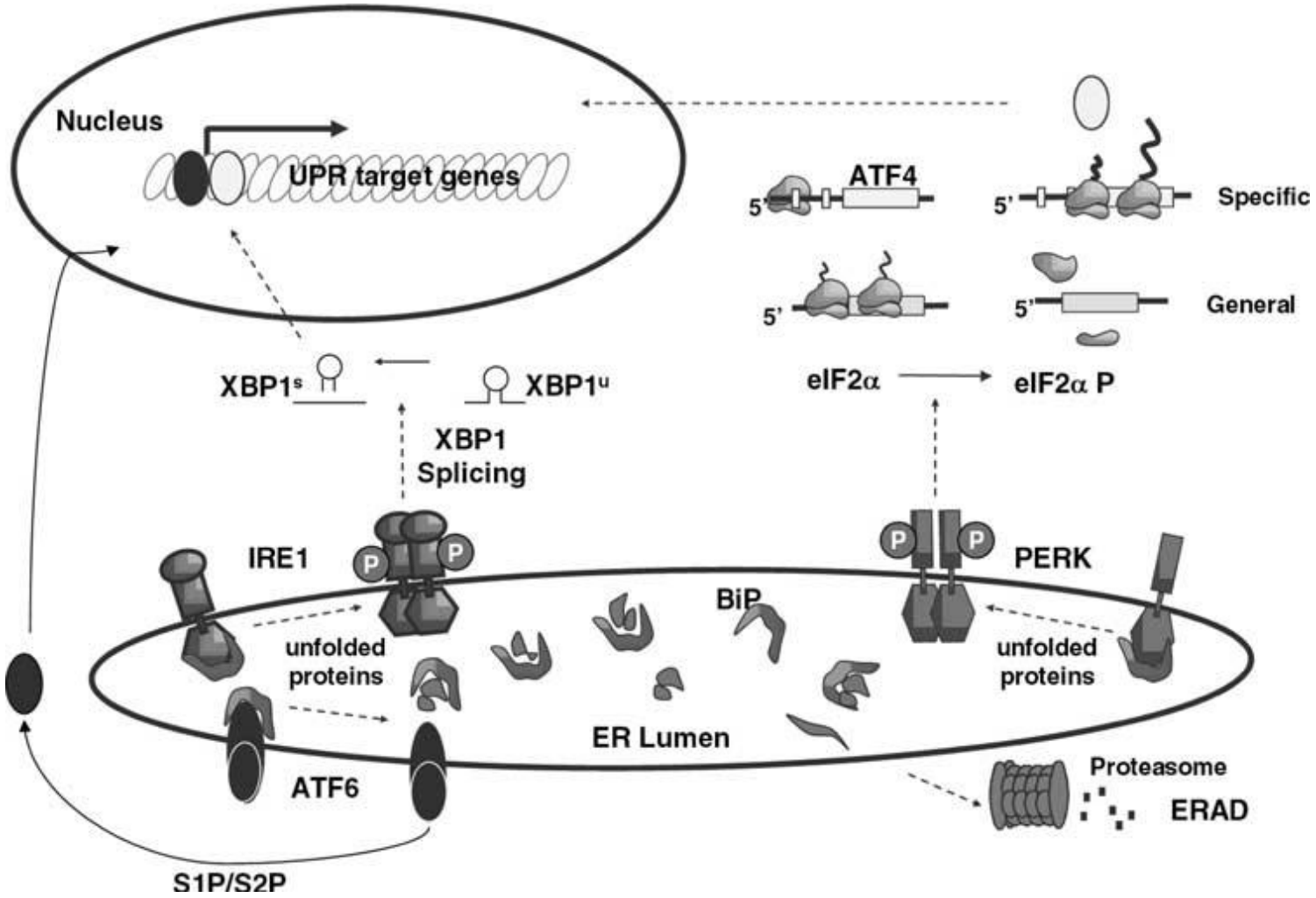
Nucleus
UPR target genes
ATF4
5'
5'
Specific
5'
5'
General
XBP1s
XBP1u
XBP1
Splicing
eIF2α
eIF2α P
IRE1
P
P
PERK
P
P
BiP
unfolded
proteins
unfolded
proteins
ER Lumen
ATF6
Proteasome
ERAD
S1P/S2P

Figure 1.10 ***The mammalian Unfolded Protein Response (from(Wu and Kaufman, 2006)).***

The mammalian UPR has three pathways coupling events in the ER lumen to regulating gene transcription in the nucleus; the IRE1, PERK, and ATF6 pathways (also see text).

preference for hydrophobic areas, while its N-terminal domain regulates dissociation via ATP hydrolysis. Upon accumulation of unfolded/misfolded proteins in the ER lumen, BiP is dissociated from all three sensors. ATF6 is shuttled to the Golgi where it is cleaved by S1P/S2P proteases and the cytosolic fragment of ATF6 migrates to the nucleus. IRE1 and PERK are oligomerized and autophosphorylated. Activated IRE1 mediates splicing of *XBP1* mRNA, which generates the active form of the XBP1 transcription factor. Phosphorylated PERK phosphorylates eIF2a, which attenuates translation and allows translation of selective mRNAs with inhibitory uORFs in their 5' UTR (i.e. ATF4). These three distinct pathways finally signal to the nucleus and induce UPR associated gene transcription acting on ERSE (Endoplasmic Reticulum Stress Response Elements) promoter elements (ATF6 nuclear fragment, spliced XBP1 and ATF4 act together on promoter elements). BiP/GRP78, GRP94, calreticulin, calnexin protein disulfide isomerases PDI, ERP57, and ERP72 are some of the activated genes. This increases ER protein folding capacity and accelerates ERAD (Endoplasmic Reticulum Associated Degradation). Finally, all three pathways are simultaneously activated; however the PERK pathway is identified as the immediate response to ER stress, while the other two pathways act subsequently.

When the ER folding capacity is restored, a negative feedback loop is activated to reinstate the basal equilibrium of transcription factors and chaperones. Initially, PERK and/or eIF2a are dephosphorylated. This effect is mediated via p-eIF2a phosphatase, CreP (constitutive repressor of eIF2a phosphorylation), and a stress-induced regulator of p-eIF2a phosphatase, GADD34 (growth arrest and DNA damage-inducible gene 34). Subsequently, the level of BiP and prevents further activation of ATF6, IRE1 and PERK by binding to their luminal domains. Little is known about inactivation of ATF6 and XBP1; it has been suggested that endogenous levels of ATF6 and XBP1 autoregulate their inactivation via negative feedback.

Finally, a microarray study in the nematode *C.elegans* (containing all 3 transducers) identified during normal development inducible UPR (i-UPR) and constitutive (c-UPR) genes that require the three transducers of UPR (termed ire1, pek1 and atf6 in *C.elegans*)(Shen et al., 2005).Although xbp1 is downstream of ire-1 and they work synergistically in regulating most i-UPR genes identified, they do not overlap in the c-UPR genes regulated, thus suggesting they might act via different

pathways. On the other hand, atf6 regulates c-UPR genes rather than i-UPR genes, suggesting it is important during development and homeostasis.

1.3.4 ER stress and disease

Apoptotic death following ER stress

If the activation of UPR associated genes and ERAD fail to restore a cells luminal balance of unfolded proteins, mitochondrial-dependent and independent cell death pathways are activated and mediate apoptotic (programmed cell death) (Wu and Kaufman, 2006). The main genes/pathways involved are:

- Bak/Bax-regulated $Ca2^{+}$ release from the ER
- procaspase-12 cleavage and activation
  and
- IRE1-mediated activation of ASK1 (apoptosis signal-regulating kinase 1)/JNK (c-Jun amino terminal kinase) (Figure 1.11)

In response to Ca^{2+} entry via Bak and Bax, m-Calpain cleaves procaspase-12, which in turn activates the entire caspase cascade via pro-caspase-9. Released calcium activates the mitochondrial apoptotic branch by releasing cytochrome c release and thus activating apoptosis via procaspase-9 and Apaf-1(apoptosis protease-activating factor 1) (Wu and Kaufman, 2006, Nicotera et al., 1999).

Apart from this well characterised pathway, individual UPR transducers signal to the apoptotic pathway. Ire1 via its interaction withTRAF2 (TNF receptor-associated factor-2) and ASK1 can lead to cell death. ATF6 and PERK/eIF2a/ATF4 regulate transcription of CHOP (CEBP homologous protein), which in turn inhibits expression of Bcl-2 and thus induces apoptosis (Wu and Kaufman, 2006).

Neurodegeneration

Apoptosis has been associated with many neurodegenerative diseases like Alzheimer's, Parkinson's, Huntington's diseases and stroke (Chan and Mattson, 1999, Nicotera et al., 1999).

Figure 1.11

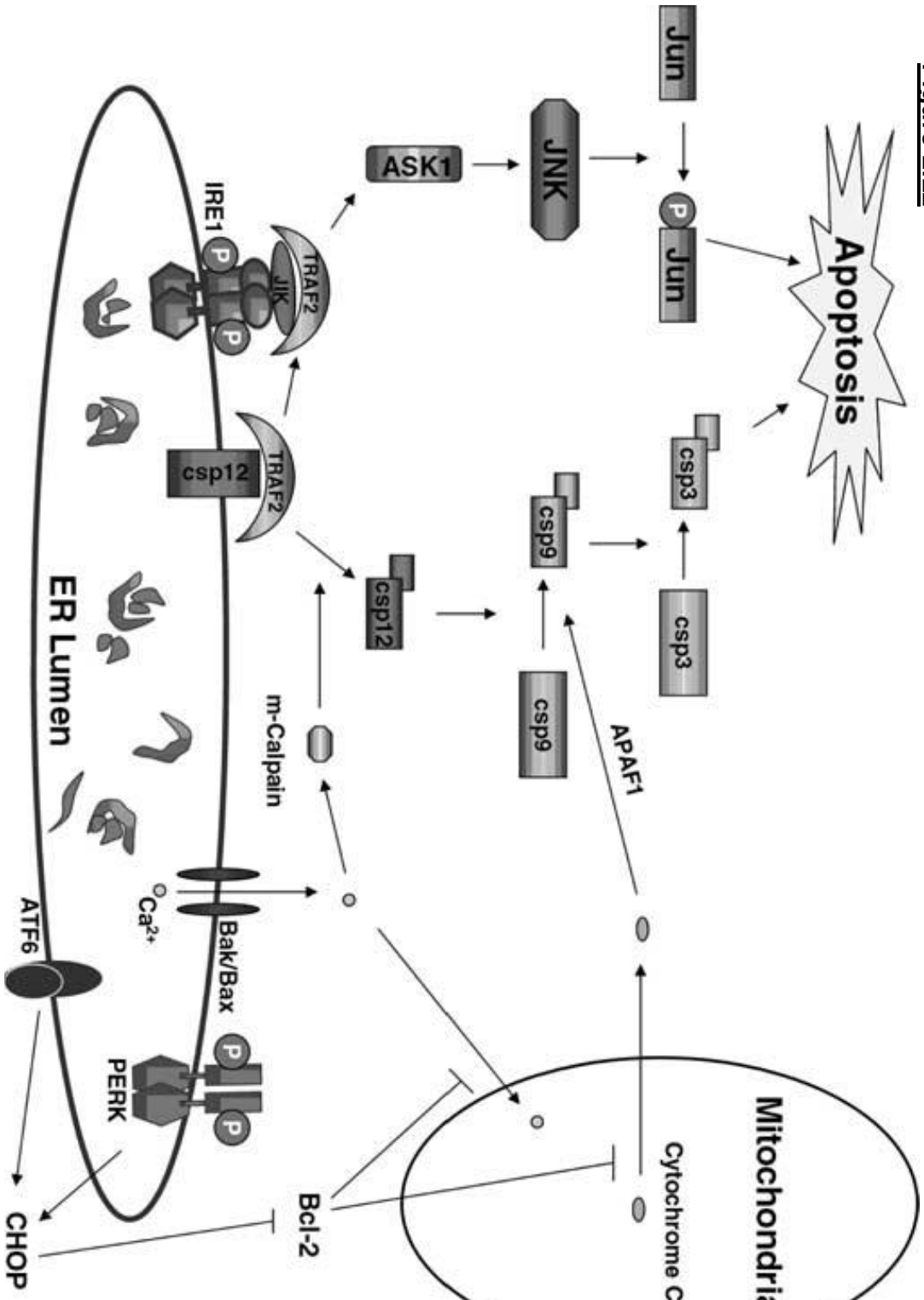
Apoptosis
Jun
P Jun
JNK
ASK1
IRE1
P
P
TRAF2
JIK
csp12
TRAF2
ER Lumen
csp12
csp9
csp3
csp3
csp9
APAF1
m-Calpain
Mitochondria
Cytochrome C
Bcl-2
Bak/Bax
P
P
PERK
ATF6
CHOP
Ca^{2+}

Figure 1.11 ***The mammalian UPR and programmed cell death (from(Wu and Kaufman, 2006))*****.**

See text 1.3.4.

The ER contributes to neuronal excitotoxicity by releasing Ca^{2+}. Excitotoxicity is a mechanism of neuronal death through overactivation of glutamate receptors, especially under metabolic and oxidative stress, resulting in cellular Ca^{2+} overload (Mody and MacDonald, 1995). Treatment of neurons with agents that reduce or block ER-mediated Ca^{2+} release protects against excitotoxicity. The same has been shown in models of cerebral ischaemia and epilepsy (Frandsen and Schousboe, 1991, Pelletier et al., 1999, Wei et al., 1998). BiP/GRP78 can suppress elevations of intracellular Ca^{2+} following exposure of neurons to glutamate; this results from reduced Ca^{2+} release from ryanodine associated calcium stores (Yu et al., 1999).

Abnormalities of ER-mediated Ca^{2+} signalling have been linked to the pathogenesis of Alzheimer's. Alzheimer's is a neurodegenerative disease that manifests through memory loss, cognitive decline, gradual loss of bodily function and ultimately death; in Alzheimer's extracellular plaques of β-amyloid are deposited and believed to be neurotoxic. Numerous mutations in presenilin 1, a transmembrane ER protein lead to early-onset inherited Alzheimer's; overexpression of presenilin 1 alters proteolysis of the β-amyloid precursor protein, which results in increased production of the neurotoxic β-amyloid peptide. Presenilin 1 interacts with RyR or RyR-associated proteins and increases channel activity of the RyR receptor (Hayrapetyan et al., 2008). Another ER amyloid-binding protein (ERAB-endoplasmic reticulum β-amyloid-peptide-binding protein) was found to be increased in neurons in the brains of individuals with Alzheimer's disease, and it was suggested that binding of β-amyloid to ERAB might be important for the cytotoxicity of the amyloid peptide (Oppermann et al., 1999).

Huntington disease is an autosomal dominant polyglutamine disorder that leads to selective loss of striatal neurons. Affected individuals exhibit involuntary, jerky movements and alterations in memory and mood. It is caused by expansion of [CAG]n repeats in the huntingtin gene. In response to ER stress, huntingtin releases from membranes and translocates into the nucleus; subsequently huntingtin can be released and re-associated with membrane; albeit mutant huntingtin does not translocate (Atwal and Truant, 2008). Mutant huntingtin also elevates BiP and CHOP levels and phosphorylation of c-Jun-N-terminal kinase (JNK) (Reijonen et al., 2008).

A common observation in Parkinson's disease (PD) is the deposition of intracytoplasmic inclusion bodies (Lewy bodies) in neurons. Affected individuals display tremor, muscle rigidity and postural instability; a common pathological finding in PD is degeneration of dopaminergic neurons in the substantia nigra. In a cellular model of PD, when 6-hydroxydopamine is added numerous UPR genes are upregulated (Ryu et al., 2002); 6-hydroxydopamine, causes a type of neurodegeneration similar to that observed in PD (Ungerstedt et al., 1974).

In conclusion, the Endoplasmic Reticulum stress response to unfolded proteins is associated with programmed cell death and upregulation of many components of the UPR are observed in a wide spectrum of neurodegenerative diseases.

1.4 Thesis Aim

VAP proteins are ER integral membrane proteins, enriched on the ER surface. Until now several functions have been ascribed to them including membrane trafficking, targeting of proteins, vesicle fusion, lipid metabolism and they interact with a broad spectrum of proteins. There is increasing literature linking VAP proteins with the Unfolded Protein Response. On the other hand, misregulation of the unfolded protein response has been implicated in neurodegenerative diseases. In this thesis we investigate the regulation of the UPR by VAP proteins and study the ALS8 associated P56S mutant in this context.

In detail:

- We investigate the interactions of VAPB with UPR components and look for specific effects on transcriptional activation of the UPR.
- We examine the neuron specificity of VAPB
- We investigate the effect of perturbation of VAPB levels in cell viability
- We perform a large scale bioinformatics screen for predicting novel protein interactors for VAPB
- We compare wild-type VAPB to the ALS8 associated $VAPB^{P56S}$ mutant

Chapter 2

Materials and Methods

2.1 Fluorescent Protein Fragment Complementation Assay (FPCA), adapted from (Remy and Michnick, 2007)

FPCA is a technique for detecting protein-protein interactions in cells. Full length CDS of *mus musculus VAPA* (NM013933) *VAPB* (NM_019806), *VAPA*^{P56S}, *VAPB*^{P56S} and human *ATF6α* (NM_007348) were amplified using standard PCR from pEGFP-C1-VAPA, pEGFP-C1-VAPB, pEGFP-C1-VAPA^{P56S}, pEGFP-C1-VAPB^{P56S} and *pCMV-ATF6-3xFLAG7.1* respectively. All PCR products had either BspEI-XbaI or NotI-ClaI flanking restriction sites. Amplified products were cloned into pVenus1 BspEI-XbaI site and pVenus2 NotI-ClaI site; the Venus plasmids are based on the Invitrogen *p-CDNA3.1Zeo(+)* backbone; pVenus1 contains residues 1-157 of YFP (Yellow Fluorescence Protein, 1YFP-PDB entry) fused to a b-leucine zipper and pVenus2, residues 158-238 fused to a b-leucine zipper. Insertion of VAP proteins or ATF6α CDS replaces the leucine zippers which were cloned in the BspEI-XbaI or NotI-ClaI sites.

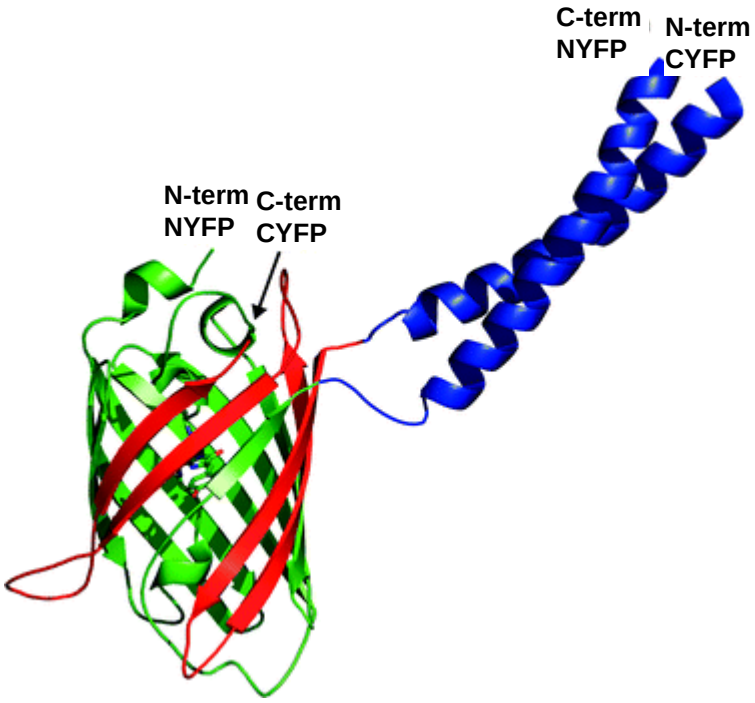

Figure 2.1 ***Schematic of split-YFP reassembly of fragments by b-leucine zippers.*** NYFP (residues 1–157) is green, CYFP (158–238) is green, and the b-leucine zippers are blue (Sarkar and Magliery, 2008)

HEK293 cells were plated and transfected at 40% confluency using INVITROGEN Lipofectamine2000 with 200 ng of each Venus plasmid; in total 400ng of plasmid DNA per transfection were used. Images of living cells were acquired 24 h after transfection on an Olympus IX70 fluorescence microscope using Openlab software (Improvision); images were prepared using ImageJ (Collins, 2007). Representative images are shown.

2.2 Dual Luciferase Transcription Assay (Promega Dual Glo™ Luciferase Assay System)

Transcriptional dual luciferase assays are widely used for transcription factors to monitor transcriptional activity from a given promoter by measuring luciferase bioluminescence. HEK293 or NSC-34 cells were plated and cultured to 40% confluency and transfected using Lipofectamine2000 (Invitrogen). Each transfection mixture contained 300 ng of *p5xATF6-GL3* (ATF6α reporter) or *pGL3-XBP1(-330)-luc*(XBP1 reporter) or *pGL3-GRP78*(-132)-luc (Bip reporter) and 100 ng of the internal control renilla luciferase reporter, *pTK-RL*. VAPB and $VAPB^{P56S}$ were expressed as EGFP-fusion proteins derived from pEGFP-C1 (Clontech), or as myc epitope tagged fusion proteins where the EGFP coding sequence was replaced with a myc epitope coding sequence. EGFP fusions of VAPB domains (MSP, MSP^{P56S} ΔH, ΔH^{P56S}, CC/CT, CT) were previously described (Middleton, 2005). The total amount of DNA per transfection when studying the endogenous response (of ATF6 or XBP1 or Bip) was 500 ng. ATF6 was over expressed as a FLAG-tagged fusion protein from pCMV-ATF6-3xFLAG7.1. When studying the expressed ATF6 effect 100 ng of each VAPB and ATF6 expression plasmid was used, with the total amount of DNA in each transfection made up to 600 ng with the vector pEGFP-C3 (Clontech). Twenty-four hours after transfection ER stress was induced for 12 h with 2 µg/ml tunicamycin (Calbiochem). Cells were assayed for firefly and renilla luciferase activity using the Dual Glo™ Luciferase Assay System (Promega).

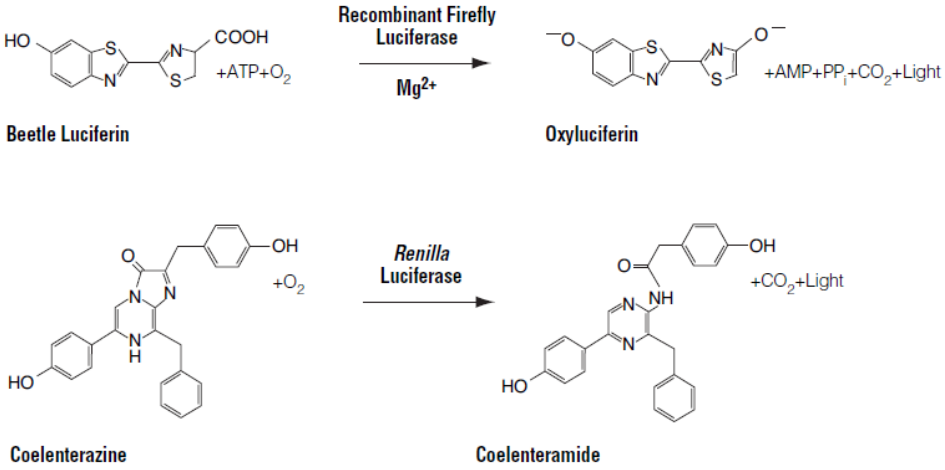

Figure 2.2 ***Bioluminescent reactions catalyzed by firefly and Renilla luciferases (image from Promega technical manual).***

Mono-oxygenation of beetle luciferin is catalyzed by *Firefly* luciferase in the presence of Mg^{2+}, ATP and O_2. Coelenterazine mono-oxygenation is catalyzed by *Renilla* luciferase and requires only O_2 (Alam and Cook, 1990).

Cells were lysed at room temperature using a proprietary lysis buffer by Promega included in the Firefly luciferase reagent. Both firefly and renilla luminescence were measured using a FLUOstar OPTIMA micro-plate reader (BMG LABTECH). Firefly luciferase luminescence was measured first and then the STOPnGLO™ reagent was added; this reagent stops the first reaction and contains the renilla luciferase substrate for the second reaction; finally the renilla luminescence was measured. Firefly luciferase luminescence values are normalized to renilla firefly luminescence values and are averages of four experiments (n=4) with SE (standard error).

2.3 Cell Death Assays

2.3.1 Propidium Iodide Cell Viability Assay

NSC34 or HEK293 cells were plated and cultured to 40% confluency and then transfected using Lipofectamine2000 (Invitrogen). Each transfection mixture

contained 100 ng of the relative expression plasmid and control samples were pEGFP-C3 and pCDNA3.1Tubulin. Twenty-four hours after transfection ER stress was induced for 12 h with 2 μg/ml tunicamycin (Calbiochem). Cells were then washed with pre-warmed (37^{o}C) PBS and growth medium was replaced. After 12 hours 1X propidium iodide from a 50X stock solution of 250μl/ml of propidium iodide (Sigma) was added to the growth medium. The cells were incubated for 20 min at 37oC and then imaged on an Olympus IX70 fluorescence microscope using Openlab software (Improvision). Viable cells were detected on a fluorescent microscope as those, which excluded the propidium iodide; dead cells could be detected using the red 650 nm filter. Results are averages of 4 experiments with SE (standard error). Rescue of cell death by addition of caspase inhibitor results were evaluated using a one-way ANOVA.

2.3.2 Bioluminescent Cell Viability Assay (Promega CytoTox-Glo^{TM} Cytotoxicity Assay)

NSC34 cells were cultured to 40% confluency and then were transfected using Lipofectamine2000 (Invitrogen). Each transfection mixture contained 100 ng of the relative expression plasmid and control samples were pEGFP-C3 and pCDNA3.1Tubulin. The caspase inhibitor Z-VAD-FMK (R&D Systems), where applied, was 50 μM and added when transfection medium was changed. Twenty-four hours after transfection ER stress was induced for 12 h with 2 μg/ml tunicamycin (Calbiochem). Cells were then washed with pre-warmed (37^{o}C) 1X phosho-buffered saline (PBS) and growth medium was replaced. After 12 hours cells were assayed for bioluminescence using the CytoTox-Glo™ Cytotoxicity Assay (Promega).

The CytoTox-Glo™ Cytotoxicity Assay (Niles et al., 2007) luminescent assay allows measurement of the number of dead cells in cell populations by measuring the activity of a protease associated with cytotoxicity. Dead-cell protease activity is measured using a luminogenic peptide substrate (alanyl-alanylphenylalanyl-aminoluciferin; AAF-Glo™ Substrate) which has high affinity for the protease released from cells that have lost their membrane integrity; conversely the intact membrane of live cells cannot be crossed by the AAF-Glo™ Substrate and thus no

signal is produced.

The AAF-Glo™ Substrate was added to live cells and luminescence was measured using a FLUOstar OPTIMA micro-plate reader (BMG LABTECH); this value corresponds to dead cells. Lysis buffer containing digitonin was then added to the cells and luminescence was measured again; this value corresponds to the total number of dead cells. Cell death values are normalised to total cell death number and are averages of 4 experiments with SE (standard error). Rescue of cell death by addition of caspase inhibitor results were evaluated using a one-way ANOVA.

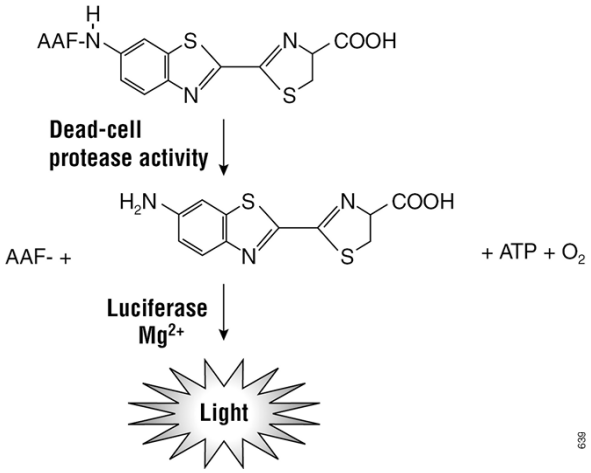

Figure 2.3 ***Bioluminescence assay based on dead-cell protease activity (image from Promega technical manual).***

Proprietary luminogenic AAF-Glo™ peptide substrate picks up released dead cell proteases and thus dead cells correspond to an increase in luminescence.

2.4 siRNA knockdown of endogenous proteins – transcription assay

10^6 HEK293 cells were nucleofected with 20 pMoles of VAPB siRNA(Appendix I, #P22, #P23, 10 pMoles each, Qiagen) or a control GFP-siRNA (Dharmacon) using the Amaxa Biosystems nucleofector. Twenty-four hours after nucleofection, cells were transfected with p5xATF6-GL3 or pGL3-XBP1(-330)-luc or pGL3-GRP78(-132)-luc and pTK-RL as described above. After a further 24 h, cells were treated with 2 µg/ml Tunicamycin (Calbiochem) for 12 h and then assayed

for luciferase activity as above. Where specified, siRNA knockdown was performed using Lipofectamine2000 instead of nucleofection, using the same amount of siRNA.

2.5 Cell Lines and Primary Neuron Culture Experiments

2.5.1 HEK293, NSC34, C6 Culture

HEK293, NSC34 or C6 cells were maintained in DMEM (Gibco) supplemented with 10% FBS (Foetal Bovine Serum) and 1% penicillin/streptomycin (Invitrogen) at 37^{o}C in 5% CO_2 in a Galaxy R (Scientific Instruments Ltd) CO_2 incubator. Early passage cell stocks were maintained in liquid nitrogen storage and cells that were used in experiments were not passaged more than 20 times.

2.5.2 Dissection and preparation of rat E18 primary cortical cultures and glial cultures

Cortices from E18 Sprague-Dawley rat embryos were dissected and transferred intact to a 35mm dish containing 2ml of Hank's/Hepes Solution on ice. 200μl of Trypsin and 20μl of DNAse solution were then added and the dish was placed in a Galaxy R (Scientific Instruments Ltd) CO_2 incubator (37^{o}C in 5% CO_2) for 20 minutes. After 20 minutes growth medium was added to the dish to stop trypsinisation. The contents of the dish were then transferred to a tube and made up to 10 ml by adding growth medium. Cells were washed twice, each time allowing cortices to settle down. Cells were then centrifuged at 800rpm for 2min and the supernatant was removed. After adding 2ml of growth medium and 20μl of DNAse, cells were then triturated using a fire polished Pasteur pipette. Finally, cells were counted using a haemocytometer (100.000 to 800.000 cells per well) and plated in poly-D-lysine coated plates or glass coverslips. The next day plating medium was removed, cells were washed with 1X PBS and fresh growth medium was added (see Appendix II, Figure 5).

For glial cultures, dissociated cells were plated in DMEM (Gibco) supplemented with 10% FBS and 1% penicillin/streptomycin (Invitrogen). At DIV7

Figure 2.4

A

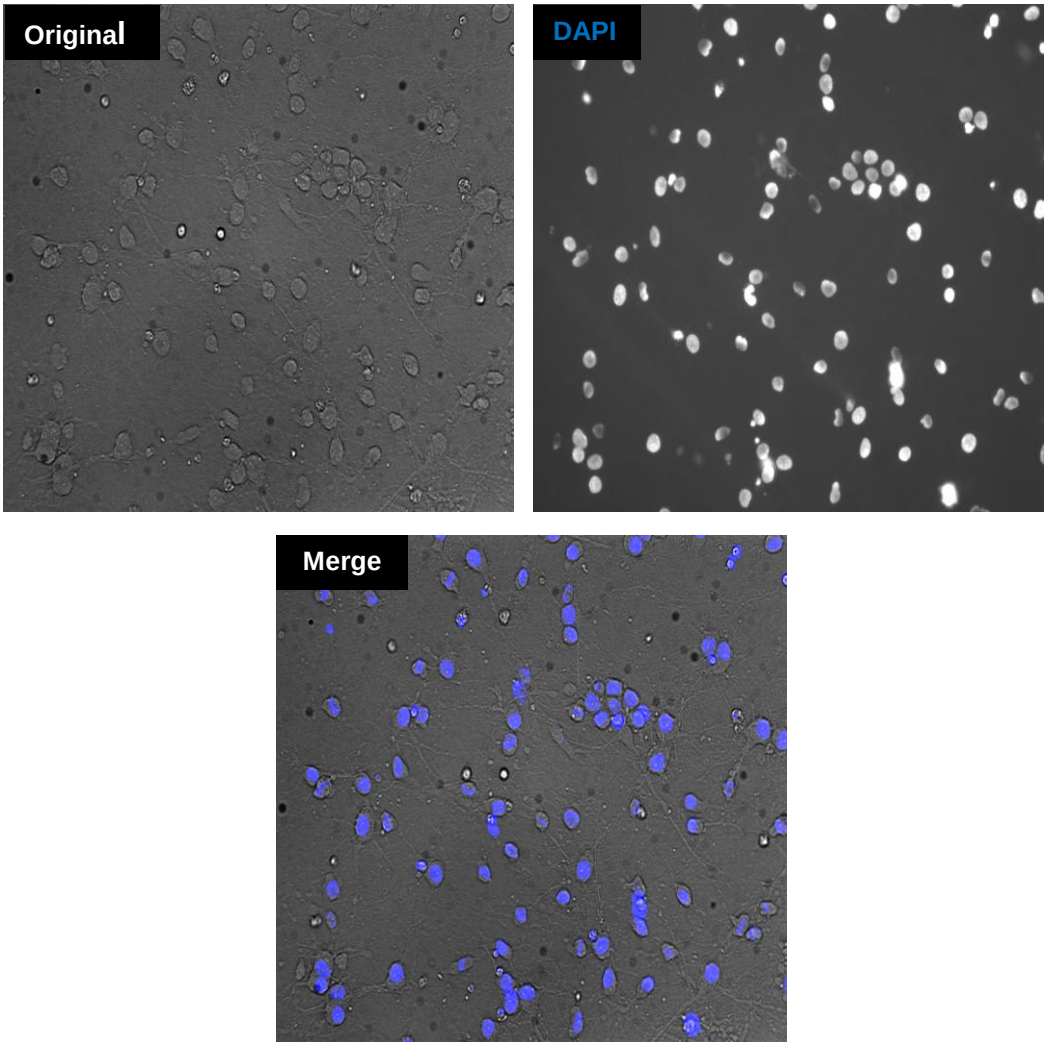

B

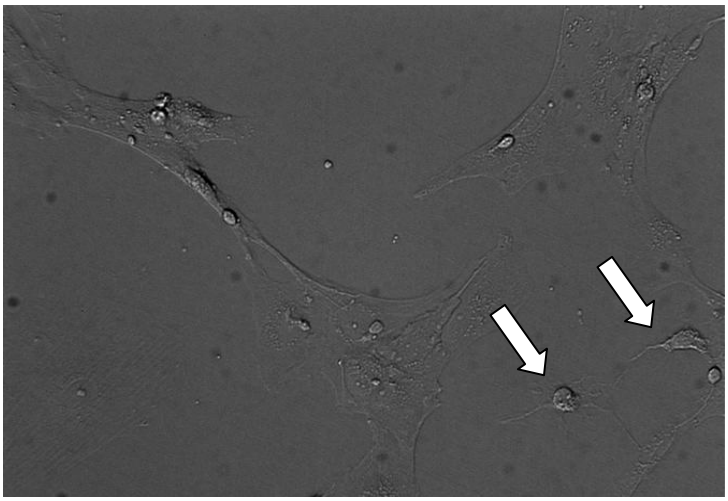

Figure 2.4 ***Dissociated primary cortical neuron and neuron-depleted glia cultures*****.**

A. Representative images from DIV2 dissociated primary cortical Sprague-Dawley rat embryos neuron cultures. Cells are stained with DAPI using VECTASHIELD DAPI containing mounting medium (VECTORLABS). DAPI is indicative of the viability of neurons in culture. Serum-free medium inhibits glial growth.

B. Representative images from dissociated DIV8 Sprague-Dawley cortical rat embryos neurons after 24 hours of treatment with NMDA (SIGMA) 1mM. Neurons are dying (indicated with white arrows), while glial cells are rapidly growing in the serum rich medium.

NMDA (SIGMA) 1mM was added for 24 hours to kill all neurons and then washed with pre-warmed 1X PBS and replaced with growth medium supplemented with 10% FBS. Cultures are washed several times in the following days and finally glia are trypsinised at DIV9 and replated.

- ***Growth medium*** for 500 ml- (500 ml *BME*(Basal Medium, GIBCO), 5 ml *Penicillin-Streptomycin*(invitrogen), 8 ml of a 32.5% *Glucose* solution (in water, sterile, SIGMA), 5 ml *Sodium Pyruvate* 100 mM (Invitrogen), 5 ml *N2 supplement*(GIBCO) and 10 ml *B27 supplement* (GIBCO)).
- ***Hanks/Hepes solution – HBSS*** (Hepes buffered Calcium and Magnesium free Earls BSS pH 7.3) 500ml + 1.19g *Hepes* (PH to 7.3 and Filtered).
- ***Trypsin solution*** -Dissolve 100 mg Trypsin (Worthington Biochemical) in 10 ml of Ca^{2+}/Mg^{2+} free PBS
- ***DNAse solution*** - 5mg DNAse (SIGMA) dissolved in 1ml of PBS.

2.5.3 Lipofectamine2000 Transfection Of Mammalian Cell Lines or Glial Cells

Cells were cultured to 40% confluency. Two hours prior to transfection, growth medium was replaced with antibiotic free medium (no penicillin/streptomycin). The DNA and lipofectamine complex was prepared in Opti-MEM® I Reduced Serum Medium (GIBCO) and added to cells. After 2 hours cells were washed in 1X PBS and the transfection complex was replaced with growth medium plus antibiotics.

2.5.4 Nucleofection Of Mammalian Cell Lines or Primary Cortical Neurons (Amaxa Cell line or Primary Neuron Nucleofector^{TM} Kit)

The required number of cells was cultured to 90% and harvested by trypsinisation. An aliquot of the trypsinised cells was taken and the cells were counted using a haemocytometer to determine cell density (for neurons cells were not trypsinised, but used immediately after dissection and dissociation). 10^6 cells per nucleofection sample were centrifuged at 800xg for 2 minutes. The supernatant was discarded and the pellet was resuspended in 100 µl of prewarmed at room

temperature Nucleofector solution V. The relative amount of DNA was added to each nucleofection reaction, gently mixed using the pippette tip and finally transferred to an electroporation cuvette, placed into the Nucleofector and electroporated using the appropriate program. Then 500µl of culture medium was added to the cuvette and cells were plated to the desired density in the appropriate culture vessels.

2.5.5 Cell Imaging and Immunofluorescence

Live cells were imaged in 6 or 12 well poly-L-Lysine coated plastic plates. An Olympus IX70 fluorescence microscope using Openlab software (Improvision); images were prepared using ImageJ.

For immunofluorescence cells cultured on poly-D-lysine coated cover slips were fixed in 3% paraformaldehyde, 0.03% glutaraldehyde (w/v) in PBS, at room temperature for 20 min. Fixative was quenched and cells permeablized with a solution of 50 mM NH_4Cl, 0.2% (w/v) Saponin (Sigma), for 15 min at room temperature. Cells were then washed once in *PGAS* (0.2% (w/v) fish skin gelatin (Sigma G-7765), 0.02% saponin, in PBS) and incubated in PGAS for 5 mins at room temperature. Antibodies were diluted in PGAS solution. Primary antibody was added to the coverslip which was incubated in a humidified chamber for 1 hour. The coverslip was then washed 3 times in PGAS and then the secondary antibody was added and incubated in a humidified chamber for 1 hour. Finally the coverslip was washed in PGAS and then was washed 3 times in PBS. Inverted cover slips were mounted in Mowoil, and examined on a Zeiss Imager Z1 microscope fitted with a LSM 510 Meta confocal excitation/acquisition system.

2.5.6 Subcellular Fractionation

Cells were then homogenised in ice-cold 20mM Hepes (pH7.4), 320mM sucrose plus COMPLETE protease inhibitors (Boeringer). The homogenate was centrifuged at 1500 rpm for 10 min at 4^{o}C in a benchtop cooled centrifuge. The supernatant was decanted into another tube leaving the P1 pellet. The supernatant or post nuclear fraction was centrifuged for a further 30 min at 20000 rpm to produce

the P2 and S2 layers. Samples were either frozen at -20 ^{o}C or immediately used.

2.6 Triton X114 (Bordier, 1981) Extraction

This method is a detergent (Triton X114) extraction of membrane proteins. The P2 layer was resuspended in resuspension buffer (10mM Hepes pH 8.0 with KOH, 400mM KCl, 1.0% Triton X114 (BDH)) and incubated for 10 min on ice (or until cleared). The resuspended P2 was layered on to 300µl of sucrose cushion (6% (w/v) Sucrose, 10 mM Hepes pH 8.0, 400 mM KCl, 0.06% Triton X114 (BDH)) and then incubated at 30^{o}C for 3 min. This was then centrifuged at 300g for 3 min. The upper aqueous layer was removed and kept. 150µl of 10% Triton X114 was centrifuged at 14000 rpm in a bench top centrifuge to remove the remaining detergent phase.

2.7 DNA Preparation, PCR, Cloning

2.7.1 Mini-Prep of Bacterial DNA (Qiagen)

A single bacterial colony was picked and incubated in 2ml Luria-Bertani (LB) medium at 37^{o}C in a rotary shaker-incubator for 16 hours. 1.5ml of the bacterial culture was pipetted into an eppendorf tube and centrifuged at 14K rpm in a tabletop microfuge. The supernatant was discarded and the pellet was resuspended in 250µl of buffer P1 containing RNase A to remove RNA contamination produced by bacterial lysis. The bacterial cells were then lysed in 250µl NaOH/SDS (buffer P2) for 5min. 350µl of buffer N3 were added to neutralize the reaction; buffer N3 replaces NaOH/SDS with KOH/SDS and bacterial chromosomal DNA and proteins precipitate out of solution, while plasmid DNA stays in solution. The suspension was then centrifuged at 14K rpm for 10 min. The supernatant was carefully pipetted to a Qiaprep column and passed through using a vacuum manifold. 0.5ml of buffer PB followed by 0.75ml of buffer PE were added to the column and washed through. The column was then centrifuged for 1min at 14K rpm to remove residual PE.

Finally, 50µl of buffer EB was added to the column. After incubation at room temperature for 1min, samples were centrifuged for 1min at 14K rpm to elute the DNA.

2.7.2 Transformation of Chemically Competent Bacteria

One 50 µl vial of TOP10 One Shot® cells (Invitrogen) or DH5α (NEB) for each transformation was thawed on ice. 1µl of DNA or ligation mix was added to the cells and after mixing gently using the pipette tip, the vial was incubated on ice for 30min. Bacteria were heat-shocked at 42^{o}C in a pre-heated water bath for 30s and placed immediately back on ice. After 2 minutes, 250µl of prewarmed SOC medium was added and cells were incubated at 37^{o}C for one hour in a rotary shaker-incubator. A fifth of the total volume was spread on the relative antibiotic selection LB agar plates.

2.7.3 Gel Electrophoresis of DNA

Gels were made from 0.8-1.0% agarose melted in 1x TAE buffer (40mM Tris-HCl, pH7.8; 20mM sodium acetate; 1mM EDTA, pH8.0) containing 0.5µg/ml ethidium bromide solution. The melted agarose was cast in a horizontal gel tray after cooling to 60°C with a suitably positioned comb to form slots in the gel. The gel, once solidified, was submerged in 1x TAE buffer. DNA solutions (0.1µg-10µg) were resuspended in loading buffer (0.25% w/v bromophenol blue; 100mM EDTA; 30% glycerol) and loaded into the wells of the gel. The samples were electrophoresed at 65V in parallel with double-stranded DNA size markers.DNA was visualised under an ultra violet light visualizer.

2.7.4 Gel Extraction of DNA (QIAGEN)

Bands were carefully excised from the agarose gel using a clean scalpel under a UV (long wave) light visualizer. Three volumes of buffer QXI were added to the weighed excised band. The Qiaex II was vortexed for 30s and then 10µl were added.

The mixture was then incubated at 50^{o}C for 10min and vortexed every 2min. The solution was then centrifuged at full speed in a tabletop microfuge for 30s and the supernatant discarded. The pellet was washed twice in 500µl of buffer QXI and then washed twice in 500µl of solution PE (70% ethanol). The pellet was air dried for 10-15min and then resuspended in 20µl of dH_2O.

2.7.5 Digestion of DNA with Restriction Endonucleases

DNA was digested with restriction enzymes using the manufacturer's recommended 10x restriction buffers and digestion temperatures (New England Biolabs). Plasmid DNA was digested for 1 hour and 30 mins at 37°C in a total volume of 10µl or 15 µl of 1x restriction buffer using between 5-10 units of restriction endonuclease, such that the volume of restriction enzyme did not exceed one tenth of the reaction volume.

2.7.6 Polymerase Chain Reaction (PCR)

The standard PCR conditions described by Ashworth (1993) were used. Each 50µl reaction contained the following components:

5µl of 10x PCR buffer (150mM Tris-HCl pH 8.8, 600mM KCl, 22.5mM, $MgCl_2$),
1.25µl of 10mM dNTPs,
1µl (10pmol) of each of two primers,
1Unit of PFU DNA polymerase
Water and 50ng template DNA to a total volume of 50µl.

The PCRs were carried out on a programmable thermocycler (ABI9700). Generally, the samples underwent 25 cycles of:

(a) denaturation at 94°C for 0.5 min.
(b) annealing at 50-55°C for 0.5 min.
(c) extension at 72°C for 1 min.
followed by 5 min. at 72°C (poly-A extension using Taq polymerase).

In most cases the products of the PCR reaction were treated with restriction enzymes

and ligated into the relative plasmid vectors. These vector constructs were then introduced into chemically competent bacteria.

2.7.7 Spectrophotometric Quantitation of Nucleic acids

Nucleic acid concentrations were determined by measuring the UV absorbance at 260nm of diluted samples (Beckman DU-7 spectrophotometer). Assuming the molecular weight of a nucleotide pair is 660 Daltons, an OD_{260} absorbance of 1 is equivalent to 50µg/ml for double stranded DNA, 40µg/ml for RNA and 33µg/ml for 20mer oligonucleotides.

2.7.8 DNA Sequencing

All samples were sequenced using the DNA sequencing service MWG Biotech AG.

2.8 Western Blotting

2.8.1 Immunoblotting

Samples in 1X SDS loading buffer were run on a 10% or 4-20% SDS gel at 125V in 1X Tris-Glycine running buffer. They were then transferred to a PVDF (Millipore or Hybond-P from Amersham) membrane in 1X CAPS buffer at 25V for 16 hours. The PVDF membrane was then incubated in 5% non-fat milk for 1hr at room temperature. The relative primary antibody was added at 1:5000 dilution for 1hr. The membrane was washed twice in PBS plus 0.1% Tween20 for 5 minutes and then incubated for 1hr in the appropriate secondary at 1:10:000 dilution. The blot was then washed three times in PBS plus 0.1% Tween20 for 10 minutes. ECL detection reagent was added to the blot, which was then exposed on Kodak film and analysed.

All chemicals purchased from SIGMA unless otherwise stated:

SDS loading Buffer (2X) – 80mM Tris (pH 6.9), 2% SDS (Bio-Rad), 100mM DTT, 10% Glycerol

(Bio-Rad), 0.004% bromophenol blue

10% Resolving Gel – 2.5ml acrylamide (Bio-Rad), 2.5ml resolving buffer (pH 8.8), 4.8ml dH_2O, 200µl 10% APS (Bio-Rad), 5µl Temed (Bio-Rad)

Stacking Gel – 0.5ml acrylamide (Bio-Rad), 1.3ml stacking buffer (pH 6.8), 3.2ml dH_2O, 40µl 10% APS (Bio-Rad), 5µl Temed (Bio-Rad)

Tris-Glycine Running buffer (10X) – 30g Trizma, 140g Glycine, 50ml 20% SDS (Bio-Rad), dH_2O to 1litre

CAPS transfer Buffer (50X) – 0.5M CAPS (pH 11.5)

2.8.2 Protein Quantification

Images of the immunoblot film were taken at 30 seconds, 90 seconds and 5 minutes. Band intensities were calculated using Image J (Collins, 2007). Where error bars are shown they are averages of all relative experiments with standard error.

2.8.3 BCA (bicinchoninic acid-containing protein assay) Protein Assay (PIERCE)

The BCA Protein Assay combines the well-known reduction of Cu^{2+} to Cu^{1+} by protein in an alkaline medium with the highly sensitive and selective colorimetric detection of the cuprous cation (Cu^{1+}) by bicinchoninic acid. The assay was performed as described in the PIERCE technical manual.

2.9 Antibodies

Antibodies used for immunoblotting or immunofluorescence are listed in Table 2.1

Table 2.1 Antibodies used in this study for immunofluorescence or immunocytochemistry

ANTIBODY	ORIGIN
anti-VAPA mouse	as described in (Skehel et al., 2000)
anti-VAPB mouse	sheep raised multi antigenic peptide (MAP) form of a peptide corresponding to amino acids 174–189 of mouse VAPB (AltaBioscience)
anti c-myc	mouse monoclonal, 9E-10 epitope (SIGMA)
anti-FLAG	mouse monoclonal (SIGMA)
donkey anti-Sheep Cy2	(Jackson Laboratories)
donkey anti-Rabbit Cy3	(Jackson Laboratories)
anti-p38	rabbit polyclonal (Abcam)
anti-ATF6α	rabbit polyclonal (Santa Cruz Biotechnology)
anti-ATF6α	mouse monoclonal (IMGENEX)
anti-GFP	rabbit polyclonal (Molecular Probes)

2.10 Statistical Analysis

Both luciferase and cell viability assays had an n=4 and results were analysed using a one-way ANOVA (ANalysis Of VAriance) statistical test; moreover each n contains duplicate samples. P-values and statistical significance are mentioned in the relative figure legends.

Chapter 3
VAPB and ATF6α

3.1 Background

ATF6α

ATF6α is one of a family of transmembrane transcription factors (Bailey and O'Hare, 2007). There are two mammalian genes, ATF6 and CREBL1(G13) encoding ATF6α and ATF6β proteins respectively (Yoshida et al., 2000). ATF6α functions in a regulated transcription pathway involved in ER homeostasis and response to stress known as the Unfolded Protein Response (UPR). ATF6β is a poor transcriptional activator of the UPR (Haze et al., 2001, Thuerauf et al., 2004). All experiments described here are based on ATF6α and hence forth wherever ATF6 is mentioned it corresponds to ATF6α protein encoded by the ATF6 gene. Upon accumulation of unfolded proteins in the lumen of the ER, ATF6α translocates from the ER to the Golgi and is proteolyzed in turn by S1P and S2P. This results in the release of the DNA binding and transcription trans-activation domain of ATF6α from the ER membrane allowing it to enter the nucleus and activate transcription (Figure 3.1).

ATF6α appears to interact with several promoter elements. A synthetic promoter has been generated that acts as an ATF6/XBP1 dependent transcription reporter (Wang et al., 2000). The luciferase gene in the p5xATF6-GL3 reporter is under the control of a synthetic promoter containing the c-fos minimal promoter and 5 tandem copies of the ATF6α consensus binding site identified by in vitro gel mobility shift assays with recombinant ATF6α; DNA oligonucleotides binding to ATF6α were selected from a pool of oligonucleotides (Shen et al., 2005). However it was shown that the UPR associated transcription factor XBP1 can bind to the same ATF6α sites with high affinity (Yoshida et al., 2001). Moreover, Yamamoto et al., 2007 showed that ATF6α forms heterodimers with XBP1. Studies with knockdown of endogenous ATF6α with siRNA have shown that the p5xGL3ATF6 is responsive to changes in ATF6α levels (Lee et al., 2003). Thus, the p5xGL3ATF6α reporter detects levels of ATF6α, but a percentage of it is due to XBP1.

Figure 3.1

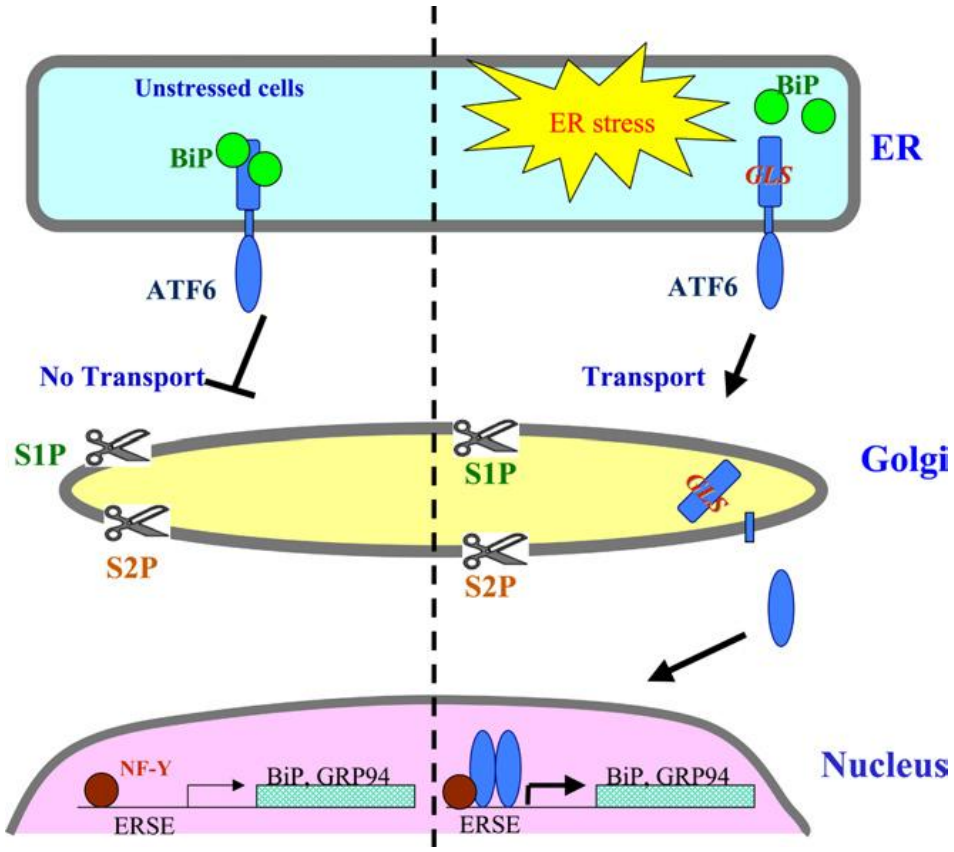

Figure 3.1 ***ATF6a transcription factor participating in the Unfolded Protein Response (from (Wang et al., 2000))***

ATF6α upon UPR activation follows the path ER→the Golgi→Nucleus. The Golgi-localization sequence (GLS) upon ER stress is unmasked by dissociation of BiP and ATF6α is transported to the Golgi. ATF6α is cleaved by S1P, S2P shuttled to the nucleus were it acts on ERSE promoters via NF-Y (a CCAAT box binding factor). The right side of the figure corresponds to ER stressed cells.

MSP and ATF6α

It was previously shown ((Middleton, 2005) and Skehel unpublished) that overexpression of the MSP domains of VAPA or VAPB as EGFP fusion proteins is toxic to HEK293 cells and primary rat hippocampal cultured neurons; moreover they form large cytoplasmic aggregates. Therefore, in order to elucidate the MSP domain

overexpression associated toxicity and discover proteins that might interact with the MSP domain a yeast two hybrid screen was performed using as bait the VAPA MSP domain. A sequence corresponding to amino acids 1-107 of mouse VAPA (MSP) was used to screen a rat brain cDNA library in a yeast two hybrid screen (Middleton, 2005). A partial clone of ATF6α was found as an interacting partner.

VAPB domains

In Chapter 1- Introduction we have described the three structural domains of VAP proteins and their participation in various protein-protein interactions (Table 1.1 and text). In Figure 3.2 we depict EGFP mouse VAPB (and ALS8 associated $VAPB^{P56S}$) full length and truncation constructs described in Middleton, 2005 that were used for the purposes of our study. These constructs are all mouse N-terminal EGFP fusion proteins:

- Full length mVAPB
- Full length $mVAPB^{P56S}$ (proline 56 substituted for a serine)
- ΔHB (containing the MSP domain and Coiled Coil domains; lacking the hydrophobic C-terminal membrane anchor)
- ΔHB^{P56S} (containing the MSP domain and Coiled Coil domains; lacking the hydrophobic C-terminal membrane anchor – proline 56 substituted for a serine)
- MSPB (containing the MSP domain; lacking the Coiled Coil and hydrophobic C-terminal membrane anchor)
- $MSPB^{P56S}$ (containing the MSP domain; lacking the Coiled Coil and hydrophobic C-terminal membrane anchor – proline 56 substituted for a serine)
- CC/CTB (containing the Coiled Coil and hydrophobic C-terminal membrane anchor; lacking the MSP domain)
- CCB (containing the Coiled Coil; lacking the hydrophobic C-terminal membrane anchor and the MSP domain)
- CTB (containing the hydrophobic C-terminal membrane anchor; lacking the Coiled Coil and the MSP domain)

In this chapter we will explore the reported VAP-ATF6α interaction.

Figure 3.2 Mouse *VAPB GFP fusion truncations (from (Middleton, 2005))*

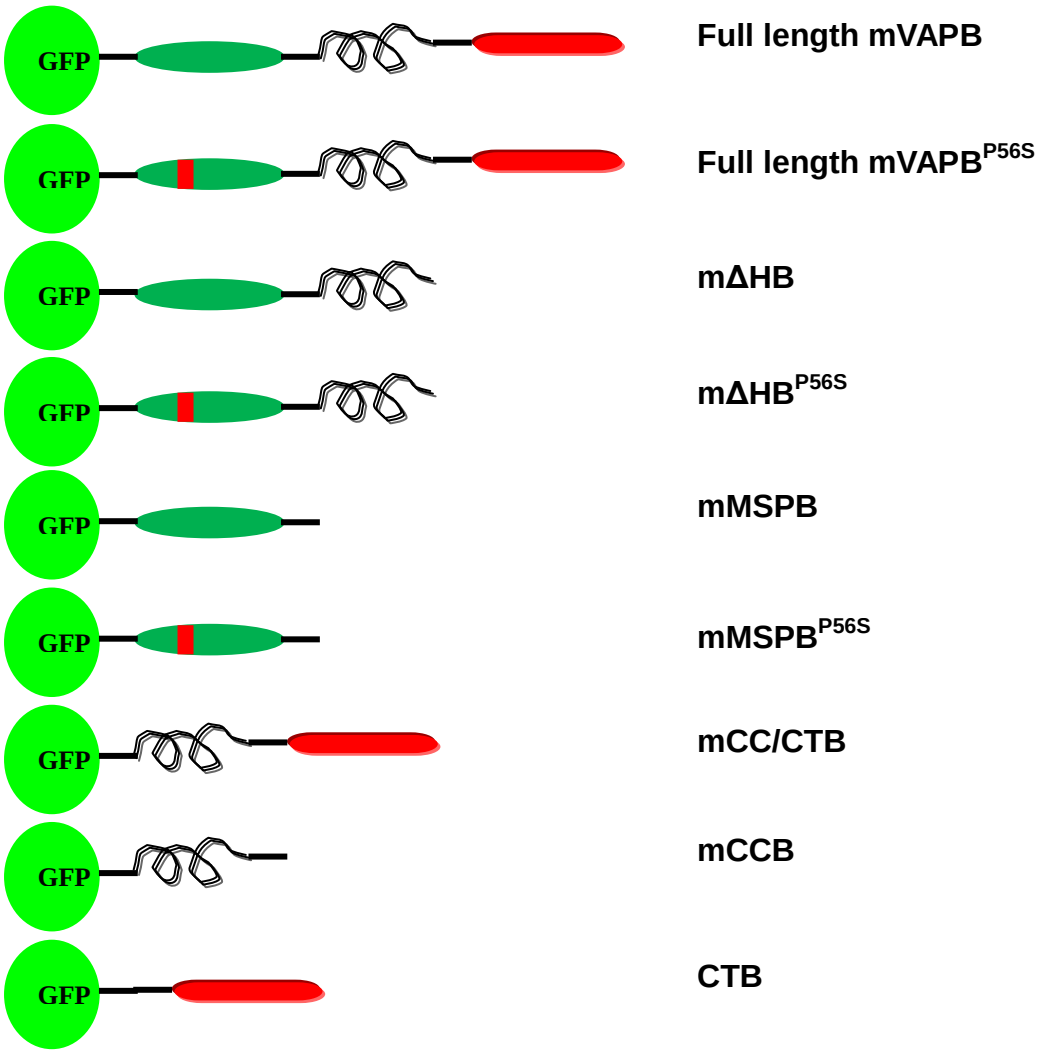

3.2 mVAPA, mVAPB, mVAPA^{P56S} and mVAPBP^{P56S} interact with ATF6α in a peptide complementation assay.

ATF6α was identified in a yeast-two-hybrid screen as a positive interactor of the VAPA MSP domain (Middleton, 2005); a sequence corresponding to amino acids 1–107 of mouse VAPA was used to screen a rat brain cDNA library. In addition to a number of FFAT- and MSP domain-containing proteins, a partial clone of the ER stress regulated transcription factor ATF6α was identified. Yeast-two-hybrid assays are powerful tools for discovering novel protein-protein interactions, but positive results should be validated with additional experiments. To characterize this interaction further, expression constructs for full-length VAPA, VAPB and ATF6α were analysed by a fluorescent peptide complementation assay (Remy et al., 2002, Remy and Michnick, 2007). In this assay, a fluorescent protein is generated from two separate parts of a split GFP, termed Venus1 and Venus2, only by the association of two test polypeptides expressed as fusion proteins. A functional fluorescent protein is generated when the two test proteins directly interact. Although the initial yeast two-hybrid interaction was between a truncated form of ATF6α and the MSP domain of VAPA, an interaction between full-length forms of VAPA and VAPB with ATF6α was readily detectable (Figure 3.3.1). Similarly, the ALS8-associated mutant VAPB^{P56S} was shown to be capable of interacting with ATF6α. No interaction was detected between VAPA, VAPB or ATF6α when co-expressed with heterologous leucine zipper-Venus fusions. The reconstitution of a fluorescent protein clearly indicates that VAPA and VAPB are capable of interacting with ATF6α. Similar results were also obtained with the converse Venus combinations, where ATF6α was expressed as a fusion with Venus 1, and the VAP proteins were fused to Venus 2 (Figure 3.3.2).

Figure 3.3.1

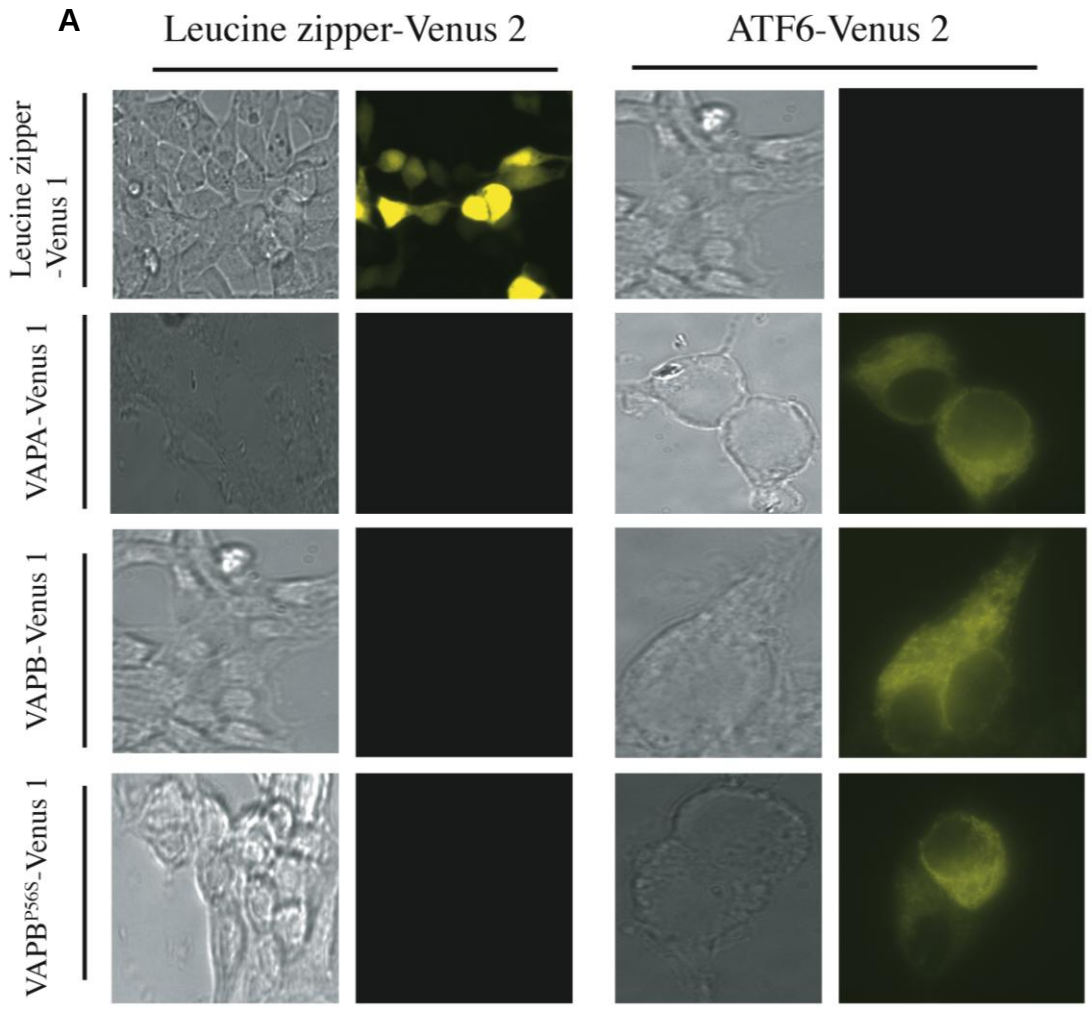
A
Leucine zipper-Venus 2
ATF6-Venus 2
Leucine zipper -Venus 1
VAPA-Venus 1
VAPB-Venus 1
VAPB^{P56S}-Venus 1

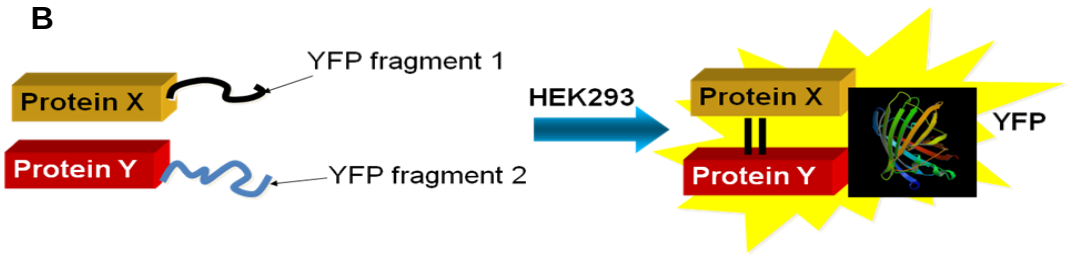
B
YFP fragment 1
Protein X
Protein Y
YFP fragment 2
HEK293
Protein X
Protein Y
YFP

Figure 3.3.1 ***Fluorescent Protein Fragment Complementation Assay.***

A. VAPA, VAPB and VAPB^{P56S} interact with ATF6α in HEK293 cells in a Fluorescent Protein Complementation Assay. The coding sequences of mouse VAPA, VAPB and VAPB^{P56S} were expressed in HEK293 cells as fusion proteins with a truncated non-fluorescent form of YFP, Venus 1. These proteins were co-expressed with the complementary ATF6α-Venus 2 fusion protein. Fluorescence indicates reconstitution of a functional YFP and therefore a direct interaction of VAPA and VAPB with ATF6α. Wild-type VAPB and mutant VAPB^{P56S} are capable of interacting with ATF6α. Controls in which a homodimerizing leucine zipper peptide was expressed as either a Venus 1 or Venus 2 fusion proteins show no fluorescence when expressed with the complementary VAP or ATF6α fusion proteins. Bright field or fluorescence images were acquired from live cells through cell culture plastic.

B. Schematic representation of a Fluorescent Protein Complementation Assay in HEK293 cells (see 2.1 Materials and Methods). An interaction between two proteins X and Y can be detected in HEK293 cells when fusion proteins fused to truncated forms of YFP (two subunits of YFP) are co-expressed. YFP reconstitution is mediated by an X-Y interaction and fluorescence indicates a positive result (interaction).

Figure 3.3.2

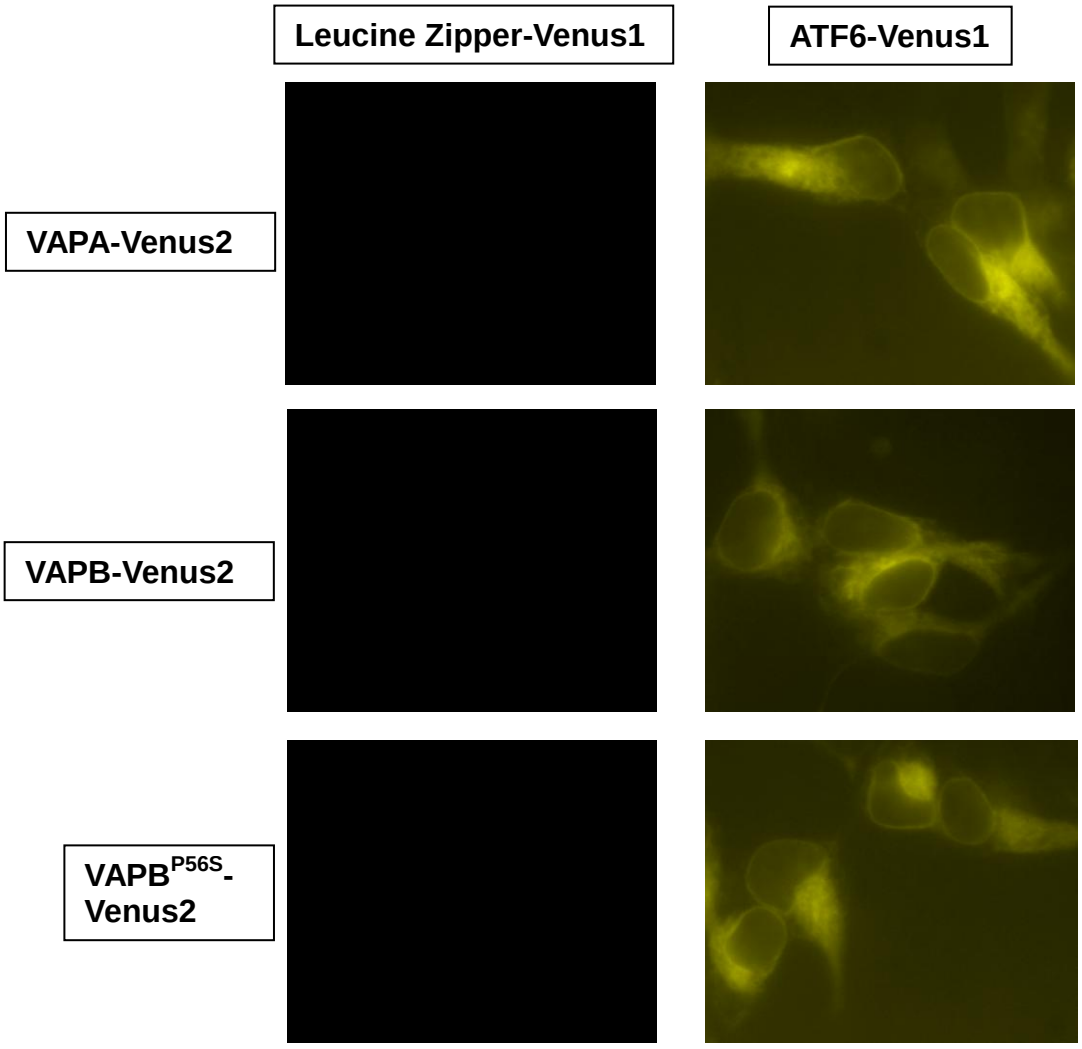
Leucine Zipper-Venus1
ATF6-Venus1
VAPA-Venus2
VAPB-Venus2
VAPB^{P56S}-Venus2

Figure 3.3.2 ***VAPA, VAPB and VAPB^{P56S} interact with ATF6α in HEK293 cells in a Fluorescent Protein Complementation Assay using converse Venus combinations from 3.3.1.***

The coding sequences of mouse VAPA, VAPB and VAPB^{P56S} were expressed in HEK293 cells as fusion proteins with a truncated non-fluorescent form of YFP, Venus 2. These proteins were co-expressed with the complementary ATF6α-Venus 1 fusion protein. Fluorescence indicates reconstitution of a functional YFP and therefore a direct interaction of VAPA and VAPB with ATF6α. Wild-type VAPB and mutant VAPB^{P56S} are capable of interacting with ATF6α. Controls in which a homodimerizing leucine zipper peptide was expressed as a Venus 1 fusion protein show no fluorescence when expressed with the complementary VAP or ATF6α fusion proteins (also see Figure 3.3.1).

3.3 Co-localisation of mVAPB or mVAPB^{P56S} and ATF6α

Fluorescence analysis of HEK293 cells expressing EGFP-VAPB and FLAG-tagged ATF6α shows extensive regions of co-localization on the ER, but also some complementary distribution (Figure 3.6). The aggregates of EGFP-VAPB^{P56S} show some but not extensive co-localization with ATF6α, although we cannot discount that low antigen accessibility may contribute to reduced ATF6α detection in VAPB^{P56S} aggregates. Expression of VAPB^{P56S} does not appear to cause gross disruption of ATF6α distribution in the ER.

Figure 3.3

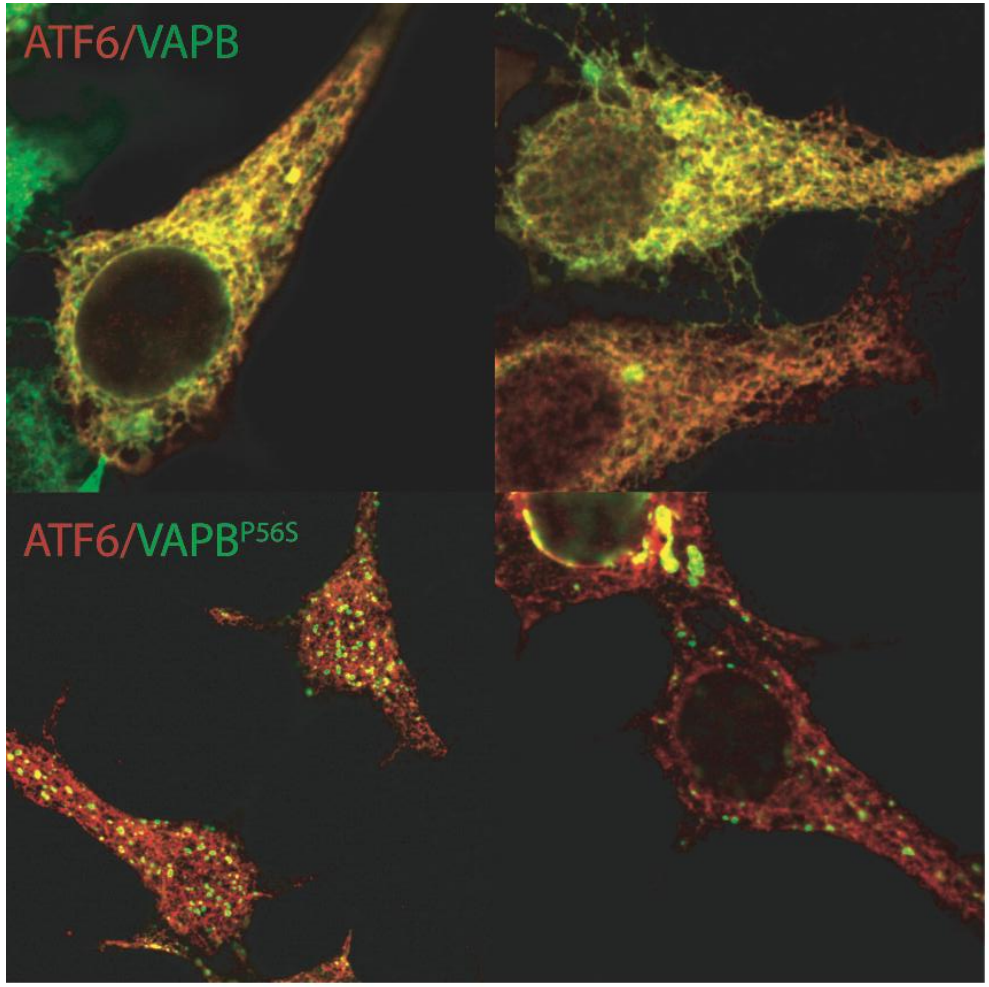

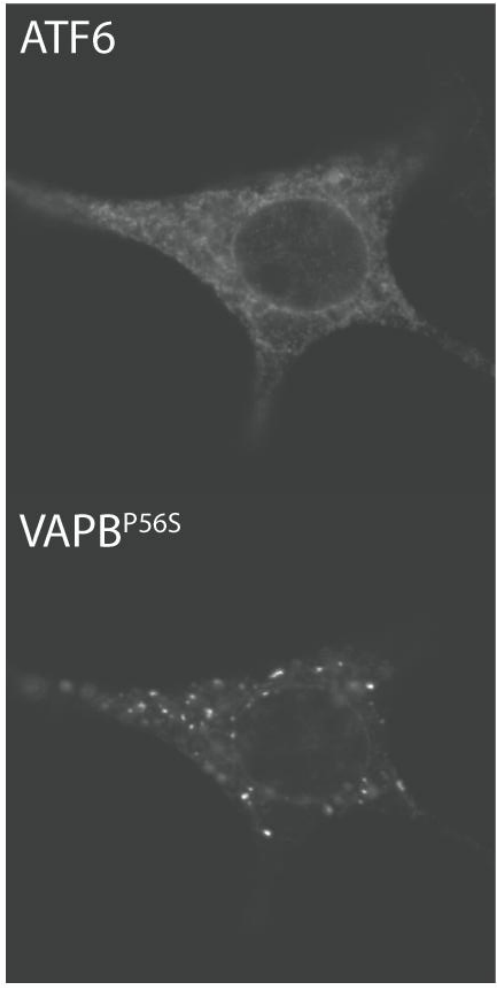

Figure 3.3 ***Co-localization of VAPB and ATF6α.***

HEK293 cells were transfected with FLAG-ATF6, EGFP-VAPB and EGFP-VAPB^{P56S}. In colour plates, FLAG-ATF6 is shown in red and EGFP-VAPB or EGFP-VAPB^{P56S} is in green. There is extensive, but not total co-localization of VAPB and ATF6α in a reticular distribution. ATF6α co-localizes with the aggregates formed by VAPB^{P56S}, but not in a punctate pattern. Note that VAPB^{P56S} does not cause a gross change in the distribution of ATF6α.

3.4 ATF6α transcriptional activation is inhibited by mVAPB and mVAPB^{P56S}.

ATF6α appears to interact with several promoter elements (Hai et al., 1989, Wang et al., 2000, Yoshida et al., 2000). A synthetic promoter has been generated that acts as an ATF6/XBP1 dependent transcription reporter (Wang et al., 2000). To determine if the interaction with VAPB affects the ability of ATF6α to activate transcription, luciferase-based transient transcription assays were done using this ATF6/XBP1-dependent reporter of transcription (Appendix I, #P18). In HEK293 cells, basal levels of transcription from this promoter are reduced by over-expression of myc-tagged forms of VAPB or VAPB^{P56S} (Figure 3.4.1A). When the UPR was activated by the glycosylation inhibitor, tunicamycin, ATF6/XBP1-mediated transcription was also significantly reduced by over expression of VAPB or VAP-B^{P56S}. Increasing levels of ATF6α by co-expression of a FLAG-tagged recombinant form of human ATF6α (Appendix I, #P17) increased basal and tunicamycin-induced expression from the ATF6αXBP1 reporter. In both cases, the elevated levels of ATF6/XBP1 dependent transcription were also reduced by over expression of either VAPB or VAPB^{P56S} (Figure 3.4.1B and C). This effect requires the cytoplasmic domains of VAPB and does not appear to be a non-specific consequence of increasing levels of protein in the ER membrane since over expression of a DsRed fluorescent fusion protein of the C-terminal hydrophobic domain of VAPB does not reduce the basal or tunicamycin-induced expression from the ATF6/XBP1 reporter (Figure 3.4.1A and Figure 3.4.2). Over expression of VAP proteins does not reduce expression levels of luciferase directed from a CMV promoter; therefore, the repressive effect on the ATF6/XBP1 reporter is unlikely to be the result of a general repression of transcription (Figure 3.4.3). A similar inhibitory effect was also seen in the motor neuron derived cell line NSC34 (Figure 3.4.1C and D). In NSC34 cells, basal levels of expression from the ATF6/XBP1 reporter are less than in HEK293, perhaps indicating lower levels of endogenous ATF6α. Finally, the p5xGL3-ATF6 reporter is responsive to changes in levels of expression of endogenous ATF6α (Figure 3.4.4).

Figure 3.4.1

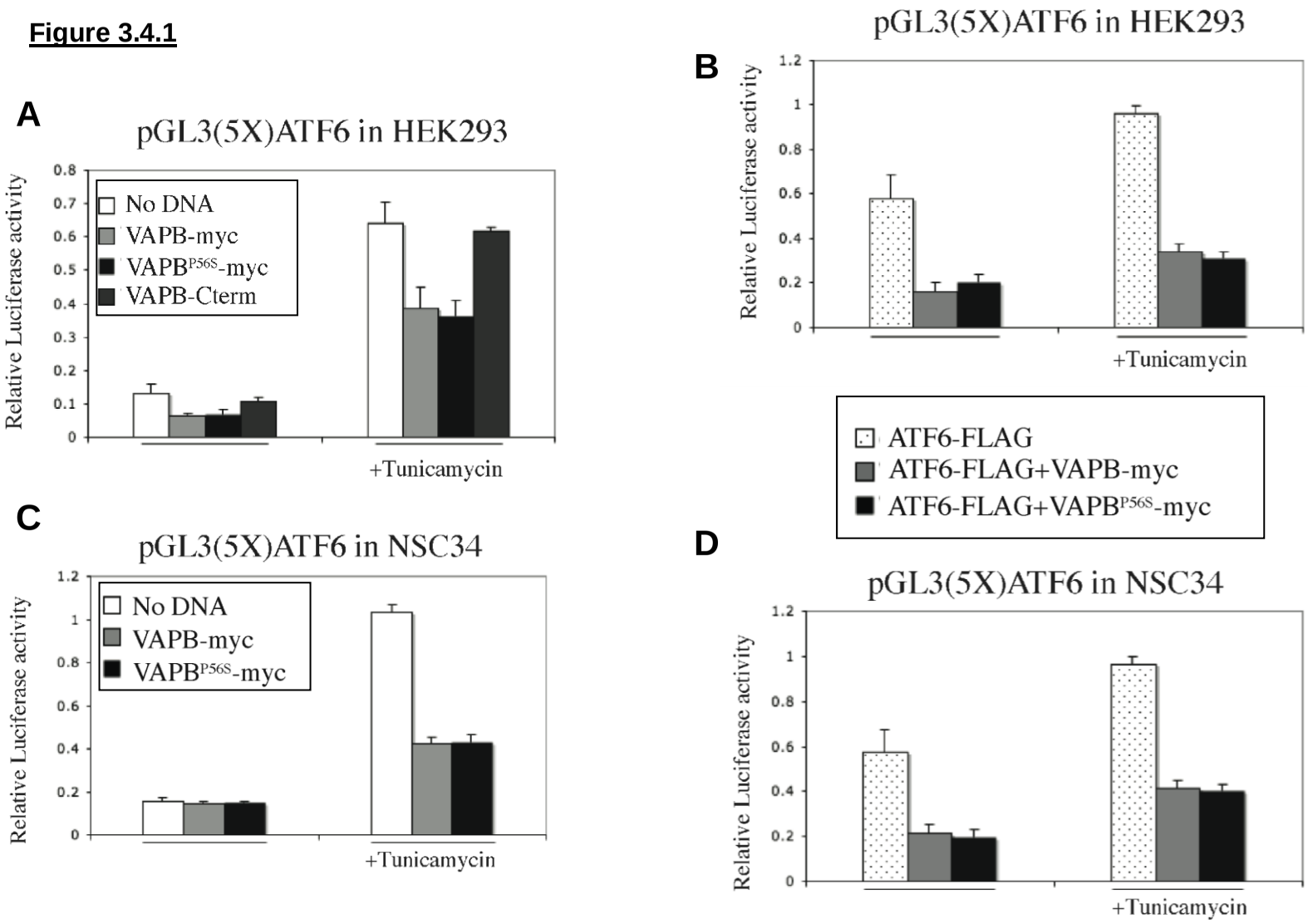
A
pGL3(5X)ATF6 in HEK293
Relative Luciferase activity
No DNA
VAPB-myc
VAPB^{P56S}-myc
VAPB-Cterm
+Tunicamycin
B
pGL3(5X)ATF6 in HEK293
Relative Luciferase activity
+Tunicamycin
ATF6-FLAG
ATF6-FLAG+VAPB-myc
ATF6-FLAG+VAPB^{P56S}-myc
C
pGL3(5X)ATF6 in NSC34
Relative Luciferase activity
No DNA
VAPB-myc
VAPB^{P56S}-myc
+Tunicamycin
D
pGL3(5X)ATF6 in NSC34
Relative Luciferase activity
+Tunicamycin

Figure 3.4.1 ***VAPB and VAPB^{P56S} inhibit transcription from an ATF6 regulated transcription reporter.***

A. HEK293 were transfected with a reporter plasmid containing the luciferase cDNA regulated by five ATF6/XBP1 binding sites, pGL3(5X)ATF6. Cell cultures were co-transfected with expression plasmids encoding VAPB or VAPB^{P56S} as myc-tagged fusion proteins (VAPB-myc and VAPB^{P56S}-myc) or a monomeric red fluorescent fusion protein containing the C-terminal 41 amino acids of VAPB (VAPB-Cterm). Where indicated cultures were treated for 12 h with 2 µg/ml tunicamycin to induce ER stress. VAPB and VAPB^{P56S} reduce constitutive levels of ATF6/XBP1 activity, while VAPB-Cterm had no effect ($p=0.012932$).

B. Over expression of ATF6α as an ATF6-FLAG fusion protein increased basal and tunicamycin-induced activity of the ATF6/XBP1 reporter gene, but in both cases, levels of activity were reduced by co-expression of VAPB-myc or VAPB^{P56S}-myc ($p=0.011491$).

C and **D.** The transcriptional assay using the motor neuron-like cell line NSC34 gave comparable results as the HEK293 experiment (p values 0.02134, 0.019345 respectively).

Figure 3.4.2

A

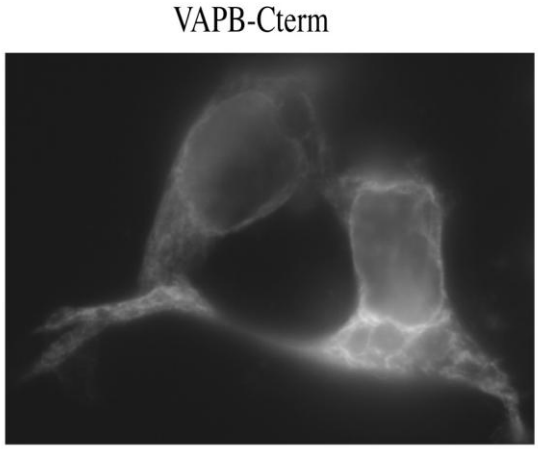

B

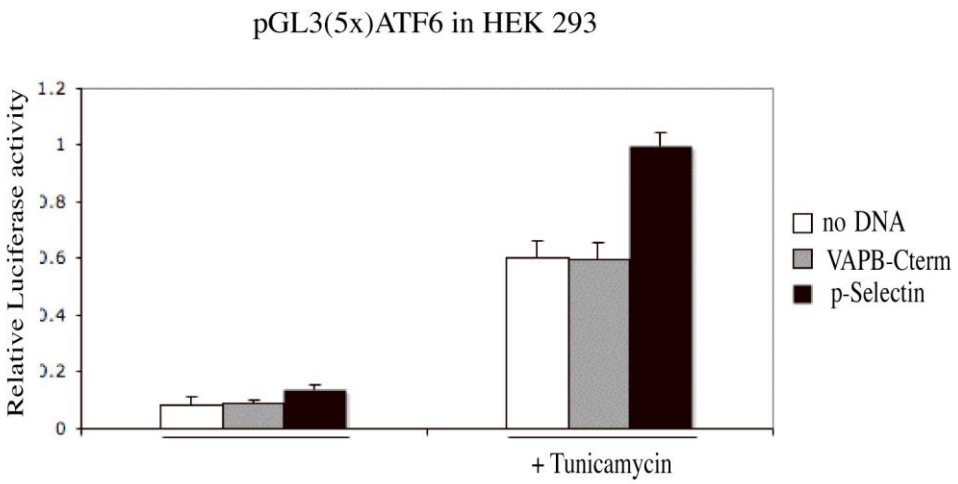

Figure 3.4.2 ***ATF6/XBP1-dependent transcription is not affected by over-expression of an ER membrane protein.***

A. A monomeric red fluorescent fusion protein containing the C-terminal 41 amino acids of VAPB (VAPB-Cterm) was expressed in HEK293 cells. Fluorescence microscopic analysis indicates that the protein is distributed throughout the cell in a reticular pattern.

B. Basal or tunicamycin-induced levels of ATF6/XBP1 dependent transcription are not affected by expression of VAPB-Cterm. Therefore the observed inhibition requires the cytoplasmic domains of VAPB, and is not simply the result of increasing levels of protein in the membrane of the ER. Increasing the synthetic load on the lumen of the ER by over expression of the integral membrane protein p-selectin enhances ATF6/XBP1-dependent transcription, as expected. Results are averages of four experiments and error bars correspond to standard error (SE) p=0.025428.

Figure 3.4.3

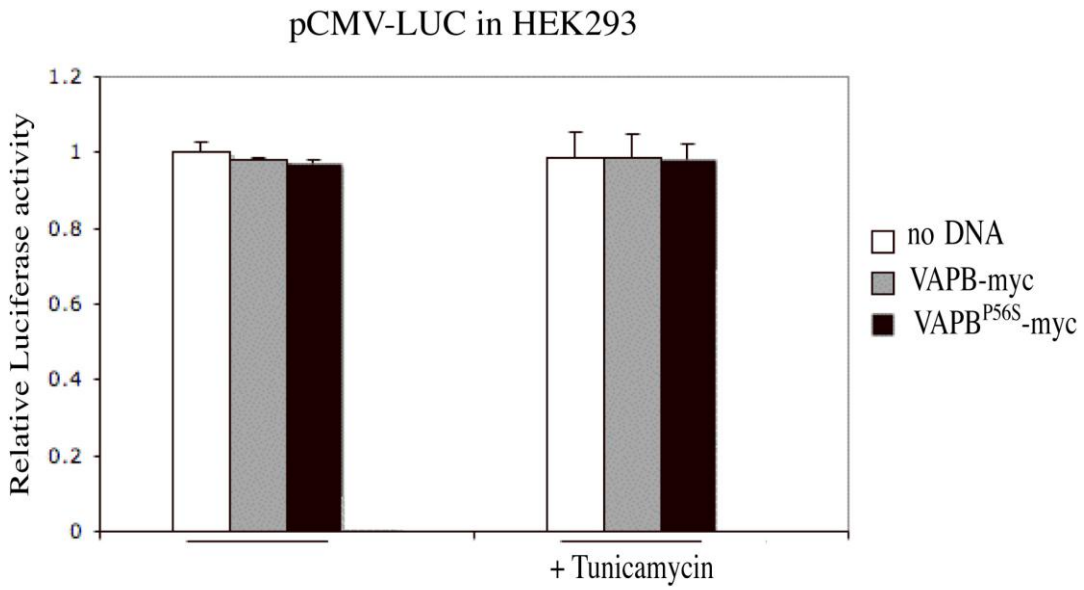

Figure 3.4.3 ***Overexpression of VAPB does not affect the activity of a CMV promoter.***

HEK293 cells were transfected with a plasmid (pCMV-GL3-luc, PROMEGA) in which the expression of luciferase was under the control of a CMV (CytoMegaloVirus) promoter. Co-expression of VAPB-myc or VAPB^{P56S}-myc had no affect on the level of luciferase expression. All transcription assays are normalised to the expression levels of a co-expressed renilla luciferase gene. Results are averages of four experiments and error bars correspond to standard error (SE), p=0.012927. Therefore, the inhibitory affect of VAPB and VAPB^{P56S} on ATF6/XBP1 dependent expression is unlikely to be a non-specific general effect of transcription.

Figure 3.4.4

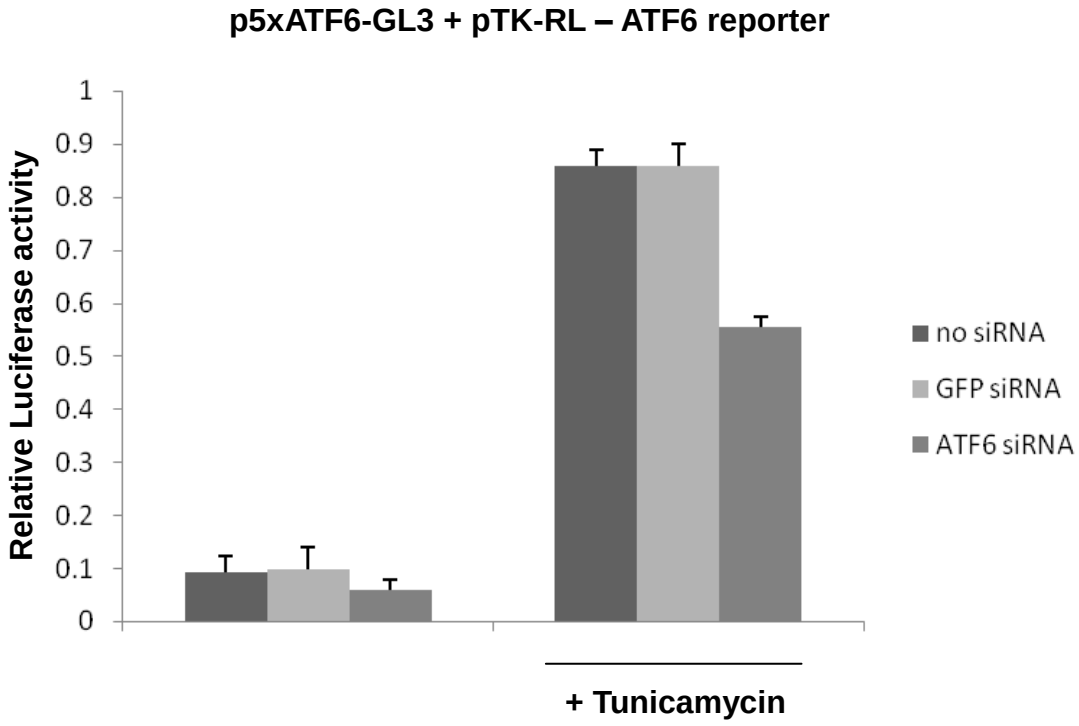

Figure 3.4.4 ***The ATF6 synthetic reporter is responsive to ATF6 siRNA.***

When HEK293 cells were transfected with GFP siRNA, there is no effect to the relative luciferase activity as measured by Firefly luciferase light units normalised to the renillin control. When the ATF6α siRNA (20 pmoles) (QIAGEN Hs_ATF6_5 HP Validated siRNA (SI03019205)) is applied, there is a reduction in relative luciferase activity in tunicamycin induced and baseline samples. Although we could not get a representative immunoblot to associate this observation with actual protein levels (the endogenous ATF6α antibodies used did not produce a signal when analysed in western blots; 2 different antibodies were used, see materials and methods chapter) this suggests that the reporter based on the synthetic ATF6α promoter is responsive to reduction of endogenous ATF6α.

3.5 VAPB siRNA reduces the levels of endogenous VAPB and increases basal ATF6/XBP1-dependent transcription

Consistent with the inhibitory affect seen by over expression of VAPB, siRNA-mediated reduction of endogenous VAPB results in an increase of basal (60%) and induced levels (30%) of ATF6/XBP1-dependent transcription (Figure 3.5). HEK293 cells were nucleofected with siRNA to endogenous hVAPB, washed and cultured for 24 hours. Then cells were transfected using Lipofectamine2000 with the ATF6 reporter, and cultured for 24 hours before being treated with 2 µg/ml tunicamycin. GFP siRNA was used as a control. This experiment was also repeated in Chapter 4 (Figure 4.4).

3.6 mVAPB^{P56S} accumulates to lower levels than mVAPB and therefore may be a stronger inhibitor of ATF6α

When equal amounts of expression plasmid DNA for VAPB and VAPB^{P56S} were used for cell-transfections, the overall level of attenuation was similar between the wild type and mutant forms of VAPB (Figure 3.4.1). Immunoblot analysis of total protein from transfected cells, however, indicated that the mutant protein, VAPB^{P56S}-myc, accumulated to significantly lower levels, reaching only 20% of the level of wild-type protein (Figure 3.6.1A). This suggests that VAPB^{P56S}-myc may exert a stronger inhibition on ATF6α than the wild-type VAPB-myc, since a similar level of inhibition is achieved from a lower amount of protein. The difference in protein levels is less pronounced when VAPB and VAPB^{P56S} are expressed as EGFP fusion proteins, which indicates that the presence of the GFP moiety may have a stabilizing affect on VAPB^{P56S}. Consistent with this, the inhibition of ATF6/XBP1-dependent transcription is more pronounced for VAPB^{P56S}-GFP than VAPB-GFP (Figure 3.6.1B). Moreover, increasing amounts of VAPB and VAPB^{P56S} DNA have a stronger inhibitory effect, while the mutant still accumulates to lower levels (Figure 3.6.2). Thus, VAPB^{P56S} appears to have a significantly greater inhibitory effect on ATF6α mediated transcription than wild-type VAPB.

Figure 3.5

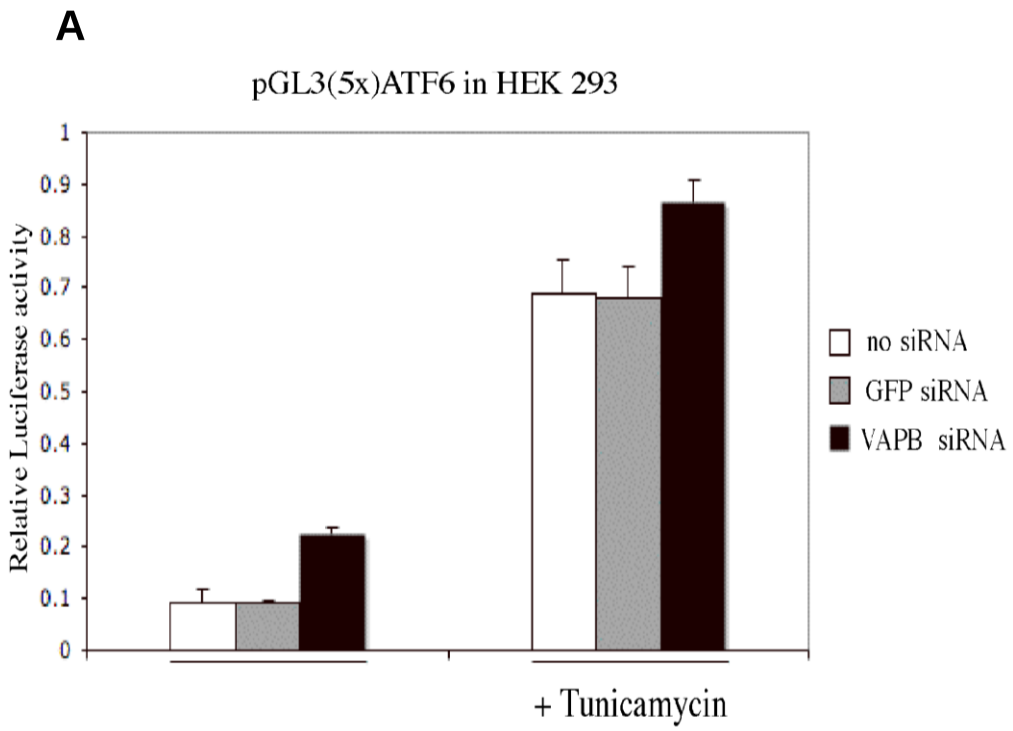
A
pGL3(5x)ATF6 in HEK 293
Relative Luciferase activity
1
0.9
0.8
0.7
0.6
0.5
0.4
0.3
0.2
0.1
0
no siRNA
GFP siRNA
VAPB siRNA
+ Tunicamycin

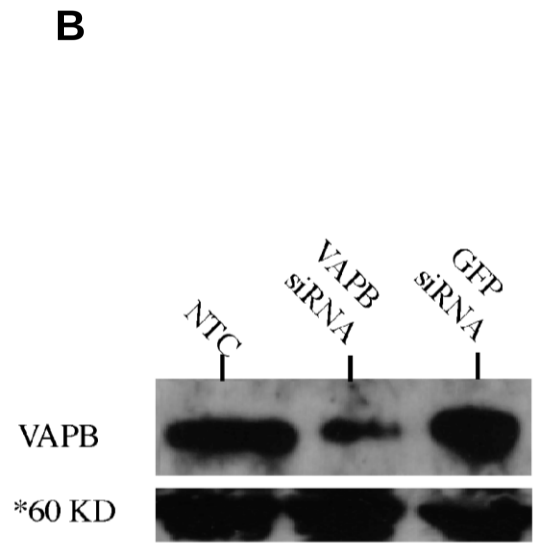
B
NTC
VAPB siRNA
GFP siRNA
VAPB
*60 KD

Figure 3.5 ***VAPB siRNA reduces the levels of endogenous VAPB and increases basal ATF6/XBP1-dependent transcription.***

A. Transcriptional Assay in HEK293 cells nucleofected with siRNA to VAPB. Reduction of endogenous VAPB expression levels increases basal and tunicamycin-induced, transcription from an ATF6/XBP1-regulated transcription promoter n=4, p=0.025817.

B. Immunoblot analysis of HEK293 cells nucleofected with VAPB siRNA or GFP siRNA and non-transfected cells shows a 25% reduction in levels of endogenous VAPB when treated with VAPB siRNA and no reduction in GFP siRNA treated cells. *A 60 kDa non-specific band from longer exposures of the immunoblot serves as a loading control. Band intensities were measured using ImageJ (NIH)-also see Figure 4.4

Figure 3.6.1

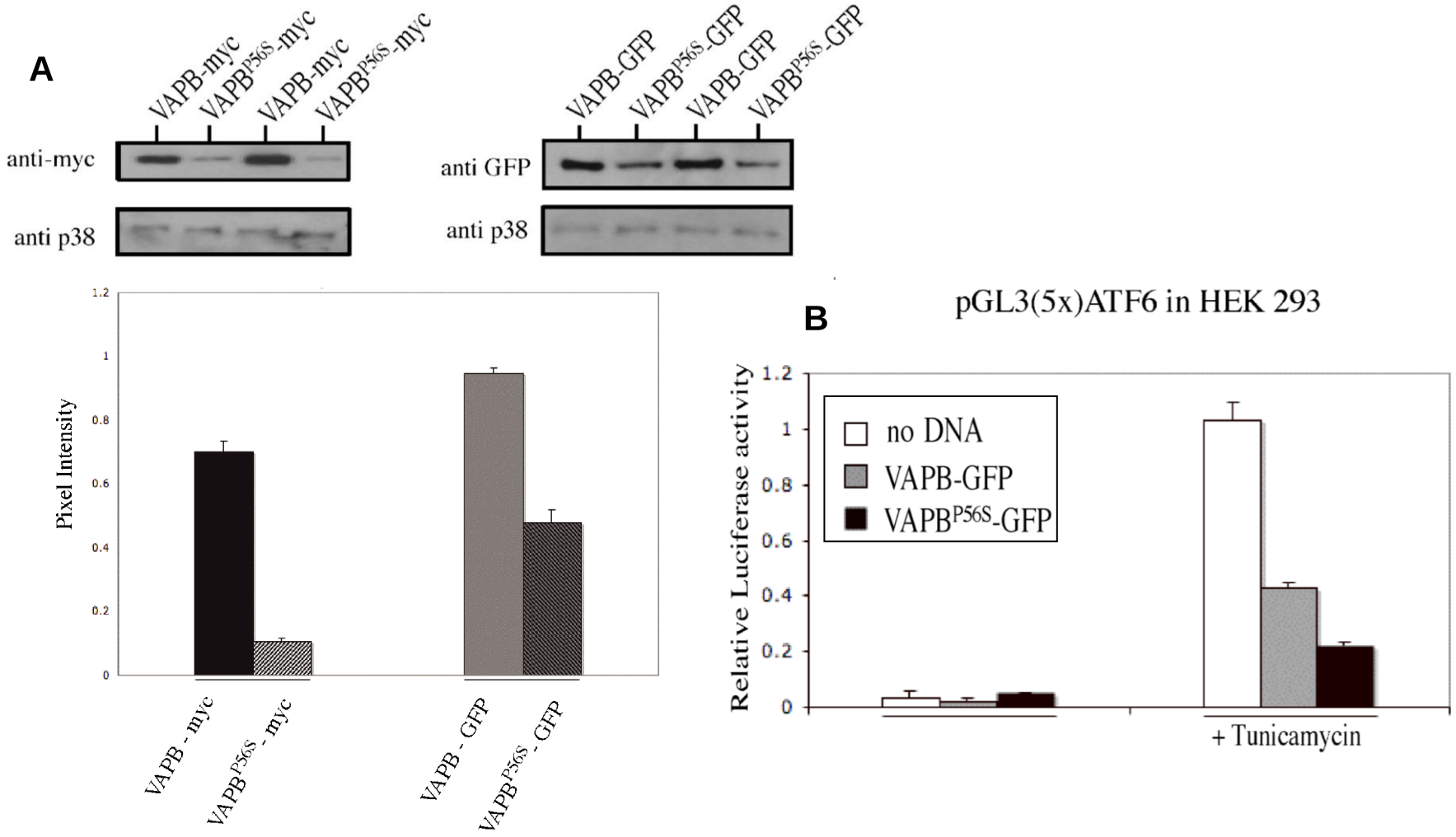
A
VAPB-myc
VAPB^{P56S}-myc
VAPB-myc
VAPB^{P56S}-myc
anti-myc
anti p38
VAPB-GFP
VAPB^{P56S}-GFP
VAPB-GFP
VAPB^{P56S}-GFP
anti GFP
anti p38
Pixel Intensity
1.2
1
0.8
0.6
0.4
0.2
0
VAPB - myc
VAPB^{P56S} - myc
VAPB - GFP
VAPB^{P56S} - GFP
B
pGL3(5x)ATF6 in HEK 293
Relative Luciferase activity
no DNA
VAPB-GFP
VAPB^{P56S}-GFP
+ Tunicamycin

Figure 3.6.1 ***VAPB^{P56S} accumulates to lower levels than VAPB.***

A. Immunoblot analysis of HEK293 cells expressing myc or GFP-tagged forms of VAPB and VAPB^{P56S}. Duplicate samples are shown, and relative levels expressed as a histogram of signal intensities. As both myc and GFP fusion proteins, VAPB^{P56S} accumulates to lower levels than VAPB. VAPB^{P56S}-myc is ~15% the level of VAPB-myc, and VAPB^{P56S}-GFP is ~50% the level of VAPB-GFP. The GFP moiety appears to have a stabilizing affect on the levels of mutant protein, allowing it to accumulate to higher levels than the myc-tagged form. Band intensities were determined using ImageJ (NIH) Intensities for both myc and GFP, VAPB and VAPB^{P56S} were normalized to the p38 loading control; error bars correspond to standard error (SE).

B. Consistent with this the inhibition of ATF6-dependent reporter gene expression is reduced to a greater relative level by VAPB^{P56S}-GFP than VAPB^{P56S}-myc; results are averages of 4 experiments and error bars correspond to standard error (SE), p=0.016827.

Figure 3.6.2

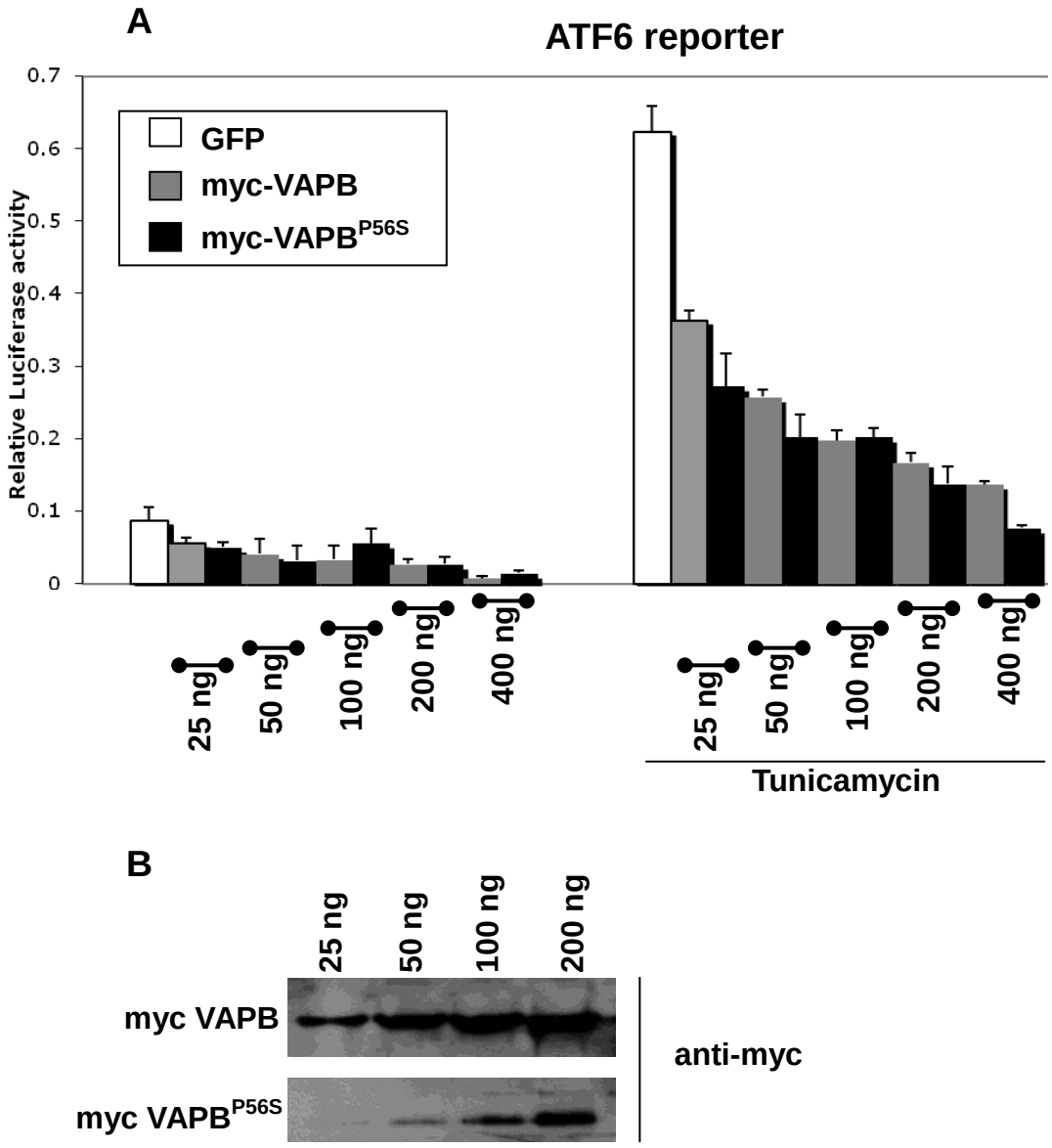
A
ATF6 reporter
Relative Luciferase activity
0.7
0.6
0.5
0.4
0.3
0.2
0.1
0
GFP
myc-VAPB
myc-VAPB^{P56S}
25 ng
50 ng
100 ng
200 ng
400 ng
25 ng
50 ng
100 ng
200 ng
400 ng
Tunicamycin
B
25 ng
50 ng
100 ng
200 ng
myc VAPB
myc VAPB^{P56S}
anti-myc

Figure 3.6.2 ***Inhibition of ATF6 activation by increasing amounts of VAPB and VAPB^{P56S} DNA.***

A. Transcriptional assay in HEK293 cells overexpressing myc-VAPB or myc-VAPB^{P56S}. Total amount of DNA is balanced with pEGFP-C3. Increasing DNA amounts of the VAP proteins cause greater inhibition of the ATF6α reporter. The concentration used in our assays is 100 ng – It is clear that the inhibitory effect is still present at low (25 ng) or high concentrations (400 ng).

B. Immunoblot of representative samples from the titration of DNA amounts assay. VAPB^{P56S} always accumulates to lower amounts than wild-type VAPB. 30 μg of total protein were loaded using a micro-BCA assay (PIERCE).

3.7 Effect of overexpression of mVAPB and mVAPB^{P56S} truncations on ATF6α reporter transcriptional activation

ATF6α was identified as a positive interactor of the VAPA MSP domain (Middleton, 2005). In addition to this we have shown that full length VAP proteins and the P56S mutant interact with ATF6α. VAP proteins have three major structural domains (MSP, CC, CT – see Figure 1.2) and we proceeded to examine their effect on ATF6α activation by overxpressing various EGFP truncations of VAP proteins. HEK293 or NSC34 cells were transfected with all the mouse VAPB and VAPB^{P56S} EGFP constructs and truncations along with the ATF6α reporter and the internal renillin control (Figure 3.7). Results are consistent in the two different cell-lines examined. Tunicamycin treatment induces the ATF6α reporter by 6-fold. Although basal levels of transcription do not seem to be affected, there is inhibition of the activity of the synthetic ATF6α promoter when cells are induced with tunicamycin. This inhibition is true for VAPB (40%), VAPB^{P56S} (45%), MSPB (65%), MSPB^{P56S} (35%), ΔHB (45%) and ΔHB^{P56S} (49%), CC/CTB (40%), CCB (38%) but not for the CTB construct. Therefore, the Coiled-Coil domain of VAPB affects ATF6α synthetic promoter dependent transcription. MSPB^{P56S} inhibits less that wild-type MSPB, which is the strongest inhibitor out of all domains; consistent with Figure 3.4.1A, the C-terminal construct had no effect on ATF6α activity.

3.8 VAPB overexpression blocks glycosylation associated activation of expressed ATF6α

The luminal domain of ATF6α contains two highly conserved cysteines that form a disulfide bond that holds together dimmers of ATF6α. When the reducing agent dithiothreitol or the N-glycosylation inhibitor tunicamycin are added ATF6α is reduced and the extent of reduction correlates with its activation (Nadanaka et al., 2007). When HEK293 cells were transfected with the FLAG-tagged expression construct of human ATF6α along with pEGFP-C3, the anti-FLAG antibody detects a

Figure 3.7

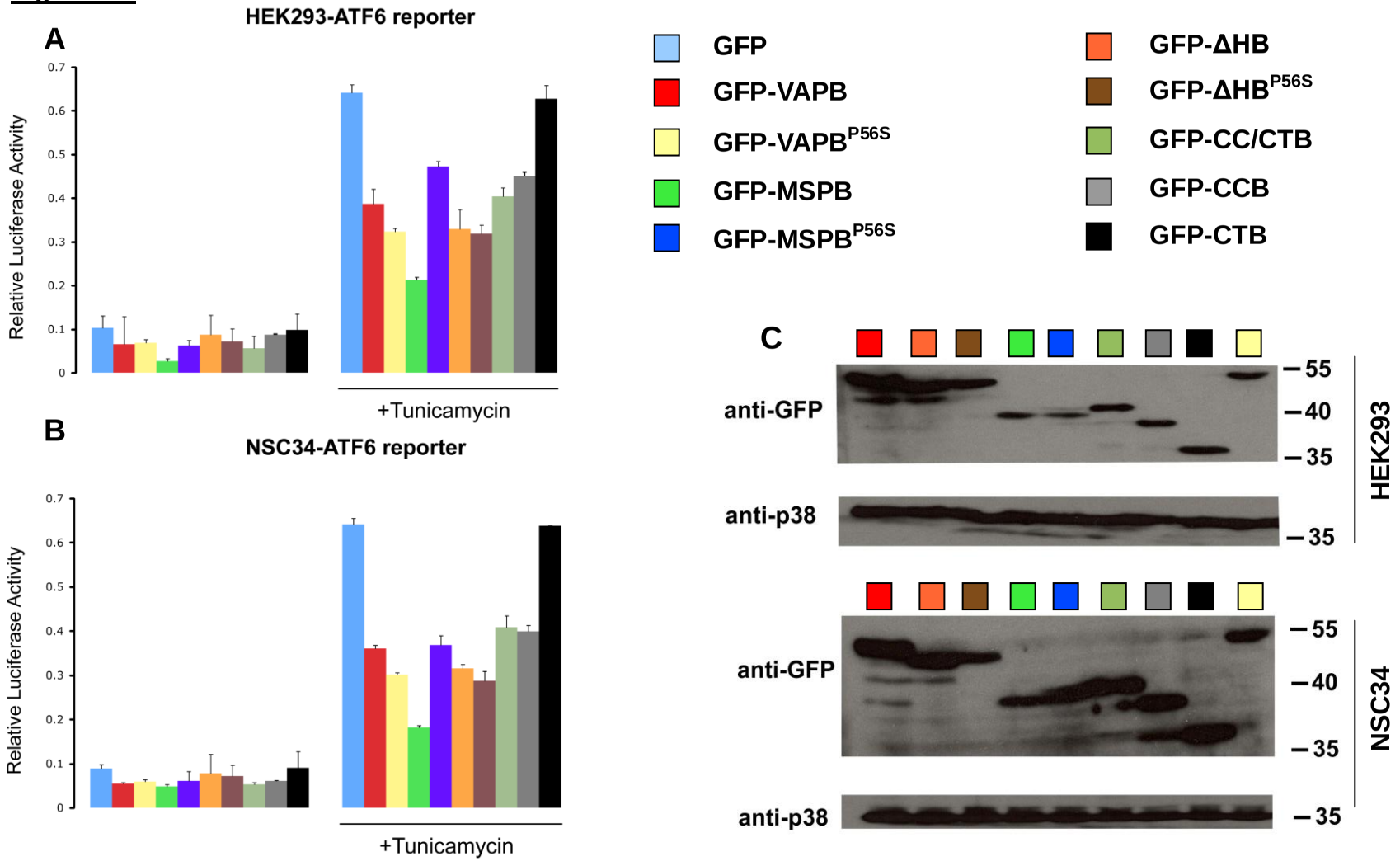
A
HEK293-ATF6 reporter
Relative Luciferase Activity
0.7
0.6
0.5
0.4
0.3
0.2
0.1
0
+Tunicamycin
B
NSC34-ATF6 reporter
Relative Luciferase Activity
0.7
0.6
0.5
0.4
0.3
0.2
0.1
0
+Tunicamycin
GFP
GFP-VAPB
GFP-VAPB P56S
GFP-MSPB
GFP-MSPB P56S
GFP-ΔHB
GFP-ΔHB P56S
GFP-CC/CTB
GFP-CCB
GFP-CTB
C
anti-GFP
anti-p38
55
40
35
35
HEK293
anti-GFP
anti-p38
55
40
35
35
NSC34

Figure 3.7 ***Effect of overexpression of mVAPB and mVAPB^{P56S} truncations on ATF6α transcriptional activation.***

A and **B.** In both HEK293 and NSC34 cells, overexpression of VAPB, VAPB^{P56S}, MSPB, MSPB^{P56S}, ΔHB, ΔHB^{P56S}, CC/CTB and CCB but not the CTB construct inhibits activation of ATF6α in tunicamycin treated samples as measured from the relative luciferase activity produced by transcriptional activation of the synthetic ATF6 promoter. Amongst the different truncations, MSP is the most potent inhibitor, while MSP^{P56S} cannot inhibit to the same extent. Results shown are averages of 4 experiments and error bars correspond to standard error (SE), p=0.031245.

C. Immunoblot of representative samples from the assayed for relative luciferase activity HEK293 and NSC34 samples. Relative expression of mVAPB, mVAPB^{P56S} and truncations EGFP constructs is shown; p38 is used as a loading control. Expression is similar for all VAPB truncation and full length constructs for HEK293 and NSC34 samples.

Figure 3.8

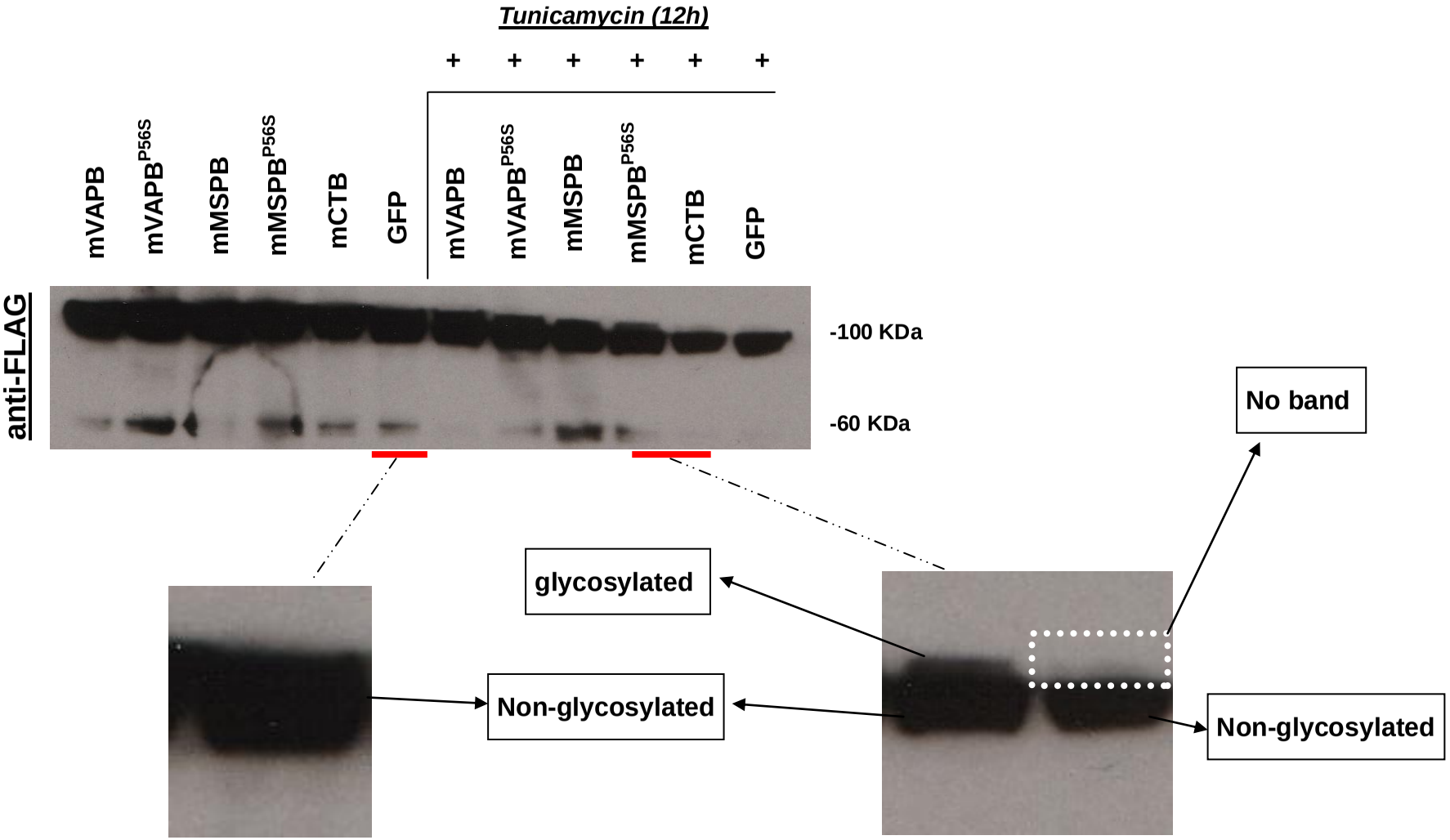
Tunicamycin (12h)
+ + + + + +
mVAPB
mVAPB^{P56S}
mMSPB
mMSPB^{P56S}
mCTB
GFP
mVAPB
mVAPB^{P56S}
mMSPB
mMSPB^{P56S}
mCTB
GFP
anti-FLAG
-100 KDa
-60 KDa
No band
glycosylated
Non-glycosylated
Non-glycosylated

Figure 3.8 ***Overexpression of mVAPB inhibits glycosylation associated activation of expressed human ATF6α in HEK293 cells***

HEK293 cells were transfected with the FLAG-tagged version of human ATF6α and co-transfected with GFP or mVAPB, mVAPB^{P56S}, mMSPB, mMSPB^{P56S} or mCTB. Cells were treated with tunicamycin for 12 hours. ATF6α when treated with tunicamycin is activated and this activation is correlated with its glycosylated and non-glycosylated forms; a doublet is formed after 1 hour of tunicamycin treatment (top band corresponds to glycosylated and lower band to non-glycosylated) while after 12 hours of treatment the top band of the doublet disappears. Magnification of the immunoblot shows the relative bands and the effect of tunicamycin treatment. Equal amounts of total protein (15 μg) were loaded in each lane, as determined using a micro-BCA protein assay.

single band in non-induced cells (equal amounts of total protein were loaded); after 12 hrs treatment with tunicamycin two bands are detected. At 100 KDa, the top band corresponds to the glycosylated form of ATFα, while the lower band is the non-glycosylated form. Consistent with the pattern of activation of ATF6α, the top band is reduced in intensity after 12 hours and this is correlated with ATF6α activation. When cells are co-transfected with mVAPB, mVAPB^{P56S}, mMSPB or mMSPB^{P56S}, we do not detect the same pattern as with GFP only. Two bands are now clearly visible at 100 KDa and both forms of ATF6α (glycosylated and non-glycosylated) are now detected; suggesting a reduced ATF6α activation. This result is consistent with the observed inhibition of ATF6α in the transcriptional assay. In addition, in the immunoblot a ~60 KDa band is detected. This band is the N-terminal proteolytic fragment of ATF6α, which migrates to the nucleus. ATF6α overexpression is known to activate promoters of various mammalian ER chaperone genes even in the absence of ER stress and induces the formation of the nuclear targeted fragment (Yoshida et al., 1998); for endogenous ATF6α, the proteolytic fragment is not formed without tunicamycin treatment, while here we can see it forming at basal condition. Nevertheless there is a difference at the quantity of the proteolytic fragment between wild-type and mutant constructs. Specifically, mVAPB^{P56S}, mMSPB and mMSPB^{P56S} overexpression samples when induced with tunicamycin for 12 hours retain the proteolytic fragment; while in CTB and GFP samples the fragment has disappeared. After tunicamycin treatment the fragment is reduced and that is basically due to its short half-life (Nadanaka et al., 2007, Yoshida et al., 2000); however we should note that these results should be verified for the endogenous protein, as expression of ATF6α interferes with the autoregulation of the molecule's activation (Yoshida et al., 1998). Despite that, this experiment clearly demonstrates that VAPB overexpression inhibits the activation of ATF6α as monitored by glycosylation of its luminal domain disulfide bond. The P56S mutant has the same effect, while the C-terminal has no effect.

3.9 Overexpression of full length and truncated wild type mVAPB but not mVAPB^{P56S}can rescue the effects of the siRNA mediated reduction of endogenous VAPB on the synthetic ATF6 promoter in HEK293 cells

ATF6α reporter transcriptional activation is inhibited by VAPB overexpression. All experiments so far were performed in cells where the endogenous protein was present while overexpressing the fusion-proteins. VAPB is known to form wild-type homodimers and heterodimers with the mutant protein, therefore when we express an EGFP VAPB or VAPB^{P56S} fusion protein (or truncation) we cannot discount the fact that they might interact with the endogenous protein. In this experiment, we used siRNA mediated reduction of endogenous hVAPB levels in HEK293 cells. Performing this experiment in HEK293 cells offers two advantages; blocking of endogenous VAPB expression with the human specific siRNA (Appendix I, #P22, #P23) and simultaneous expression of mouse EGFP constructs of VAPB, VAPB^{P56S} and truncations. As it can be seen in Figure 3.7B, application of the human specific siRNA does not block expression of VAPB EGFP fusion proteins and truncations. This can be explained by the fact that mouse and human sequences recognised by the siRNA are different as depicted in Figure 3.8. HEK293 cells were transfected with siRNA to endogenous hVAPB or GFP siRNA. After 24 hours cells were transfected with the ATF6 reporter and EGFP VAPB and VAPB^{P56S} full length proteins and truncations. Cells were cultured for another 24 hours and then treated with tunicamycin for 12 hours to induce an unfolded protein response of the ER (Figure 3.7A). None of the mP56S mutation constructs (full length VAPB^{P56S} MSPB^{P56S} and ΔHB^{P56S}) retain their full inhibitory effect on ATF6α when endogenous hVAPB expression is reduced by the siRNA; the relative luciferase activity measured is now comparable to the levels of the GFP control transfected samples. In contrast, wild type constructs: full length VAPB, MSPB and ΔHB constructs, retain their inhibitory effect on ATF6α activation. Moreover, Coiled-Coil and C-terminal tail CC/CTB, CCB do not inhibit ATF6α activation, when the endogenous hVAPB is blocked; while the CTB construct still exhibits no

Figure 3.7

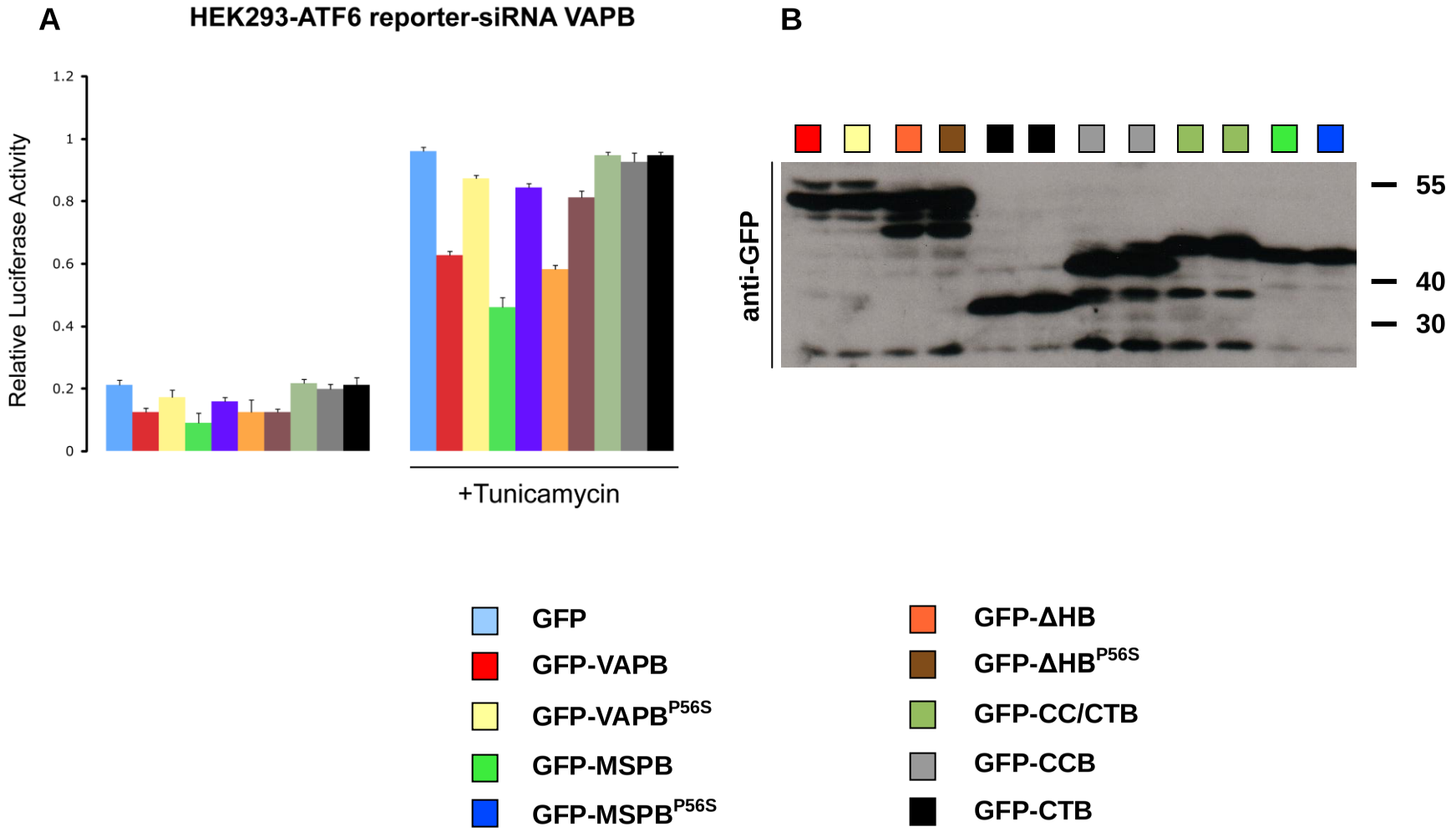
A
HEK293-ATF6 reporter-siRNA VAPB
Relative Luciferase Activity
1.2
1
0.8
0.6
0.4
0.2
0
+Tunicamycin
B
anti-GFP
55
40
30
GFP
GFP-VAPB
GFP-VAPB^P56S
GFP-MSPB
GFP-MSPB^P56S
GFP-ΔHB
GFP-ΔHB^P56S
GFP-CC/CTB
GFP-CCB
GFP-CTB

Figure 3.7 ***Effect of overexpression of mVAPB and mVAPB^{P56S} truncations on ATF6α transcriptional activation, when endogenous hVAPB is blocked by siRNA.***

A. HEK293 cells were transfected with siRNA to endogenous VAPB and then with the ATF6α reporter along with wild-type mVAPB and mVAPB^{P56S} full length and truncations EGFP constructs. P56S mutant constructs are no longer able to suppress transcriptional activation of ATF6α, while the wild-type constructs still retain their inhibitory effect. This trend is now evident and in baseline (no tunicamycin induction) levels of relative luciferase activity. Moreover the Coiled-Coil constructs (CC/CT and CCB) that displayed inhibition previously now have lost their repressive effect. Results shown are averages of 4 experiments and error bars correspond to standard error (SE)), p=0.031245.

B. Immunoblot of representative samples from the transcriptional assay in siRNA VAPB transfected HEK293 cells. This blot demonstrates that mouse constructs are not affected by the application of the siRNA and are expressed to similar levels as when the siRNA is not present (Figure 3.7C). On this blot some sample duplicates have been loaded. There is a discrepancy observed from other transcriptional assay immunoblots; the P56S full length now accumulates to similar levels as the wild-type. 30 μg of total protein were loaded; protein concentration was determined using a micro-BCA assay.

Figure 3.8

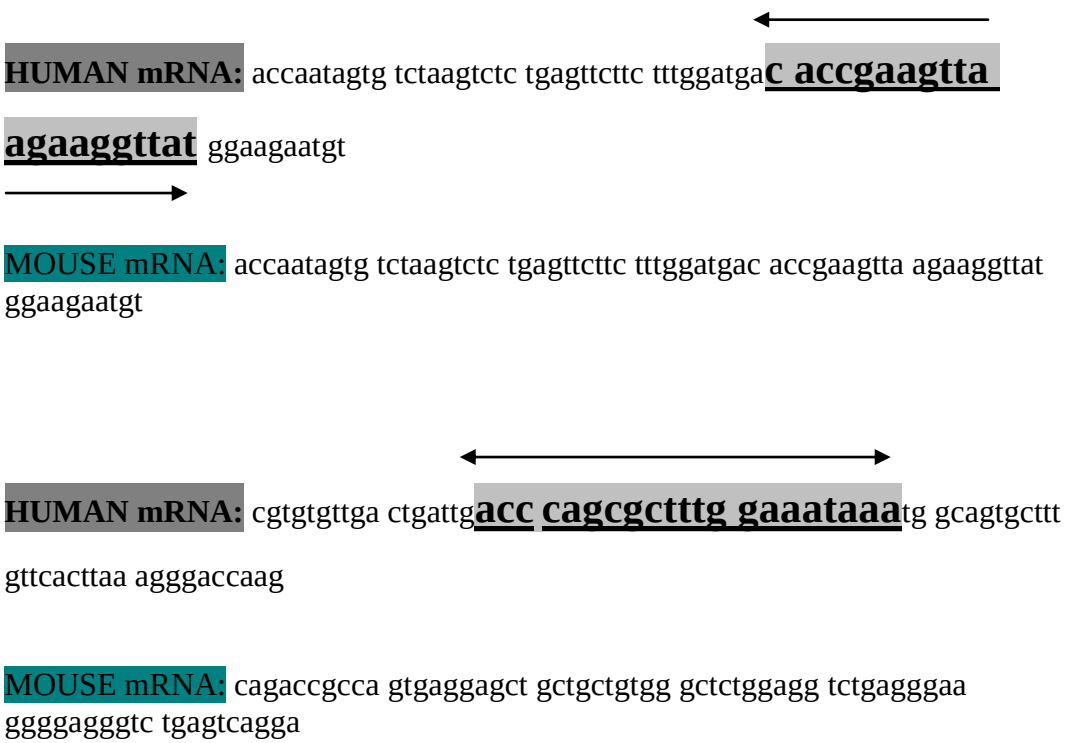

Figure 3.8 ***mRNA sequences of mouse and human vapB genes.***

Mouse and human mRNA sequences of vapB around areas where the two siRNAs bind (Appendix I, #P22, #P23). The two areas where the siRNAs bind (denoted by arrows) are different between mouse and human; a BLAST search with the nucleotides of the siRNAs returns only human vapB sequences and no mouse ones.

effect. This shows that the previously observed inhibitory effect of P56S and Coiled-Coil constructs on ATF6α transcriptional activation is dependent on the presence of the endogenous VAPB protein; this could be explained by the fact that VAPB homodimerizes, and thus P56S and Coiled-Coil expressed constructs can interact with the endogenous hVAPB gene in HEK293 cells.

3.10 Discussion

VAP proteins are integral membrane proteins that are enriched on the ER membrane. Data presented in this chapter support the earlier finding (Middleton, 2005) that VAPB interacts with the ER stress associated transcription factor ATF6α. In addition, VAP proteins modulate the activity of this transcription factor and therefore can potentially regulate a cell's response to stress induced by unfolded or misfolded protein accumulation in its Endoplasmic Reticulum (UPR). The ATF6α branch of the UPR includes many points of regulation, as ATF6α migrates from ER to Golgi, where it is proteolysed and subsequently targeted to the nucleus and interacts with ERSE promoter elements (Wang et al., 2000). Thus it can be concluded that ATF6α regulation can occur in different subcellular compartments and therefore a multitude of genes can be present at a given place. This chapter reports the novel interaction of ATF6α with VAP proteins and suggests a direct effect of it in ER stress modulation; also, it proposes a different regulation by the ALS8 associated P56S mutant.

VAP proteins interact with ATF6α

In this chapter we present evidence for a direct interaction between VAP proteins and ATF6α. As it was previously shown the MSP domain of VAPA interacts with ATF6α in a yeast two hybrid assay (Middleton, 2005). We demonstrate that VAPA, VAPB and VAPB^{P56S} interact with ATF6α in a fluorescent protein complementation assay, while the relevant b-zipper controls do not. This observation is important because it shows that full length VAP proteins can interact with ATF6α in HEK293 cells. Moreover ATF6α and VAPB and VAPB^{P56S} when expressed as fusion proteins display extensive colocalization. Although we were not able to co-

immunoprecipitate VAPB and ATF6α in a pull-down assay, this does not necessarily suggest that the interaction might be a false positive. Usually transient interactions cannot always be verified with a co-ip pulldown; moreover the commercial ATF6α antibody is not a particularly good antibody, as for the purposes of this study it has never worked to satisfactory standards. The direct interaction we are proposing is supported by the effect we are describing in this chapter. VAP overexpression or reduction of endogenous VAP by siRNA affect ATF6α activity as measured by the p5xGL3ATF6 luciferase reporter; in addition we demonstrate how VAPB can interfere with glycosylation associated activation of ATF6α. Nevertheless, a direct pull-down verification of the interaction would strengthen the hypothesis that we formulate in this chapter.

VAPB inhibits ATF6/XBP1 dependent transcription

As outlined in this chapter's background paragraph 3.1, the promoter used in p5xGL3ATF6 is not the endogenous promoter of ATF6α, but a synthetic promoter which has been shown to be responsive to changes in endogenous or expressed ATF6α (Wang et al., 2000). We have also shown that the reporter's activity is reduced when cells are co-transfected with ATF6α siRNA, but not GFP siRNA (Figure 3.4.4) and that the reporter is induced when FLAG tagged ATF6α is expressed. However we cannot discount the fact that as described in Wang et al. the promoter can be affected by other ER stress related components i.e. XBP1. Even so, in the next Chapter we proceed to demonstrate that VAPB affects the entire Unfolded Protein Response. In conclusion, from the aforementioned data and in conjunction with the proposed VAP-ATF6α interaction we can deduct that a significant amount of the observed inhibition or activation of the ATF6α reporter is ATF6α dependent.

Overexpression of VAPB and VAPB^{P56S} inhibits transcriptional activation of the ATF6α reporter in HEK293 and NSC34 cells. Conversely, siRNA mediated inhibition of endogenous VAPB induces the ATF6 reporter. Those two results clearly display a modulation of ATF6α activation as monitored by this reporter. After showing evidence for a direct interaction between VAPB and ATF6α we now demonstrate that this interaction has a functional effect. It becomes clear that levels of VAP proteins affect a cell's response to ER stress via ATF6α; as it has been shown

by other groups VAP overexpression and reduction of endogenous levels affect the UPR (Kanekura et al., 2006).

The ALS8 associated P56S mutant may be a stronger inhibitor of ATF6α than the wild-type

When VAPB and VAPB^{P56S} are overexpressed, they both inhibit ATF6α activation to the same extent; however, when samples from the assay are probed for protein expression, VAPB^{P56S} always accumulated to lower levels than the wild-type protein. This finding may suggest that for the same amount of protein, the P56S mutant is a stronger inhibitor of ATF6α. In both myc and EGFP fusion proteins, the mutant is always found in lower levels, but the GFP moiety seems to have a stabilizing effect on the mutant protein and in the EGFP fusions, the difference is less than the myc between wild-type and mutant. This finding is true in both HEK293 and NSC34 cells. Moreover when increasing amounts of DNA are used, the mutant P56S for the same amount of protein inhibits ATF6α more (Figure 3.6.2). While other groups have associated VAPB^{P56S} with the UPR in general (Kanekura et al., 2006), this is the first reported difference regarding the ATF6α branch of the UPR. Evidently, this suggests that the UPR can be misregulated by P56S, as greater inhibition of ATF6α can lead to a reduced response to ER stress, which can lead a cell (or a motor neuron in ALS8) to death. However, the P56S mutant forms cytoplasmic aggregates that may increase the insolubility of the protein and render it less accessible to the antibody. In addition, the P56S mutant may not be as stable as the wild-type and therefore proteolysed and degraded. Our VAPB domain analysis in this chapter highlights a different aspect of this issue.

ATF6α and the various domains of VAPB

The ATF6α-VAP interaction was first identified using the MSP domain. When VAPB truncations (EGFP fusions of functional domains of VAPB as predicted from its sequence and homology or similarity to known protein architectures) are overexpressed, they still display the inhibitory effect observed for the full length sequences (apart from the hydrophobic tail construct); MSP is the most potent inhibitor of ATF6α and MSP^{P56S} does not inhibit to the same levels as the wild-type;

the CC/CTB and CCB constructs still inhibit, while the C-terminal anchor does not. This analysis reveals that the MSP domain is the strongest inhibitor of the ATF6α reporter, while the P56S mutant of the MSP cannot retain this functionality; the same trend is not observed for the ΔH constructs, as ΔH^{P56S} inhibits the same as ΔH; the coiled-coil domain of VAPB inhibits ATF6α activation, while the C-terminal anchor has no effect.

Thus, the cytoplasmic domains of VAPB when overexpressed modulate the activity of ATF6α; as predicted, the C-terminal has no effect. This functional effect reveals a potentional regulatory complex formed on the ER membrane by VAPB and ATF6α, with their cytoplasmic portions interacting and affecting activation of ATF6α. The MSP domain has the highest affinity for ATF6α and the Coiled-Coil also participates in this modulation. For the VAPB mutant, the Coiled-Coil still has the same effect, but the P56S MSP cannot inhibit to the same extent as wild-type MSP. This preliminary observation is further discussed and more aspects of it are revealed when the interaction of expressed fusion proteins with the endogenous protein is considered.

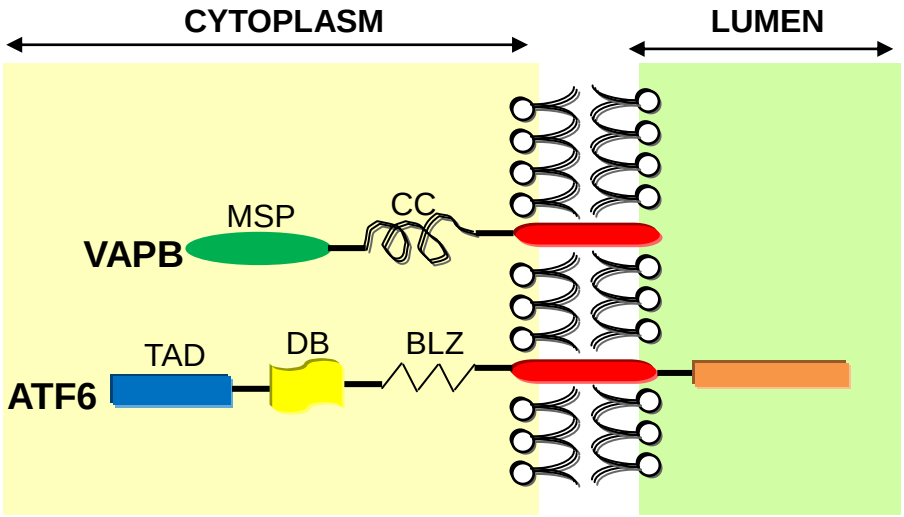

Figure 3.9 ***ATF6α and VAPB on the ER membrane.***

The cytoplasmic portion of VAPB contains the MSP and CC domains. The transmembrane anchor is buried in the phospholipid bilayer of the ER membrane.

ATF6's cytoplasmic part contains the Transcriptional Activation Domain, the Basic DNA Binding Motif and a Basic Leucine Zipper.

The effect of the P56S mutant on ATF6α is dependent on the presence of the endogenous protein

When VAPB fusion proteins are expressed in HEK293 or NSC34 cells, the endogenous protein is present. The endogenous protein affects (without any VAPB construct expressed) ATF6α activation, because siRNA mediated blocking of endogenous VAPB expression induces the ATF6α reporter (Figure 3.5). VAPB overexpression could affect endogenous VAPB as VAP proteins are known to homo/heterodimirize. In HEK293 cells we can reduce the endogenous human protein expression and simultaneously express the mouse EGFP fusion proteins that are "insensitive" to the siRNA, as the recognition sequence varies between mouse and human (see Figure 3.7B and Figure 3.8). By doing this we can study the effect of overexpression when the endogenous protein levels are reduced. This experiment reveals that the P56S mutant (full length and truncations) are dependent on the presence of the endogenous protein, as the previously observed inhibitory effect is now reduced or totally abolished; the P56S constructs cannot rescue the overexpression effect. Conversely, the wild-type VAPB full length, ΔH and MSP still inhibit ATF6α activation.

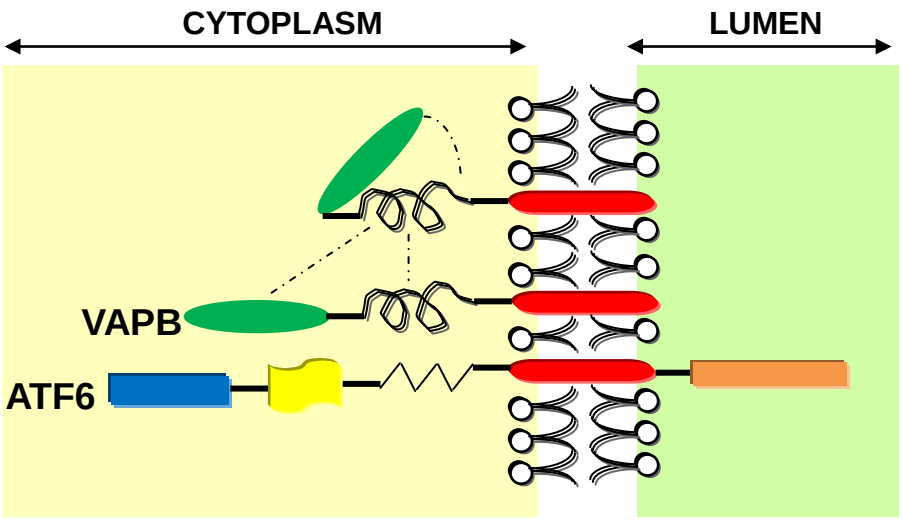

Figure 3.10 ***Model for the modulation of ATF6α activity via the VAPB Coiled-Coil domain.***

Overexpression of the CC domain of VAPB inhibits activation of ATF6α; this effect is dependent on the presence of the endogenous protein during overexpression. The CC could potentially modulate the activity of ATF6α by interfering with other VAPB molecules (their MSP or CC domains) or autoregulate a given VAPB molecule (by interacting with the MSP domain).

This experiment also highlights an important aspect of the CC effect on ATF6α. SiRNA mediated reduction of expression of endogenous VAPB blocks the effect of overexpression of the CCB; activation levels are now comparable to the GFP control. From this we can speculate that the overexpression of CCB interferes with endogenous VAPB in a way that ATF6α activation is blocked; this effect is not seen when the endogenous protein levels are reduced. Therefore, CCB overexpression could potentially interfere with the VAP-ATF6α interaction by interacting with the endogenous protein Coiled-Coil or the MSP domain. Nevertheless, the Coiled-Coil of VAPB could affect the regulation of ATF6α activity by VAPB either via other VAPB molecules or via interactions within a VAPB molecule (MSP-CC interaction, see Figure 3.10).

One possible mechanism for ATF6α regulation by VAPB

When VAPB and VAPB^{P56S} are overexpressed in the presence of the endogenous VAPB protein, ATF6 activitation as monitored by the p5xGL3ATF6 reporter is inhibited. This inhibition observed can be either by retention of ATF6 on the ER membrane, or by blocking its migration to Golgi, or even by blocking binding of nuclear ATF6α on ERSE promoter elements. Reduction of the luminal disulfide bond and glycosylation of ATF6α are correlated with activation of ATF6α. Here we show that overexpression of VAPB, VAPB^{P56S}, MSP, MSP^{P56S} but not CTB or GFP inhibit glycosylation associated activation of ATF6. This could be one of the regulation points of VAPB over ATF6α. The experiment provides one possible explanation for the observed inhibition; however VAPB could be acting in the Golgi

or nucleus where ATF6α is shuttled.

Chapter Conclusion

In this chapter we show a direct effect of the VAPB-ATF6α interaction; overexpression of VAPB and $VAPB^{P56S}$ inhibit ATF6α activation, while siRNA to endogenous VAPB induces ATF6α. The mutant protein accumulates to lower levels than the wild-type protein. VAPB domains (MSP, CC but not CT; MSP is the most potent inhibitor) inhibit ATF6α activation and the observed effect is dependent on the presence of the endogenous protein. In conclusion, the ALS8 associated P56S mutant displays a gain of negative function (inhibition) behaviour regarding ATF6α activity, which is dependent on its wild-type allele.

Chapter 4

VAPB, regulation of the UPR and cell death

4.1 Background

In the previous Chapter we show that VAPB interacts with and modulates the activity of the Unfolded Protein Response associated transcription factor ATF6α (Gkogkas et al., 2008). The reporter used in the previous Chapter is a synthetic reporter (Wang et al., 2000) that apart from ATF6α binds other UPR associated elements like XBP1. This suggests that apart from the VAP-ATF6α interaction, VAP might participate in regulation of the UPR via other promoter elements. Moreover, ATF6α and XBP1 form heterodimers (Yamamoto et al., 2007) and display single and combined action in UPR activation. ATF6 and XBP1 act on Endoplasmic Reticulum Stress Response Elements – ERSEs (CCAAT-N9-CCACG motif) and activate transcription of UPR chaperones (i.e. BiP/GRP78) and associated genes. For that matter we will study regulation of the UPR by VAP proteins using the following two reporter-constructs:

- pGL3-XBP1(-330)-luc (Yoshida et al., 2000)(Appendix I, #P19-termed the XBP1 reporter)
- pGL3-GRP78(-132)-luc (Yoshida et al., 1998) (Appendix I, #P20-termed the BiP reporter)

The XBP1 reporter contains the human XBP1 promoter fused to the firefly luciferase gene. Transcription is regulated by the hXBP1 promoter which has a size of 459 bp (-330 to +129, 0 indicates beginning of transcription – Figure 4.1A). This reporter is responsive to ER stress inducers. The hXBP1 promoter contains an ERSE element in the region from +32 to +65. When this element is deleted, the relative XBP1 reporter is no longer responsive to ER stress induction (Figure 4.1.A).

The BiP/GRP78 reporter contains the human BiP promoter fused to the firefly luciferase gene. Transcription is regulated by the hBiP/GRP78 promoter which has a size of 397 bp (-363 to +34, 0 indicates beginning of transcription – figure 4.1.A and B). This reporter is responsive to ER stress inducers. The hBiP promoter contains 3

Figure 4.1

Taken from Yoshida et al., 1998 and 2000

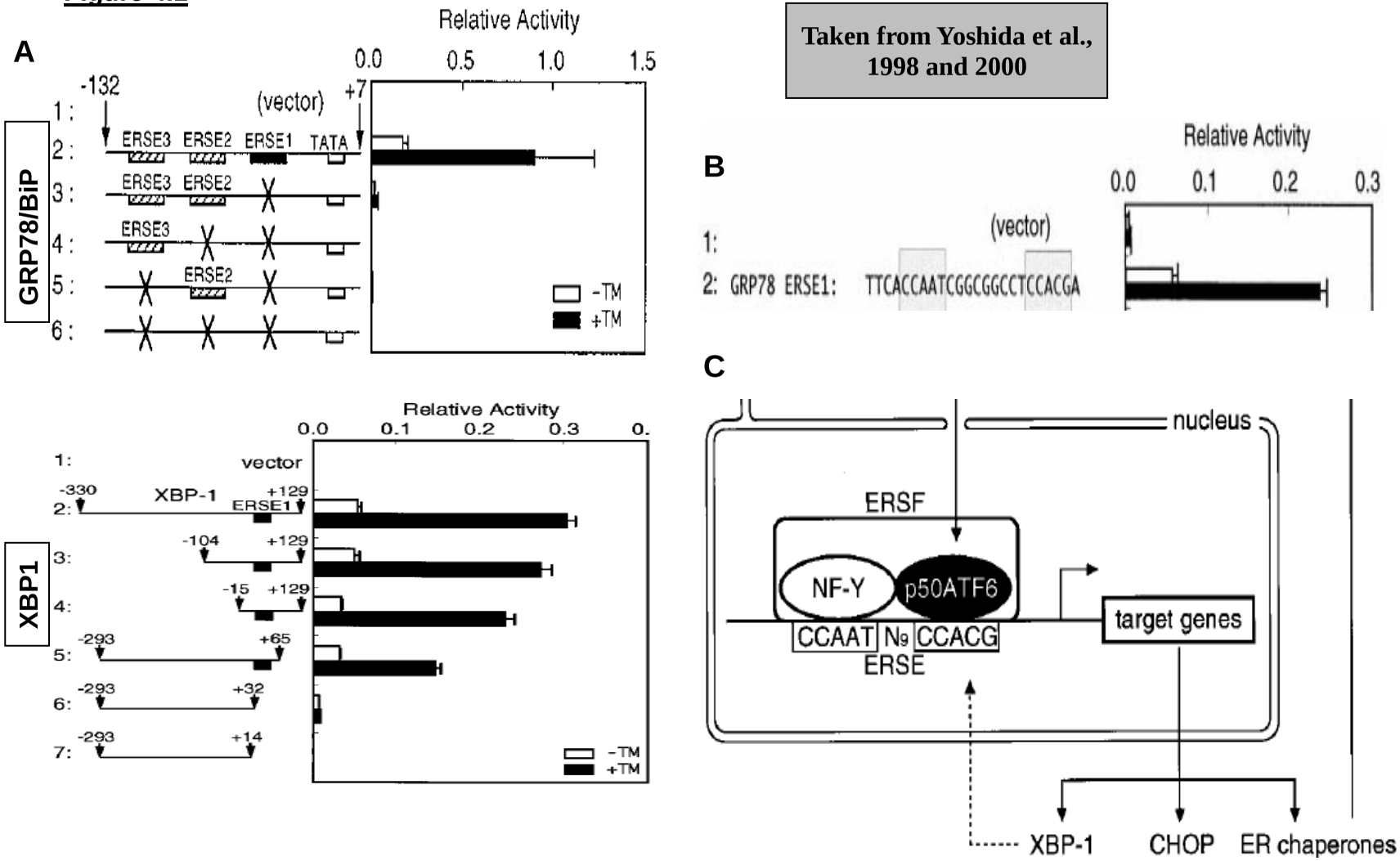

Figure 4.1 XBP1 and BiP *UPR associated promoter elements (from (Yoshida et al., 1998, Yoshida et al., 2000).*

A., B. Analysis of the XBP1 and BiP promoters using Luciferase based transcription assays. HeLa cells were transfected with human XBP1 or GRP78 promoter luciferase based reporter constructs and scrambled versions (deletion of promoter regions or mutation of ERSE elements) and then ER stress was induced with 2 μg/ml tunicamycin for 16 hours. The right panels depict relative luciferase activity. For BiP, scrambling ERSE1 makes the promoter insensitive to ER stess induction with tunicamycin. ERSE2 and ERSE3 together or individually cannot induce transcription after ER stress, while ERSE1 (seen in B) can induce transcription of a luciferase construct following ER stress. Deletion analysis of the human XBP1 promoter fused to the firefly luciferase gene reveals that the ERSE1 sequence is essential for initiating transcription following ER stress. Results are averages of 4 experiments and error bars correspond to standard error (SE).

C. Schematic representation of ATF6 and XBP1 binding to ERSE promoter elements in the nucleus and subsequent activation of transcription of UPR associated chaperones.

ERSE elements termed ERSE1 (-61 to -37), ERSE2 (-94 to -76) and ERSE3 (-126 to -114). ERSE1 is the only element out of three that can initiate transcription of a luciferase gene in a reporter construct following ER stress. Thus, the role of the ERSE2 and ERSE3 elements is not known.

Kanekura et al., 2006 showed that VAPB overexpression can induce the IRE1 pathway by promoting splicing of an immature XBP1 mRNA reporter construct, while the P56S mutant of VAPB cannot. In addition, siRNA to endogenous VAPB reduces splicing of the reporter construct. This study reveals a connection of VAP proteins with the IRE1 branch of the UPR.

In this Chapter we will study regulation of the UPR by VAP proteins using the XBP1 and BiP human endogenous promoters in luciferase based reporter contructs. As with ATF6α we will examine here also the effect of VAPB domains (Table 3.1) and especially the MSP domain.

4.2 VAPB and XBP1 and BiP promoters

4.2.1 Overexpression of full length and truncated forms of mVAPB and mVAPB^{P56S} in HEK293 and NSC34 cells inhibits transcriptional activation from the human promoter of XBP1

In Chapter 3 we showed that VAPB interacts with and modulates the activity of the ER stress associated transcription factor ATF6α and in order to investigate whether the other pathways of the Unfolded Protein Response were affected we used a human XBP1 promoter luciferase based construct (Appendix I, #P19). HEK293 or NSC34 cells were transfected with all the mouse VAPB and VAPB^{P56S} EGFP constructs previously described along with the XBP1 reporter and the internal renillin (Appendix I, #P21) control plasmid (Figure 4.2). Tunicamycin treatment induces the XBP1 reporter by 6-fold. Although basal levels of transcription do not seem to be affected, there is inhibition of the activity of the XBP1 promoter when cells are induced with tunicamycin. This inhibition is true for VAPB (50%), VAPB^{P56S} (50%), MSPB (66%), MSPB^{P56S} (33%), ΔHB (49%) and ΔHB^{P56S} (48%), but not for the CC/CTB, CCB and CTB constructs. To strengthen this finding we use HEK293 cells and motor neuron-like NSC34 cells and results are consistent in the two different cell types. Therefore, the Coiled-Coil and C-terminal anchor domains of VAPB do not seem to affect XBP1 promoter dependent transcription, while MSPB^{P56S} inhibits less that wild-type MSPB. Expression of VAPB-EGFP constructs is previously shown in Figure 3.7 Chapter 3.

4.2.2 Overexpression of full length and truncated forms of mVAPB and mVAPB^{P56S} in HEK293 and NSC34 cells induces transcriptional activation from the human promoter of BiP/GRP78

BiP/GRP78 is a key component of the Unfolded Protein Response. We have shown that VAPB affects the activity of the ATF6α synthetic promoter and the hXBP1 promoter and to check whether the hBiP promoter is affected, we used a human GRP78 promoter luciferase based construct (Appendix I, #P20, #P21).

Figure 4.2

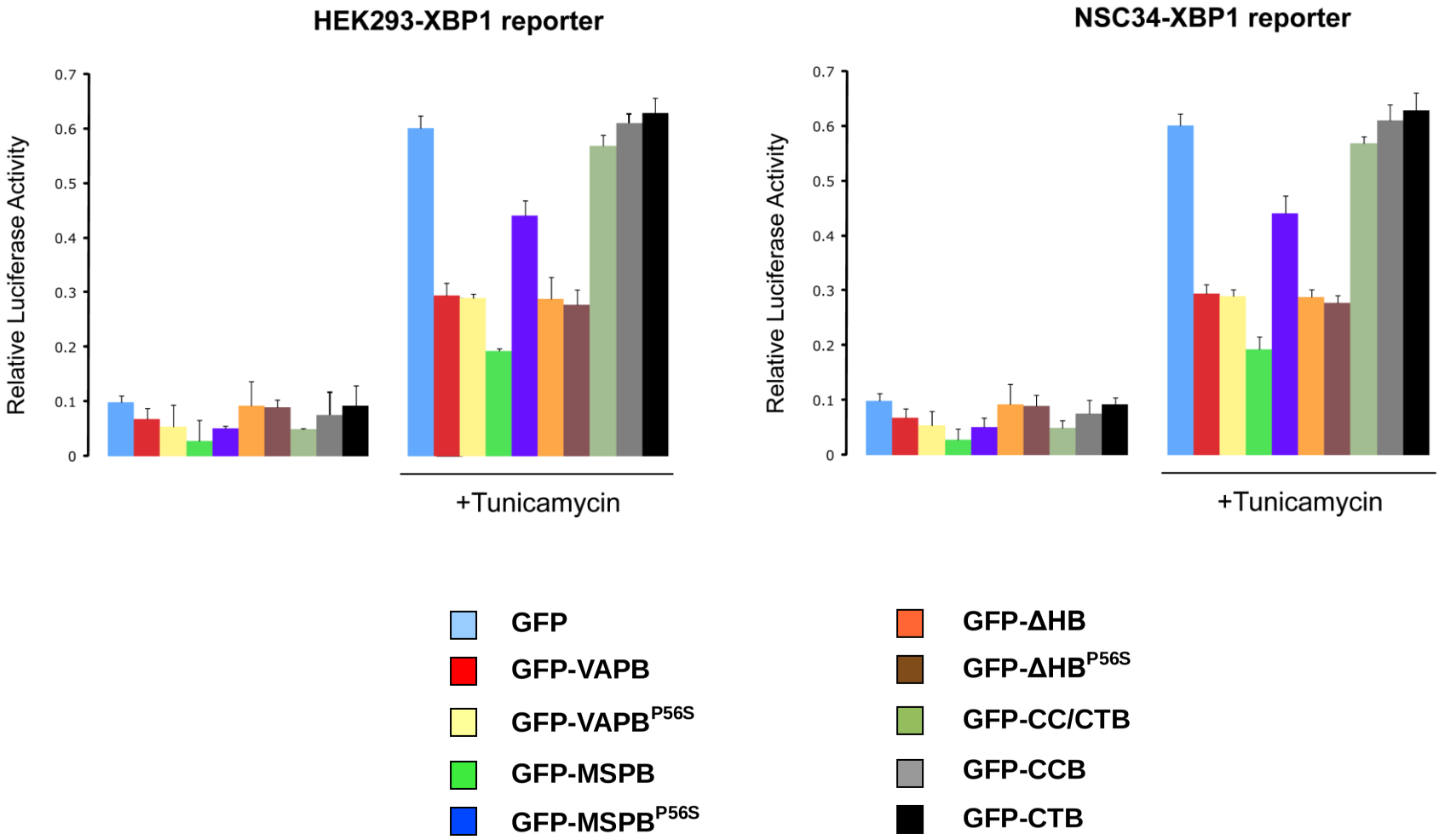
HEK293-XBP1 reporter
NSC34-XBP1 reporter
Relative Luciferase Activity
0.7
0.6
0.5
0.4
0.3
0.2
0.1
0
+Tunicamycin
GFP
GFP-VAPB
GFP-VAPB P56S
GFP-MSPB
GFP-MSPB P56S
GFP-ΔHB
GFP-ΔHB P56S
GFP-CC/CTB
GFP-CCB
GFP-CTB

Figure 4.2 ***Effect of overexpession of mVAPB and mVAPB^{P56S} on human XBP1 promoter dependent transcription.***

In both HEK293 and NSC34 cells, overexpression of VAPB, VAPB^{P56S}, MSPB, MSPB^{P56S}, ΔHB and ΔHB^{P56S}, but not CC/CTB, CCB and CTB constructs inhibits activation of the XBP1 reporter in tunicamycin treated samples as measured from the relative luciferase activity produced by transcriptional activation of the human XBP1 promoter. Amongst the different truncations, MSP is the most potent inhibitor, while MSP^{P56S} cannot inhibit to the same extent. Results shown are averages of 4 experiments and error bars correspond to standard error (SE)), p=0.027114).

Figure 4.3

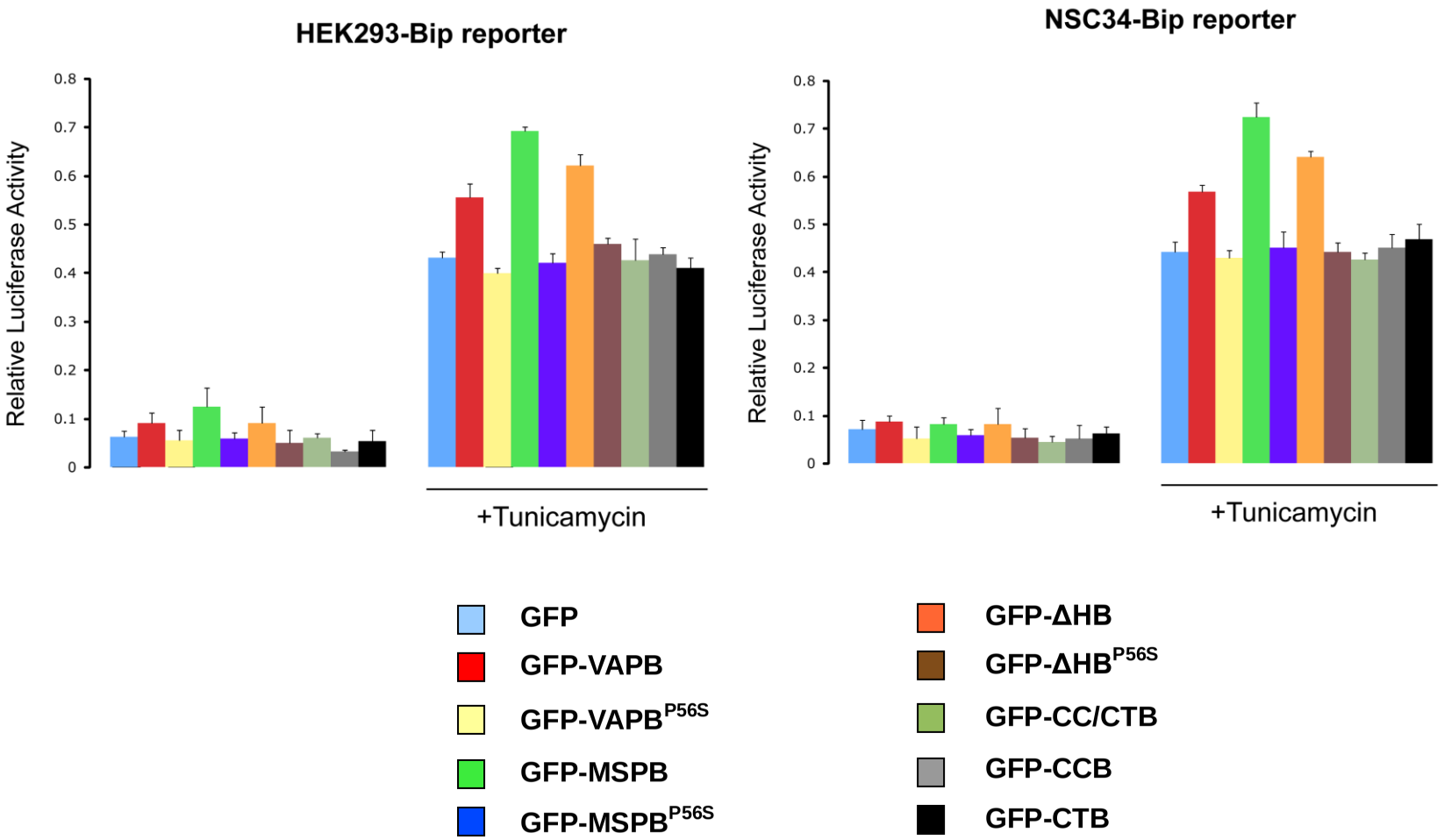
HEK293-Bip reporter
NSC34-Bip reporter
Relative Luciferase Activity
0.8
0.7
0.6
0.5
0.4
0.3
0.2
0.1
0
+Tunicamycin
GFP
GFP-VAPB
GFP-VAPB^P56S
GFP-MSPB
GFP-MSPB^P56S
GFP-ΔHB
GFP-ΔHB^P56S
GFP-CC/CTB
GFP-CCB
GFP-CTB

Figure 4.3 ***Effect of overexpession of VAPB and VAPB^{P56S} on human BiP promoter dependent transcription.***

In both HEK293 and NSC34 cells, overexpression of VAPB, MSPB and ΔHB but not VAPB^{P56S}, MSPB^{P56S}, ΔHB^{P56S}, CC/CTB, CCB and CTB constructs potentiate activation of the BiP reporter in tunicamycin treated samples as measured from the relative luciferase activity produced by transcriptional activation of the human BiP promoter. Amongst the different truncations, MSP is the most potent activator, while MSP^{P56S} does not affect BiP activity. Results shown are averages of 4 experiments and error bars correspond to standard error (SE)), p=0.021568.

Transcriptional assay was carried out as previously. Overexpression of the various constructs does not affect basal levels of transcription but there is potentiation of the activity of the BiP reporter when cells are induced with tunicamycin (Figure 4.3). This potentiation is true for VAPB (25%), MSPB (62%) and ΔHB (50%) but not for the $VAPB^{P56S}$, $MSPB^{P56S}$, ΔHB^{P56S}, CC/CTB, CCB and CTB constructs. Thus, it seems that the P56S mutation in VAPB and its truncations that contain the MSP domain cannot induce the BiP reporter, unlike the wild-type constructs. Moreover, overexpression of the Coiled-Coil and C-terminal anchor domains of VAPB do not activate transcription from the human BiP promoter more than control samples (GFP).

4.2.3 siRNA mediated reduction of expression of endogenous hVAPB in HEK293 cells has a differential effect on basal and induced activity levels of the XBP1 and Bip reporters

As it was previously shown for ATF6α, reducing endogenous VAPB levels using siRNA induces the activity of the ATF6α reporter, which is the opposite effect from overexpressing mVAPB. The same experiment was conducted for the XBP1 and BiP reporters to check whether reduced expression of the endogenous protein had the opposite effect from overexpression (Figure 4.4). For the XBP1 reporter, siRNA to VAPB increases basal and induced levels of transcription; in Figure 4.2 it is shown that overexpression of VAPB inhibits the activation of the XBP1 reporter and now we show that siRNA mediated reduction of endogenous VAPB levels has the opposite effect. Conversely, siRNA to endogenous VAPB reduces the activity of the BiP reporter in non-induced and induced samples; this is the opposite from the activation of the BiP reporter that is observed when VAPB is overexpressed in Figure 4.3. In this experiment GFP siRNA is used as a control. Western blot analysis of representative samples shows that VAPB siRNA reduces the amount of expressed endogenous VAPB in HEK293 cells, while GFP siRNA does not.

Figure 4.4

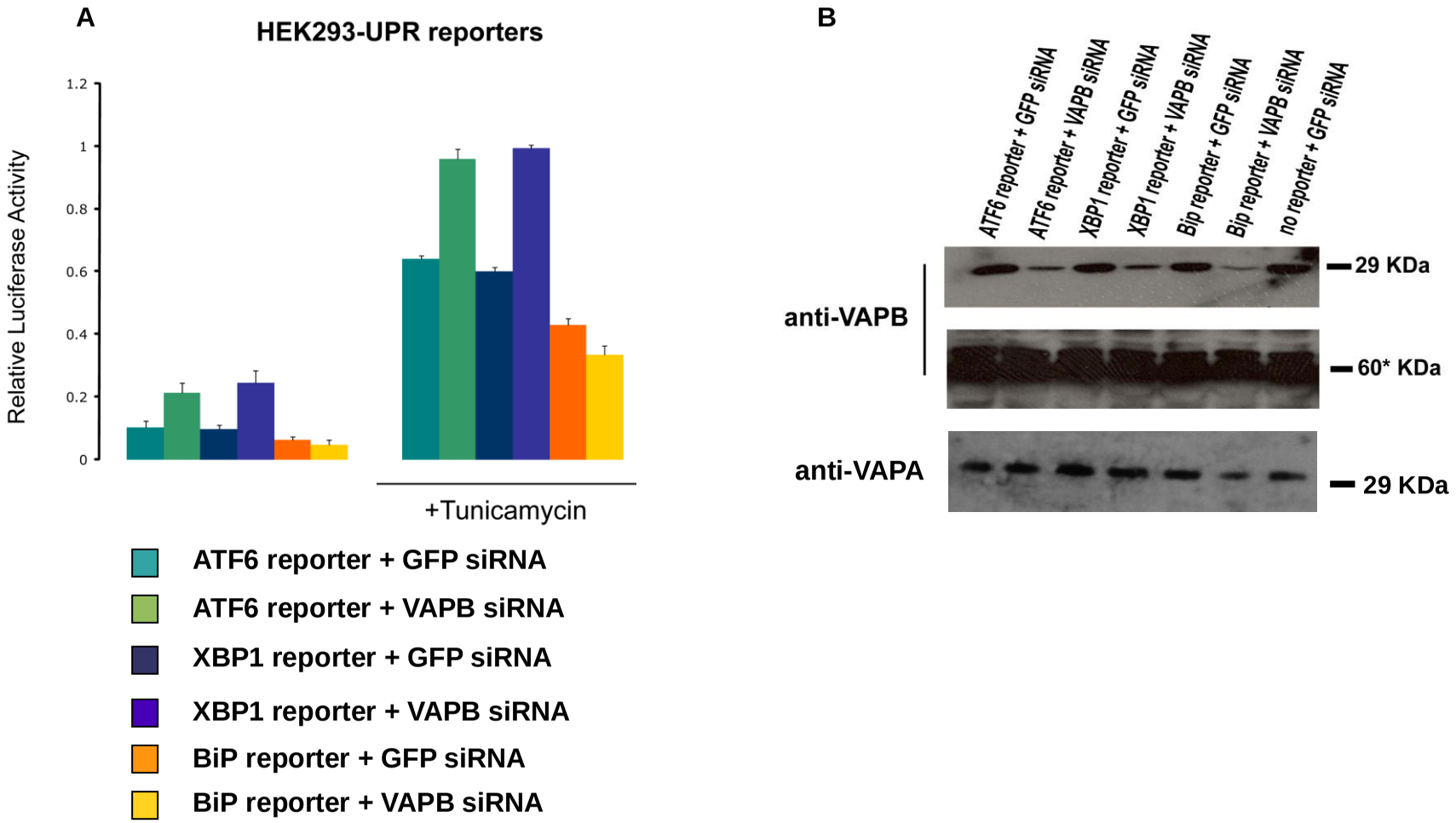
A
HEK293-UPR reporters
Relative Luciferase Activity
1.2
1
0.8
0.6
0.4
0.2
0
+Tunicamycin
ATF6 reporter + GFP siRNA
ATF6 reporter + VAPB siRNA
XBP1 reporter + GFP siRNA
XBP1 reporter + VAPB siRNA
BiP reporter + GFP siRNA
BiP reporter + VAPB siRNA
B
ATF6 reporter + GFP siRNA
ATF6 reporter + VAPB siRNA
XBP1 reporter + GFP siRNA
XBP1 reporter + VAPB siRNA
Bip reporter + GFP siRNA
Bip reporter + VAPB siRNA
no reporter + GFP siRNA
anti-VAPB
29 KDa
60* KDa
anti-VAPA
29 KDa

Figure 4.4 ***Effect of siRNA mediated reduction of endogenous VAPB expression on the transcriptional activation of XBP1 and BiP reporters.***

A. HEK293 cells were transfected with siRNA to endogenous VAPB and then with ATF6, XBP1 or BiP reporters; ATF6 results are a repeat of the Chapter 3.7, Figure 3.5 experiment. Reduction of endogenous VAPB levels affects both basal and induced levels of XBP1 and BiP reporters. For XBP1, there is an increase in relative luciferase activity by 33%, while for BiP there is a 5% reduction which is statistically significant by a one-way ANOVA ($p=0.001238$). Results shown are averages of 4 experiments and error bars correspond to standard error (SE).

B. Immunoblot of representative samples from the assayed for luciferase activity HEK293 cells. GFP siRNA is used as a control. There is a significant reduction of endogenous VAPB in siRNA treated samples but there is not a 100% inhibition of expression of endogenous VAPB protein. *A 60 kDa non-specific band from longer exposures of the immunoblot serves as a loading control. Also staining with the endogenous VAPA antibody is shown.

4.2.4 Wild type mVAPB but not mVAPB^{P56S} can rescue the effects of the siRNA mediated reduction of endogenous hVAPB protein levels on XBP1 and BiP reporters in HEK293 cells

In order to examine whether inhibition of XBP1 and induction of BiP reporter activities are dependent on the presence of the endogenous VAPB protein we used siRNA mediated reduction of expression of endogenous hVAPB in HEK293 cells as described in Chapter 3.9. None of the mP56S mutation constructs (full length VAPB^{P56S} MSPB^{P56S} and ΔHB^{P56S}) retain their full inhibitory effect on XBP1 reporter activation when siRNA to endogenous hVAPB is applied; the relative luciferase activity measured is now comparable to the levels of the GFP control transfected samples. In contrast, wild type constructs: full length VAPB, MSPB and ΔHB constructs, retain their inhibitory effect on the XBP1 reporter, while coiled-coil and C-terminal tail CC/CTB, CCB and CTB constructs still exhibit no effect. This shows that the previously observed inhibitory effect of P56S constructs on transcriptional activation from the hXBP1 promoter is dependent on the presence of the endogenous hVAPB protein in HEK293 cells (Figure 4.5). For the BiP reporter in HEK293 cells, P56S constructs did not have an effect on BiP activation in Figure 4.3. When VAPB siRNA is applied, overexpression of wild type mVAPB constructs: VAPB, MSPB and ΔHB, still potentiates the transcriptional activity of the BiP reporter. P56S mutation, coiled coil and C-terminal tail constructs still did not have an effect on transcriptional activation via the BiP promoter (Figure 4.5).

Figure 4.5

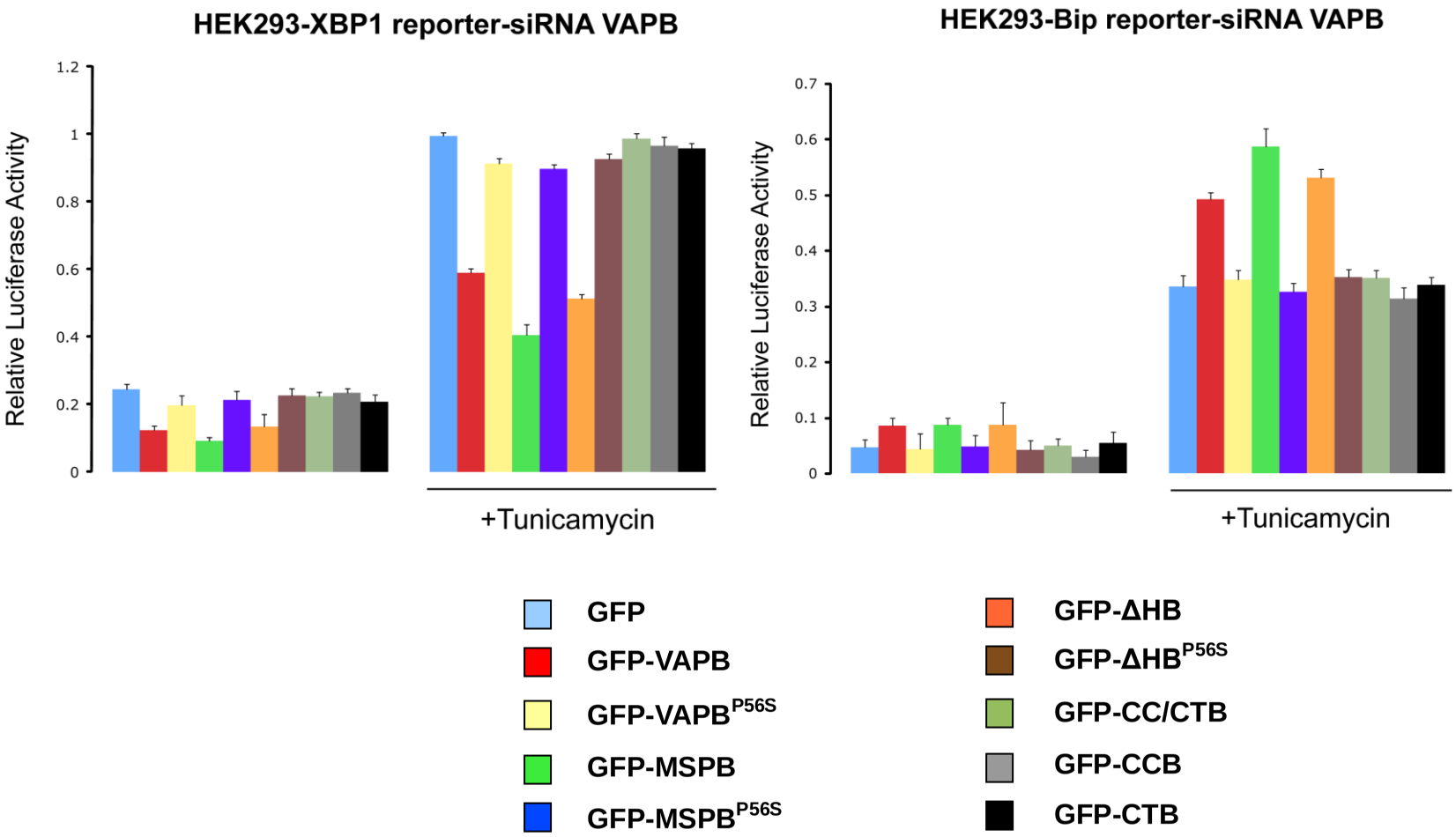
HEK293-XBP1 reporter-siRNA VAPB
Relative Luciferase Activity
1.2
1
0.8
0.6
0.4
0.2
0
+Tunicamycin
HEK293-Bip reporter-siRNA VAPB
Relative Luciferase Activity
0.7
0.6
0.5
0.4
0.3
0.2
0.1
0
+Tunicamycin
GFP
GFP-VAPB
GFP-VAPB P56S
GFP-MSPB
GFP-MSPB P56S
GFP-ΔHB
GFP-ΔHB P56S
GFP-CC/CTB
GFP-CCB
GFP-CTB

Figure 4.5 ***Effect of overexpression of mVAPB and mVAPB^{P56S} full length proteins and truncations on XBP1 and BiP reporters' activity in HEK293 cells, when endogenous hVAPB expression is reduced by siRNA.***

HEK293 cells were transfected with siRNA to endogenous hVAPB and then with XBP1 or BiP reporters along with wild-type mVAPB and mVAPB^{P56S} full length and truncated EGFP constructs. In tunicamycin treated samples, for XBP1, overexpression of the P56S mutant did not suppress the activation of the XBP1 reporter, while the wild-type constructs retained their inhibitory effect. This trend is now evident and in baseline (no tunicamycin induction) levels of relative luciferase activity. Similarly, for the BiP reporter, reduction of endogenous hVAPB expression levels does not affect potentiation by overexpression of wild-type VAPB. However, overexpression of P56S mutation constructs still had no effect. Results shown are averages of 4 experiments and error bars correspond to standard error (SE), p=0.018248.

4.3 Overexpression of mVAPB and mVAPB^{P56S} domains in NSC34 increases cell death following ER stress

Misregulation of the UPR has been associated with neurodegeneration (Paschen and Mengesdorf, 2005). We proceeded to examine whether overexpression of the MSP domain and other VAPB domains had an effect on cell survival after ER stress. There is increasing evidence in literature associating misregulation of the Unfolded Protein Response with apoptotic cell death in neurodegenerative disease (Paschen and Mengesdorf, 2005, Wu and Kaufman, 2006). Therefore we wanted to investigate whether the observed regulation of the UPR by overexpression of VAPB domains had an effect on cell viability following ER stress in the motor-neuron like cell line NSC34. For this experiment NSC34 cells were transfected with VAPB expression plasmids, washed, induced with 2 μg/ml tunicamycin for 12 hours, washed again, cultured for another 12 hours and finally assayed for viability using propidium iodide or the Cytotox Glo^{TM} cytotoxicity assay (Figure 4.6.1). NSC34 cells overexpressing GFP, tubulin or the C-terminal of VAPB (CTB) did not display reduced viability after ER stress. However, cells overexpressing VAPB, VAPB^{P56S}, MSPB, MSPB^{P56S}, ΔHB, ΔHB^{P56S}, CC/CTB, CCB but not CTB display an increase in cell death as measured by the two assays after tunicamycin induced ER stress (also see Figure 4.6.2).

Figure 4.6.1

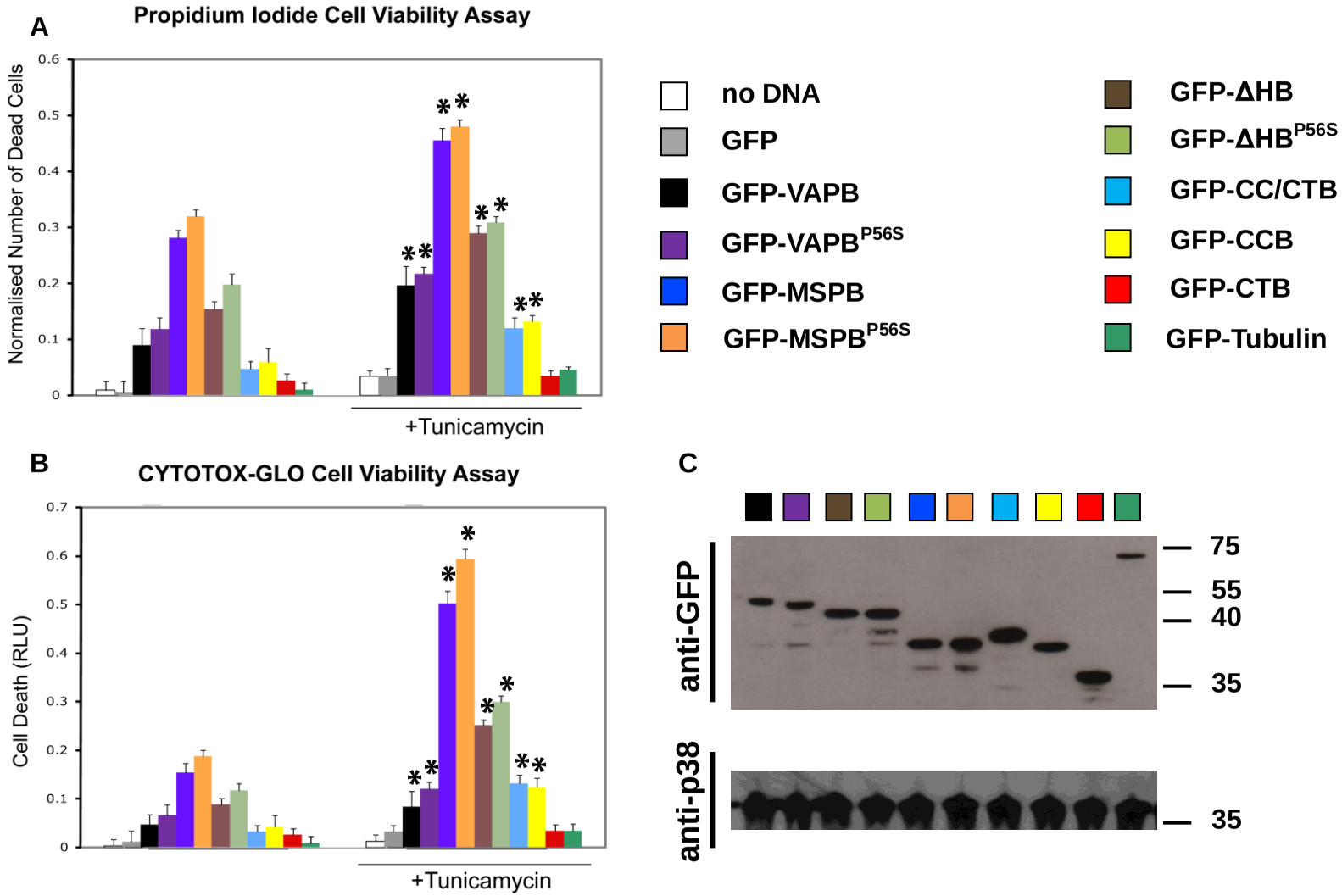
A
Propidium Iodide Cell Viability Assay
Normalised Number of Dead Cells
0
0.1
0.2
0.3
0.4
0.5
0.6
+Tunicamycin
no DNA
GFP
GFP-VAPB
GFP-VAPB P56S
GFP-MSPB
GFP-MSPB P56S
GFP-ΔHB
GFP-ΔHB P56S
GFP-CC/CTB
GFP-CCB
GFP-CTB
GFP-Tubulin
B
CYTOTOX-GLO Cell Viability Assay
Cell Death (RLU)
0
0.1
0.2
0.3
0.4
0.5
0.6
0.7
+Tunicamycin
C
anti-GFP
anti-p38
75
55
40
35
35

Figure 4.6.1 ***Effect of overexpression of full length and truncated mVAPB and mVAPB^{P56S} on NSC34 viability after ER stress.***

A., B. Propidium iodide and Cytotox-Glo cell viability assays. Results are consistent for both assays. NSC34 cells were transfected with full length mVAPB and mVAPB^{P56S} and truncations and after 24 hours induced with 2 μg/ml tunicamycin for 12 hours, washed and cultured a further 12 hours before assayed for cell death. Overexpression of MSPB and MSPB^{P56S} in non-induced and induced samples scores the highest in both assays while ΔH and ΔH^{P56S} come next. Samples marked with * have a $p<0.002$ by a one-way ANOVA. Cells recovering from treatment with tunicamycin when overexpressing VAPB, VAPB^{P56S}, MSPB, MSPB^{P56S}, ΔHB and ΔHB^{P56S}, CC/CTB, CCB but not CTB die more than the control samples (no DNA, GFP or GFP-tubulin overexpressing cells or non-transfected cells). Results shown are averages of 4 experiments and error bars correspond to standard error (SE).

C. Immunoblot of representative samples from the assayed for cell death NSC34 samples. Relative expression of mVAPB, mVAPB^{P56S} and truncated EGFP constructs is shown; p38 is used as a loading control. Expression levels in NSC34 cells are equivalent to those previously seen (Chapter 3 Figure 3.7C).

Figure 4.6.2

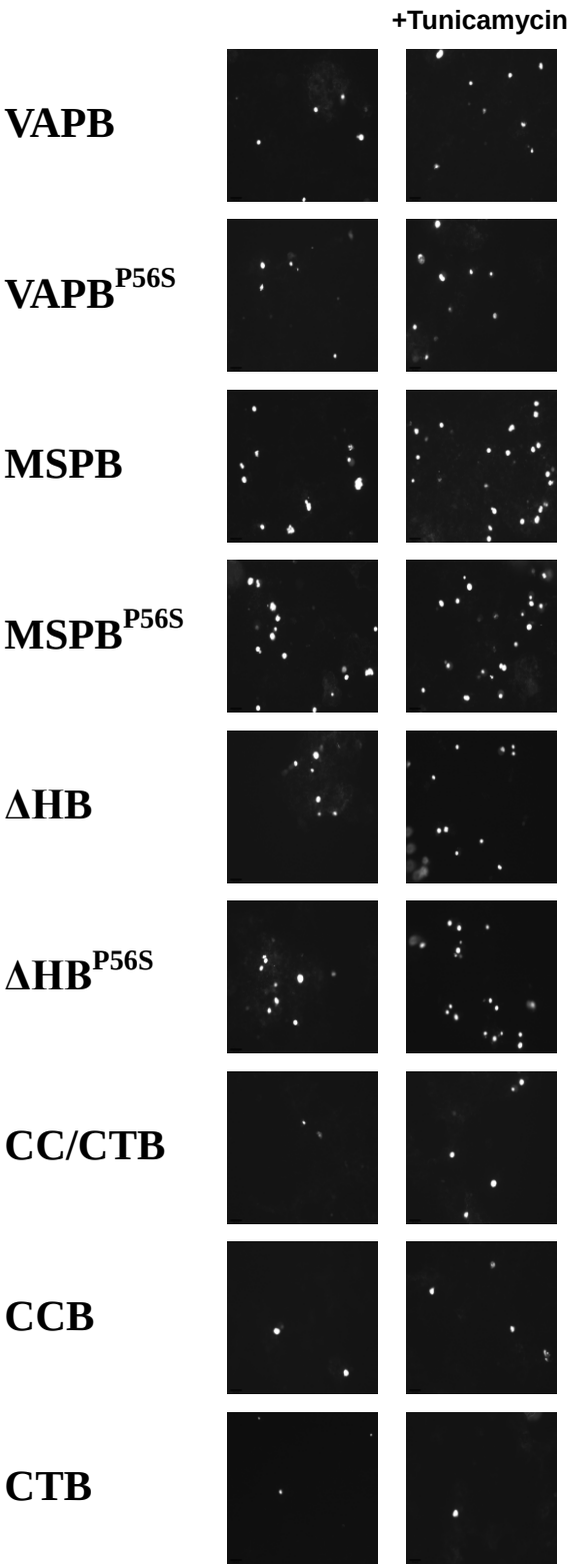
+Tunicamycin
VAPB
VAPB^P56S
MSPB
MSPB^P56S
ΔHB
ΔHB^P56S
CC/CTB
CCB
CTB

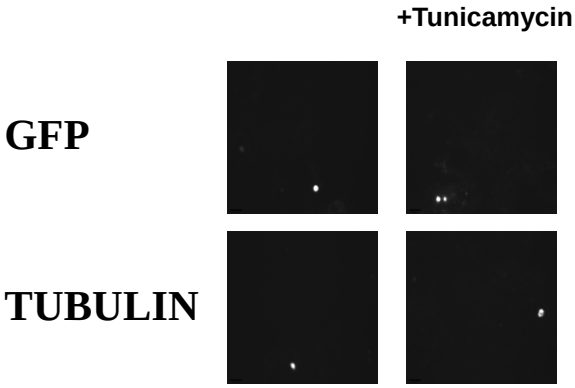

Figure 4.6.2 ***Propidium Iodide Cell Viability assay from Figure 4.10.1B.***

Representative images are shown from the propidium iodide cell viability assay shown in Figure 4.10.1B. Cells that have lost their membrane integrity allow the vital dye propidium iodide to enter their cytoplasm. Cells recovering from treatment with tunicamycin when overexpressing VAPB, VAPB^{P56S}, MSPB, MSPB^{P56S}, ΔHB and ΔHB^{P56S}, CC/CTB, CCB but not CTB die more than the control samples (GFP and tubulin).

4.4 ER stress vulnerability of NSC34 cells overexpressing mVAPB and mVAPB^{P56S} domains is caspase dependent

In 4.3 we showed that overexpression of VAPB and VAPB^{P56S} domains renders cells more vulnerable to ER stress. It is a common theme in neurodegenerative disease for cells to die via programmed cell death pathways, especially apoptosis (Paschen and Mengesdorf, 2005, Wu and Kaufman, 2006). Caspases are the effector molecules of apoptotic cell death. In order to examine whether the cell death observed in our aforementioned experiments is caspase dependent, we used the pan-caspase blocker zVAD-FMK (carbobenzoxy-valyl-alanyl-aspartyl -[O-methyl] -fluoromethylketone), which binds to the caspase catalytic site and inhibits induction of apoptosis (Craighead et al., 1999). Application of zVAD-FMK at 50 μM increases survival after tunicamycin induced ER stress of cells overexpressing MSPB, MSPB^{P56S}, ΔHB, ΔHB^{P56S}, CC/CTB or CCB and thus reduces cells death and reverses a significant amount of the effect previously observed (Figure 4.7). Therefore, cell death observed after ER stress in NSC34 cells overexpressing mVAPB or mVAPB^{P56S} domains, is caspase dependent.

Figure 4.7

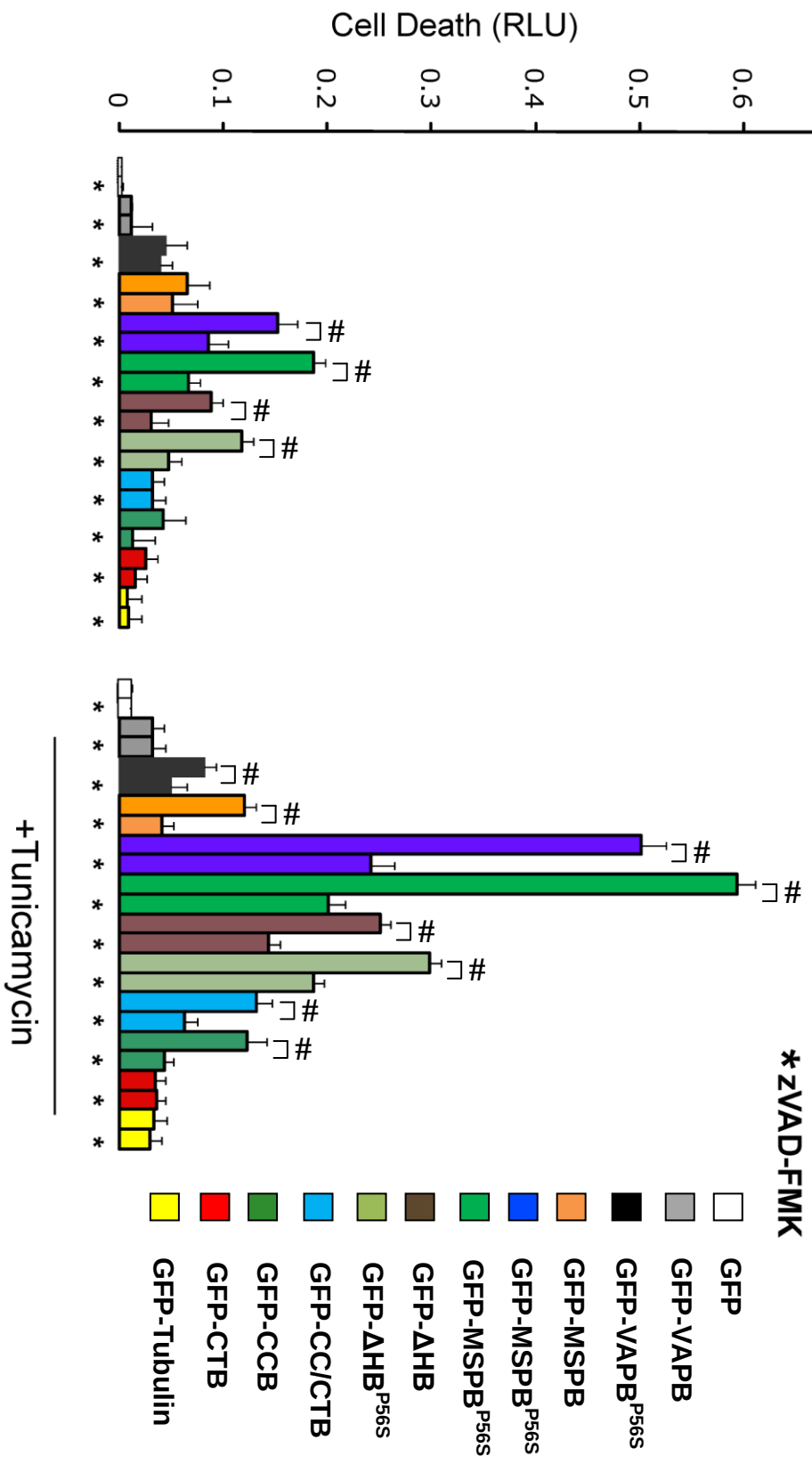
CYTOTOX-GLO Cell Viability Assay
Cell Death (RLU)
0
0.1
0.2
0.3
0.4
0.5
0.6
0.7
*zVAD-FMK
+Tunicamycin
GFP
GFP-VAPB
GFP-VAPB^{P56S}
GFP-MSPB
GFP-MSPB^{P56S}
GFP-MSPB^{P56S}
GFP-ΔHB
GFP-ΔHB^{P56S}
GFP-CC/CTB
GFP-CCB
GFP-CTB
GFP-Tubulin

Figure 4.7 ***Cell death induced by overexpression of VAPB domains is caspase dependant.***

The Cytotox-Glo™ cell viability assay was used to examine whether cell death observed after ER stress of NSC34 cells overexpressing mVAPB or mVAPB^{P56S} domains is caspase dependent. In samples marked with * 50 μM of zVAD-FMK pan-caspase inhibitor has been applied. Samples marked with # have a $p<0.002$ by a one-way ANOVA test. Application of zVAD-FMK increases cell viability which indicates that cell death after overexpression of VAPB domains and ER stress is caspase dependent. Results shown are averages of 4 experiments and error bars correspond to standard error (SE).

4.5 Discussion

In the previous Chapter, we have shown that VAPB interacts with and modulates the activity of the Unfolded Protein Response (UPR) associated transcription factor ATF6α. Moreover, the various domains of VAPB have a different effect on ATF6α activation. Regulation of a cell's ER stress response is essential for its survival and there is increasing literature linking misregulation of such pathways with neurodegenerative diseases (Hoozemans et al., 2005, Paschen and Mengesdorf, 2005, Xu et al., 2005). In this chapter we explore how VAP proteins affect two ERSE containing endogenous promoters (XBP1 and BiP) and potentially affect cell viability.

VAP proteins and XBP1, BiP promoters

Here we show that overexpression of VAPB, $VAPB^{P56S}$ MSPB, $MSPB^{P56S}$, ΔHB and ΔHB^{P56S}, but not CC/CTB, CCB and CTB inhibit transcriptional activation of an XBP1 luciferase based reporter (under the control of the human XBP1 promoter). This result is similar to that previously shown for ATF6α, but the CC/CTB and CCB constructs do not have an effect on XBP1 reporter activation. Also, we have presented evidence for a direct interaction between ATF6 and VAP proteins, while there is no evidence for a VAP-XBP1 interaction. Therefore it cannot be discounted the fact that maybe the XBP1 promoter effect is not a direct effect – or that it is mediated via ATF6α. XBP1 and ATF6α form a heterodimer (Yamamoto et al., 2007), especially under ER stress conditions. Additionally, we show that this modulation of XBP1 reporter (as we have shown for ATF6α) depends on the expression levels of the endogenous protein. When levels of endogenous VAPB are reduced with siRNA interference, overexpression of the P56S constructs ($VAPB^{P56S}$, MSP^{P56S} and ΔH^{P56S}) fails to inhibit XBP1 reporter activation. Similar to ATF6α this clearly shows that the P56S mutation's functionality depends on the presence of the endogenous protein. This is a finding that might explain why in some instances the mutant behaves like a gain of function (Chai et al., 2008) or rather like a gain of a negative function (i.e. inhibition of ATF6α activation) instead of a dominant loss of function (Ratnaparkhi et al., 2008); which becomes more important when

considering that in humans there are two alleles of VAPB and in ALS patients one of them is the mutant P56S. Therefore, the presence of the wild-type protein could potentially stabilize the mutant protein, which on its own does not display the same stability as the wild-type.

Overexpression of VAPB, MSPB and ΔHB but not $VAPB^{P56S}$, $MSPB^{P56S}$, ΔHB^{P56S}, CC/CTB, CCB or CTB potentiates transcriptional activation of a BiP luciferase based reporter (under the control of the human BiP promoter). Clearly the overexpression of the P56S mutation cannot activate the BiP promoter; the same thing applies for the Coiled-Coil and C-terminal domains of VAPB. This pattern is not altered when the endogenous protein expression levels are reduced with siRNA. Thus, in this context, the P56S mutation is a loss of function and effectively may fail to activate the cascade of chaperones and genes associated with BiP activation and the UPR.

VAP and ERSE

All three promoters in the relative reporter constructs (ATF6α synthetic promoter and hXBP1 and hBip endogenous promoters) examined in this study are associated with ERSE elements. The synthetic ATF6α promoter can bind both ATF6α and XBP1, while both proteins bind to ERSE elements. The human XBP1 promoter contains one ERSE element which is essential for transcriptional activation of the reporter upon ER stress, while the BiP promoter contains three ERSE elements; only one of those three ERSE elements is necessary for transcriptional activation upon ER stress. Our data show a differential effect on the aforementioned promoters; inhibition for the ATF6α and XBP1 reporters and potentiation of the BiP reporter. Given the fact that all three promoters contain ERSE elements, the prediction would be that VAP proteins should have the same effect on the reporters. However, our results suggest that the inhibition and induction observed on similar promoter elements could be due to other elements within those promoters. For example the BiP promoter contains two ERSE elements that are not transcriptionally activated after ER stress; it could be that VAPB has an affinity for ERSE elements and in the BiP promoter its association with the two “inactive” ERSEs could modulate transcriptional activation.

VAPB, cell death and ER stress

Apart from the MSP domain, we show that the other domains of VAPB (Coiled Coil and C-terminal anchor) are not toxic to cells; it is only the MSP domain or truncations of VAPB that contain the MSP (ΔH) that display increased death levels (both wild-type and P56S). When cells are stressed for 12 hours with the N-glycosylation inhibitor tunicamycin and then cultured for another 12 hours, overexpression of VAPB domains apart from the C-terminal anchor reduces the viability of cells in a caspase dependent manner; compared to controls (GFP and GFP-tubulin). This observation suggests that overexpression of VAP protein domains renders cells more vulnerable after their ER stress pathway has been induced; while in non-induced cells, their overexpression does not increase cell death (apart from the MSP domain). These results reveal that the balance of VAP proteins and VAP protein domains is essential for the survival of a cell when its UPR has been initiated; overexpression might interfere with the homeostasis of endogenous VAP proteins or their interactions with other cellular components. In this study we highlight the regulation of the UPR by VAP proteins and the ALS8 associated mutant, therefore caspase dependent cell death after recovery from ER stress might be a result of misregulation of transcriptional activation of ERSE containing promoters by VAP proteins. Failure to regulate the UPR might lead to programmed cell death (Paschen and Mengesdorf, 2005).

Chapter conclusion

The ER stress response to unfolded proteins in the ER lumen is based on an intricate network of interactions between transcription factors, chaperones and a plethora of other genes. VAP proteins are present on the ER membrane and our data suggest that they can be part of this regulatory network via regulation of ERSE promoter elements. Misregulation of this balance can lead to apoptotic cell death.

Chapter 5

Regulation of the UPR by the MSP domain

5.1 Background

The MSP domain is the most conserved domain of VAP proteins from *A.* Californica to humans. Previous results of the laboratory indicate that the MSP domain when overexpressed is toxic to primary hippocampal neurons and HEK293 cells (Middleton, 2005). Moreover, Skehel et al., 2000 showed that endogenous mouse VAPA in whole mouse brain homogenates apart from the predominant ~33 KDa band displayed an 18KDa proteolytic product.

If VAP proteins are proteolyzed, this could result in release of various domains (i.e. MSP or CC). In the previous two chapters we have shown that overexpression of VAP protein domains affects differentially regulation of the UPR via ERSE elements on UPR associated promoters. Moreover we showed that VAP protein domains overexpression reduces cell viability following an ER stress insult.

In this chapter we will study expression of VAP proteins in neuronal and non-neuronal tissues.

5.2 VAPA and VAPB are expressed ubiquitously but at differing levels in different tissues

We proceeded to examine VAPA and VAPB expression in various tissues. Immunoblot analysis of selected tissues from an adult male Sprague-Dawley rat demonstrated that both VAPA and VAPB proteins are present in all tissues examined, but at different relative levels (Figure 5.1A) This is in agreement with the wide expression profile of mRNA published previously (Nishimura et al., 1999, Skehel et al., 2000, Weir et al., 1998). VAPA is expressed at higher levels in testis, cerebellum and forebrain while for VAPB pancreas is the tissue with the highest expression.

5.3 Endogenous VAPA and VAPB are cleaved; VAPB cleavage is restricted in neuronal tissue

In Figure 5.1A an additional, less abundant, protein of approximately 14 kDa is detected by both VAPA and VAPB antisera in Figure 5.1A. The VAPB-related signal is a doublet, the expression of which is tightly restricted to neuronal tissue (forebrain and cerebellum extracts) and not detected in the other tissues tested (Figure 5.1A). The 14 kDa VAPA-related polypeptide is more widely expressed and detectable in pancreas, liver, forebrain, lung and thymus, kidney and testis; low levels are seen in the cerebellum and no signal is detected in heart or skeletal muscle. A peptide of similar size has been predicted from a splice variant of VAPB, termed VAPC. However, the peptide used to generate the VAPB anti-serum is not present in VAPC (Nishimura et al., 1999), and the VAPA antisera do not cross react significantly with VAPB-derived species (Figure 5.1C). Moreover VAPB does not behave like a typical integral membrane protein when extracted with Triton X114 as it is found predominantly in the aqueous phase, while VAPA is seen exclusively in the detergent phase (Figure 5.1C, also see (Bordier, 1981) and (Middleton, 2005)). It is concluded that these smaller molecular weight immunoreactive species are most likely generated by proteolysis of the VAP proteins. Finally our results published in Gkogkas et al., 2008 were also confirmed by Tsuda et. al., 2008, who showed that Drosophila VAP gets cleaved and the MSP domain is released.

Figure 5.1

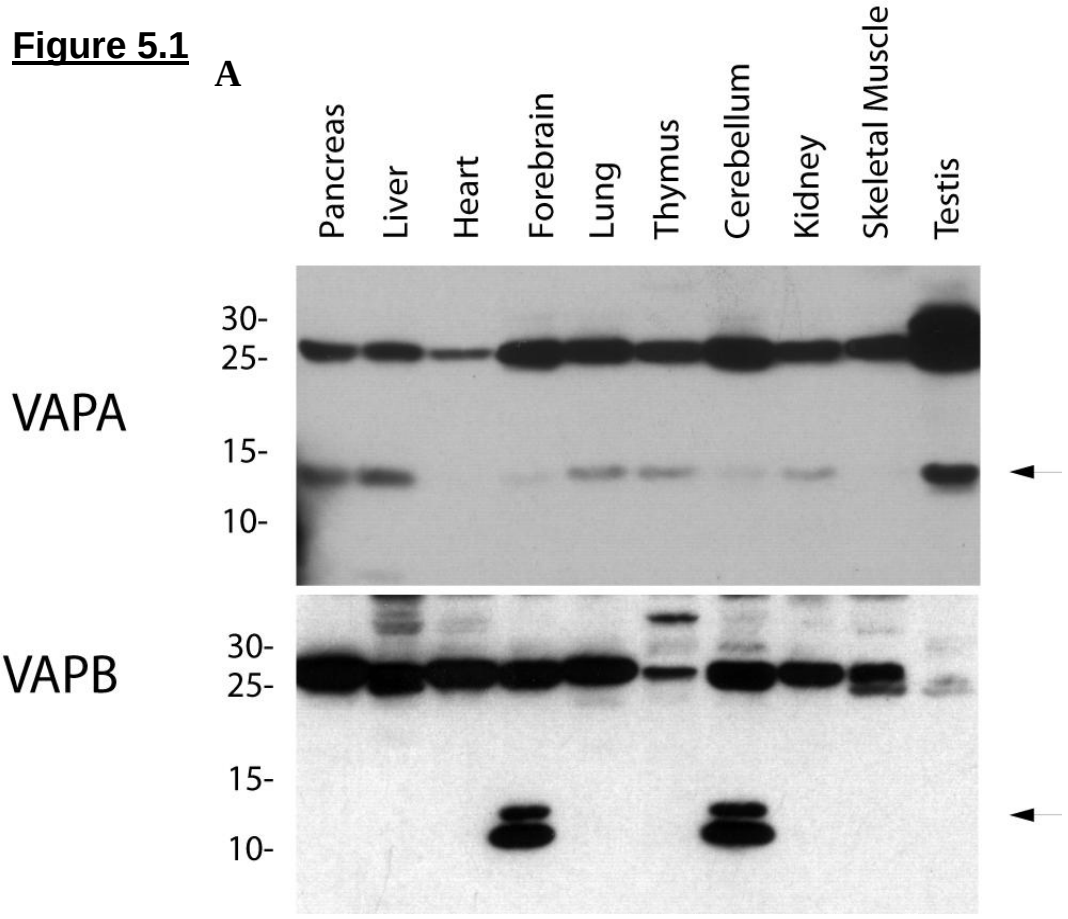
A
Pancreas
Liver
Heart
Forebrain
Lung
Thymus
Cerebellum
Kidney
Skeletal Muscle
Testis
VAPA
30-
25-
15-
10-
VAPB
30-
25-
15-
10-
B
VAPA
VAPB
C
Triton X114
PNF
D
Aq
anti-VAPA
anti-VAPB

Figure 5.1 ***Expression of VAPA and VAPB in different adult male rat tissues.***

A. ***Detection of VAPA and VAPB in different tissues.***

Anti-peptide anti-serum was raised to residues 174–189 of mouse VAPB. In the tissues indicated, the predominant immunoreactivity is at approximately 27 kDa, in agreement with the molecular weight predicted from the cDNA. Both VAPA and VAPB are expressed widely but at different levels. A faster migrating VAPB-related doublet signal of approximately 14 kDa is clearly detected in forebrain and cerebellum protein extracts (arrows). The immunoblot is deliberately over exposed to demonstrate the restricted nature of this expression pattern. A faster migrating immunoreactive species of approximately 14 kDa is also seen with VAPA antisera, however, in contrast to that seen for VAPB; this species is detectable in pancreas, liver, forebrain, lung and thymus, kidney and testis. Low levels are seen in the cerebellum and no signal is detected in heart or skeletal muscle.

B. ***Loading and Transfer control for immunoblot analysis of tissue extracts*****.**

The membranes used for immunoblotting of tissue extracts with VAPA and VAPB antisera were stained with a Ponceau S solution prior to blocking with non-fat milk and antibody incubation. Antisera used on relative membranes are marked. Even abundant proteins such as cytoskeletal constituents are not expressed equally in different tissues. Therefore, a general protein detection reagent such as Ponceau S is a more appropriate control for loading. Comparable lanes between each blot have transferred equally and contain equivalent amounts of protein. Picture is shown in grayscale – original colour is red.

C. ***Specificity control for VAPA and VAPB antisera.***

A post-nuclear fraction (PNF) from a rat brain homogenate was extracted with 1% Triton X114. Aqueous and detergent phases were then separated and analysed with either VAPA or VAPB specific antisera. VAPA is seen predominantly as a doublet that is almost completely extracted into the detergent phase. VAPB is a single 27kD species that is present largely in the aqueous phase. There is negligible cross reactivity between the two antisera.

5.4 Proteolysis of endogenous and expressed hVAPB

VAPA and VAPB are cleaved and VAPB is cleaved only in neuronal tissue. The fact that the VAPB antibody was raised to aminoacids 174–189 which lies between the MSP and Coiled Coil regions of VAPB, suggests that the 14 KDa truncation observed in the tissue blot (Figure 5.1A) is most likely a proteolytic product of VAPB that contains the coiled coil. VAPB when extracted with Triton X114 does not behave as a typical membrane protein as it is found predominantly in the aqueous phase instead of the detergent phase (Skehel et al., 2000). When whole brain extract from an adult Sprague Dawley rat was extracted using Triton X114, the 14 KDa band was found only in the detergent fraction, while the 27 KDa full length protein was in the aqueous phase (Figure 5.2B also see (Bordier, 1981), (Middleton, 2005) and Figure 5.1C). This suggests two things:

-The 14 KDa band is hydrophobic and therefore must contain the C-terminal membrane anchor of VAPB.

-The presence of the 14 KDa fragment missing has a significant effect on the hydrophobicity of the protein as it is essential for the protein to extract in the aqueous phase. Moreover the 14 KDa missing correspond to the predicted molecular weight of the MSP domain in isolation.

Thus, the MSPB domain is cleaved and in full length VAPB satisfies the protein's hydrophobicity and promotes its solubility in aqueous solutions.

Neuron specific cleavage of VAPB was observed in adult Sprague-Dawley rats in Figure 5.1A. In post-nuclear fractions of homogenized brain and spinal cord from E18 Sprague-Dawley embryos, the 14 KDa truncation can be again detected when probed with the VAPB antisera (Figure 5.2A). When E18 cortical cells were dissociated and cultured for 11 days in vitro (DIV11) endogenous VAPB was proteolysed in a similar manner. Surprisingly, in DIV1 E18 cortical neurons endogenous VAPB was not cleaved and appeared as a single 29 KDa band. No cleavage products were detected in cultured glial cells (depleted of neurons by NMDA induced toxicity) from the same E18 embryos and in the 3 cell-lines examined: HEK293 (kidney), NSC34 (motor-neuron like), C6 (glioma); Figure 5.2A.

Apart from the endogenous VAPB protein, we wanted to examine whether

Figure 5.2

A
anti-VAPB
Spinal Cord
Whole Brain
CN DIV11
CN DIV1
Glia
HEK293
NSC34
C6
15 KDa
29 KDa
B
anti-VAPB
P2
S2
D
Aq
Triton X114
15 KDa
29 KDa
C
anti-β-tub
anti-myc
myc-hVAPB
myc-hVAPB^P56S
myc-hVAPB^D130E
myc-hVAPB^del160
50 KDa
15 KDa
30 KDa
D
anti-myc
myc-hVAPB
myc-hVAPB^P56S
myc-hVAPB^D130E
myc-hVAPB^del160
NTC
70* KDa
15 KDa
30 KDa

Figure 5.2 Neuron specific proteolysis of *endogenous and myc-tagged VAPB.*

A. Immunoblot of post-nuclear fractions from homogenate of spinal cord, whole brain and primary cortical neurons in culture DIV11 and DIV1 and glia, from E18 Sprague-Dawley rat embryos, as well as HEK293, NSC34 (motor-neuron like) and C6 (glioma) cell line extracts. Cleaved VAPB is detected only in spinal cord, whole brain and DIV11 neurons. 30 μg of total protein were loaded in each lane; protein concentration was determined by a micro-BCA assay.

B. Immunoblot of P2 and S2 from post-nuclear fraction and Triton X114 extracted P2 of adult Sprague-Dawley rat whole brain. When extracted with Triton X114, endogenous VAPB does not behave as a typical membrane protein as it is found predominantly in the aqueous phase instead of the detergent phase. If extracted using Triton X114, the 14 KDa band is found only in the detergent fraction, while the 27 KDa full length protein is in the aqueous phase.

C. Immunoblot of DIV5 primary cortical Sprague-Dawley rat neurons nucleofected with hVAPB wild-type and mutant N-terminally c-myc tagged expression constructs. No cleavage products are detected for any of the expressed VAPB contructs; β-tubulin is used as a loading control.

D. Immunoblot of DIV11 primary cortical Sprague-Dawley rat neurons nucleofected with hVAPB wild-type and mutant N-terminally c-myc tagged expression constructs. Wild-type VAPB, $VAPB^{D130E}$ and $VAPB^{del160}$ are cleaved, but not $VAPB^{P56S}$. Human $VAPB^{D130}$ gets cleaved more than all the other constructs, as the intensity of the band corresponding to the proteolytic 14 KDa fragment is higher for D130E than for the other constructs. After 11 DIV, the amount of protein is significantly reduced, albeit the cleavage pattern is clear. *A 70 kDa non-specific band from longer exposures of the immunoblot serves as a loading control.

expressed VAPB behaves in the same manner in neurons in terms of its proteolysis. In HEK293 or NSC34 cells we have not detected proteolysis of expressed mVAPB or mVAPB^{P56S} (Chapter 3,4 Skehel unpublished and Middleton, 2005). Recently two novel ALS associated human VAPB mutations, D130E and del160 have been described (Landers et al., 2008). When D130E and del160 mutants were expressed as EGFP fusion proteins they display subcellular localization similar to wild-type (Landers et al., 2008). In order to study those new mutants along with the already known P56S we cloned hVAPB, hVAPB^{P56S}, hVAPB^{D130E} and hVAPB^{del160} in the pEGFP-C1 vector where the EGFP fusion protein was replaced with a c-myc epitope (cloning performed by Dr. Caroline Wardrope). We expressed myc-tagged versions of wild-type hVAPB, hVAPB^{P56S}, hVAPB^{D130E} and hVAPB^{del160} by nucleofecting primary dissociated cortical E18 Sprague-Dawley neurons. At DIV5 of culture, when cell extracts are probed with the anti-myc antibody no cleavage products are detected for any the expressed VAP constructs (Figure 5.2C). After 11 DIV, wild-type VAPB, VAPB^{D130E} and VAPB^{del160} were cleaved, but not VAPB^{P56S}. Moreover, the D130E mutant seems to be cleaved more than the wild-type protein, while the del160 mutant does not seem to be different from wild-type VAPB. The 14 KDa band detected in the immunoblot is an N-terminal myc tagged product, since all hVAP constructs were N-terminally tagged with the c-myc epitope. The size of this band corresponds to the size of the MSP domain and is consistent with our hypothesis that VAPB is cleaved in a neuron specific manner; the P56S mutant is not proteolysed after 11 DIV, while the D130E is proteolysed more.

5.5 The effect of the proteolysis of VAPB on the Unfolded Protein Response

In order to study the effect of the release of the MSP domain in the regulation of the Unfolded Protein Response we used HEK293 cells and “simulated” the cleavage of VAPB (wild-type and mutant). This was done using the EGFP truncations of mVAPB and mVAPB^{P56S}. Co-expression of MSPB and CC/CTB or MSPB^{P56S} and CC/CTB “simulates” cleavage of full length mVAPB and mVAPB^{P56S} and release of the MSP domain – the CC/CT stays bound to membranes. Cells were

Figure 5.3

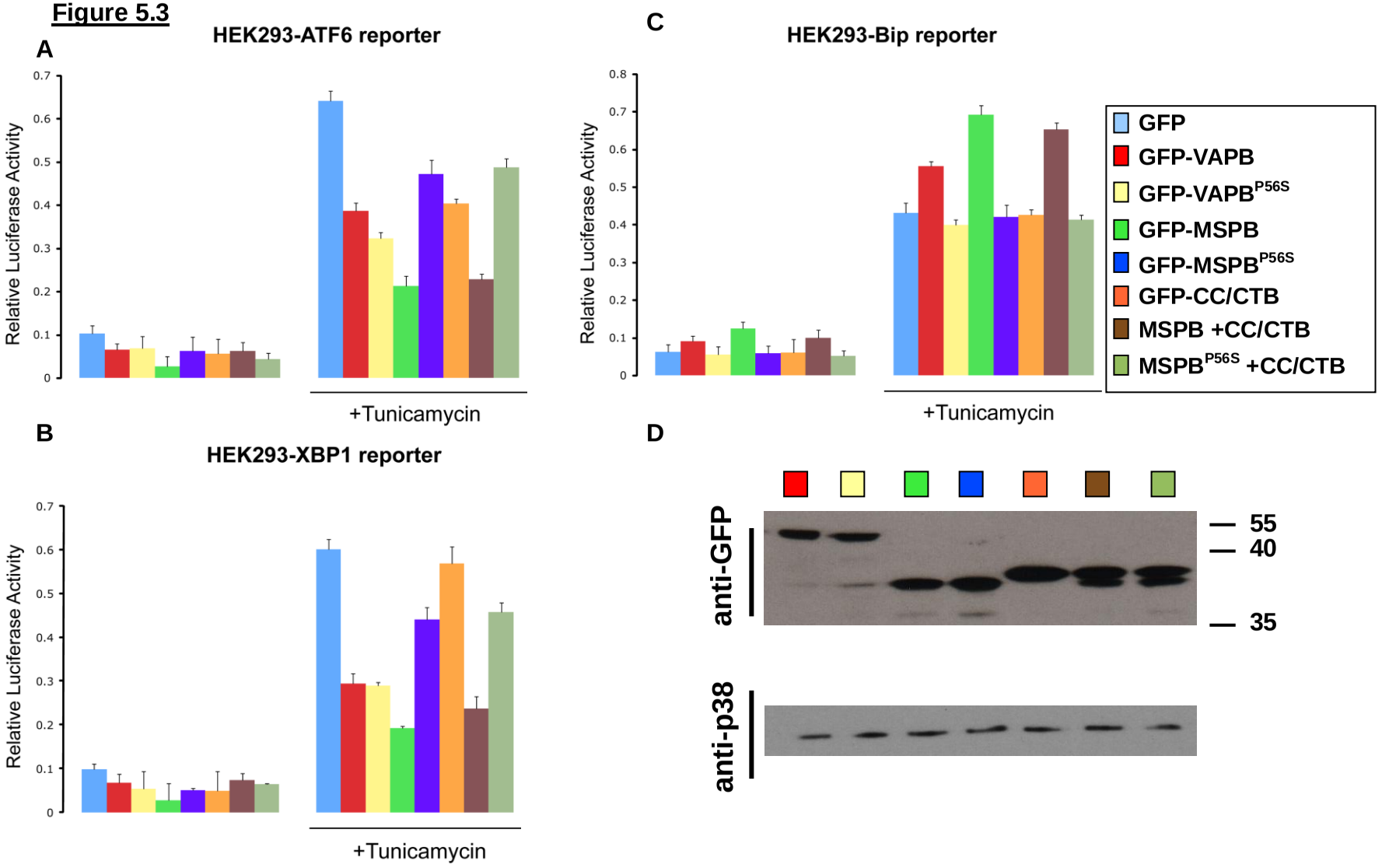
A
HEK293-ATF6 reporter
Relative Luciferase Activity
+Tunicamycin
B
HEK293-XBP1 reporter
Relative Luciferase Activity
+Tunicamycin
C
HEK293-Bip reporter
Relative Luciferase Activity
+Tunicamycin
GFP
GFP-VAPB
GFP-VAPB P56S
GFP-MSPB
GFP-MSPB P56S
GFP-CC/CTB
MSPB +CC/CTB
MSPB P56S +CC/CTB
D
anti-GFP
anti-p38
55
40
35

Figure 5.3 ***Simulation of VAPB cleavage by co-expression of the complementary VAPB truncations and its effect on transcriptional activation of the Unfolded Protein Response.***

A, B, C. HEK293 cells were transfected with complementary truncations of VAPB and VAPB^{P56S} that "simulate" cleavage of full length proteins to MSP and CC/CT domains along with ATF6, XBP1 and Bip reporters. Co-expression of MSP and CC/CT has an effect similar to that of MSP on its own, which is more potent than full length or CC/CTB single expression. The P56S MSP mutant, still has no effect on BiP reporter activation, but inhibits both ATF6 and XBP1 reporter activities. However, for the ATF6 reporter the inhibition is 16% for MSP^{P56S} + CC/CTB and 33% for MSP^{P56S} only. Results shown are averages of 4 experiments and error bars correspond to standard error (SE).

D. Immunoblot of representative samples from the transcriptional assay simulating VAPB cleavage. Relative expression of mVAPB, mVAPB^{P56S} and truncations EGFP constructs is shown. Co-expression of MSP and CC/CT can be seen as a doublet in the relative samples.

co-transfected with ATF6 or XBP1 or BiP reporters as previously and DNA quantities are balanced using pEGFP-C3. This experiment clearly shows that simulation of VAPB cleavage by co-expression of the two complementary truncations (MSPB+CC/CTB) that make up the full length protein has the same effect as expression of only the MSP domain (Figure 5.3). For ATF6 and XBP1 reporters this means more potent inhibition of their activation and for the BiP reporter more potentiation than full length or CC/CTB single expression. The P56S mutant of the MSP domain when co-expressed with CC/CTB still has no effect on BiP reporter activation, but inhibits both ATF6 and XBP1 reporter activities; albeit for the ATF6 reporter the inhibition is 16% for MSP^{P56S} + CC/CTB and 33% for MSP^{P56S} only. This suggests that co-expression of the MSP^{P56S} domain along with CC/CTB blocks the effect of the CC/CTB domain (when it's expressed on its own). From all this data we conclude that in cases where the MSP domain is cleaved, there can be differential modulation of the Unfolded Protein Response.

5.6 The A130E mutant of mVAPB gets cleaved and affects transcriptional activation of the UPR

In DIV11 cortical neurons, $hVAPB^{D130E}$ is cleaved more than hVAPB, and $hVAPB^{del160}$. In mouse VAPB, at position 130 there is an alanine instead of the aspartic acid in the human sequence. We proceeded to subclone $VAPB^{A130E}$, $VAPB^{A130D}$ and $VAPB^{del160}$ as c-myc fusion proteins as previously described for the relative human constructs (cloning performed by Dr. Caroline Wardrope). HEK293 cells were transfected with the ATF6, XBP1 or BiP reporters as previously. Overexpression of $mVAPB^{A130E}$ inhibits ATF6α and XBP1 reporters and induces the BiP reporter activity more than wild type VAPB, $VAPB^{P56S}$, $VAPB^{del160}$ or $mVAPB^{A130D}$ (Figure 5.4A, B and C); the last construct has an aspartic acid in the position of the alanine in the mouse sequence, which makes the mouse sequence identical to the human wild-type sequence. Moreover, an immunoblot of samples from the assayed cells (Figure 5.4D) shows that the N-terminal tagged A130E mutant of mVAPB is cleaved in HEK293 cells, while wild type VAPB, $VAPB^{P56S}$,

Figure 5.4

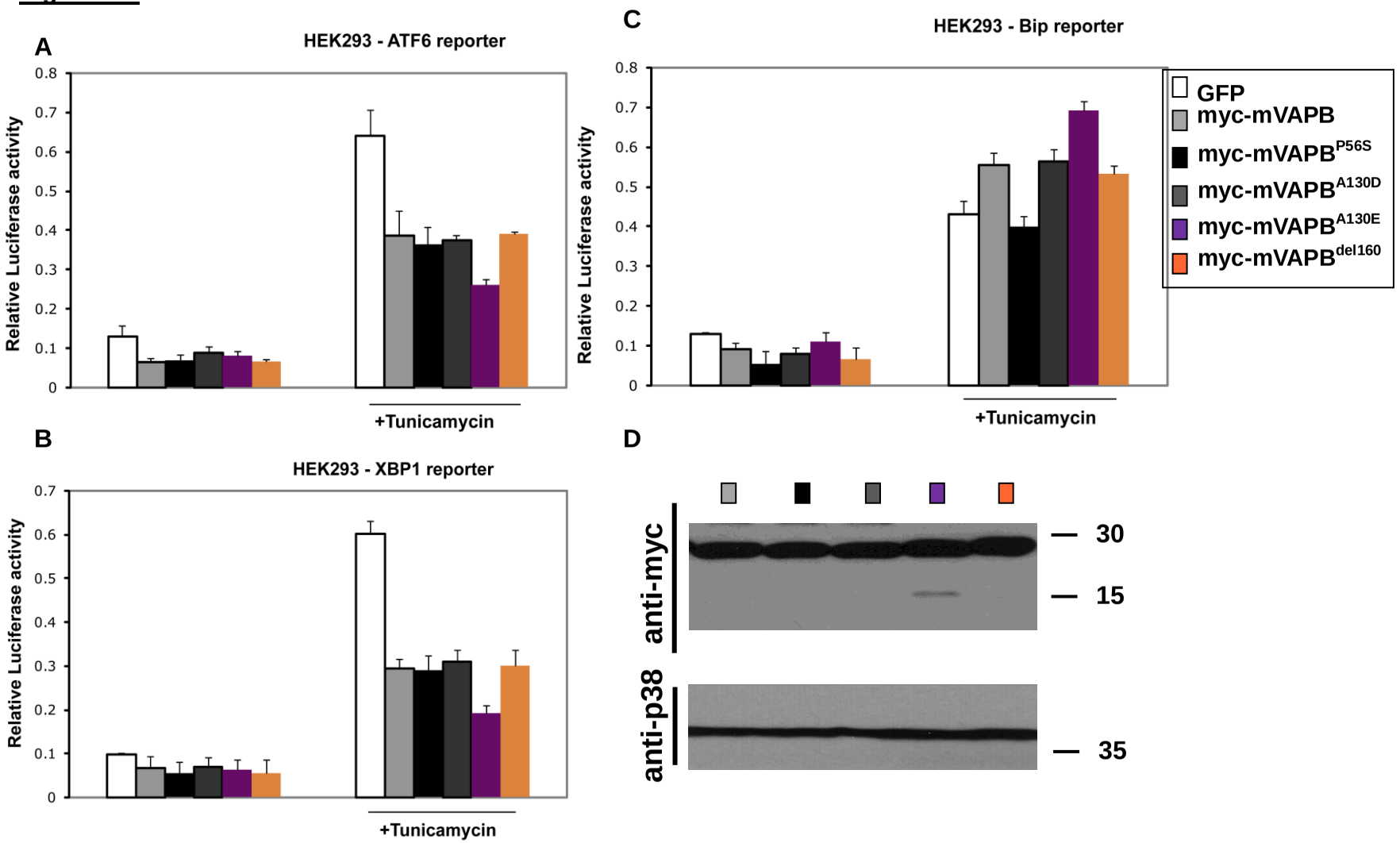
A
HEK293 - ATF6 reporter
Relative Luciferase activity
0.8
0.7
0.6
0.5
0.4
0.3
0.2
0.1
0
+Tunicamycin
B
HEK293 - XBP1 reporter
Relative Luciferase activity
0.7
0.6
0.5
0.4
0.3
0.2
0.1
0
+Tunicamycin
C
HEK293 - Bip reporter
Relative Luciferase activity
0.8
0.7
0.6
0.5
0.4
0.3
0.2
0.1
0
+Tunicamycin
GFP
myc-mVAPB
myc-mVAPB P56S
myc-mVAPB A130D
myc-mVAPB A130E
myc-mVAPB del160
D
anti-myc
anti-p38
30
15
35

Figure 5.4 ***Effect of the 130E ALS associated mutation on ER stress response in HEK293 cells.***

A., B., C. Transcriptional assay using ATF6α, XBP1 and BiP reporters in HEK293 cells. Full length wild type mVAPB, mVAPB^{P56S}, mVAPB^{A130E}, mVAPB^{A130D} and mVAPB^{del160} are overexpressed. Mouse VAPB^{A130E} inhibits ATF6α and XBP1 reporters and induces the BiP reporter more than all the other constructs. Since in the mouse sequence there is an A at position 130, we used mVAPB^{A130D} as a control to introduce the D that is in the wild-type human sequence at that position. Results shown are averages of 4 experiments and error bars correspond to standard error (SE), p=0.014398.

D. Immunoblot of representative samples from the transcriptional assay in HEK293 cells. None of the mVAPB constructs is cleaved apart from the mVAPB^{A130E}. The proteolytic fragment generated is approximately 15 KDa which corresponds to the predicted size of the MSP domain – the c-myc constructs are N-terminally tagged.

VAPB^{del160} and mVAPB^{A130D} are not. This suggests that the substitution of the alanine at position 130 for a glutamic acid in mVAPB renders the protein more susceptible to proteolysis, and as predicted this has a profound effect on regulation of the Unfolded Protein Response, as the MSP domain is probably released.

5.7 Overexpression of mMSPB and mMSPB^{P56S} is toxic to NSC34 cells

Our data suggest that the MSP domain of VAPB is released after cleavage in a neuron specific manner. In order to examine the effect that released MSP has on cells, we overexpressed an EGFP fusion construct of MSPB and MSPB^{P56S} in the motor-neuron like NSC34 cells. It was previously suggested (Middleton, 2005) that overexpression of wild-type MSP is toxic in cell lines and primary neurons. We verified that result and confirmed that MSPB^{P56S} is also toxic to NSC34 cells (Chapter 4, Figure 4.6.1A and 4.6.2B) by using a vital dye assay (propidium iodide-cells that have lost membrane integrity allow the dye to enter the cell) or a cytotoxixity assay (CytoTox-Glo™, Promega). GFP and GFP-tubulin are used as controls. Moreover we showed in Chapter 4 Figure 4.7 that MSP and MSP^{P56S} overexpression render cells more vulnerable to ER stress.

5.8 Discussion

In this Chapter we show neuron specific proteolysis of VAPB and release of the MSP domain. The MSP domain is a key regulator of the UPR and affects cell viability. Moreover we show in a disease paradigm (D130E mutation) how release of the MSP domain can misregulate the UPR.

The MSP domain – neuron specificity and UPR regulation

We had already shown in the previous chapter that the MSP domain is a potent inhibitor of ATF6α activity and that the MSP^{P56S} does not display the same functionality. But, there was no evidence that the MSP exists in isolation, separately

from the full length VAPB. We clearly demonstrated in this chapter (and (Gkogkas et al., 2008)) that VAPB gets cleaved in a neuron specific manner and also that this proteolytic event releases the MSP domain. Moreover, Tsuda et. al., 2008 also demonstrated that the Drosophila homologue of VAPB is cleaved and the MSP domain released. Therefore, the MSP domain can exist in isolation in cells and this is restricted to neuronal tissue. Furthermore, we have shown that VAPB is cleaved only in neurons and not glial cells (or HEK293, NSC34 or C6 cells) and that in dissociated cultures from E18 rat embryos the proteolytic event cannot be seen at DIV1 but at DIV11; albeit VAPB is cleaved in extracts from cortex and spinal cord of embryos. This pattern of cleavage suggests that VAPB is cleaved in adult and in embryo, but when cortical cells are dissociated and cultured in vitro VAPB is not cleaved from DIV1, but at DIV11. The same applies for expressed VAPB in this model of primary cortical cultures. However, the P56S mutant is not proteolyzed after 11 days in culture.

VAPB cleavage is present in organised structures of neurons (whole tissue adult or embryo, DIV11 culture) but is not present in dissociated neurons DIV1. This observation highlights a dynamic regulation of VAPB cleavage that is associated with neuronal structure; at DIV0 when the dissociated neurons are plated, they are extracted from an already organised structure in the embryonic brain and after plating they start growing their processes. At DIV11 cortical neurons have formed a complex structure where cells have more synapses and their processes are considerably longer than DIV1. Moreover, this result could highlight a dynamic regulation of VAPB proteolysis dependent on neuron morphology and synaptic activity.

In terms of the regulation of the Unfolded Protein Response, the MSP domain out of all the VAP protein domains has the most profound effect on ATF6α and XBP1 reporter inhibition and BiP reporter potentiation. If we “simulate” cleavage of VAP proteins by co-expressing complementary truncations (MSP + CC/CT) we observe the same effect as overexpressing the MSP domain; which in the case of ATF6α and XBP1 reporters is stronger inhibition and for the BiP reporter stronger induction compared to the full-length protein. These results suggest that the MSP domain elicits a profound regulatory effect on ER homeostasis; this becomes important in a neuronal context where we have shown the cleavage of VAP proteins and potential

release of the MSP domain. Conversely, the MSP^{P56S} does not have the same inhibitory effect as the wild-type MSP for ATF6 and XBP1 reporters, while it has no effect on BiP activation. Moreover, when the endogenous protein expression is reduced by siRNA, MSP^{P56S} displays reduced ability in rescuing its previously observed effect, which suggests its dependency on the presence of the wild-type protein. This potentially shows that the P56S mutation results in loss or reduction of the functionality of the protein, and that the interaction of the mutant protein with the wild-type protein may stabilise the mutant and allow it to exert its inhibitory (ATF6α, XBP1) or potentiating effect (BiP).

The aforementioned prediction of the effect of the release of the MSP domain on ER homeostasis is confirmed in a disease example. We show that the published VAPB D130E mutation (Conforti et al., 2006, Landers et al., 2008) -A130E in mouse- gets cleaved and produces a proteolytic fragment in HEK293 cells. The fact that the protein gets cleaved in non-neuronal tissue, may suggest that the substitution D→E can render the protein more susceptible to proteolysis than the wild-type; even in non-neuronal tissue. In addition, substitution of the mouse A130→D (which is the residue in the human sequence) does not lead to cleavage of the protein, which shows that it is the introduction of the E residue at position 130 that is associated with the observed cleavage. Also, in primary cortical DIV11 neurons the $hVAPB^{D130E}$ gets cleaved more than wild-type hVAPB or $hVAPB^{del160}$ when equal amounts of protein are loaded. As we predict earlier, the $mVAPB^{A130E}$ inhibits ATF6α and XBP1 reporters and potentiates the BiP reporter more than wild-type mVAPB, $mVAPB^{P56S}$, $mVAPB^{A130D}$ or $mVAPB^{del160}$; which is consistent with the profound effect the MSP domain has.

So far, we have presented evidence that the MSP domain of VAPB is a key regulator of the ER stress response and that cleavage of VAPB that produces the MSP domain is neuron specific. It has been previously shown by our lab (Middleton, 2005) that overexpression of the MSP domain is toxic to cells and primary hippocampal neurons. We confirmed this result in the motor-neuron like NSC34 cells and show that $MSPB^{P56S}$ is also toxic using two independent death assays. In addition to this we now show that this cell death observed is caspase-dependent, because the pan-caspase inhibitor zVAD-FMK rescues cell-death to a certain extent.

Therefore, when increased amounts of the MSP or MSP^{P56S} are accumulated, this is toxic for cells and induces programmed cell death via apoptosis. This result shows that the balance of free MSP domain in cells can be crucial for cell survival; wild type MSP is cleaved and MSP is produced in a cell, but when this balance is disturbed by overexpression, cells die.

Chapter conclusion

The MSP domain of VAP proteins is a highly conserved protein domain that is a key regulator of the UPR and can be toxic when overexpressed. Neuron specific cleavage of VAPB which releases the MSP domain and aberrant behaviour of the P56S mutant can offer a new avenue for ER stress regulation in motor neurons in ALS8.

Therefore the data presented in chapters 3, 4 and 5 suggest that VAP proteins participate in regulation of the UPR and that the MSP is the most potent modulator the ER stress response. The fact that the MSP domain can be cleaved of the full length VAP protein reveals a novel regulatory mechanism for regulation of the UPR in cells. Motor neuronshave long processes and such signalling to distal sites of the ER could be important for their survival. It could be that in ALS8 the mutant P56S fails to get cleaved and thus disturbs the balance of available MSP in motor neurons. Recapitulation of this study in motor neurons would contribute to our knowledge of ALS8 pathogenesis.

Chapter 6

In silico analysis of the VAP MSP domain

6.1 Background

The MSP domain is an s-type Immunoglobulin-like fold (Ig-fold), which is also found in several other proteins, including human growth hormone receptor, fibronectin and CD4 (Bork et al., 1994). It comprises of a seven stranded b sandwich composed of a three-stranded sheet opposed by a four stranded sheet. These sheets of the Ig-fold interact with sheets of other Ig-like domains and therefore can mediate protein-protein interactions. MSP in nematodes, apart from a cytoskeletal element, is exported from the sperm cytoplasm into the proximal gonad where via the Eph receptor blocks CaMKII signalling (Corrigan et al., 2005). Therefore, despite the fact that Ig-like domains are thought to be mainly involved in binding functions, a signalling role for the MSP domain architecture is emerging.

VAP proteins contain an N-terminal domain that is homologous to the nematode Major Sperm Protein. The VAP MSP domain shares more than 60% sequence similarity with nematode MSP, while in VAP proteins the average sequence similarity is more than 70%. This high conservation of the MSP sequence from nematodes to human suggests that the protein architecture is associated with elementary cellular processes and thus is conserved through evolution.

The Evolutionary Trace (ET) is a method for discovering novel clusters on a given protein architecture that are hotspots for protein-protein interactions (Madabushi et al., 2002, Lichtarge et al., 1996). The algorithm uses phylogenetic information from a protein family to rank the residues on a sequence according to their evolutionary importance (high conservation amongst family members). These residues can be then projected onto the known 3D structure of a protein thus defining the evolutionary conserved cluster that is likely to participate in protein-protein interactions; therefore a prerequisite is a known structure for the protein. The 3D structure of VAPA MSP has been resolved with X-ray crystallography (1Z9L, Protein data bank (PDB)) (Kaiser et al., 2005). Moreover in the Protein Families Database (PFAM) there is a non-redundant set of 348 MSP containing proteins.

ET has been used to describe functional clusters on known protein architectures; using ET the ligand binding sites of the SH2 and SH3 domains have been described (Lichtarge et al., 1996). In this chapter we will use ET with a slight

modification. The input for ET is an alignment of proteins in a family, which is then scored for conservation of residues. Alignments generated by software such as Clustal-X (Thompson et al., 2002) show amino acid conservation in family by shifting a given protein sequence and introducing gaps in order to create columns of highly conserved amino acids; if a position is not conserved, or partially conserved, a gap may be introduced. This method does not take into account the fact that when a region corresponds to a secondary structure (i.e. β-sheet) if some of the residues are not well conserved then the alignment algorithm can introduce a gap; secondary structure organization defines tertiary folding of protein domains. When describing a protein family via an alignment (so that it can be used by ET), gaps in areas of secondary structure reduce the amount of available information for a specific spot, as a gap reduces scoring for a given position. Evidently, by using an automated method for creating an alignment of a protein family, some positions of secondary structure could be misrepresented in the alignment and thus this alignment would not be a good description of the protein family. Therefore we proceed to manually process the alignment for the dataset of MSP containing protein by manually deleting or introducing gaps in order to get a good representation of secondary structure residues.

6.2 Evolutionary Trace (ET) Analysis of the MSP domain

6.2.1 Alignment of MSP domains

In order to highlight “hotspots” for protein interactions on the MSP domain 3D structure we carried out an ET analysis of a non-redundant set of 348 MSP containing proteins from the PFAM database. As we described earlier we will be using as input for the ET algorithm a manually edited version of the alignment. The dataset was aligned using Clustal-X and then gaps around areas of secondary structure were deleted or gaps were inserted in order to ensure good quality of alignment (Figure 6.2). The secondary structure of the MSP domain as observed from the 1Z9L crystal structure is seen in Figure 6.1.

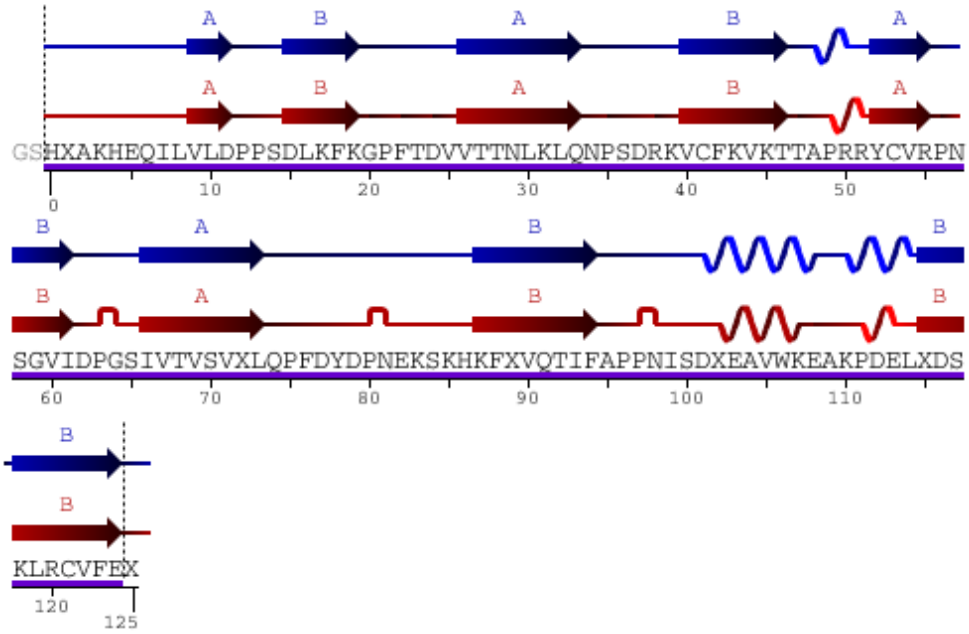

Figure 6.1 ***Secondary structure of the VAPA rat MSP domain.***

Schematic representation of the predicted by DSSP (blue) and observed by crystallographers (red) secondary structure of the MSP domain. Arrows indicate β-sheets, three-loops indicate α-helices and single loops indicate turns. Letters A,B correspond to Ig-fold sheets.

6.2.2 Conserved amino acid patch on the MSP structure

We used the manually edited alignment as input to the ET algorithm (Lichtarge et al., 1996). The algorithm returned a proposed 29 amino acid cluster on the surface of the MSP domain that is predicted to be evolutionary conserved and could participate in protein interactions (Figure 6.3C). Trace results are commonly expressed in terms of coverage: the residue is important if its coverage is small - that is if it belongs to some small top percentage of residues [100% is all of the residues in a protein], according to trace. The ET results are presented in the form of a table, usually limited to top 25% percent of residues (or to some nearby percentage), sorted by the strength of the presumed evolutionary pressure. (I.e. the smaller the coverage, the stronger the pressure on the residue) Starting from the top of that list, mutating a

Figure 6.2

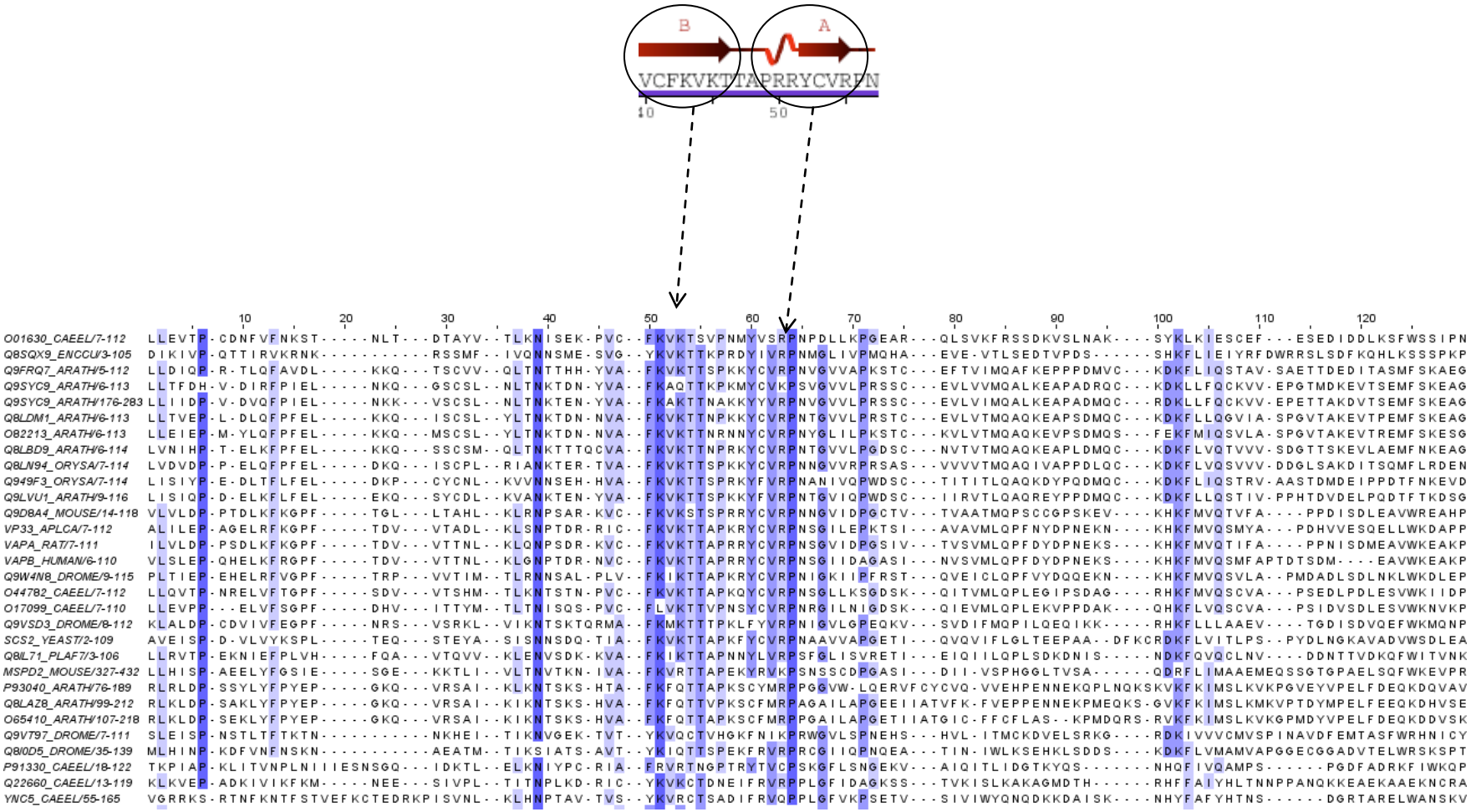
B
A
VCFKVKTTAPRRYCVRPN
10
50
O01630_CAEEL/7-112
Q8SQX9_ENCCU/3-105
Q9FRQ7_ARATH/5-112
Q9SYC9_ARATH/6-113
Q9SYC9_ARATH/176-283
Q8LDM1_ARATH/6-113
O82213_ARATH/6-113
Q8LBD9_ARATH/6-114
Q8LN94_ORYSA/7-114
Q949F3_ORYSA/7-114
Q9LVU1_ARATH/9-116
Q9DBA4_MOUSE/14-118
VP33_APLCA/7-112
VAPA_RAT/7-111
VAPB_HUMAN/6-110
Q9W4N8_DROME/9-115
O44782_CAEEL/7-112
O17099_CAEEL/7-110
Q9VSD3_DROME/8-112
SCS2_YEAST/2-109
Q8IL71_PLAF7/3-106
MSPD2_MOUSE/327-432
P93040_ARATH/76-189
Q8LAZ8_ARATH/99-212
O65410_ARATH/107-218
Q9VT97_DROME/7-111
Q8I0D5_DROME/35-139
P91330_CAEEL/18-122
Q22660_CAEEL/13-119
YNC5_CAEEL/55-165

Figure 6.2 Manual correction of the Clustal-X generated alignment for 348 MSP domain containing proteins from the PFAM database.

Schematic representation of manual "alignment correction", using the secondary MSP structure as a guide. Along with the published 3D structure of the 1Z9L VAPA rat MSP domain crystallographers submit to the Protein Database a secondary structure file as observed from the crystal. We generated an automated alignment using Clustal-X for the 348 MSP domain containing proteins from the PFAM database; using the secondary structure as a guide we manually corrected the alignment around areas of gaps. When a gap is present in one of the sequences and that area corresponds to a secondary structure (i.e. β-sheet) the gap is removed and the sequence shifted. This manual correction ensures that there is sequence information for areas of secondary structure and that the algorithm will use this information in its prediction. Not all 348 sequences of the alignment are shown and the part of the MSP secondary structure that includes the P56 is depicted.

Figure 6.3

A

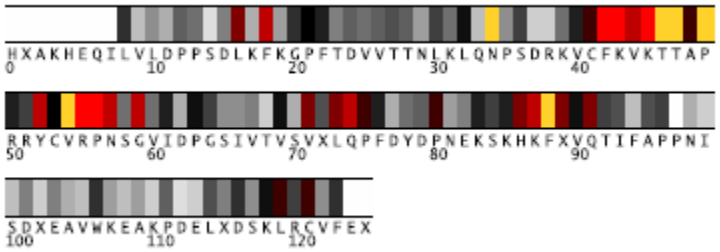

B

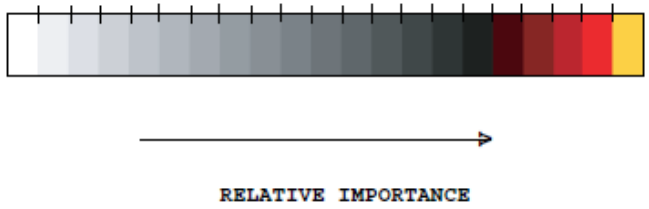

C

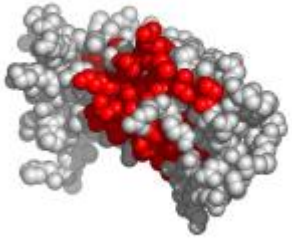

Cluster colour	size	Member residues
red	29	16,18,41, 42,43,44, 45,46,48, 49,52,53, 54,55,**56**, 57,59,71, 73,74,75, 86,87,88, 89,91

D

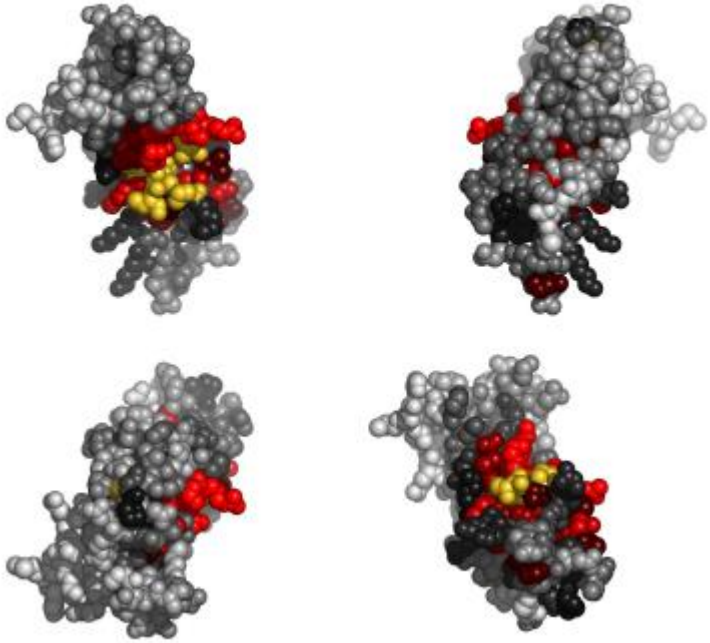

Figure 6.3 ***Evolutionary Trace analysis of the 1Z9L crystal structure of rat VAPA MSP domain.***

A. Residues 0-125 in 1Z9L coloured by their relative importance as scored by the ET algorithm. The ET algorithm receives as input an alignment of protein sequences of a given family; we here introduce a manually edited alignment "corrected" around areas of secondary structure for 348 MSP containing proteins from PFAM.

B. Colour scheme for residue scoring by the ET algorithm

C. The cluster identified by ET in red. 29 surface amino acids form an evolutionary conserved cluster predicted to participate in protein-protein interactions. The P56 belongs in this cluster.

D. Residues in 1Z9L, coloured by their relative importance. Clockwise: front, back, top and bottom views. Original view as defined by the PDB 1Z9L pdb file.

couple of residues should affect the protein somehow, with the exact effects to be determined experimentally (Table 6.1). To detect candidates for novel functional interfaces, the algorithm first looks for residues that are solvent accessible (according to DSSP program, copyright W. Kabsch, C.Sander and MPI-MF) by at least 10 $Å^2$ (square Angstrom), which is roughly the area needed for one water molecule to come in contact with the residue. Furthermore, the algorithm requires that these residues form a cluster of residues which have a neighbour within 5 Å from any of their heavy atoms.

Table 6.1

res	type	disruptive mutations
54	V	(Y) (R) (H) (KE)
49	P	(Y) (T) (R) (H)
47	T	(K) (FW) (MR) (H)
46	T	(K) (R) (Q) (M)
43	K	(Y) (FTW) (CG) (SVAH)
56	P	(R) (YH) (K) (E)
42	F	(K) (E) (Q) (D)
55	R	(T) (YD) (SVCAG) (FELWPI)
45	K	(Y) (FW) (T) (SVA)
52	Y	(K) (Q) (M) (E)
57	N	(Y) (H) (FW) (R)
87	K	(Y) (T) (FW) (VA)
44	V	(R) (Y) (KE) (H)
74	Q	(Y) (FW) (T) (H)
59	G	(R) (KE) (H) (FW)
86	H	(E) (QM) (K) (T)
91	Q	(Y) (H) (FTW) (CG)
89	X	(Y) (R) (E) (H)
121	C	(R) (K) (H) (E)
41	C	(R) (K) (E) (QH)
75	P	(YR) (H) (T) (KE)
119	L	(R) (Y) (T) (H)
48	A	(Y) (E) (R) (K)
53	C	(E) (KR) (D) (QH)

Table 6.1 ***Predicted disruptive mutations to the MSP protein-protein interactions or ligand binding.***

The algorithm proposes disruptive mutations by using residue properties as follows: small [AV GSTC], medium [LPNQDEMIK], large [WFY HR], hydrophobic [LPV AMWFI], polar [GTCY], positively [KHR], or negatively [DE] charged, aromatic [WFY H], long aliphatic chain [EKRQM], OH-group possession [SDETY], and NH2 group possession [NQRK]. The suggestions are listed according to how different they appear to be from the original amino acid, and they are grouped in round brackets if they appear equally disruptive. From left to right, each bracketed group of amino acid types resembles more strongly the original (i.e. is, presumably, less disruptive).

6.2.3 The FFAT binding site on the MSP domain partially overlaps with the predicted evolutionary conserved patch

Kaiser et al., 2005 published the 3D structure of rat VAPA MSP domain as a dimer and as a complex with the FFAT motif. The FFAT motif is a targeting signal found in proteins shuttled to the ER surface or nuclear membrane. The interaction between FFAT containing proteins and VAP MSP domain has been shown to be essential for targeting these proteins to the relative subcellular location.

The FFAT binding site is shown in Figure 6.4C (as mapped from the 1Z9L complex file from PDB). The P56S proline is not part of the FFAT binding surface, but as hypothesized by Teuling et al., 2007, the carbon backbone of the proline could be interfering with the FFAT cluster. Moreover as seen in Figure 5.4D the predicted 29 amino acid cluster from ET only partially overlaps with the FFAT binding surface. This means that not all FFAT residues are highly conserved in all MSP containing proteins. Conversely the P56 is one of the 29 residues of the ET cluster.

Figure 6.4

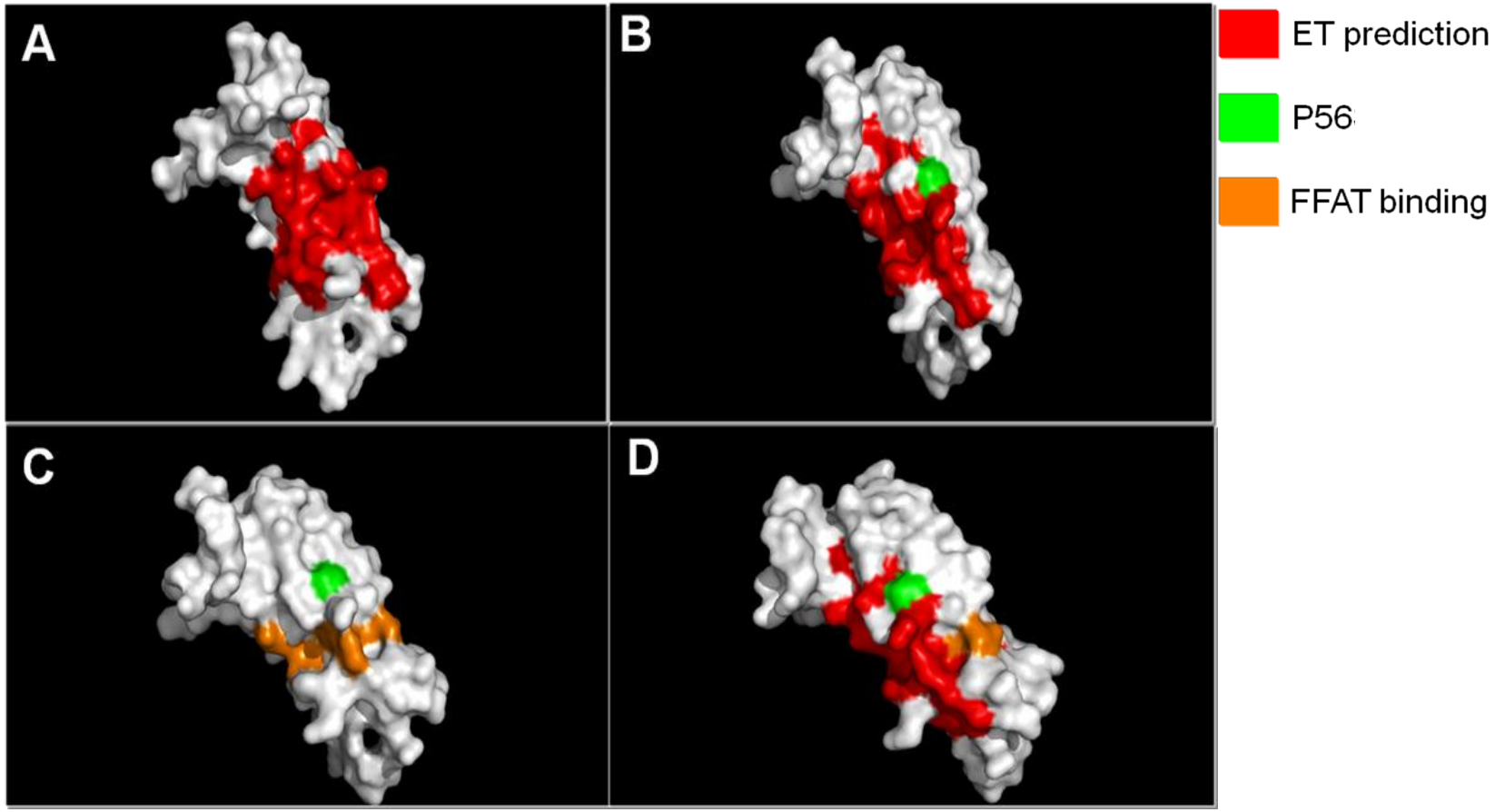

Figure 6.4 ***The predicted conserved patch on rat VAPA MSP domain contains the P56 but partially overlaps with the FFAT binding site.***

A. Results of the Evolutionary Trace mapped onto the 1Z9L crystal structure of rat VAPA MSP domain. A 29 amino acid "patch" on the surface of the MSP domain is predicted to be highly conserved and therefore might participate in protein-protein interactions

B. Results of the Evolutionary Trace mapped onto the 1Z9L crystal structure of rat VAPA MSP domain - highlighting the P56. Proline 56 is one of the 29 amino acids of the conserved "patch" and is a high scoring amino acid in this Evolutionary Trace.

C, D. Results of the Evolutionary Trace mapped onto the 1Z9L crystal structure of rat VAPA MSP domain - highlighting the P56 and the FFAT motif binding surface. The point mutation lies outside the FFAT binding site. Moreover the FFAT binding site partially overlaps with the ET cluster.

All pictures were prepared using PyMol and ET files as input. ET cluster shown in red, P56 in green and FFAT binding site in orange.

6.3 Discussion

In this Chapter we identify an evolutionary conserved 29 amino acid patch on the known 3D structure of rat VAP MSP domain (Figure 5.3). The MSP domain participates in various protein interactions (Table 1.1), while we show in Chapters 3 and 4 that it is a key regulator of the Unfolded Protein Response and that the MSP could be released after neuron-specific proteolysis of VAPB; finally overexpression of MSP is toxic to cells and renders them more vulnerable to ER stress. The conserved cluster model built by the algorithm suggests disruptive mutations for the 29 amino acids that belong to the ET cluster; this could disrupt ligand binding or protein interactions. Moreover, mutagenesis of some of those 29 amino acids could be used to investigate the MSP-ATF6 interaction and the observed effect in the transcriptional assay.

Finally, the FFAT binding cluster which is one of the key functions of the VAP MSP is not well conserved in all known MSP containing proteins, therefore it could be a function primarily associated with mammalian VAP MSP domains rather than all MSP containing proteins. The P56 which is mutated to a Serine in ALS8 patients is highly conserved and is an important residue of the ET cluster. Teuling et al., report that P56S disrupts FFAT binding; in the mutant MSP^{P56S} the residue at position 56 could be at a different position than the wild-type and thus could be part of the ET cluster. Solving the crystallographic structure of the mutant MSP would address this question.

Chapter conclusion

We have shown in this study that the MSP domain is a toxic factor and key regulator of the UPR and that VAPB MSP is released only in neuronal tissue. Evolutionary Trace analysis of the known 3D structure of rat VAPA MSP domain provides a surface 29 ligand cluster that is pivotal in the MSP architecture in terms of its protein-protein interactions. Future design of MSP ligands that would block MSP functionality could benefit from the disruptive mutations suggested by the ET model.

Chapter 7
General Discussion

7.1 General Discussion

Various functions have been ascribed to VAP proteins; lipid and inositol metabolism, vesicle trafficking, FFAT binding, ER to Golgi trafficking and regulation of the Unfolded Protein Response. VAP proteins are type-II integral membrane proteins enriched on the ER surface. A mutation (P56S) in VAPB has been associated with a late-onset form of ALS (ALS8), while recently two new (D130E, del160) ALS associated mutations have been described. The P56S mutant forms cytoplasmic aggregates; protein aggregation in brain patients is seen in many neurodegenerative diseases like Parkinson's, Alzheimer's or Huntington's (Gorman, 2008). P56S aggregation has been associated with FFAT binding (Prosser et al., 2008, Teuling et al., 2007), while FFAT overexpression dissolves P56S aggregates. In a recent report (Jaarsma D., 2008) from FENS 2008, $VAPB^{P56S}$ overexpressing transgenic mice form tubular aggregates that are continuous with ER tubules, while wild-type overexpressing lines do not; however none of the mutant lines displayed any disease symptoms. Therefore, while FFAT binding is a pivotal function of VAP proteins and has been found to be impaired in P56S mutants, it might not be the only function of VAPB linked to motor neuron degeneration in ALS8. It looks like P56S aggregates when P56S is overexpressed do not have an acute or clear effect on cell viability.

In this study we highlight the role of VAPB in regulation of the Unfolded Protein Response. We show that the N-terminal Major Sperm Protein homology domain of VAPB is a key regulator of the UPR; in addition VAPB is cleaved in a neuron specific manner and the MSP domain is released. VAPB interacts with and modulates the activity of the UPR transcription factor ATF6α. Moreover, VAPB levels affect transcriptional activation of two other ERSE containing promoters (XBP1 and BiP). In addition, VAP protein levels affect the viability of motor-neuron like cells (NSC34) recovering from ER stress. Finally, we study the highly conserved structure of the MSP domain and identify an evolutionary conserved patch of aminoacids that may be important for VAP protein function.

VAPB and ATF6α

Full length VAPB, VAPB^{P56S} and VAPA were shown to interact with full length ATF6α. Both ATF6α and VAPB are transmembrane ER proteins; ATF6α upon ER stress translocates to the Golgi where it's cleaved; the proteolytic fragment of ATF6α is shuttled to the nucleus where it activates UPR associated genes transcription. Additionally, VAPB overexpression blocks ATF6α glycosylation associated activation. These two lines of evidence suggest that VAPB-ATF6α interaction can happen on the ER membrane, but do not exclude it from occurring anywhere in the trafficking of ATF6α from ER to Golgi.

We proceed to show a functional effect of this identified interaction; overexpression of VAPB and VAPB^{P56S} inhibit activation of ATF6α as measured by the synthetic promoter of the ATF6 reporter. Conversely, siRNA mediated reduction of endogenous VAPB expression induces the reporter, reversing the inhibitory effect observed. Overexpression of VAPB truncations in the transcriptional assay shows that the MSP domain is the most potent inhibitor, the Coiled-coil is an inhibitor and the hydrophobic tail has no effect. The P56S mutant is a more potent inhibitor of ATF6α as it accumulates to lower amounts than the wild-type protein; albeit the inhibition observed for the P56S mutant constructs and the coiled-coil is dependent on the presence of the endogenous protein during overexpression.

Our data establish a link between VAP proteins and the ATF6α response to unfolded proteins in the ER lumen. The ATF6α branch of the UPR is considered to be a slower response than PERK or IRE1 (Yamamoto et al., 2007). Also, ATF6α dependent UPR associated genes are constitutive rather than induced, which suggests that ATF6α participates in development and homeostasis (Shen et al., 2005). ALS8 is a late onset neurodegenerative disease, and since ATF6 is not immediately activated in UPR this may suggest that the VAPB-ATF6 interaction becomes important later in life; PERK and IRE1 pathways are the main UPR transducers and ATF6α may constitute a complementary pathway; later in life the ATF6α pathway could be required to substitute or complement the IRE1 and PERK pathways. Failure to regulate the ATF6α pathway via VAPB could render the cells incapable to respond to accumulation of unfolded/misfolded proteins. In ALS8 the VAPB^{P56S} allele could exert a greater inhibition on ATF6α activation and thus fail to communicate with the

nucleus and initiate the UPR response.

From the aforementioned data it becomes clear that the VAPB-ATF6α interaction should be further investigated. In Figure 7.1 we depict all the potential points of regulation of ATF6 by VAPB.

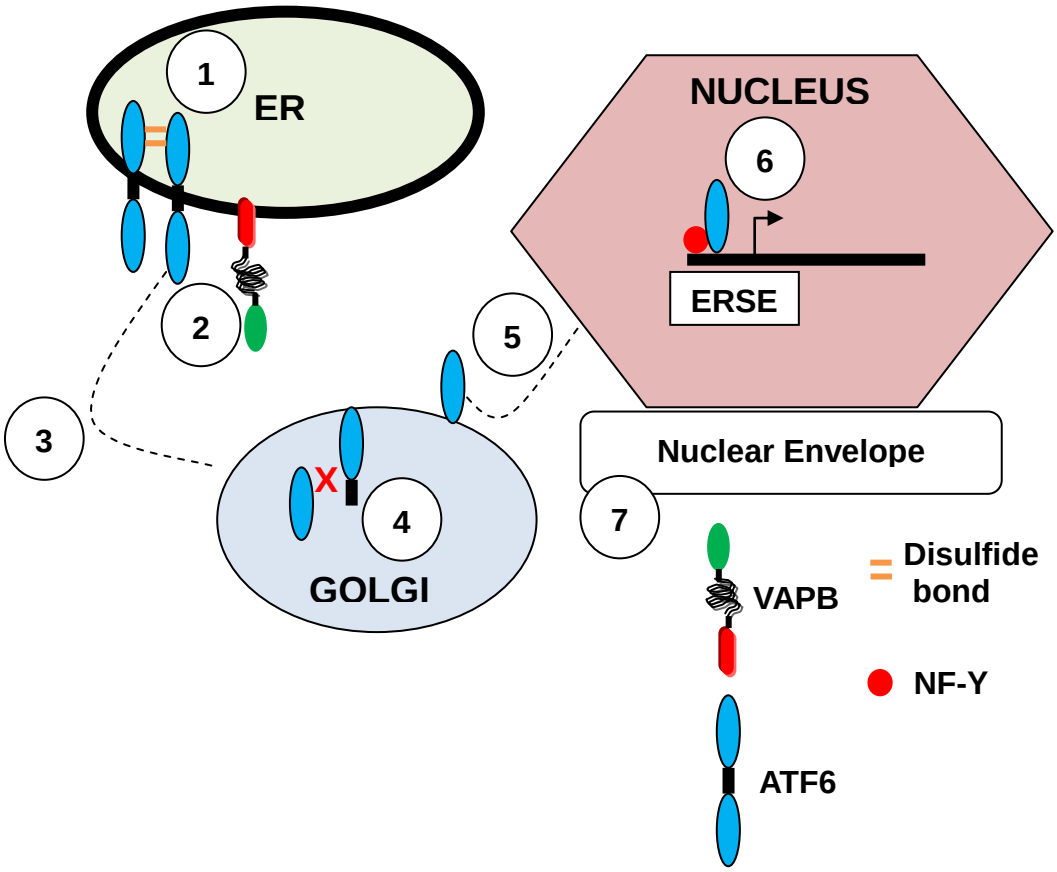

Figure 7.1 ***ATF6 and its potential regulation by VAPB***

1: VAPB overexpression blocks glycosylation associated activation of ATF6α (luminal domains of ATF6 forms disulfide bonds).

2: VAPB could be dimerizing with ATF6α on the ER membrane.

3: VAPB could block translocation of ATF6α to the Golgi cisternae.

4: VAPB could interfere with proteolysis of ATF6 by S1P and S2P.

5: VAPB could interfere with nuclear shuttling of ATF6α from the Golgi.

6: VAPB similarly to yeast (Opi1) could control ERSE binding and transcription

mediated by ATF6α in the nucleus.

7: VAPB could be interacting with ATF6α on the nuclear envelope.

Similarly to yeast, VAPB could be blocking transcription of ERSE element dependent genes by ATF6α and NF-Y. In yeast Opi1 is on the ER membrane and it's binding to the Scs2 MSP domain can regulate INO1 transcription. In yeast UPR (inositol starvation) the transcription factor Hac1 controls binding of Opi1 to INO1 promoter elements (Kagiwada and Zen, 2003). Binding of ATF6α to promoter elements could be regulated in a similar way. In order to verify this, chromatin immunoprecipitation experiments (Kuo and Allis, 1999) would need to be performed; check whether VAPB overexpression or reduction of expression with siRNA can affect binding of ATF6α to promoter elements.

ER to Golgi transport is inhibited when VAPA and $VAPB^{P56S}$ are overexpressed (Prosser et al., 2008), but VAPB has no effect. VAPA and VAPB form heterodimers and thus VAPB overexpression could block ATF6α trafficking to the Golgi via VAPA; the same applies to $VAPB^{P56S}$. $VAPB^{P56S}$ could be a stronger inhibitor of ATF6α because it might have a higher affinity for VAPA than wild-type VAPB.

Proteolysis of ATF6α in the Golgi apparatus is performed by S1P and S2P proteases. VAPB is not enriched in the Golgi cisternae, but nevertheless is present. VAPB-ATF6α association could potentially inhibit proteolysis of ATF6α thus reducing the amounts of the active N-terminal portion of ATF6α that translocates to the nucleus. Fluorescent live microscopy following ATF6α translocation while VAPB is overexpressed or reduced with siRNA could reveal if VAPB can interfere with this part of the ATF6α cycle. Finally, the nuclear envelope is an ER subdomain surrounding the nucleus; VAPB and ATF6α are present in the nuclear envelope and their interaction there could regulate ATF6α activation.

VAPB and the UPR

We show in this study that VAPB overexpression or reduction by siRNA affects transcriptional activation from the following promoters fused to a luciferase reporter gene:

- A synthetic ATF6 promoter in p5xGL3ATF6 that has been shown to be responsive not only to endogenous ATF6α but also XBP1(Wang et al., 2000).
- The human XBP1 endogenous promoter in pGL3-XBP1-(-330)-luc .
- The human BiP endogenous promoter in pGL3-GRP78-(-132)-luc.

Luciferase assays are powerful tools for investigating various effects on promoter elements; the ATF6α promoter is sensitive to ATF6α levels but also to XBP1 levels as ATF6α and XBP1 dimerize and both bind to these promoter elements (also see chapter 3.1, background); we show that VAPB can interact with ATF6α and therefore the inhibition observed is most likely due to this interaction. We also proceed to show that VAPB overexpression inhibits XBP1 reporter activation from the endogenous XBP1 promoter; conversely the BiP reporter is induced by VAPB overexpression. In accordance with this, siRNA mediated reduction of endogenous VAPB expression reverses the overexpression effect observed for XBP1 and BiP reporters. For XBP1 and BiP reporters the effect is observed for the endogenous promoter of the relative human genes which suggests a transcriptional regulation of those promoters from VAPB and VAPB^{P56S} levels. ATF6α and XBP1 heterodimerize (Yamamoto et al., 2007) and for both reporters the effect of VAPB overexpression is inhibitory, which might suggest an active participation of VAPB in regulating the dynamics of this dimer and thus UPR regulation. Activation of the BiP chaperone constitutes the main part of the UPR response to unfolded protein accumulation in the ER lumen; VAPB induces BiP activation, while VAPB^{P56S} does not. In ALS8, failing to activate the BiP response could impede folding of unfolded proteins and lead to cell death. Interestingly the VAPB^{P56S} effect observed for XBP1 and BiP transcriptional activation is dependent on the presence of the endogenous protein. On the other hand, overexpression of VAPB and VAPB^{P56S} but not GFP or tubulin reduces cell viability after ER stress. This shows that when the balance of VAP proteins is perturbed, cells are more susceptible to apoptotic death once their UPR has been activated.

In conclusion, VAP proteins are here shown to be involved in regulation of the transcriptional activation of the UPR by a) acting on several UPR-ERSE associated promoter elements and b) by directly interacting with the UPR transducer ATF6α. The P56S ALS8 associated mutant displays a similar effect (which might be

more potent for the same amount of protein) which is however dependent on the presence of the endogenous protein. Nevertheless VAP protein levels seem to regulate the UPR and affect cell viability once the UPR is activated. Apart from the activation phase of the UPR, VAPs could be acting on the recovery phase of the cell.

The MSP domain

The MSP domain is the most conserved domain of VAP proteins and its Ig-like fold has been implicated in various protein-protein interactions (Tarr and Scott, 2005). Middleton, 2005 showed that MSP overexpression is toxic to cells and primary neurons and also that MSP of VAPA interacts with ATF6α.We have shown that VAP MSP is released after VAP protein cleavage and that VAPB cleavage is neuron tissue specific (Gkogkas et al., 2008) and Tsuda et al., 2008 showed that drosophila VAP is cleaved and secreted.

In this study we show that VAPB MSP is a key regulator of the UPR and affects cell viability. When overexpressed MSP inhibits transcriptional activation of the ATF6α and XBP1 reporters and is the most potent inhibitor amongst VAPB domains; the BiP reporter is induced and MSP is again the most potent activator amongst VAPB domains. The MSP in all three aforementioned instances retains its overexpression effect when the endogenous VAPB is blocked with siRNA. MSP^{P56S} inhibits ATF6 and XBP1 reporters but has no effect on BiP activation. Moreover the MSP^{P56S} overexpression effect is dependent on the presence of endogenous VAPB. Furthermore, overexpression of MSP and MSP^{P56S} EGFP fusion proteins forms large cytoplasmic aggregates and is toxic to cells (Middleton, 2005); in addition, MSP and MSP^{P56S} overexpression in cells that have been induced with the N-glycosylation inhibitor tunicamycin (UPR is induced) reduces cell viability via apoptosis.

We additionally show that neuron specific VAPB cleavage can occur in a dissociated cortical neuron culture, in spinal cord tissue but not in glial primary cultures, HEK293, NSC34 or C6 glioma cells. Although proteolysis can be seen in embryonic brain tissue, it is not observed at day 1 in vitro of the dissociated cultured cells but can be seen at day 11. In accordance with this, overexpressed human VAPB, $VAPB^{P56S}$, $VAPB^{D130E}$, $VAPB^{del160}$ are not cleaved at DIV1. At DIV11 VAPB, $VAPB^{D130E}$ and $VAPB^{del160}$ are cleaved while $VAPB^{P56S}$ is not; also the D130E

mutant is proteolysed more. Remarkably, mouse $VAPB^{A130E}$ but not $VAPB^{A130D}$ inhibits ATF6α, XBP1 reporters and induces the BiP reporter more than wild-type VAPB or $VAPB^{P56S}$ in HEK293 cells; From all the aforementioned constructs in HEK293 cells only $VAPB^{A130E}$ is proteolysed and it's that construct that has a more potent effect on UPR activation (the three reporters used).

To sum up, endogenous VAPB and not VAPA are cleaved in a neuron specific manner and this proteolysis most likely releases the MSP domain. The MSP monomer overexpression is toxic to cells and reduces cell viability after ER stress; moreover the wild-type MSP is a potent inhibitor of ATF6 and XBP1 and a potent inducer of BiP; the P56S mutant functionality depends on the endogenous VAPB protein. Our data suggests that MSP^{P56S} is not cleaved, while the D130E increases the proteolysis of the protein. The fact that VAPB gets cleaved only in neurons could be highlighting an important physiological function of the protein. Non-cleavage of $VAPB^{P56S}$ and enhanced cleavage of $VAPB^{D130E}$ are two paradigms of aberrant proteolysis of VAPB in neurons associated with ALS8 mutations. Finally, the proposed secretion of the MSP domain (Tsuda et al., 2008) could be a mechanism via which neurons act on glial cells or other neurons.

VAPB domains

We have shown using ATF6, XBP1 and BiP reporters that overexpression of VAPB truncations has different effects on transcriptional activation of these reporters. The C-terminal hydrophobic tail of VAPB localizes to the ER membrane and when overexpressed has no effect on any of the three reporters. The Coiled-Coil domain participates in promiscuous protein-protein interactions and inhibits the ATF6 reporter activation but has no effect on XBP1 and BiP reporters. Moreover when the endogenous VAPB expression is blocked with siRNA, the Coiled-Coil effect is abolished, suggesting a dependency from the endogenous VAPB Coiled-Coil or MSP domain or another unidentified factor. These data reveal that the cytoplasmic domains of VAPB can participate in UPR regulation. Additionally, overexpression of CC reduces viability of NSC34 cells after ER stress by inducing apoptosis, suggesting that CC levels are important for UPR regulation and can lead to cell death when their balance is perturbed. The MSP and CC domains might interact on the

same molecule or in VAPB dimers. VAPA and VAPB high sequence similarity and the fact that they heterodimirize could suggest a VAPA-VAPB modulation of the observed Coiled-Coil effect. Nevertheless, VAPB dimmers, multimers or VAPA-VAPB heterodimers could affect regulation of the UPR by masking or titrating regulatory UPR VAP domains (MSP, CC). A mutagenesis study of the observed inhibition or induction of the luciferase reporters could highlight important residues.

A model for ALS8 motor neuron degeneration

Neuron specificity of VAPB cleavage and subsequent release of the MSP domain becomes extremely important in a motor neuron context. We have shown that the MSP domain when overexpressed is toxic and renders cells more vulnerable after ER stress, while it has a profound effect on UPR transducers activation. Motor neurons have long processes that enervate muscles; many cellular factors are transported along the axon and reach the terminals of long processes (Van Den Bosch and Robberecht, 2008).

The fact that VAPB is cleaved only in neurons might reflect a need for local regulation in the long neuronal processes or crosstalk with other cells (glia) in the nervous system. We show that increased amounts of MSP are toxic and kill cells via apoptosis; it could be that intracellular amounts of free MSP domain need to be regulated and the cell cannot handle the excess protein. Apart from the observed toxicity, overexpression of MSP has a profound effect on the UPR response; we show that overexpression of MSP after ER stress reduces cell viability by inducing apoptotic death. Therefore, apart from the profound effect on transcriptional activation, increased intracellular MSP reduces cell viability and renders cells more vulnerable to induction of apoptosis following ER stress. Full length VAPB overexpression has a similar effect but not as profound (for transcriptional regulation and cell death). On the other hand, MSP^{P56S} transcriptional regulation for ATF6 and XBP1 reporters is dependent on endogenous VAPB, while the MSP^{P56S} has no effect on BiP reporter activity; moreover, expressed human $VAPB^{P56S}$ does not get cleaved in neurons. These data suggest that the P56S mutation might block VAPB neuron specific cleavage. In drosophila Tsuda et al., 2008 showed that the P56S mutant also gets cleaved and secreted but cannot interact with the ephrin receptor.

Figure 7.2

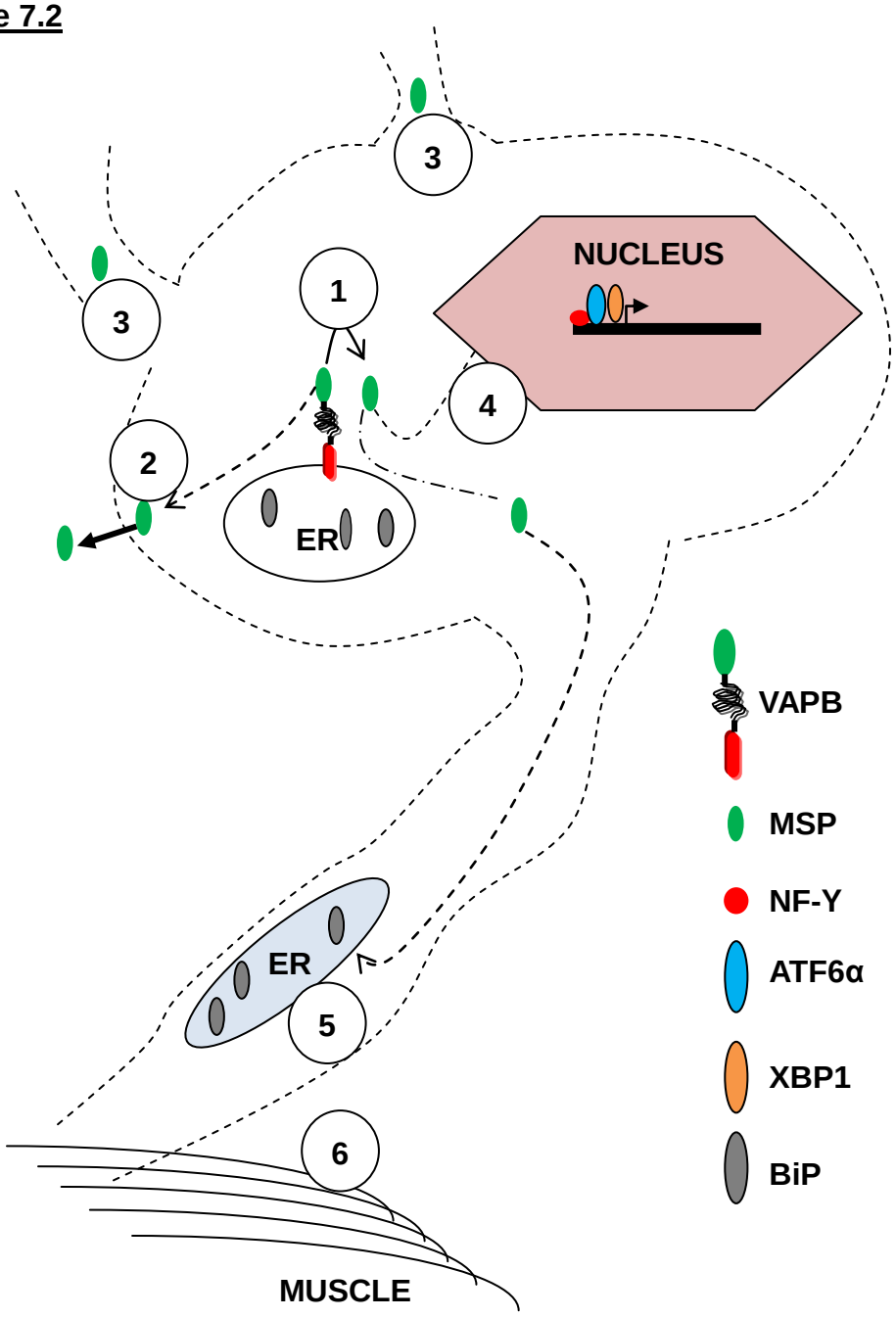

Figure 7.2 ***A model for MSP function in neurons.***

Schematic representation of a motor neuron and the effect of VAPB neuron specific cleavage.

1: VAPB gets cleaved on the ER or other membranes and the MSP domain is

released in the cytoplasm.

2: MSP gets secreted and can act on other cells either via the ephrin receptor (Tsuda et al., 2008) or another unidentified route.

3: MSP is targeted to dendrites where it could associate with the UPR machinery on ER microdomains.

4: MSP could be acting indirectly on UPR gene transcription in the nucleus or directly by being transported in the nucleoplasm where it could associate with nuclear ATF6α. Nevertheless, the MSP domain could be acting on various ERSE elements.

5: MSP could act on ER microdomains in synapses along the motor neuron axon.

6: MSP could act on muscle cells in the motor neuron Neuromuscular Junction.

Our data suggest that human $VAPB^{P56S}$ in a rat neuron dissociated culture does not get cleaved. Conversely, D130E and del160 VAPB mutants get cleaved and the D130E mutant displays enhanced cleavage (and potent inhibition of ATF6, XBP1 and induction of BiP).

As depicted in Figure 7.2, enhanced cleavage or no cleavage could potentially interfere with the proposed MSP pathway in motor neurons. MSP could be in the cytoplasm after cleavage of membrane bound VAPB and subsequently could be secreted and act on other cells. MSP could be transported down the axon and act on distal ER microdomains by interacting with ATF6α or affect nuclear UPR response indirectly or by nuclear internalization. Also, MSP could be acting on muscle cells at the Neuromuscular junction (NMJ). In this context non-cleavage (P56S) or enhanced cleavage (D130E) could affect the various points of regulation by the MSP domain.

In P56S ALS8 patients described so far there two alleles of VAPB; wild-type VAPB and the P56S mutant. Interaction between the two alleles could be pivotal for development of motor neuron degeneration; non-cleavage of P56S could affect the balance of VAPB proteins by heterodimerization. Our data suggest that the MSP^{P56S} can have a regulatory effect on UPR provided the endogenous protein is present. However non-cleavage of $VAPB^{P56S}$ suggests that the MSP^{P56S} monomer might not exist as a monomer in neurons; if it does get cleaved as Tsuda et al., 2008 suggest for

the drosophila protein our data supports that the domain produced is non-functional regarding transcriptional activation of the UPR.

Tsuda et al., 2008 suggest that the MSP domain behaves like a hormone by acting on the ephrin receptors of neighbour cells. We propose that the MSP domain has a key intracellular UPR regulatory role which affects motor neuron viability in uninduced or ER stress induced cells; this physiological function can be perturbed by ALS8 associated mutations (P56S, D130E, del160).

VAP and ALS

Motor neuron degeneration in late onset ALS (like ALS8) suggests that neurons die as a result of an accumulation of insults (protein misfolding, oxidative stress, mitochondrial dysfunction, inflammation) throughout life or as a result of an acute change in cell physiology underlined by a change in gene interactions that is correlated with aging or environmental cues; most likely a cellular factor gains some form of toxicity that accelerates disease progression or manifestation (Boillee et al., 2006). Moreover, sporadic and familial cases display similar pathology.

Recently, the participation of non-neuronal cells in motor neuron degeneration is being extensively studied (Nagai et al., 2007). ALS is a multifactorial disease and ultimately cell death is a combination of multiple pathway participation in a non-cell autonomous manner.

Perturbation of transcriptional regulation within motorneurons can lead to cell death as it has been shown for many neurodegenerative diseases (Chu et al., 2007). We have shown that VAP proteins and their ALS associated mutants participate in UPR associated promoter elements regulation. It could be that VAP proteins contribute to ALS pathogenesis by misregulating transcription factor promoter elements. Studying VAP proteins and their involvement in late-onset ALS in neuronal and nonneuronal cells could highlight new therapeutic avenues.

Conclusion

This study highlights a novel interaction for the ALS8 associated VAPB gene with the Unfolded Protein Response of the Endoplasmic Reticulum. ALS is a disease of motor neurons and therefore validation for this interaction and modulatory effect

of VAPB levels on UPR regulation in motor neurons is necessary. We have developed and applied three straightforward assays for monitoring the effect of VAPB levels on the UPR; a luciferase based transcriptional assay and a cell death assay and a fluorescent protein complementation assay. If VAPB proves to be a biomarker for ALS8 in motor neurons then these assays can be used for drug discovery. Until now VAPB has been associated with ALS8 via the large Brazilian pedigree (Nishimura et al., 2004); further epidemiological studies might highlight VAPB as an ALS8 candidate gene and therefore elucidating its participation in the various cellular processes is of high importance.

References

ALAM, J. & COOK, J. L. (1990) Reporter genes: application to the study of mammalian gene transcription. Anal Biochem, 188, 245-54.

AMARILIO, R., RAMACHANDRAN, S., SABANAY, H. & LEV, S. (2005) Differential regulation of endoplasmic reticulum structure through VAP-Nir protein interaction. J Biol Chem, 280, 5934-44.

ATURALIYA, R. N., FINK, J. L., DAVIS, M. J., TEASDALE, M. S., HANSON, K. A., MIRANDA, K. C., FORREST, A. R., GRIMMOND, S. M., SUZUKI, H., KANAMORI, M., KAI, C., KAWAI, J., CARNINCI, P., HAYASHIZAKI, Y. & TEASDALE, R. D. (2006) Subcellular localization of mammalian type II membrane proteins. Traffic, 7, 613-25.

ATWAL, R. S. & TRUANT, R. (2008) A stress sensitive ER membrane-association domain in Huntingtin protein defines a potential role for Huntingtin in the regulation of autophagy. Autophagy, 4, 91-3.

BACK, S. H., SCHRODER, M., LEE, K., ZHANG, K. & KAUFMAN, R. J. (2005) ER stress signaling by regulated splicing: IRE1/HAC1/XBP1. Methods, 35, 395-416.

BAILEY, D. & O'HARE, P. (2007) Transmembrane bZIP transcription factors in ER stress signaling and the unfolded protein response. Antioxid Redox Signal, 9, 2305-21.

BOILLEE, S., VANDE VELDE, C. & CLEVELAND, D. W. (2006) ALS: a disease of motor neurons and their nonneuronal neighbors. Neuron, 52, 39-59.

BORDIER, C. (1981) Phase separation of integral membrane proteins in Triton X-114 solution. J Biol Chem, 256, 1604-7.

BORGESE, N., FRANCOLINI, M. & SNAPP, E. (2006) Endoplasmic reticulum architecture: structures in flux. Curr Opin Cell Biol, 18, 358-64.

BORK, P., HOLM, L. & SANDER, C. (1994) The immunoglobulin fold. Structural classification, sequence patterns and common core. J Mol Biol, 242, 309-20.

BOYD, A. W. & LACKMANN, M. (2001) Signals from Eph and ephrin proteins: a

developmental tool kit. Sci STKE, 2001, RE20.

BRUNGER, A. T. (2005) Structure and function of SNARE and SNARE-interacting proteins. Q Rev Biophys, 38, 1-47.

BURRI, L., VARLAMOV, O., DOEGE, C. A., HOFMANN, K., BEILHARZ, T., ROTHMAN, J. E., SOLLNER, T. H. & LITHGOW, T. (2003) A SNARE required for retrograde transport to the endoplasmic reticulum. Proc Natl Acad Sci U S A, 100, 9873-7.

CARETTE, J. E., VERVER, J., MARTENS, J., VAN KAMPEN, T., WELLINK, J. & VAN KAMMEN, A. (2002) Characterization of plant proteins that interact with cowpea mosaic virus '60K' protein in the yeast two-hybrid system. J Gen Virol, 83, 885-93.

CHAI, A., WITHERS, J., KOH, Y. H., PARRY, K., BAO, H., ZHANG, B., BUDNIK, V. & PENNETTA, G. (2008) hVAPB, the causative gene of a heterogeneous group of motor neuron diseases in humans, is functionally interchangeable with its Drosophila homologue DVAP-33A at the neuromuscular junction. Hum Mol Genet, 17, 266-80.

CHAN, S. L. & MATTSON, M. P. (1999) Caspase and calpain substrates: roles in synaptic plasticity and cell death. J Neurosci Res, 58, 167-90.

CHEN, Y. A. & SCHELLER, R. H. (2001) SNARE-mediated membrane fusion. Nat Rev Mol Cell Biol, 2, 98-106.

CHU, C. T., PLOWEY, E. D., WANG, Y., PATEL, V. & JORDAN-SCIUTTO, K. L. (2007) Location, location, location: altered transcription factor trafficking in neurodegeneration. J Neuropathol Exp Neurol, 66, 873-83.

CLAMP, M., CUFF, J., SEARLE, S. M. & BARTON, G. J. (2004) The Jalview Java alignment editor. Bioinformatics, 20, 426-7.

COLLINS, T. J. (2007) ImageJ for microscopy. Biotechniques, 43, 25-30.

CONFORTI, F. L., SPROVIERI, T., MAZZEI, R., UNGARO, C., TESSITORE, A., TEDESCHI, G., PATITUCCI, A., MAGARIELLO, A., GABRIELE, A., LABELLA, V., SIMONE, I. L., MAJORANA, G., MONSURRO, M. R., VALENTINO, P., MUGLIA, M. & QUATTRONE, A. (2006) Sporadic ALS is

not associated with VAPB gene mutations in Southern Italy. J Negat Results Biomed, 5, 7.

CORRIGAN, C., SUBRAMANIAN, R. & MILLER, M. A. (2005) Eph and NMDA receptors control Ca2+/calmodulin-dependent protein kinase II activation during C. elegans oocyte meiotic maturation. Development, 132, 5225-37.

CRAIGHEAD, M. W., TIWARI, P., KEYNES, R. G. & WATERS, C. M. (1999) Human oligodendroglial cell line, MO3.13, can be protected from apoptosis using the general caspase inhibitor zVAD-FMK. J Neurosci Res, 57, 236-43.

DUDEN, R. (2003) ER-to-Golgi transport: COP I and COP II function (Review). Mol Membr Biol, 20, 197-207.

ETTAYEBI, K. & HARDY, M. E. (2003) Norwalk virus nonstructural protein p48 forms a complex with the SNARE regulator VAP-A and prevents cell surface expression of vesicular stomatitis virus G protein. J Virol, 77, 11790-7.

FOSTER, L. J., WEIR, M. L., LIM, D. Y., LIU, Z., TRIMBLE, W. S. & KLIP, A. (2000) A functional role for VAP-33 in insulin-stimulated GLUT4 traffic. Traffic, 1, 512-21.

FRANDSEN, A. & SCHOUSBOE, A. (1991) Dantrolene prevents glutamate cytotoxicity and Ca2+ release from intracellular stores in cultured cerebral cortical neurons. J Neurochem, 56, 1075-8.

GAVIN, A. C., BOSCHE, M., KRAUSE, R., GRANDI, P., MARZIOCH, M., BAUER, A., SCHULTZ, J., RICK, J. M., MICHON, A. M., CRUCIAT, C. M., REMOR, M., HOFERT, C., SCHELDER, M., BRAJENOVIC, M., RUFFNER, H., MERINO, A., KLEIN, K., HUDAK, M., DICKSON, D., RUDI, T., GNAU, V., BAUCH, A., BASTUCK, S., HUHSE, B., LEUTWEIN, C., HEURTIER, M. A., COPLEY, R. R., EDELMANN, A., QUERFURTH, E., RYBIN, V., DREWES, G., RAIDA, M., BOUWMEESTER, T., BORK, P., SERAPHIN, B., KUSTER, B., NEUBAUER, G. & SUPERTI-FURGA, G. (2002) Functional organization of the yeast proteome by systematic analysis of protein complexes. Nature, 415, 141-7.

GKOGKAS, C., MIDDLETON, S., KREMER, A. M., WARDROPE, C., HANNAH, M.,

GILLINGWATER, T. H. & SKEHEL, P. (2008) VAPB interacts with and modulates the activity of ATF6. Hum Mol Genet, 17, 1517-26.

GONG, Y., LEE, J. N., BROWN, M. S., GOLDSTEIN, J. L. & YE, J. (2006) Juxtamembranous aspartic acid in Insig-1 and Insig-2 is required for cholesterol homeostasis. Proc Natl Acad Sci U S A, 103, 6154-9.

GORMAN, A. M. (2008) Neuronal cell death in neurodegenerative diseases: recurring themes around protein handling. J Cell Mol Med.

GOUGEON, P. Y. & NGSEE, J. K. (2005) Purification and functional properties of prenylated Rab acceptor 2. Methods Enzymol, 403, 799-807.

HAI, T. W., LIU, F., COUKOS, W. J. & GREEN, M. R. (1989) Transcription factor ATF cDNA clones: an extensive family of leucine zipper proteins able to selectively form DNA-binding heterodimers. Genes Dev, 3, 2083-90.

HAMAMOTO, I., NISHIMURA, Y., OKAMOTO, T., AIZAKI, H., LIU, M., MORI, Y., ABE, T., SUZUKI, T., LAI, M. M., MIYAMURA, T., MORIISHI, K. & MATSUURA, Y. (2005) Human VAP-B is involved in hepatitis C virus replication through interaction with NS5A and NS5B. J Virol, 79, 13473-82.

HANADA, K., KUMAGAI, K., TOMISHIGE, N. & KAWANO, M. (2007) CERT and intracellular trafficking of ceramide. Biochim Biophys Acta, 1771, 644-53.

HAYRAPETYAN, V., RYBALCHENKO, V., RYBALCHENKO, N. & KOULEN, P. (2008) The N-terminus of presenilin-2 increases single channel activity of brain ryanodine receptors through direct protein-protein interaction. Cell Calcium, 44, 507-18.

HAZE, K., OKADA, T., YOSHIDA, H., YANAGI, H., YURA, T., NEGISHI, M. & MORI, K. (2001) Identification of the G13 (cAMP-response-element-binding protein-related protein) gene product related to activating transcription factor 6 as a transcriptional activator of the mammalian unfolded protein response. Biochem J, 355, 19-28.

HOOZEMANS, J. J., VEERHUIS, R., VAN HAASTERT, E. S., ROZEMULLER, J. M., BAAS, F., EIKELENBOOM, P. & SCHEPER, W. (2005) The unfolded protein response is activated in Alzheimer's disease. Acta Neuropathol, 110, 165-72.

HOSAKA, K., NIKAWA, J., KODAKI, T. & YAMASHITA, S. (1992) A dominant mutation that alters the regulation of INO1 expression in Saccharomyces cerevisiae. J Biochem, 111, 352-8.

JAARSMA D., T. E., AHMED S., HAASDIJK E., VAN DIS V. & HOOGENRAAD C. C. (2008) Transgenic mice expressing ALS-mutant VAPB develop endoplasmic reticulum-derived tubular aggregates in motor neurons. FENS Forum 2008. Geneva, Switzerland.

JU, W., MORISHITA, W., TSUI, J., GAIETTA, G., DEERINCK, T. J., ADAMS, S. R., GARNER, C. C., TSIEN, R. Y., ELLISMAN, M. H. & MALENKA, R. C. (2004) Activity-dependent regulation of dendritic synthesis and trafficking of AMPA receptors. Nat Neurosci, 7, 244-53.

KAGIWADA, S. & HASHIMOTO, M. (2007) The yeast VAP homolog Scs2p has a phosphoinositide-binding ability that is correlated with its activity. Biochem Biophys Res Commun, 364, 870-6.

KAGIWADA, S., HOSAKA, K., MURATA, M., NIKAWA, J. & TAKATSUKI, A. (1998) The Saccharomyces cerevisiae SCS2 gene product, a homolog of a synaptobrevin-associated protein, is an integral membrane protein of the endoplasmic reticulum and is required for inositol metabolism. J Bacteriol, 180, 1700-8.

KAGIWADA, S. & ZEN, R. (2003) Role of the yeast VAP homolog, Scs2p, in INO1 expression and phospholipid metabolism. J Biochem, 133, 515-22.

KAISER, S. E., BRICKNER, J. H., REILEIN, A. R., FENN, T. D., WALTER, P. & BRUNGER, A. T. (2005) Structural basis of FFAT motif-mediated ER targeting. Structure, 13, 1035-45.

KANEKURA, K., NISHIMOTO, I., AISO, S. & MATSUOKA, M. (2006) Characterization of amyotrophic lateral sclerosis-linked P56S mutation of vesicle-associated membrane protein-associated protein B (VAPB/ALS8). J Biol Chem, 281, 30223-33.

KAWANO, M., KUMAGAI, K., NISHIJIMA, M. & HANADA, K. (2006) Efficient trafficking of ceramide from the endoplasmic reticulum to the Golgi apparatus

requires a VAMP-associated protein-interacting FFAT motif of CERT. J Biol Chem, 281, 30279-88.

KOSINSKI, M., MCDONALD, K., SCHWARTZ, J., YAMAMOTO, I. & GREENSTEIN, D. (2005) C. elegans sperm bud vesicles to deliver a meiotic maturation signal to distant oocytes. Development, 132, 3357-69.

KUO, M. H. & ALLIS, C. D. (1999) In vivo cross-linking and immunoprecipitation for studying dynamic Protein:DNA associations in a chromatin environment. Methods, 19, 425-33.

LANDERS, J. E., LECLERC, A. L., SHI, L., VIRKUD, A., CHO, T., MAXWELL, M. M., HENRY, A. F., POLAK, M., GLASS, J. D., KWIATKOWSKI, T. J., AL-CHALABI, A., SHAW, C. E., LEIGH, P. N., RODRIGUEZ-LEYZA, I., MCKENNA-YASEK, D., SAPP, P. C. & BROWN, R. H., JR. (2008) New VAPB deletion variant and exclusion of VAPB mutations in familial ALS. Neurology, 70, 1179-85.

LAPIERRE, L. A., TUMA, P. L., NAVARRE, J., GOLDENRING, J. R. & ANDERSON, J. M. (1999) VAP-33 localizes to both an intracellular vesicle population and with occludin at the tight junction. J Cell Sci, 112 (Pt 21), 3723-32.

LAURENT, F., LABESSE, G. & DE WIT, P. (2000) Molecular cloning and partial characterization of a plant VAP33 homologue with a major sperm protein domain. Biochem Biophys Res Commun, 270, 286-92.

LEE, A. H., IWAKOSHI, N. N. & GLIMCHER, L. H. (2003) XBP-1 regulates a subset of endoplasmic reticulum resident chaperone genes in the unfolded protein response. Mol Cell Biol, 23, 7448-59.

LEHTO, M., HYNYNEN, R., KARJALAINEN, K., KUISMANEN, E., HYVARINEN, K. & OLKKONEN, V. M. (2005) Targeting of OSBP-related protein 3 (ORP3) to endoplasmic reticulum and plasma membrane is controlled by multiple determinants. Exp Cell Res, 310, 445-62.

LEV, S., BEN HALEVY, D., PERETTI, D. & DAHAN, N. (2008) The VAP protein family: from cellular functions to motor neuron disease. Trends Cell Biol, 18, 282-90.

LICHTARGE, O., BOURNE, H. R. & COHEN, F. E. (1996) An evolutionary trace method defines binding surfaces common to protein families. J Mol Biol, 257, 342-58.

LOEWEN, C. J. & LEVINE, T. P. (2005) A highly conserved binding site in vesicle-associated membrane protein-associated protein (VAP) for the FFAT motif of lipid-binding proteins. J Biol Chem, 280, 14097-104.

LOEWEN, C. J., ROY, A. & LEVINE, T. P. (2003) A conserved ER targeting motif in three families of lipid binding proteins and in Opi1p binds VAP. Embo J, 22, 2025-35.

LOTZ, G. P., BRYCHZY, A., HEINZ, S. & OBERMANN, W. M. (2008) A novel HSP90 chaperone complex regulates intracellular vesicle transport. J Cell Sci, 121, 717-23.

LUNDIN, M., LINDSTROM, H., GRONWALL, C. & PERSSON, M. A. (2006) Dual topology of the processed hepatitis C virus protein NS4B is influenced by the NS5A protein. J Gen Virol, 87, 3263-72.

LUPAS, A., VAN DYKE, M. & STOCK, J. (1991) Predicting coiled coils from protein sequences. Science, 252, 1162-1164.

MADABUSHI, S., YAO, H., MARSH, M., KRISTENSEN, D. M., PHILIPPI, A., SOWA, M. E. & LICHTARGE, O. (2002) Structural clusters of evolutionary trace residues are statistically significant and common in proteins. J Mol Biol, 316, 139-54.

MATLACK, K. E., MOTHES, W. & RAPOPORT, T. A. (1998) Protein translocation: tunnel vision. Cell, 92, 381-90.

MIDDLETON, S. (2005) A VAP-33 homologue: a possible role in intracellular signalling and membrane structure in neurons. Centre For Neuroscience Research. University of Edinburgh.

MILLER, M. A., RUEST, P. J., KOSINSKI, M., HANKS, S. K. & GREENSTEIN, D. (2003) An Eph receptor sperm-sensing control mechanism for oocyte meiotic maturation in Caenorhabditis elegans. Genes Dev, 17, 187-200.

MITNE-NETO, M., RAMOS, C. R., PIMENTA, D. C., LUZ, J. S., NISHIMURA, A. L.,

GONZALES, F. A., OLIVEIRA, C. C. & ZATZ, M. (2007) A mutation in human VAP-B--MSP domain, present in ALS patients, affects the interaction with other cellular proteins. Protein Expr Purif, 55, 139-46.

MODY, I. & MACDONALD, J. F. (1995) NMDA receptor-dependent excitotoxicity: the role of intracellular Ca2+ release. Trends Pharmacol Sci, 16, 356-9.

MORIISHI, K. & MATSUURA, Y. (2007) Host factors involved in the replication of hepatitis C virus. Rev Med Virol, 17, 343-54.

NADANAKA, S., OKADA, T., YOSHIDA, H. & MORI, K. (2007) Role of disulfide bridges formed in the luminal domain of ATF6 in sensing endoplasmic reticulum stress. Mol Cell Biol, 27, 1027-43.

NAGAI, M., RE, D. B., NAGATA, T., CHALAZONITIS, A., JESSELL, T. M., WICHTERLE, H. & PRZEDBORSKI, S. (2007) Astrocytes expressing ALS-linked mutated SOD1 release factors selectively toxic to motor neurons. Nat Neurosci, 10, 615-22.

NICOTERA, P., LEIST, M. & MANZO, L. (1999) Neuronal cell death: a demise with different shapes. Trends Pharmacol Sci, 20, 46-51.

NIKAWA, J., MURAKAMI, A., ESUMI, E. & HOSAKA, K. (1995) Cloning and sequence of the SCS2 gene, which can suppress the defect of INO1 expression in an inositol auxotrophic mutant of Saccharomyces cerevisiae. J Biochem, 118, 39-45.

NILES, A. L., MORAVEC, R. A., ERIC HESSELBERTH, P., SCURRIA, M. A., DAILY, W. J. & RISS, T. L. (2007) A homogeneous assay to measure live and dead cells in the same sample by detecting different protease markers. Anal Biochem, 366, 197-206.

NISHIMURA, A. L., AL-CHALABI, A. & ZATZ, M. (2005) A common founder for amyotrophic lateral sclerosis type 8 (ALS8) in the Brazilian population. Hum Genet, 118, 499-500.

NISHIMURA, A. L., MITNE-NETO, M., SILVA, H. C., RICHIERI-COSTA, A., MIDDLETON, S., CASCIO, D., KOK, F., OLIVEIRA, J. R., GILLINGWATER, T., WEBB, J., SKEHEL, P. & ZATZ, M. (2004) A mutation

in the vesicle-trafficking protein VAPB causes late-onset spinal muscular atrophy and amyotrophic lateral sclerosis. Am J Hum Genet, 75, 822-31.

NISHIMURA, Y., HAYASHI, M., INADA, H. & TANAKA, T. (1999) Molecular cloning and characterization of mammalian homologues of vesicle-associated membrane protein-associated (VAMP-associated) proteins. Biochem Biophys Res Commun, 254, 21-6.

OKADA, T., HAZE, K., NADANAKA, S., YOSHIDA, H., SEIDAH, N. G., HIRANO, Y., SATO, R., NEGISHI, M. & MORI, K. (2003) A serine protease inhibitor prevents endoplasmic reticulum stress-induced cleavage but not transport of the membrane-bound transcription factor ATF6. J Biol Chem, 278, 31024-32.

O'LEARY, D. D. & WILKINSON, D. G. (1999) Eph receptors and ephrins in neural development. Curr Opin Neurobiol, 9, 65-73.

OPPERMANN, U. C., SALIM, S., TJERNBERG, L. O., TERENIUS, L. & JORNVALL, H. (1999) Binding of amyloid beta-peptide to mitochondrial hydroxyacyl-CoA dehydrogenase (ERAB): regulation of an SDR enzyme activity with implications for apoptosis in Alzheimer's disease. FEBS Lett, 451, 238-42.

PASCHEN, W. & MENGESDORF, T. (2005) Endoplasmic reticulum stress response and neurodegeneration. Cell Calcium, 38, 409-15.

PELLETIER, M. R., WADIA, J. S., MILLS, L. R. & CARLEN, P. L. (1999) Seizure-induced cell death produced by repeated tetanic stimulation in vitro: possible role of endoplasmic reticulum calcium stores. J Neurophysiol, 81, 3054-64.

PENNETTA, G., HIESINGER, P. R., FABIAN-FINE, R., MEINERTZHAGEN, I. A. & BELLEN, H. J. (2002) Drosophila VAP-33A directs bouton formation at neuromuscular junctions in a dosage-dependent manner. Neuron, 35, 291-306.

PERETTI, D., DAHAN, N., SHIMONI, E., HIRSCHBERG, K. & LEV, S. (2008) Coordinated lipid transfer between the endoplasmic reticulum and the Golgi complex requires the VAP proteins and is essential for Golgi-mediated transport. Mol Biol Cell, 19, 3871-84.

PERRY, R. J. & RIDGWAY, N. D. (2005) Molecular mechanisms and regulation of ceramide transport. Biochim Biophys Acta, 1734, 220-34.

PRATT, W. B. & TOFT, D. O. (2003) Regulation of signaling protein function and trafficking by the hsp90/hsp70-based chaperone machinery. Exp Biol Med (Maywood), 228, 111-33.

PROSSER, D. C., TRAN, D., GOUGEON, P. Y., VERLY, C. & NGSEE, J. K. (2008) FFAT rescues VAPA-mediated inhibition of ER-to-Golgi transport and VAPB-mediated ER aggregation. J Cell Sci, 121, 3052-61.

RATNAPARKHI, A., LAWLESS, G. M., SCHWEIZER, F. E., GOLSHANI, P. & JACKSON, G. R. (2008) A Drosophila model of ALS: human ALS-associated mutation in VAP33A suggests a dominant negative mechanism. PLoS ONE, 3, e2334.

REIJONEN, S., PUTKONEN, N., NORREMOLLE, A., LINDHOLM, D. & KORHONEN, L. (2008) Inhibition of endoplasmic reticulum stress counteracts neuronal cell death and protein aggregation caused by N-terminal mutant huntingtin proteins. Exp Cell Res, 314, 950-60.

REMY, I., GALARNEAU, A. & MICHNICK, S. W. (2002) Detection and visualization of protein interactions with protein fragment complementation assays. Methods Mol Biol, 185, 447-59.

REMY, I. & MICHNICK, S. W. (2007) Application of protein-fragment complementation assays in cell biology. Biotechniques, 42, 137, 139, 141 passim.

ROSSI, A. E. & DIRKSEN, R. T. (2006) Sarcoplasmic reticulum: the dynamic calcium governor of muscle. Muscle Nerve, 33, 715-31.

RUSS, W. P. & ENGELMAN, D. M. (2000) The GxxxG motif: a framework for transmembrane helix-helix association. J Mol Biol, 296, 911-9.

RYU, E. J., HARDING, H. P., ANGELASTRO, J. M., VITOLO, O. V., RON, D. & GREENE, L. A. (2002) Endoplasmic reticulum stress and the unfolded protein response in cellular models of Parkinson's disease. J Neurosci, 22, 10690-8.

SAITO, S., MATSUI, H., KAWANO, M., KUMAGAI, K., TOMISHIGE, N., HANADA, K., ECHIGO, S., TAMURA, S. & KOBAYASHI, T. (2008) Protein phosphatase 2Cepsilon is an endoplasmic reticulum integral membrane protein

that dephosphorylates the ceramide transport protein CERT to enhance its association with organelle membranes. J Biol Chem, 283, 6584-93.

SARKAR, M. & MAGLIERY, T. J. (2008) Re-engineering a split-GFP reassembly screen to examine RING-domain interactions between BARD1 and BRCA1 mutants observed in cancer patients. Mol Biosyst, 4, 599-605.

SCALES, S. J., CHEN, Y. A., YOO, B. Y., PATEL, S. M., DOUNG, Y. C. & SCHELLER, R. H. (2000) SNAREs contribute to the specificity of membrane fusion. Neuron, 26, 457-64.

SCHRODER, M. & KAUFMAN, R. J. (2005) The mammalian unfolded protein response. Annu Rev Biochem, 74, 739-89.

SHEN, X., ELLIS, R. E., SAKAKI, K. & KAUFMAN, R. J. (2005) Genetic interactions due to constitutive and inducible gene regulation mediated by the unfolded protein response in C. elegans. PLoS Genet, 1, e37.

SKEHEL, P. A., FABIAN-FINE, R. & KANDEL, E. R. (2000) Mouse VAP33 is associated with the endoplasmic reticulum and microtubules. Proc Natl Acad Sci U S A, 97, 1101-6.

SKEHEL, P. A., MARTIN, K. C., KANDEL, E. R. & BARTSCH, D. (1995) A VAMP-binding protein from Aplysia required for neurotransmitter release. Science, 269, 1580-3.

SOUSSAN, L., BURAKOV, D., DANIELS, M. P., TOISTER-ACHITUV, M., PORAT, A., YARDEN, Y. & ELAZAR, Z. (1999) ERG30, a VAP-33-related protein, functions in protein transport mediated by COPI vesicles. J Cell Biol, 146, 301-11.

TARR, D. E. & SCOTT, A. L. (2005) MSP domain protein-1 from Ascaris suum and its possible role in the regulation of major sperm protein-based crawling motility. Mol Biochem Parasitol, 143, 165-72.

TARR, D. E. & SCOTT, A. L. (2005) MSP domain proteins. Trends Parasitol, 21, 224-31.

TASKER, P. N., MICHELANGELI, F. & NIXON, G. F. (1999) Expression and distribution of the type 1 and type 3 inositol 1,4, 5-trisphosphate receptor in

developing vascular smooth muscle. Circ Res, 84, 536-42.

TEULING, E., AHMED, S., HAASDIJK, E., DEMMERS, J., STEINMETZ, M. O., AKHMANOVA, A., JAARSMA, D. & HOOGENRAAD, C. C. (2007) Motor neuron disease-associated mutant vesicle-associated membrane protein-associated protein (VAP) B recruits wild-type VAPs into endoplasmic reticulum-derived tubular aggregates. J Neurosci, 27, 9801-15.

THOMPSON, J. D., GIBSON, T. J. & HIGGINS, D. G. (2002) Multiple sequence alignment using ClustalW and ClustalX. Curr Protoc Bioinformatics, Chapter 2, Unit 2 3.

THUERAUF, D. J., MORRISON, L. & GLEMBOTSKI, C. C. (2004) Opposing roles for ATF6alpha and ATF6beta in endoplasmic reticulum stress response gene induction. J Biol Chem, 279, 21078-84.

THUERAUF, D. J., MORRISON, L. E., HOOVER, H. & GLEMBOTSKI, C. C. (2002) Coordination of ATF6-mediated transcription and ATF6 degradation by a domain that is shared with the viral transcription factor, VP16. J Biol Chem, 277, 20734-9.

TSUDA, H., HAN, S. M., YANG, Y., TONG, C., LIN, Y. Q., MOHAN, K., HAUETER, C., ZOGHBI, A., HARATI, Y., KWAN, J., MILLER, M. A. & BELLEN, H. J. (2008) The amyotrophic lateral sclerosis 8 protein VAPB is cleaved, secreted, and acts as a ligand for Eph receptors. Cell, 133, 963-77.

TU, H., GAO, L., SHI, S. T., TAYLOR, D. R., YANG, T., MIRCHEFF, A. K., WEN, Y., GORBALENYA, A. E., HWANG, S. B. & LAI, M. M. (1999) Hepatitis C virus RNA polymerase and NS5A complex with a SNARE-like protein. Virology, 263, 30-41.

UNGERSTEDT, U., LJUNGBERG, T. & STEG, G. (1974) Behavioral, physiological, and neurochemical changes after 6-hydroxydopamine-induced degeneration of the nigro-striatal dopamine neurons. Adv Neurol, 5, 421-6.

VAN DEN BOSCH, L. & ROBBERECHT, W. (2008) Crosstalk between astrocytes and motor neurons: what is the message? Exp Neurol, 211, 1-6.

VELDINK, J. H., VAN DEN BERG, L. H. & WOKKE, J. H. (2004) The future of motor

neuron disease: the challenge is in the genes. J Neurol, 251, 491-500.

VERKHRATSKY, A. (2005) Physiology and pathophysiology of the calcium store in the endoplasmic reticulum of neurons. Physiol Rev, 85, 201-79.

VOELTZ, G. K., ROLLS, M. M. & RAPOPORT, T. A. (2002) Structural organization of the endoplasmic reticulum. EMBO Rep, 3, 944-50.

WANG, Y., SHEN, J., ARENZANA, N., TIRASOPHON, W., KAUFMAN, R. J. & PRYWES, R. (2000) Activation of ATF6 and an ATF6 DNA binding site by the endoplasmic reticulum stress response. J Biol Chem, 275, 27013-20.

WEI, H., WEI, W., BREDESEN, D. E. & PERRY, D. C. (1998) Bcl-2 protects against apoptosis in neuronal cell line caused by thapsigargin-induced depletion of intracellular calcium stores. J Neurochem, 70, 2305-14.

WEIR, M. L., KLIP, A. & TRIMBLE, W. S. (1998) Identification of a human homologue of the vesicle-associated membrane protein (VAMP)-associated protein of 33 kDa (VAP-33): a broadly expressed protein that binds to VAMP. Biochem J, 333 (Pt 2), 247-51.

WEIR, M. L., XIE, H., KLIP, A. & TRIMBLE, W. S. (2001) VAP-A binds promiscuously to both v- and tSNAREs. Biochem Biophys Res Commun, 286, 616-21.

WU, J. & KAUFMAN, R. J. (2006) From acute ER stress to physiological roles of the Unfolded Protein Response. Cell Death Differ, 13, 374-84.

WYLES, J. P., MCMASTER, C. R. & RIDGWAY, N. D. (2002) Vesicle-associated membrane protein-associated protein-A (VAP-A) interacts with the oxysterol-binding protein to modify export from the endoplasmic reticulum. J Biol Chem, 277, 29908-18.

WYLES, J. P. & RIDGWAY, N. D. (2004) VAMP-associated protein-A regulates partitioning of oxysterol-binding protein-related protein-9 between the endoplasmic reticulum and Golgi apparatus. Exp Cell Res, 297, 533-47.

XU, C., BAILLY-MAITRE, B. & REED, J. C. (2005) Endoplasmic reticulum stress: cell life and death decisions. J Clin Invest, 115, 2656-64.

YAMAMOTO, K., SATO, T., MATSUI, T., SATO, M., OKADA, T., YOSHIDA, H.,

HARADA, A. & MORI, K. (2007) Transcriptional induction of mammalian ER quality control proteins is mediated by single or combined action of ATF6alpha and XBP1. Dev Cell, 13, 365-76.

YOSHIDA, H., HAZE, K., YANAGI, H., YURA, T. & MORI, K. (1998) Identification of the cis-acting endoplasmic reticulum stress response element responsible for transcriptional induction of mammalian glucose-regulated proteins. Involvement of basic leucine zipper transcription factors. J Biol Chem, 273, 33741-9.

YOSHIDA, H., MATSUI, T., YAMAMOTO, A., OKADA, T. & MORI, K. (2001) XBP1 mRNA is induced by ATF6 and spliced by IRE1 in response to ER stress to produce a highly active transcription factor. Cell, 107, 881-91.

YOSHIDA, H., OKADA, T., HAZE, K., YANAGI, H., YURA, T., NEGISHI, M. & MORI, K. (2000) ATF6 activated by proteolysis binds in the presence of NF-Y (CBF) directly to the cis-acting element responsible for the mammalian unfolded protein response. Mol Cell Biol, 20, 6755-67.

YOSHIDA, H., OKADA, T., HAZE, K., YANAGI, H., YURA, T., NEGISHI, M. & MORI, K. (2001) Endoplasmic reticulum stress-induced formation of transcription factor complex ERSF including NF-Y (CBF) and activating transcription factors 6alpha and 6beta that activates the mammalian unfolded protein response. Mol Cell Biol, 21, 1239-48.

YOSHIDA, H., OKADA, T., HAZE, K., YANAGI, H., YURA, T., NEGISHI, M. & MORI, K. (2001) Endoplasmic reticulum stress-induced formation of transcription factor complex ERSF including NF-Y (CBF) and activating transcription factors 6alpha and 6beta that activates the mammalian unfolded protein response. Mol Cell Biol, 21, 1239-48.

YU, Z., LUO, H., FU, W. & MATTSON, M. P. (1999) The endoplasmic reticulum stress-responsive protein GRP78 protects neurons against excitotoxicity and apoptosis: suppression of oxidative stress and stabilization of calcium homeostasis. Exp Neurol, 155, 302-14.

ZHENG, Y., GAO, B., YE, L., KONG, L., JING, W., YANG, X., WU, Z. & YE, L. (2005)

Hepatitis C virus non-structural protein NS4B can modulate an unfolded protein response. J Microbiol, 43, 529-36.

APPENDIX I- PLASMIDS, DNA, EXPRESSION CONSTRUCTS

#P1 (Gkogkas et al., 2008)

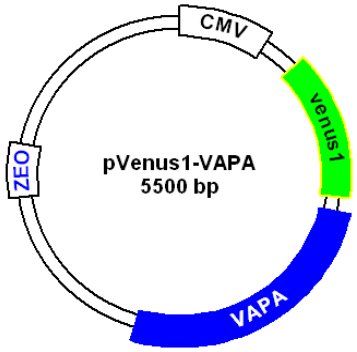

#P2 (Gkogkas et al., 2008)

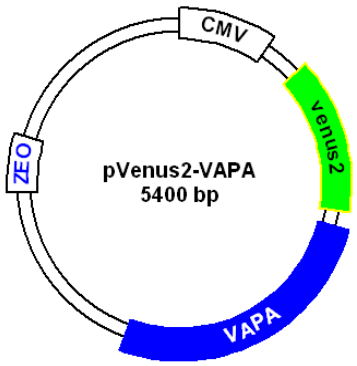

#P3 (Gkogkas et al., 2008)

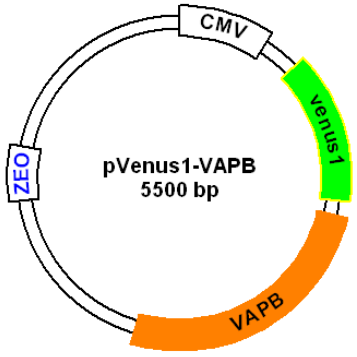

#P4 (Gkogkas et al., 2008)

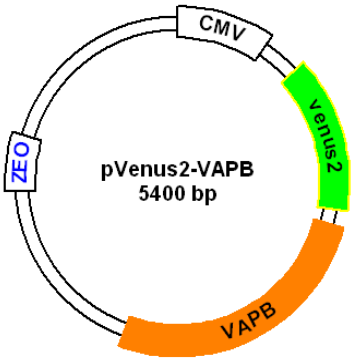

#P5 (Gkogkas et al., 2008)

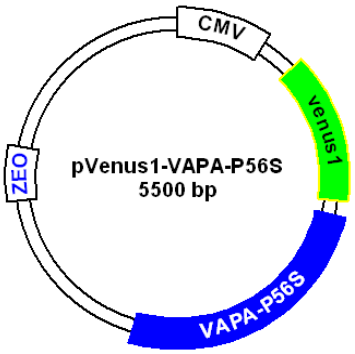

#P6 (Gkogkas et al., 2008)

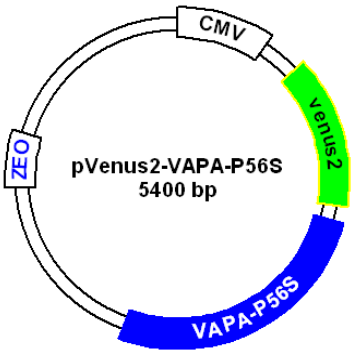

#P7 (Gkogkas et al., 2008)

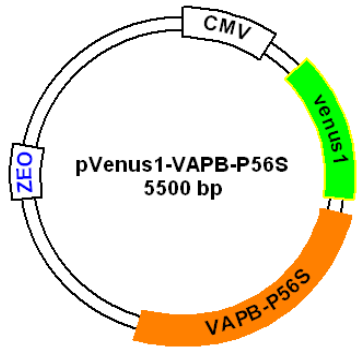

#P8 (Gkogkas et al., 2008)

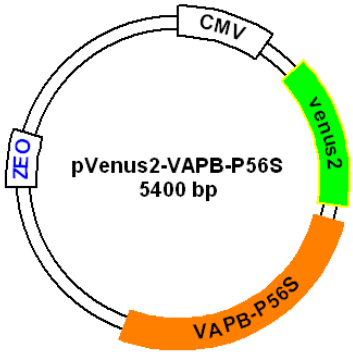

#P9 (Gkogkas et al., 2008)

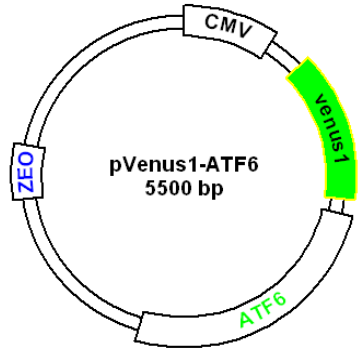

#P10 (Gkogkas et al., 2008)

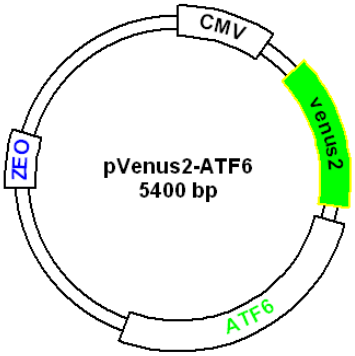

#P11 (Middleton, 2005)

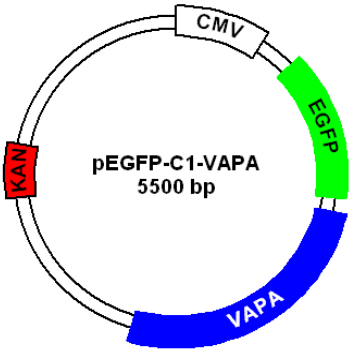

#P12 (Middleton, 2005)

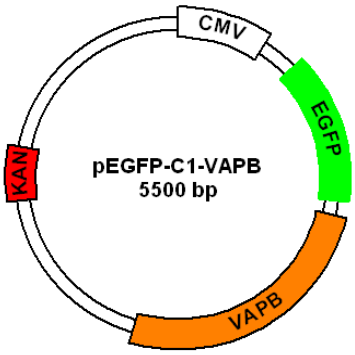

#P13 (Middleton, 2005)

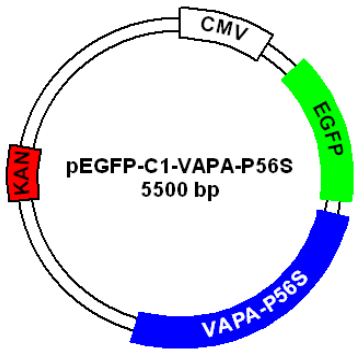

#P14 (Middleton, 2005)

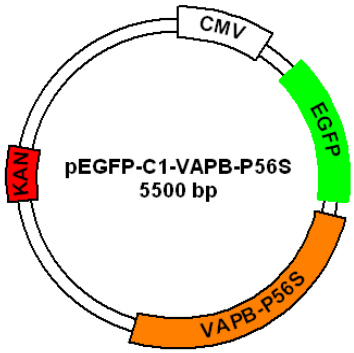

#P15 (Middleton, 2005)

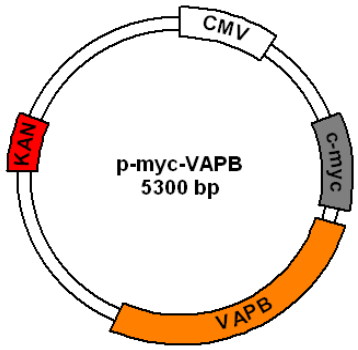

#P16 (Middleton, 2005)

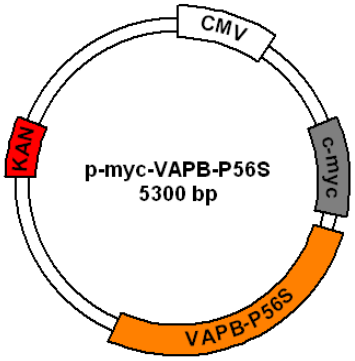

#P17 (Wang et al., 2000)

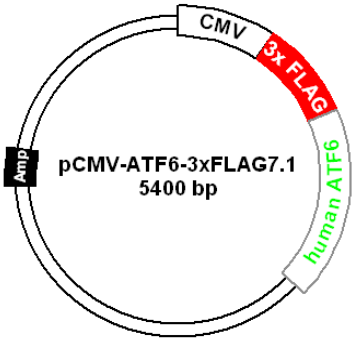

#P18 (Wang et al., 2000)

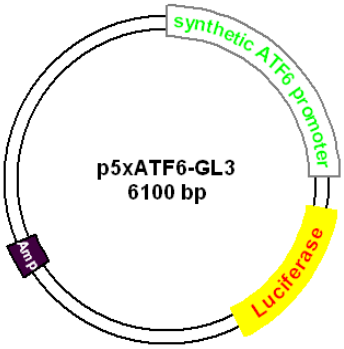

#P19 (Yamamoto et al., 2007, Yoshida et al., 2000)

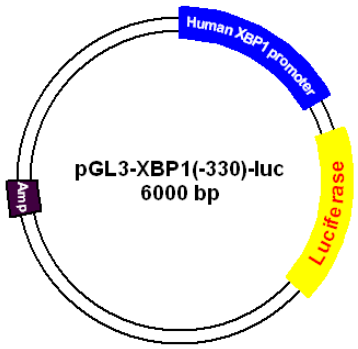

#P20 (Yamamoto et al., 2007, Yoshida et al., 1998)

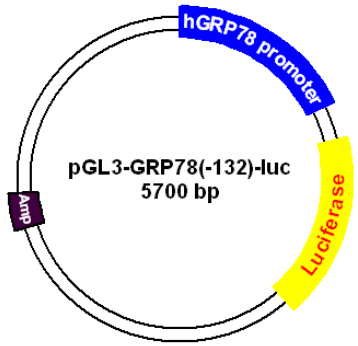

#P21 (PROMEGA)

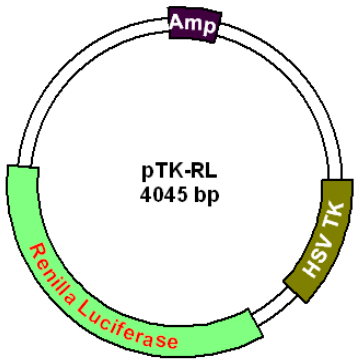

#P22 (QIAGEN)

Hs_VAPB_5_HP siRNA

#P23 (QIAGEN)

Hs_VAPB_2_HP siRNA

#P24 (made by Dr. Caroline Wardrope)

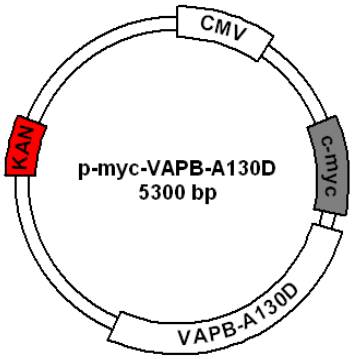

#P25 (made by Dr. Caroline Wardrope)

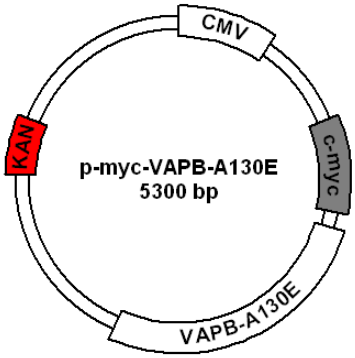

#P26 (made by Dr. Caroline Wardrope)

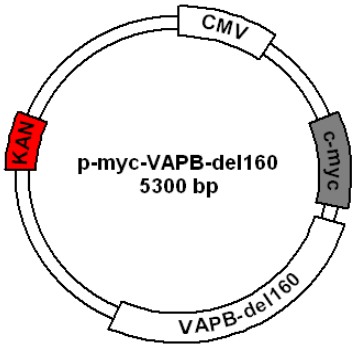

#P27 (made by Dr. Caroline Wardrope)

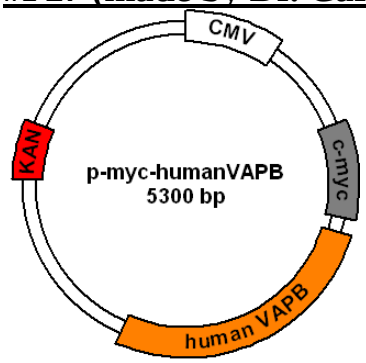

#P28 (made by Dr. Caroline Wardrope)

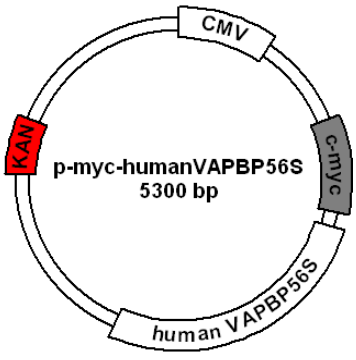

#P29 (made by Dr. Caroline Wardrope)

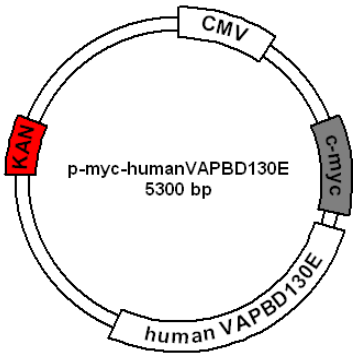

#P30 (made by Dr. Caroline Wardrope)

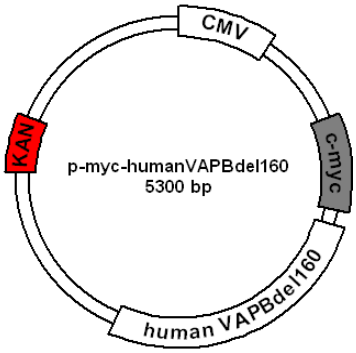

Human Molecular Genetics

VAPB interacts with and modulates the activity of ATF6

Christos Gkogkas, Susan Middleton, Anna M. Kremer, Caroline Wardrope, Matthew Hannah, Thomas H. Gillingwater and Paul Skehel

Hum. Mol. Genet. 17:1517-1526, 2008. First published 8 Feb 2008;
doi:10.1093/hmg/ddn040

Human Molecular Genetics, 2008, Vol. 17, No. 11 ***1517–1526***
doi:10.1093/hmg/ddn040
Advance Access published on February 8, 2008

VAPB interacts with and modulates the activity of ATF6

Christos Gkogkas[1], Susan Middleton[1], Anna M. Kremer[1], Caroline Wardrope[1], Matthew Hannah[2], Thomas H. Gillingwater[1] and Paul Skehel[1,*]

[1]The Centre for Neuroscience Research, The University of Edinburgh, The Hugh Robson Building, George Square, Edinburgh EH8 9XD, UK and [2]Division of Molecular Neuroendocrinology, Medical Research Council, National Institute for Medical Research, The Ridgeway, Mill Hill, London NW7 1AA, UK

Received December 7, 2007; Revised and Accepted February 6, 2008

A mis-sense point mutation in the human *VAPB* gene is associated with a familial form of motor neuron disease that has been classified as Amyotrophic Lateral Sclerosis type VIII. Affected individuals suffer from a spinal muscular atrophy (SMA), amyotrophic lateral sclerosis (ALS) or an atypical slowly progressing form of ALS. Mammals have two homologous VAP genes, *vapA* and *vapB*. VAPA and VAPB share 76% similar or identical amino acid residues; both are COOH-terminally anchored membrane proteins enriched on the endoplasmic reticulum. Several functions have been ascribed to VAP proteins including membrane trafficking, cytoskeleton association and membrane docking interactions for cytoplasmic factors. It is shown here that VAPA and VAPB are expressed in tissues throughout the body but at different levels, and that they are present in overlapping but distinct regions of the endoplasmic reticulum. The disease-associated mutation in VAPB, VAPB^{P56S}, lies within a highly conserved N-terminal region of the protein that shares extensive structural homology with the major sperm protein (MSP) from nematodes. The MSP domain of VAPA and VAPB is found to interact with the ER-localized transcription factor ATF6. Over expression of VAPB or VAPB^{P56S} attenuates the activity of ATF6-regulated transcription and the mutant protein VAPB^{P56S} appears to be a more potent inhibitor of ATF6 activity. These data indicate that VAP proteins interact directly with components of ER homeostatic and stress signalling systems and may therefore be parts of a previously unidentified regulatory pathway. The mis-function of such regulatory systems may contribute to the pathological mechanisms of degenerative motor neuron disease.

INTRODUCTION

A dominantly inherited familial form of motor neuron disease characterized in a large Brazilian family was recently shown to be associated with a mis-sense mutation in the human *vapB* gene (1). Affected individuals suffer from three different pathological conditions; a late on-set slowly progressing spinal muscular atrophy (SMA), a slowly progressing late on-set atypical amyotrophic lateral sclerosis ALS8 or a typical severe rapidly progressing ALS (2,3). Although familial forms of disease may represent less than 5% of the total incidences of ALS (4,5), they exhibit the same phenotypic heterogeneity as the more common sporadic disease (6–8). Information on the mechanistic basis of familial motor neuron diseases may, therefore, be relevant to all forms of motor neuron disease.

The first VAP protein was identified in *Aplysia californica* from its interaction in a yeast two-hybrid screen with VAMP/Synaptobrevin, hence the nomenclature VAMP/Synaptobrevin Associated Protein (9). VAP proteins are highly conserved, with homologous proteins found in all eukaryotes (10–15). There are two mammalian genes *VapA* and *VapB* (16). The proteins contain three prominent structural features; the N-terminal domain of approximately 120 amino acids is highly homologous to the nematode major sperm protein (MSP) (17), the central domain is amphipathic and predicted to form a coiled–coil structure, and the C-terminal 20 amino acids are hydrophobic and act as an intracellular membrane anchor (13,15,16).

The MSP domain binds to the 'two phenylalanines in an acid tract', or 'FFAT' motif found in several cytoplasmic

*To whom correspondence should be addressed. Tel: +44 1316511961; Fax: +44 1316506530; Email: paul.skehel@ed.ac.uk

lipid-binding proteins (18–20). The structural basis of this interaction was recently determined for the MSP domain of VAPA (21). Thus, VAP proteins may act as docking sites for cytoplasmic factors to interact with the ER. VAP proteins may also act to maintain the structure of intracellular membranes such as the ER, by interacting with the cytoskeleton and mediating membrane trafficking (13,15,22).

The disease-associated mutation in ALS8 is a C to T substitution within exon 2 of the *vapB* gene replacing a proline residue with a serine in a highly conserved region of the protein. The mutant protein, $VAPB^{P56S}$, forms aggregates when expressed in cultured cell lines or primary hippocampal neurons (1). The relationship of these aggregates to the pathological mechanism of the disease is not known. It has been suggested that the presence of aggregates containing $VAPB^{P56S}$ may result in disruption of the proteasome, activation of ER stress responses, fragmentation of the Golgi apparatus and induction of apoptosis (23). Teuling *et al*. (24) have also demonstrated that expression of $VAPB^{P56S}$ recruits the wild-type protein into aggregates and causes disruption of ER structure.

In this report, we show that both VAPA and VAPB are ubiquitously expressed but at differing levels in different tissues and that they accumulate on overlapping but distinct regions of the ER. Both VAPA and VAPB are shown to be capable of interacting with the ER stress regulated transcription factor ATF6, and over expression of VAPB or $VAPB^{P56S}$ attenuates the activity of an ATF6/XBP1 regulated promoter. This suggests that VAPB can have an inhibitory effect on ATF6 dependent transcription and that the disease-associated mutant, $VAPB^{P56S}$, has an enhanced inhibitory activity towards ATF6-dependent transcription compared to the wild-type protein. An interaction between VAP proteins and ATF6 may represent a previously uncharacterized mechanism of ER homeostatic and stress response regulation.

It is concluded that the mis-regulation of ER stress response and homeostatic regulatory systems may contribute to the pathological mechanism of degenerative motor neuron disease associated with the $VAPB^{P56S}$ mutation.

RESULTS

VAPA and VAPB are expressed ubiquitously but at differing levels in different tissues

Immunoblot analysis of selected tissues from an adult male rat demonstrated that both VAPA and VAPB proteins are present in all tissues examined, but at different relative levels (Fig. 1A). This is in agreement with the wide expression profile of mRNA published previously (13,16,25). A second protein of slightly larger molecular weight is detected in the testis by VAPA anti-sera. An additional, less abundant, protein of approximately 14 kDa is detected by both anti-serum. The VAPB-related signal is a doublet, the expression of which is tightly restricted to the forebrain and cerebellum extracts, and not detected in the other tissues tested (Fig. 1A). The 14 kDa VAPA-related polypeptide is more widely expressed and detectable in pancreas, liver, forebrain, lung and thymus, kidney and testis; low levels are seen in the cerebellum and no signal is detected in heart or skeletal muscle. A peptide of similar size has been predicted from a splice variant of VAPB, termed VAPC. However, the peptide used to generate the VAPB anti-serum is not present in VAPC (16), and the VAPA anti-sera do not cross react significantly with *vapB*-derived species (Supplementary Material, Figure S1). It is concluded that these smaller molecular weight immunoreactive species are most likely generated by proteolysis of the VAP proteins.

It has been shown previously that both VAPA and VAPB are enriched on the ER membrane (13,15,21). A distinct sub-cellular distribution for the two proteins is seen by co-immunostaining of HEK293 cells (Fig. 1B). Both proteins are localized in a reticular pattern, but they exhibit only a modest level of co-localization. This distinct sub-cellular distribution of VAPA and VAPB is most striking in skeletal muscle (Fig. 1C). Fluorescent immunocytochemistry indicates a complementary distribution of VAPA and VAPB in the sarcoplasmic reticulum. VAPA is enriched on the A- and H-bands and the Z-line, while VAPB is restricted to the I-band and T-system regions (Fig. 1C). The I-band is enriched for IP_3 receptors and RyR localize mainly at the T-system (26); VAPA and VAPB may therefore be associated with distinct intracellular calcium stores.

Interactions of the VAP MSP domain

The ALS8-associated mutation in the VAPB protein lies within a highly conserved region of the MSP domain. In a previous series of experiments, we had observed that, when expressed as an EGFP fusion protein, the MSP domains of both VAPA and VAPB formed intensely fluorescent, large intracellular aggregates and were toxic to HEK293 and PC12 cell lines, and to primary cultures of rodent hippocampal neurons (Skehel, unpublished). To investigate possible mechanisms of the MSP domain toxicity, a yeast two-hybrid screen was done to identify potential MSP interacting proteins. A sequence corresponding to amino acids 1–107 of mouse VAPA was used to screen a rat brain cDNA library. In addition to a number of FFAT- and MSP domain-containing proteins, a partial clone of the ER stress regulated transcription factor ATF6 was identified (27).

To characterize this interaction further, expression constructs for full-length VAPA, VAPB and ATF6 were analysed by a fluorescent peptide complementation assay (28) (Fig. 2). In this assay, a fluorescent protein is generated from two separate parts of a split GFP, termed Venus1 and Venus2, only by the association of two test polypeptides expressed as fusion proteins. A functional fluorescent protein is generated when the two test proteins directly interact. Although the initial yeast two-hybrid interaction was between a truncated form of ATF6 and the MSP domain of VAPA, an interaction between full-length forms of VAPA and VAPB with ATF6 was readily detectable (Fig. 2). Similarly, the ALS8-associated mutant $VAPB^{P56S}$ was shown to be capable of interacting with ATF6 (Fig. 2). No interaction was detected between VAPA, VAPB or ATF6 when co-expressed with heterologous leucine zipper-Venus fusions. The reconstitution of a fluorescent protein clearly indicates that VAPA and VAPB are capable of interacting with ATF6. Similar results were also obtained with the converse Venus combinations, where

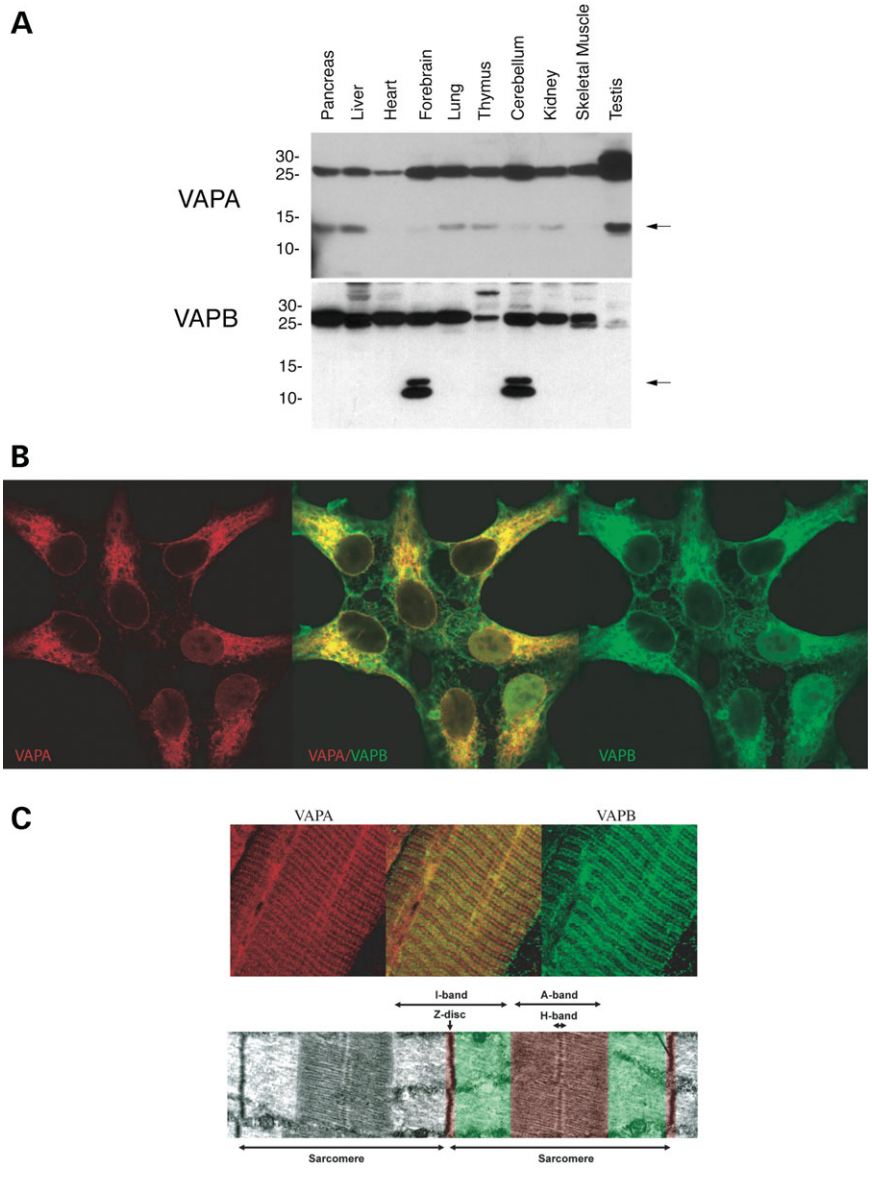

Figure 1. (**A**) Detection of VAPA and VAPB in different tissues. Anti-peptide anti-serum was raised to residues 174–189 of mouse VAPB. In the tissues indicated, the predominant immunoreactivity is at approximately 27 kDa, in agreement with the molecular weight predicted from the cDNA. Both VAPA and VAPB are expressed widely but at different levels. A faster migrating VAPB-related doublet signal of approximately 14 kDa is clearly detected in forebrain and cerebellum protein extracts (arrows). The immunoblot is deliberately over exposed to demonstrate the restricted nature of this expression pattern. A faster migrating immunoreactive species of approximately 14 kDa is also seen with VAPA anti-sera, however, in contrast to that seen for VAPB; this species is detectable in pancreas, liver, forebrain, lung and thymus, kidney and testis; low levels are seen in the cerebellum and no signal is detected in Heart or skeletal muscle. (**B**) VAPA and VAPB are expressed in distinct reticular patterns. Indirect immunoflouroescence analysis of VAPA and VAPB in HEK293 cells reveals a reticular pattern of expression, but detects very little co-localization of the two proteins. VAPA is shown in red and VAPB in green. (**C**) VAPA and VAPB are enriched in a complementary distribution in skeletal muscle. Confocal micrographs of an immunocytochemically labelled transversus abdominis muscle from a 2 month old mouse (VAPA in red, VAPB in green). The staining patterns of VAPB were consistent with it being located around putative I—band and T-system regions. In contrast, VAPA was absent from these regions, and appeared to be more strongly expressed in the regions associated with A- and H-bands and Z-lines. A pseudo-coloured electron micrograph is shown to indicate the position of VAPA and VAPB staining in relation to the structure of a muscle sarcomere.

ATF6 was expressed as a fusion with Venus 1, and the VAP proteins were fused to Venus 2 (data not shown) (28).

Fluorescence analysis of HEK293 cells expressing EGFP-VAPB and FLAG-tagged ATF6 shows extensive regions of co-localization on the ER, but also some complementary distribution (Fig. 3). The aggregates of EGFP-VAPB^{P56S} show some but not extensive co-localization with ATF6, although we cannot discount that low antigen accessibility may contribute to reduced ATF6 detection in VAPB^{P56S} aggregates. Expression of VAPB^{P56S} does not appear to cause gross disruption of ATF6 distribution in the ER (Fig. 3).

ATF6 is inhibited by VAPB and VAPB^{P56S}

ATF6 is one of a family of transmembrane transcription factors (29). It functions in a regulated transcription pathway

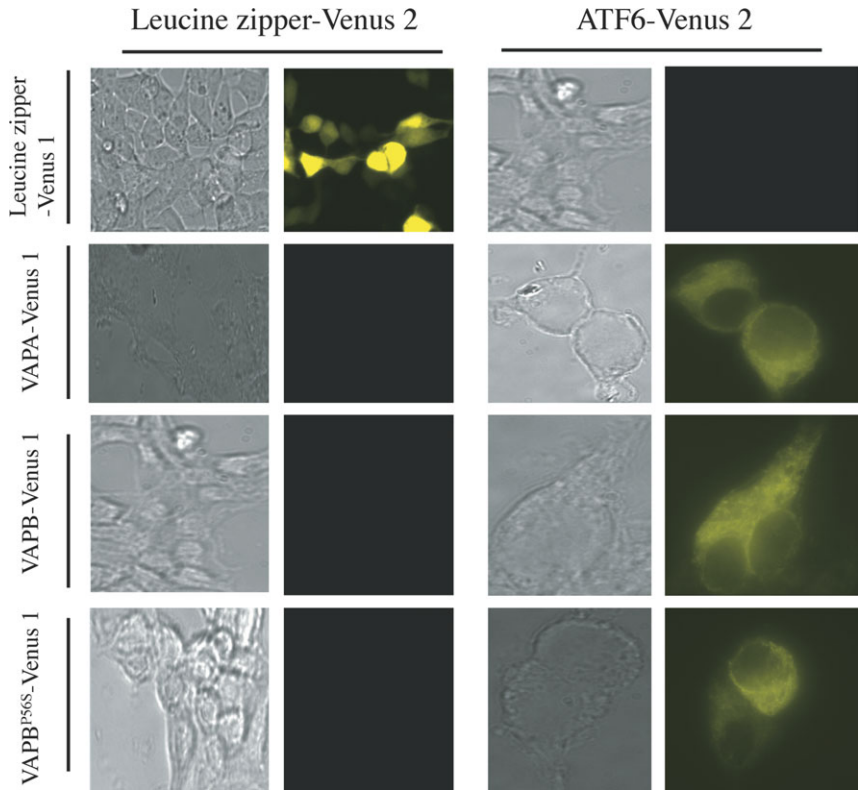

Figure 2. Peptide complementation assay for the interaction of VAPA and VAPB with ATF6. The coding sequences of mouse VAPA, VAPB and VAPB^{P56S} were expressed in HEK293 cells as fusion proteins with a truncated non-fluorescent form of YFP, Venus 1 (28). These proteins were co-expressed with the complementary ATF6-Venus 2 fusion protein. Fluorescence indicates reconstitution of a functional YFP and therefore a direct interaction of VAPA and VAPB with ATF6. Wild-type VAPB and mutant VAPB^{P56S} are capable of interacting with ATF6. Controls in which a homodimerizing leucine zipper peptide was expressed as either a Venus 1 or Venus 2 fusion proteins show no fluorescence when expressed with the complementary VAP or ATF6 fusion proteins. Bright field or fluorescence images were acquired from live cells through cell culture plastic.

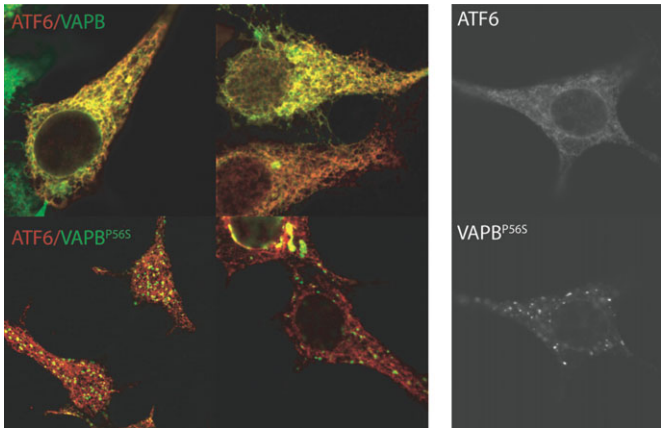

Figure 3. Co-localization of VAPB and ATF6. HEK293 cells were transfected with FLAG-ATF6, EGFP-VAPB and EGFP-VAPB^{P56S}. In colour plates, FLAG-ATF6 is shown in red and EGFP-VAPB or EGFP-VAPB^{P56S} is in green. There is extensive, but not total co-localization of VAPB and ATF6 in a reticular distribution. ATF6 co-localizes with the aggregates formed by VAPB^{P56S}, but not in a punctate pattern. Note that VAPB^{P56S} does not cause a gross change in the distribution of ATF6.

involved in ER homeostasis and response to stress known as the unfolded protein response (UPR) (30–32). Upon accumulation of unfolded proteins in the lumen of the ER, ATF6 translocates from the ER to the Golgi and is proteolyzed in turn by S1P and S2P. This results in the release of the DNA binding and transcription transactivation domain of ATF6 from the ER membrane allowing it to enter the nucleus and activate transcription (27,33).

ATF6 appears to interact with several promoter elements (31,34,35). A synthetic promoter has been generated that acts as an ATF6/XBP1 dependent transcription reporter (31). To determine if the interaction with VAPB affects the ability of ATF6 to activate transcription, luciferase-based transient transcription assays were done using this ATF6/XBP1-dependent reporter of transcription (31). In HEK293 cells, basal levels of transcription from this promoter are reduced by over-expression of myc-tagged forms of VAPB or VAPB^{P56S} (Fig. 4A). ATF6/XBP1-mediated transcription activated by the glycosylation inhibitor, tunicamycin, was also significantly reduced by over expression of VAPB or VAP-B^{P56S} (Fig. 4A) (36,37). Increasing levels of ATF6 by co-expression of a FLAG-tagged recombinant form of human ATF6 (38) increased basal and tunicamycin-induced expression from the ATF6/XBP1 reporter. In both cases, the elevated levels of ATF6/XBP1 dependent transcription were also reduced by over expression of either VAPB or VAPB^{P56S} (Fig. 4B). This effect requires the cytoplasmic domains of VAPB and does not appear to be a non-specific consequence of increasing levels of protein in the ER membrane since over expression of a DsRed fluorescent fusion protein of the C-terminal

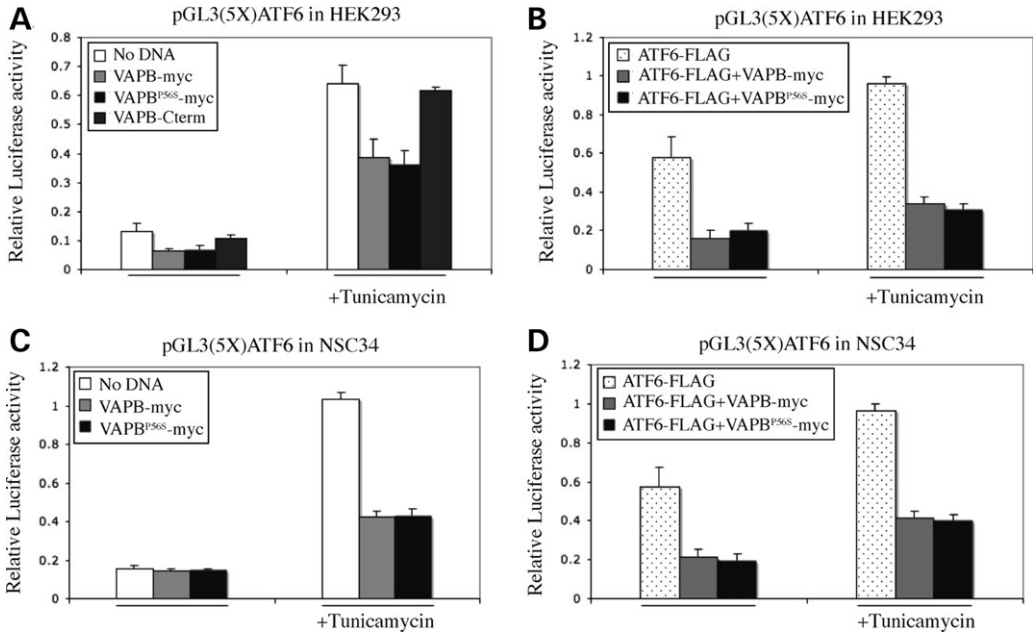

Figure 4. VAPB and VAPB^{P56S} inhibit transcription from an ATF6 regulated transcription reporter. (**A**) HEK293 were transfected with a reporter plasmid containing the luciferase cDNA regulated by five ATF6/XBP1 binding sites, pGL3(5X)ATF6. Cell cultures were co-transfected with expression plasmids encoding VAPB or VAPB^{P56S} as myc-tagged fusion proteins (VAPB-myc and VAPB^{P56S}-myc) or a monomeric red fluorescent fusion protein containing the C-terminal 41 amino acids of VAPB (VAPB-Cterm). Where indicated cultures were treated for 12 h with 2 μg/ml Tunicamycin to induce ER stress. VAPB and VAPB^{P56S} reduce constitutive levels of ATF6/XBP1 activity, while VAPB-Cterm had no effect. (**B**) Over expression of ATF6 as a ATF6-FLAG fusion protein increased basal and tunicamycin-induced activity of the ATF6/XBP1 reporter gene, but in both cases, levels of activity were reduced by co-expression of VAPB-myc or VAPB^{P56S}-myc. (**C** and **D**) The same experiments using the motor neuron-like cell line NSC34 gave similar results.

hydrophobic domain of VAPB does not reduce the basal or tunicamycin-induced expression from the ATF6/XBP1 reporter (Fig. 4A and Supplementary Material, Figure S3). Over expression of VAP proteins does not reduce expression levels of luciferase directed from a CMV promoter; therefore, the repressive affect on the ATF6/XBP1 reporter is unlikely to be the result of a general repression of transcription (Supplementary Material, Figure S4).

A similar inhibitory affect was also seen in the motor neuron derived cell line NSC34 (Fig. 4C and D). In NSC34 cells, basal levels of expression from the ATF6/XBP1 reporter are less than in HEK293, perhaps indicating lower levels of endogenous ATF6.

Consistent with the inhibitory affect seen by over expression of VAPB, siRNA-mediated reduction of endogenous VAPB results in an increase of basal and induced levels of ATF6/XBP1-dependent transcription (Fig. 5).

When equal amounts of expression plasmid DNA for VAPB and VAPB^{P56S} were used for cell-transfections, the overall level of attenuation was similar between the wild type and mutant forms of VAPB (Fig. 4). Immunoblot analysis of total protein from transfected cells, however, indicated that the mutant protein, VAPB^{P56S}-myc, accumulated to significantly lower levels, reaching only 20% of the level of wild-type protein (Fig. 6). This suggests that VAPB^{P56S}-myc may exert a stronger inhibition on ATF6 than the wild-type VAPB-myc, since a similar level of inhibition is achieved from a lower amount of protein. The difference in protein levels is less pronounced when VAPB and VAPB^{P56S} are expressed as EGFP fusion proteins (Fig. 6), which indicates that the presence of the GFP moiety may have a stabilizing affect on VAP-B^{P56S}. Consistent with this, the inhibition of ATF6/XBP1-dependent transcription is more pronounced for VAPB^{P56S}-GFP than VAPB-GFP (Fig. 6). Thus, VAPB^{P56S} appears to have a significantly greater inhibitory affect on ATF6 mediated transcription than wild-type VAPB. These results suggest that mis-regulation of ER stress responses may be important for the pathological effect of VAPB^{P56S} that leads to motor neuron degeneration.

DISCUSSION

The identification of a mutated gene responsible for a familial form of motor neuron disease greatly facilitates molecular and cellular studies of potential disease mechanisms. Understanding the cellular function of VAPB may indicate what molecular and cellular events are associated with the disease process of ALS8. It is likely that this information will be of relevance to both the inherited condition and the more common sporadic forms of disease.

Previous studies have demonstrated a role for VAP proteins on the ER. The N-terminal MSP domain contains an FFAT-motif binding site (21). This interaction has been shown to localize a number of cytoplasmic lipid-binding proteins to the ER and ER-derived membranes (18–20,39). FFAT-dependent interactions between VAPA and Nir2 and 3 have also been shown to affect the gross structure of the ER (22). Both VAPA and VAPB appear to be expressed at different relative levels in specific tissues [(16,25) and this study].

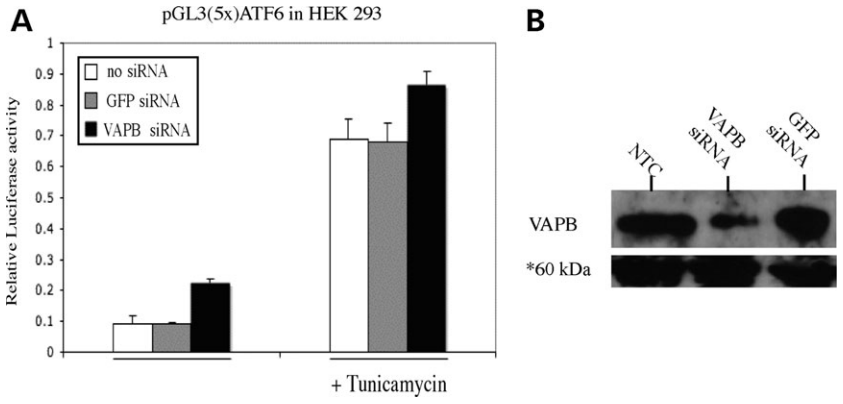

Figure 5. VAPB siRNA reduces the levels of endogenous VAPB and increases basal ATF6/XBP1-dependent transcription. (**A**) Immunoblot analysis of HEK293 cells nucleofected with VAPB siRNA or GFP siRNA and non-transfected cells shows a 25% reduction in levels of endogenous VAPB when treated with VAPB siRNA and no reduction in GFP siRNA treated cells. *A 60 kDa non-specific band from longer exposures of the immunoblot serves as a loading control. Band intensities were measured using ImageJ (NIH). (**B**) siRNA to VAPB increases basal and tunicamycin-induced, transcription from an ATF6/XBP1-regulated transcription promoter.

Both proteins are enriched on the ER and co-localize to a large extent (24). There are, however, many regions where the two proteins do not co-localize, suggesting they are present in distinct functional regions of the ER. This is most clearly seen in skeletal muscle where VAPA is enriched within the A and H bands and Z-line, whereas VAPB is seen predominantly in the I-bands and T-region. The localization of VAPA is similar to that of the IP_3 receptor (26), whereas VAPB more closely resembles the distribution of Ryanodine receptors (40). Any disruption of VAPB function caused by the P56S mutation associated with ALS8 might, therefore, affect intracellular Ca^{2+} storage and Ca^{2+} signalling capacities. Intracellular Ca^{2+} levels have been implicated in many degenerative conditions (reviewed in 41), and inhibition of Ryanodine receptor activity has been recently suggested as a possible pathological mechanism for motor neuron disease (42).

The proline residue at codon 56 within the MSP domain does not appear to contribute directly to FFAT-binding but co-immunoprecipitation of FFAT-containing proteins is reduced for $VAPB^{P56S}$ (24). Perturbation of FFAT-dependent association with the ER could disrupt the sorting of lipids within and between cellular membranes (19,20). A phosphoinositide-binding activity has been identified in the MSP domain of the yeast protein SCS2 that is a homologue of VAPA and VAPB (43).

Disruption of the MSP domain in $VAPB^{P56S}$ could affect a similar activity in the mammalian proteins. Changes in membrane composition have been suggested as a cause of neurodegeneration (44), and hyperlipidaemia is one of the clinical effects reported for $VAPB^{P56S}$ families (3). Disruption of ER and Golgi structure and/or function has been suggested previously as a possible pathological mechanism for degenerative diseases of neurons (45–47). More recently, ER stress in particular has been associated with sporadic and experimental models of motor neuron disease (48–50), and neurodegeneration in general (reviewed in 46,47,51). A recent report has also suggested that VAPB levels may induce the ER UPR by affecting the activity of IRE1 (23). In this report, we show that VAPA and VAPB can interact directly with the ER-localized transcription factor ATF6. Moreover, increasing the expression of VAPB attenuates the activity of ATF6, whereas reducing VAPB levels enhance ATF6-dependent transcription. Over expression of the mutant protein $VAPB^{P56S}$ appears to attenuate the activity of ATF6 more profoundly than does wild-type VAPB. The pertinacious aggregates formed by $VAPB^{P56S}$ do not appear to sequester ATF6 to a significant extent. The enhanced inhibitory affect of $VAPB^{P56S}$ levels on ATF6 activity may not, therefore, be due simply to a reduction in available ATF6. There are a number of stages in the activation of ATF6 that VAPB could influence. In response to accumulation of unfolded protein in the ER lumen ATF6 translocates from the ER to the Golgi. There it is sequentially processed by S1P and S2P proteases to release an amino terminal portion of the protein containing DNA binding and trans-activation domains (33). The lumental COOH-terminal domain of ATF6 is required to detect the accumulation of unfolded proteins in the lumen of the ER. As VAPB has very little luminal structure, it is unlikely to directly inhibit the ability of ATF6 to detect ER stress. Over expression of VAPB can disrupt membrane trafficking and so may indirectly inhibit the activation of ATF6 by reducing the translocation of ATF6 to the Golgi (15). Alternatively, VAP proteins might directly inhibit the translocation of ATF6 to the Golgi. It is also possible that VAP acts after translocation of ATF6 to the Golgi by a mechanism similar to that of Nucleobindin1 which represses S1P activation of ATF6 (52).

VAPB may act at the level of transcription. The yeast VAP homologue SCS2, originally identified as a suppressor of inositol auxotrophy, has been shown to localize activated genes to the nuclear membrane via an interaction with a FFAT domain-containing protein, Opi1 (10,53). The localization to the nuclear membrane was essential for gene expression (53). If an analogous situation existed in mammals, over expression of VAPB could directly affect the activity of ATF6 at promoters adjacent to the nuclear membrane.

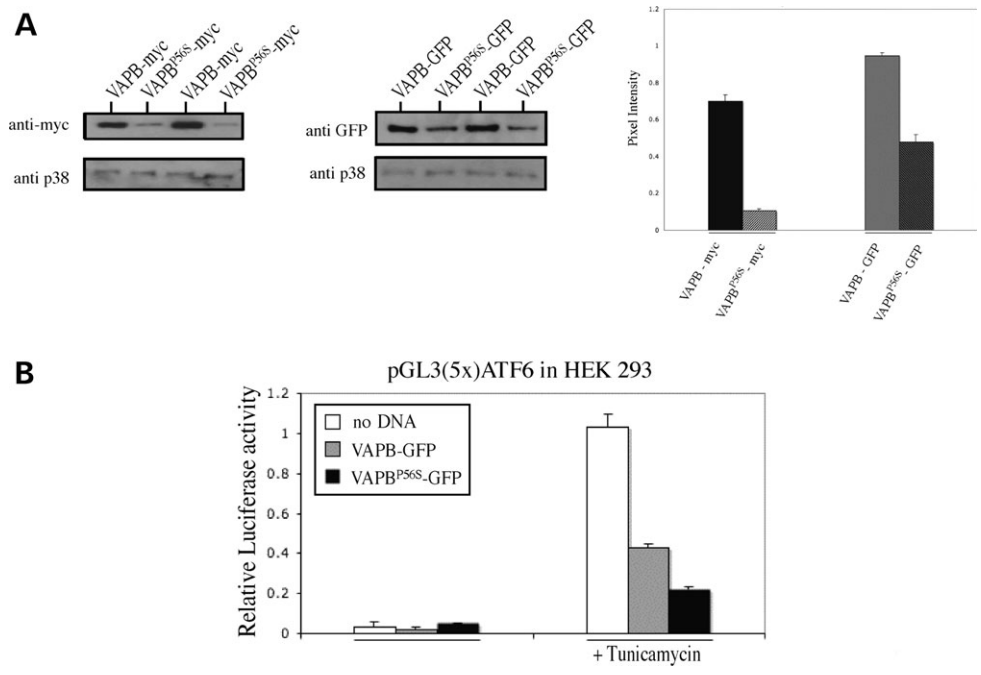

Figure 6. VAPB^{P56S} accumulates to lower levels than VAPB. Immunoblot analysis of HEK293 cells expressing myc or GFP-tagged forms of VAPB and VAPB^{P56S}. Duplicate samples are shown, and relative levels expressed as a histogram of signal intensities. As both myc and GFP fusion proteins, VAPB^{P56S} accumulates to lower levels than VAPB. VAPB^{P56S}-myc is ~15% the level of VAPB-myc, and VAPB^{P56S}-GFP is ~50% the level of VAPB-GFP. (**A**) The GFP moiety appears to have a stabilizing affect on the levels of mutant protein, allowing it to accumulate to higher levels than the myc-tagged form. (**B**) Consistent with this the inhibition of ATF6-dependent reporter gene expression is reduced to a greater relative level by VAPB^{P56S}-GFP than VAPB^{P56S}-myc. Band intensities were determined using ImageJ (NIH) Intensities for both myc and GFP, VAPB and VAPB^{P56S} were normalized to the p38 loading control.

A regulatory role for VAP proteins on the surface of the ER

The UPR and ERAD systems respond to the environment of the lumen of the ER. Perhaps the interaction between the VAP proteins and ATF6 represents an additional element of ER regulation that responds to levels of proteins associating with the surface of the ER, or to proteins that do not have significant amounts of luminal structure.

VAP proteins interact with a broad range of other coiled–coil containing proteins such as VAMP/Synaptobrevin and syntaxin (12). If interactions of the coiled/coil domain also affected the MSP domain-dependent inhibition of ATF6, they could enable the levels of membrane proteins on the surface of the ER to activate ATF6.

VAP proteins and Hepatitis C virus replication

The Hepatitis C virus has exploited potential structural and regulatory functions of the VAP proteins. Hepatitis C replicates in association with the ER. Two of the viral proteins required for this association, NS5A and NS5B, can bind to both VAPA and B, interacting with the coiled–coil and MSP domains, respectively (54,55). Disrupting these interactions or down-regulating VAPA and VAPB protein levels inhibits virus replication (55,56). Hepatitis C protein expression can also induce ER stress, activating both ATF6 and XBP1. This does not lead to a full UPR (57,58), and it has been suggested that mis-regulation of the ER stress response may in someway favour viral replication (58). Perhaps a similar mechanism may contribute to the pathogenesis of VAPB^{P56S}. The mutant protein could lead to a mis-regulation of ER stress regulatory pathways via aberrant ATF6 activity. Such mis-regulation could also have a role in the pathological affects of Hepatitis C infection.

ATF6 activity and neurodegeneration

The increased level of ATF6 inhibition by VAP^{P56S} suggests that a possible pathological mechanism for ALS8 is mis-function of homeostatic regulatory systems of the ER. Kanekura *et al*. (23) recently demonstrated that increased VAPB levels could induce the UPR as indicated by activation of XBP1, and that the affect of VAPB^{P56S} was to diminish this activation. Our study suggests that VAP proteins can also affect the activity of ATF6, and that the mutation VAPB^{P56S} may, have a greater effect than the wild-type protein VAPB. From gene transcription analysis on the UPR in *C. elegans*, it has been shown that ATF6 mainly contributes to tonic levels of gene expression (59). In mammals, ATF6 appears to have a more extensive role in the ER stress response, where it is required for the induced expression of principal ER chaperones, and also acts as a heterodimer with XBP1 to induce components of the ER associated degradation pathway (ERAD) (30).

The direct interaction between VAP proteins and ATF6 represents a previously uncharacterized mechanism for the

regulation of transcriptional responses made to changes in ER metabolism. Overall, VAP proteins may have structural and regulatory functions based on interactions of the MSP domain. The pathological mechanism in ALS8, therefore, may be the result of an inability to deal appropriately with different forms of ER stress.

MATERIALS AND METHODS

Antisera. VAPB-specific anti-serum was raised in sheep to a multi antigenic peptide (MAP) form of a peptide corresponding to amino acids 174–189 of mouse VAPB (Alta Bioscience). This sequence is identical in rats and mice. The serum was affinity purified using the immunizing peptide. The VAPA anti-serum has been described previously (13). Anti-myc was monoclonal 9E10 and anti-FLAG was M2 (Sigma).

Muscle staining

Muscle tissue was fixed in 0.1 M PBS containing 4% paraformaldehyde for 1–2 h.

Muscles were blocked in 4% BSA and 0.5% Triton-X (both Sigma) in PBS for 30 min before incubation in primary antibodies overnight at 4°C. The primary antibodies used were sheep anti-VAPB (1:200) and rabbit anti-VAPA (1:300). After washing for 30 min in blocking solution, muscles were incubated for 4–5 h in PBS containing secondary antibodies. The secondary antibodies used were Donkey anti-Sheep Cy2 (1:100, Jackson Laboratories) and Donkey anti-Rabbit Cy3 (1:100, Jackson Laboratories). After a 2 h wash in PBS, muscles were mounted on glass slides in mowoil mounting medium [2.4 g mowoil (Poly vinyl Alcohol, Calbiochem), 6 g glycerol, 2.5% 1,4-diazobicyclo-octane (DABCO, antifade, Sigma), 12 ml 200 mM Tris (pH 8.5)). These experiments are not shown.

Preparations were analysed using a laser confocal scanning microscope (Biorad Radiance 2000). The strobing function was always enabled to prevent signal bleeding through from one channel to another. Confocal z-series were merged using Lasersharp (Biorad) software. All images were analysed and prepared for presentation in Adobe Photoshop.

Cell staining

HEK293 cells grown on poly-D-lysine coated cover slips were fixed in 3% paraformaldehyde, 0.03% glutaraldehyde (w/v) in PBS, at room temperature for 20 min. Fixative was quenched and cells permeablized with a solution of 50 mM NH_4Cl, 0.2% (w/v) Saponin (Sigma), for 15 min at room temperature. Cells were washed, and antibodies diluted in a solution containing 0.2% (w/v) fish skin gelatin (Sigma G-7765), 0.02% saponin, in PBS. Inverted cover slips were mounted in Mowoil, and examined on a Zeiss Imager.Z1 microscope fitted with a LSM 510 Meta confocal excitation/acquisition system.

Peptide complementation

Full-length coding sequences for mouse VAPA, VAPB, $VAPA^{P56S}$, $VAPB^{P56S}$ and human ATF6α (NM_007348) were amplified in a PCR that introduced flanking BspEI and XbaI, or NotI and ClaI restriction sites, and sub-cloned into pcDNA3.1(zeo)-Venus[1] or pcDNA3.1(zeo)-Venus[2], respectively (28). HEK293 were transfected using Lipofectamine 2000 (Invitrogen). For each transfection 200 ng of total DNA was used. Images of living cells were acquired 24 h after transfection on an Olympus IX70 fluorescence microscope using Openlab software (Improvision). Representative images are shown.

Transcription assay

HEK293 or NSC-34 cells were grown in Dulbecco's Modified Eagle's Medium supplemented with 10% foetal bovine serum. Cells were transfected using Lipofectamine2000 (Invitrogen). Each transfection mixture contained 300 ng of p5xATF6-GL3 (31) and 100 ng of the internal control renilla luciferase reporter, pTK-RT. VAPB and $VAPB^{P56S}$ were expressed as EGFP-fusion proteins derived from pEGFP-C1 (Clontech), or as myc epitope tagged fusion proteins where the EGFP coding sequence was replaced with a myc epitope coding sequence. The total amount of DNA per transfection was 500 ng. ATF6 was over expressed as a FLAG-tagged fusion protein from pCMV-ATF6-3xFLAG7.1 (60). One hundred nanogram of each VAPB and ATF6 expression plasmid was used, with the total amount of DNA in each transfection made up to 600 ng with the vector pEGFP-C3 (Clontech). Twenty-four hours after transfection ER stress was induced for 12 h with 2 μg/ml tunicamycin (Calbiochem). Cells were then lysed and assayed for firefly and renilla luciferase activity using the Dual Glo™ Luciferase Assay System (Promega). Firefly and renilla luminescence were measured using a FLUOstar OPTIMA micro-plate reader (BMG LABTECH). Firefly luciferase luminescence values are normalized to renilla firefly luminescence values and are averages of four experiments with SE.

siRNA transfection

10^6 HEK293 cells were nucleofected with 200 pMoles of VAPB siRNA (Quiagen) or a control GFP-siRNA (Dharmacon) using the Amaxa Biosystems nucleofector. Twenty-four hours after nuclofection, cells were transfected with p5xATF6-GL3 and pTK-RT as described above. After a further 24 h, cells were treated with 2 μg/ml Tunicamycin (Calbiochem) for 12 h and then assayed for luciferase activity as above.

SUPPLEMENTARY MATERIAL

Supplementary Material is available at HMG Online.

ACKNOWLEDGEMENTS

The authors wish to thank and acknowledge Dr Francesc Soriano, Dr Giles Hardingham and Dr Mandy Jackson for

help and advice during the course of this work. Prof. Ron Prywes generously supplied pCMV-ATF6-3xFLAG7.1 and p5xATF6-GL3. Prof. Steve Michnick generously supplied the plasmid vectors of the Peptide Complementation assays.

Conflict of Interest Statement. None declared.

FUNDING

The work was supported by The Wellcome Trust (Grant number 063502), Scottish Motor Neuron Disease Association, BBSRC (T.H.G.) Medical Research Scotland (T.H.G.), and The Medical Research Council (S.M.).

REFERENCES

1. Nishimura, A.L., Mitne-Neto, M., Silva, H.C., Richieri-Costa, A., Middleton, S., Cascio, D., Kok, F., Oliveira, J.R., Gillingwater, T., Webb, J. *et al.* (2004) A mutation in the vesicle-trafficking protein VAPB causes late-onset spinal muscular atrophy and amyotrophic lateral sclerosis. *Am. J. Hum. Genet.*, **75**, 822–831.
2. Nishimura, A., Mitne-Neto, M., Silva, H., Oliveira, J., Vainzof, M. and Zatz, M. (2004) A novel locus for late onset amyotrophic lateral sclerosis/motor neurone. *J. Med. Genet.*, **41**, 315–320.
3. Marques, V.D., Barreira, A.A., Davis, M.B., Abou-Sleiman, P.M., Silva, W.A., Jr, Zago, M.A., Sobreira, C., Fazan, V. and Marques, W., Jr (2006) Expanding the phenotypes of the Pro56Ser VAPB mutation: proximal SMA with dysautonomia. *Muscle Nerve*, **34**, 731–739.
4. Logroscino, G., Beghi, E., Zoccolella, S., Palagano, R., Fraddosio, A., Simone, I.L., Lamberti, P., Lepore, V. and Serlenga, the Sclerosi Laterale Amiotrofica - Puglia registry. (2005) Incidence of amyotrophic lateral sclerosis in southern Italy: a population based study. *J. Neurol. Neurosurg. Psychiatry*, **76**, 1094–1098.
5. Piemonte and Valle d'Aosta Register for Amyotrophic Lateral Sclerosis (PARALS). (2001) Incidence of ALS in Italy: evidence for a uniform frequency in Western countries. *Neurology*, **56**, 239–244.
6. Bradley, W.G. (1995) Overview of motor neuron disease: classification and nomenclature. *Clin. Neurosci.*, **3**, 323–236.
7. Swash, M. and Desai, J. (2000) Motor neuron disease: classification and nomenclature. *Amyotroph. Lateral Scler. Other Motor Neuron Disord.*, **1**, 105–112.
8. Schymick, J.C., Talbot, K. and Traynor, B.J. (2007) Genetics of sporadic amyotrophic lateral sclerosis. *Hum. Mol. Genet.*, **16**, R233–R242.
9. Skehel, P., Martin, K., Kandel, E. and Bartsch, D. (1995) A VAMP-binding protein from Aplysia required for neurotransmitter release. *Science*, **269**, 1580–1583.
10. Kagiwada, S., Hosaka, K., Murata, M., Nikawa, J. and Takatsuki, A. (1998) The Saccharomyces cerevisiae SCS2 gene product, a homolog of a synaptobrevin-associated protein, is an integral membrane protein of the endoplasmic reticulum and is required for inositol metabolism. *J. Bacteriol.*, **180**, 1700–1708.
11. Pennetta, G., Hiesinger, P., Fabian-Fine, R., Meinertzhagen, I. and Bellen, H. (2002) Drosophila VAP-33A directs bouton formation at neuromuscular junctions in a Dosage-Dependent Manner. *Neuron*, **35**, 291–306.
12. Weir, M., Xie, H., Klip, A. and Trimble, W. (2001) VAP-A binds promiscuously to both v- and tSNAREs. *Biochem. Biophys. Res. Commun.*, **286**, 616–621.
13. Skehel, P., Fabian-Fine, R. and Kandel, E. (2000) Mouse VAP33 is associated with the endoplasmic reticulum and microtubules. *Proc. Natl Acad. Sci. USA*, **97**, 1101–1106.
14. Laurent, F., Labesse, G. and Wit, P.d. (2000) Molecular cloning and partial characterization of a plant VAP33 homologue. *Biochem. Biophys. Res. Commun.*, **270**, 286–292.
15. Soussan, L., Burakov, D., Daniels, M., Toister-Achituv, M., Porat, A., Yarden, Y. and Elazar, Z. (1999) ERG30, a VAP-33-related protein, functions in protein transport mediated. *J. Cell. Biol.*, **146**, 301–311.
16. Nishimura, Y., Hayashi, M., Inada, H. and Tanaka, T. (1999) Molecular cloning and characterization of mammalian homologues of vesicle-associated membrane protein-associated (VAMP-associated) proteins. *Biochem. Biophys. Res. Commun.*, **254**, 21–26.
17. Sepsenwol, S., Ris, H. and Roberts, T.M. (1989) A unique cytoskeleton associated with crawling in the amoeboid sperm of the nematode, Ascaris suum. *J. Cell. Biol.*, **108**, 55–66.
18. Loewen, C., Roy, A. and Levine, T. (2003) A conserved ER targeting motif in three families of lipid binding proteins. *EMBO J.*, **22**, 2025–2035.
19. Wyles, J., McMaster, C. and Ridgway, N. (2002) Vesicle-associated membrane protein-associated protein-A (VAP-A) interacts. *J. Biol. Chem.*, **277**, 29908–29918.
20. Kawano, M., Kumagai, K., Nishijima, M. and Hanada, K. (2006) Efficient trafficking of ceramide from the endoplasmic reticulum to the Golgi apparatus requires a VAMP-associated protein-interacting FFAT motif of CERT. *J. Biol. Chem.*, **281**, 30279–30288.
21. Kaiser, S.E., Brickner, J.H., Reilein, A.R., Fenn, T.D., Walter, P. and Brunger, A.T. (2005) Structural basis of FFAT motif-mediated ER targeting. *Structure*, **13**, 1035–1045.
22. Amarilio, R., Ramachandran, S., Sabanay, H. and Lev, S. (2005) Differential regulation of endoplasmic reticulum structure through VAP-Nir protein interaction. *J. Biol. Chem.*, **280**, 5934–5944.
23. Kanekura, K., Nishimoto, I., Aiso, S. and Matsuoka, M. (2006) Characterization of amyotrophic lateral sclerosis-linked P56S mutation of vesicle-associated membrane protein-associated protein B (VAPB/ALS8). *J. Biol. Chem.*, **281**, 30223–30233.
24. Teuling, E., Ahmed, S., Haasdijk, E., Demmers, J., Steinmetz, M.O., Akhmanova, A., Jaarsma, D. and Hoogenraad, C.C. (2007) Motor neuron disease-associated mutant vesicle-associated membrane protein-associated protein (VAP) B recruits wild-type VAPs into endoplasmic reticulum-derived tubular aggregates. *J. Neurosci.*, **27**, 9801–9815.
25. Weir, M., Klip, A. and Trimble, W. (1998) Identification of a human homologue of the vesicle-associated membrane. *Biochem. J.*, **333**, 247–251.
26. Tasker, P.N., Michelangeli, F. and Nixon, G.F. (1999) Expression and distribution of the type 1 and type 3 inositol 1,4,5-trisphosphate receptor in developing vascular smooth muscle. *Circ. Res.*, **84**, 536–542.
27. Yoshida, H., Haze, K., Yanagi, H., Yura, T. and Mori, K. (1998) Identification of the cis-acting endoplasmic reticulum stress response element responsible for transcriptional induction of mammalian glucose-regulated proteins. Involvement of basic leucine zipper transcription factors. *J. Biol. Chem.*, **273**, 33741–33749.
28. Remy, I., Galarneau, A. and Michnick, S.W. (2002) Detection and visualization of protein interactions with protein fragment complementation assays. *Methods Mol. Biol.*, **185**, 447–459.
29. Bailey, D. and O'Hare, P. (2007) Transmembrane bZIP transcription factors in ER stress signaling and the unfolded protein response. *Antioxid. Redox. Signal.*, **9**, 2305–2322.
30. Yamamoto, K., Sato, T., Matsui, T., Sato, M., Okada, T., Yoshida, H., Harada, A. and Mori, K. (2007) Transcriptional induction of mammalian ER quality control proteins is mediated by single or combined action of ATF6alpha and XBP1. *Dev. Cell*, **13**, 365–376.
31. Wang, Y., Shen, J., Arenzana, N., Tirasophon, W., Kaufman, R.J. and Prywes, R. (2000) Activation of ATF6 and an ATF6 DNA binding site by the endoplasmic reticulum stress response. *J. Biol. Chem.*, **275**, 27013–27020.
32. Ron, D. and Walter, P. (2007) Signal integration in the endoplasmic reticulum unfolded protein response. *Nat. Rev. Cell. Biol.*, **8**, 519–529.
33. Ye, J., Rawson, R.B., Komuro, R., Chen, X., Dave, U.P., Prywes, R., Brown, M.S. and Goldstein, J.L. (2000) ER stress induces cleavage of membrane-bound ATF6 by the same proteases that process SREBPs. *Mol. Cell*, **6**, 1355–1364.
34. Hai, T.W., Liu, F., Coukos, W.J. and Green, M.R. (1989) Transcription factor ATF cDNA clones: an extensive family of leucine zipper proteins able to selectively form DNA-binding heterodimers. *Genes. Dev.*, **3**, 2083–2090.
35. Yoshida, H., Okada, T., Haze, K., Yanagi, H., Yura, T., Negishi, M. and Mori, K. (2000) ATF6 activated by proteolysis binds in the presence of NF-Y (CBF) directly to the cis-acting element responsible for the mammalian unfolded protein response. *Mol. Cell. Biol.*, **20**, 6755–6767.

36. Tkacz, J. (1981) *Antibiotics, Modes and Mechanisms of Microbial Growth Inhibitors*, **6**, 1–52.
37. Haze, K., Yoshida, H., Yanagi, H., Yura, T. and Mori, K. (1999) Mammalian transcription factor ATF6 is synthesized as a transmembrane protein and activated by proteolysis in response to endoplasmic reticulum stress. *Mol. Biol. Cell*, **10**, 3787–3799.
38. Shen, J., Snapp, E.L., Lippincott-Schwartz, J. and Prywes, R. (2005) Stable binding of ATF6 to BiP in the endoplasmic reticulum stress response. *Mol. Cell. Biol.*, **25**, 921–932.
39. Loewen, C.J. and Levine, T.P. (2005) A highly conserved binding site in vesicle-associated membrane protein-associated protein (VAP) for the FFAT motif of lipid-binding proteins. *J. Biol. Chem.*, **280**, 14097–14104.
40. Lesh, R.E., Nixon, G.F., Fleischer, S., Airey, J.A., Somlyo, A.P. and Somlyo, A.V. (1998) Localization of ryanodine receptors in smooth muscle. *Circ. Res.*, **82**, 175–185.
41. Mattson, M.P. (2007) Calcium and neurodegeneration. *Aging Cell*, **6**, 337–350.
42. Kihira, T., Utunomiya, H. and Kondo, T. (2005) Expression of FKBP12 and ryanodine receptors (RyRs) in the spinal cord of MND patients. *Amyotrophic Lateral Sclerosis*, **6**, 94–99.
43. Kagiwada, S. and Hashimoto, M. (2007) The yeast VAP homolog Scs2p has a phosphoinositide-binding ability that is correlated with its activity. *Biochem. Biophys. Res. Commun.*, epub ahead of print.
44. Koudinov, A.R. and Koudinova, N.V. (2005) Cholesterol homeostasis failure as a unifying cause of synaptic degeneration. *J. Neurol. Sci.*, **229**, 233–240.
45. Mourelatos, Z., Gonatas, N.K., Stieber, A., Gurney, M.E., Dal Canto, M.C., Chen, Y., Gonatas, J.O., Appel, S.H., Hays, A.P., Hickey, W.F. *et al.* (1996) The Golgi apparatus of spinal cord motor neurons in transgenic mice expressing mutant Cu,Zn superoxide dismutase becomes fragmented in early, preclinical stages of the disease Fragmentation of the Golgi apparatus of motor neurons in amyotrophic lateral sclerosis. *Proc. Natl Acad. Sci. USA*, **93**, 5472–5477.
46. Paschen, W. and Frandsen, A. (2001) Endoplasmic reticulum dysfunction—a common denominator for cell injury in acute and degenerative diseases of the brain? *J. Neurochem.*, **79**, 719–725.
47. Lehotsky, J., Kaplan, P., Babusikova, E., Strapkova, A. and Murin, R. (2003) Molecular pathways of endoplasmic reticulum dysfunctions: possible cause of cell death in the nervous system. *Physiol. Res.*, **52**, 269–274.
48. Nagata, T., Ilieva, H., Murakami, T., Shiote, M., Narai, H., Ohta, Y., Hayashi, T., Shoji, M. and Abe, K. (2007) Increased ER stress during motoneuron degeneration in a transgenic mouse model of ALS. *Neurol. Res*, **29**, 767–771.
49. Kikuchi, H., Almer, G., Yamashita, S., Guegan, C., Nagai, M., Xu, Z., Sosunov, A.A., McKhann, G.M., 2nd and Przedborski, S. (2006) Spinal cord endoplasmic reticulum stress associated with a microsomal accumulation of mutant superoxide dismutase-1 in an ALS model. *Proc. Natl Acad. Sci. USA*, **103**, 6025–6030.
50. Ilieva, E.V., Ayala, V., Jove, M., Dalfo, E., Cacabelos, D., Povedano, M., Bellmunt, M.J., Ferrer, I., Pamplona, R. and Portero-Otin, M. (2007) Oxidative and endoplasmic reticulum stress interplay in sporadic amyotrophic lateral sclerosis. *Brain*, epub. ahead of print.
51. Yoshida, H. (2007) ER stress and diseases. *FEBS J.*, **274**, 630–658.
52. Tsukumo, Y., Tomida, A., Kitahara, O., Nakamura, Y., Asada, S., Mori, K. and Tsuruo, T. (2007) Nucleobindin 1 controls the unfolded protein response by inhibiting ATF6 activation. *J. Biol. Chem.*, **282**, 29264–29272.
53. Brickner, J.H. and Walter, P. (2004) Gene recruitment of the activated INO1 locus to the nuclear membrane. *PLoS Biol.*, **2**, e342.
54. Gao, L., Aizaki, H., He, J. and Lai, M.M.C. (2004) Interactions between viral nonstructural proteins and host protein hVAP-33. *J. Virol.*, **78**, 3480–3488.
55. Hamamoto, I., Nishimura, Y., Okamoto, T., Aizaki, H., Liu, M., Mori, Y., Abe, T., Suzuki, T., Lai, M.M., Miyamura, T. *et al.* (2005) Human VAP-B is involved in hepatitis C virus replication through interaction with NS5A and NS5B. *J. Virol.*, **79**, 13473–13482.
56. Zhang, J., amada, O., Sakamoto, T., Yoshida, H., Iwai, T., Matsushita, Y., Shimamura, H., Araki, H. and Shimotohno, K. (2004) Down-regulation of viral replication by adenoviral-mediated expression of. *Virology*, ..siRNA against cellular cofactors for hepatitis C virus. **320**, 135–143.
57. Tardif, K.D., Mori, K. and Siddiqui, A. (2002) siRNA against cellular cofactors for Hepatitis C virus subgenomic replicons induce endoplasmic reticulum stress activating an intracellular signaling pathway. *J. Virol.*, **76**, 7453–7459.
58. Zheng, Y., Gao, B., Ye, L., Kong, L., Jing, W., Yang, X., Wu, Z. and Ye, L. (2005) Hepatitis C virus non-structural protein NS4B can modulate an unfolded protein response. *J. Microbiol.*, **43**, 529–536.
59. Shen, X., Ellis, R.E., Sakaki, K. and Kaufman, R.J. (2005) Genetic interactions due to constitutive and inducible gene regulation mediated by the unfolded protein response in C. elegans. *PLoS genet.*, **1**, e37.
60. Shen, J., Chen, X., Hendershot, L. and Prywes, R. (2002) ER stress regulation of ATF6 localization by dissociation of BiP/GRP78 binding and unmasking of Golgi localization signals. *Dev. Cell*, **3**, 99–111.